2K Initiation Systems for Radical Polymerization of Dental Formulations

PhD Thesis

Dissertation

ausgeführt zum Zwecke der Erlangung

des akademischen Grades eines Doktors der technischen Wissenschaften

unter der Leitung von

Univ. Prof. Dipl.-Ing. Dr. techn. Robert Liska

und der Betreuung von

Senior Scientist Dipl.-Ing. Dr. techn. Patrick Knaack

am

Institut für Angewandte Synthesechemie

eingereicht an der Technischen Universität Wien

Fakultät für Technische Chemie

von

Dipl.-Ing. Florian Pieringer, BSc

01427132

Danksagung

Abstract

Free radical polymerization is one of the most important tools for the production of polymer materials. Dental applications of such materials require a convenient polymerization process at room temperature and ambient atmosphere, which is where two-component (2K) systems based on redox initiated radical polymerization truly stand out. However, these radical polymerization systems often come with drawbacks such as instability, toxicity and bad taste.

In order to surpass these limitations, the synthesis of a vitamin-C derivative was performed as a new reducing agent for redox initiated polymerization in the first part of this work (Part A). The reactivity of the initiated polymerization, as well as thermomechanical and mechanical properties of the resulting polymer networks were investigated.

In the second part of the work (Part B), the use of diboranes as labile bonds and copper complexes that catalyse their cleavage was found to be a very efficient radical initiation system. Mechanistic details of the new initiation system are analysed and a mechanism is proposed. Reactivity of this radical polymerization system was characterized with respect to multiple diborane compounds and copper compounds, as well as various concentrations. The resulting polymer networks were investigated regarding their thermomechanical and mechanical properties. Homogeneous networks are presented that show high double bond conversions and mechanical properties that are comparable to the state of the art.

Kurzfassung

Die radikalische Polymerisation ist eines der wichtigsten Werkzeuge für die Herstellung von Polymermaterialien. Für die zahnmedizinische Anwendung solcher Materialien ist ein bequemer Polymerisationsprozess bei Raumtemperatur und Umgebungsatmosphäre erforderlich, wobei sich Zweikomponentensysteme (2K), die auf redox-initiierter radikalischer Polymerisation basieren, auszeichnen. Diese radikalischen Polymerisationssysteme sind jedoch häufig mit Nachteilen wie Instabilität, Toxizität und schlechtem Geschmack verbunden.

Um diese Einschränkungen zu überwinden, wurde im ersten Teil dieser Arbeit (Part A) die Synthese eines Vitamin-C-Derivats als neues Reduktionsmittel für die redox-initiierte Polymerisation durchgeführt. Die Reaktivität der initiierten Polymerisation sowie die thermomechanischen und mechanischen Eigenschaften der resultierenden Polymernetzwerke wurden untersucht.

Im zweiten Teil der Arbeit (Teil B) wurde festgestellt, dass die Verwendung von Diboranen als labile Bindungen und von Kupferkomplexen, die ihre Spaltung katalysieren, ein effizientes System zur Erzeugung von Radikalen darstellt. Die mechanistischen Details des neuen Initiationssystems wurden analysiert und ein Mechanismus vorgeschlagen. Die Reaktivität dieses radikalischen Polymerisationssystems wurde im Hinblick auf mehrere Diboranverbindungen und Kupferverbindungen sowie verschiedene Konzentrationen charakterisiert. Die resultierenden Polymernetzwerke wurden auf ihre thermomechanischen und mechanischen Eigenschaften hin untersucht. Es werden homogene Netzwerke vorgestellt, die hohe Doppelbindungsumsätze und ausgezeichnete mechanische Eigenschaften aufweisen, die mit dem Stand der Technik vergleichbar sind.

Table of Contents

Introduction

Dental Restoratives

Oral diseases, including dental caries, impact over 3.5 billion people worldwide and impose significant health burdens on the countries affected. As reported by the Global Burden of Disease 2017, untreated dental caries in permanent teeth was the most prevalent health condition. However, the majority of oral health issues are preventable and can be managed if addressed in their early stages.[1]

One method of treating these dental conditions is through the use of fillings in the affected teeth. Amalgam was historically the most widely used dental restorative because of its ease of application in tooth cavities, low cost, and excellent durability. This alloy is composed of approximately 50% mercury, along with other metals like silver, tin, and copper. However, with advancements in analytical techniques, concerns were raised regarding the potential health risks associated with the high mercury content in amalgam.[2, 3] The demand for alternatives led to the creation of composite materials, which were required to replicate various properties of the tooth.

In order to understand the requirements for such a material better, the structure of the tooth has to be understood first, which is displayed in Figure 1.
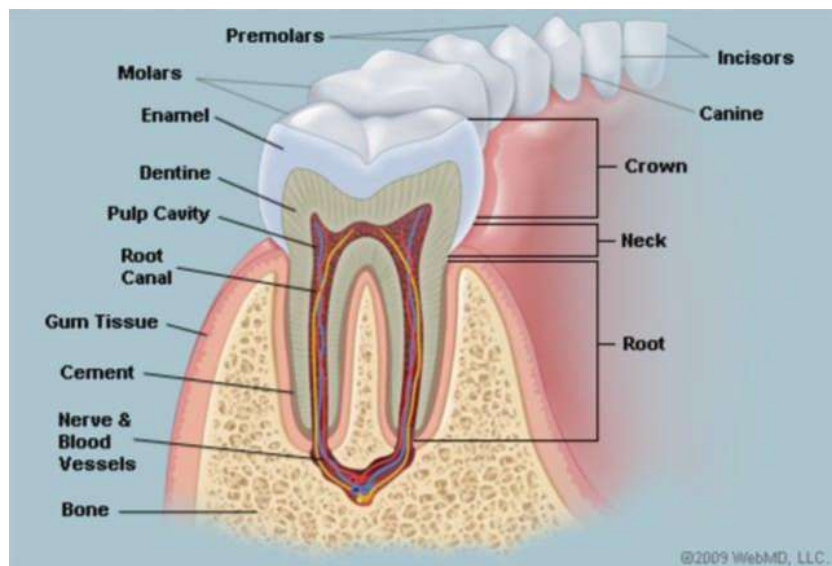
Figure 1: Schematic picture of the inner structure of a tooth.[4]

The enamel layer is composed of nearly 100% inorganic material, specifically hydroxyapatite. These hydroxyapatite crystals are, however, embedded within layers of organic collagen filaments. While this structure offers significant mechanical stability, it also has the disadvantage of being vulnerable to acids, particularly lactic acid. The dentine layer, located beneath the enamel, is made of the same material as the enamel but has a higher collagen content and contains small pores filled with dentine liquid.[2, 5] The dental restorative has to match the properties of the natural tooth as closely as possible regarding the mechanical properties, color and biocompatibility.

Dental materials

Resin-based dental composites serve as a highly effective alternative to the commonly used amalgam fillings. These composites are made up of a polymeric matrix, composed of difunctional methacrylates, along with a dispersed reinforcing phase of radiopaque silica glass. The composite material also includes coupling agents, initiators, and stabilizers as essential components.[6-8]

The organic matrix is composed of a blend of several difunctional monomers. BisGMA (bisphenol-A-glycidyldimethacrylate) is the most commonly used monomer because it shows excellent mechanical properties to the hardened matrix. However, its high viscosity limits its processability, so other monomers are incorporated into the mixture. UDMA (urethanedimethacrylate), TEGDMA (triethyleneglycoldimethacrylate), and D3MA (1,10-decanedioldimethacrylate) are frequently used due to their lower viscosity while maintaining similar mechanical properties. Figure 2 shows the structures of these monomers.[6, 8-10]

BisGMA
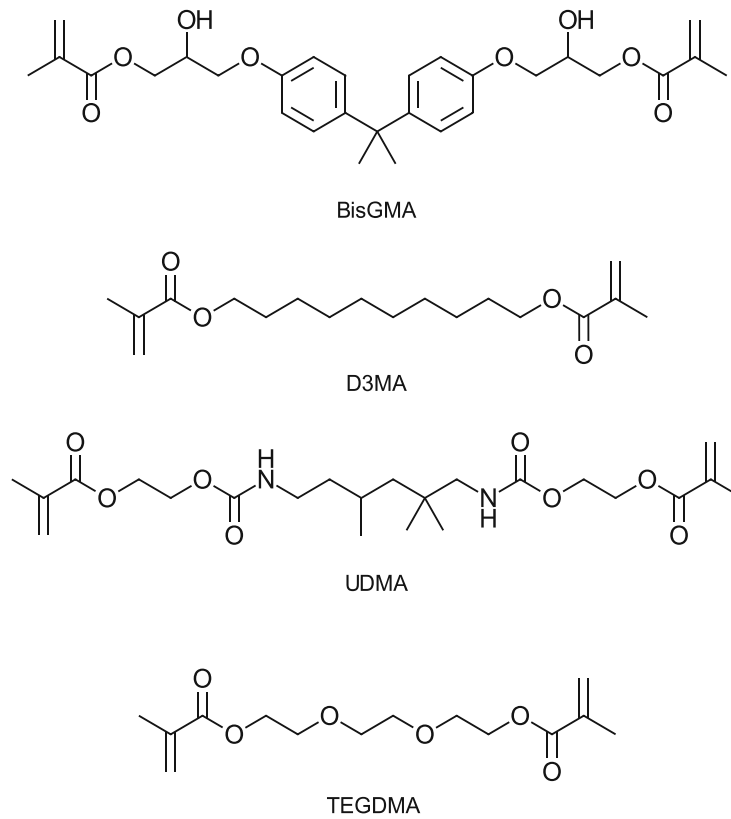
D3MA

UDMA

TEGDMA

Figure 2: Chemical structure of common monomers used for dental composite matrices, including BisGMA, D3MA, UDMA and TEGDMA.

The properties of dental restorative materials are significantly affected by the reinforcing filler materials, which account for over 60wt% of the filling. These properties include radiopacity, mechanical toughness, viscosity, and appearance. Commonly used fillers include strontium- and germanium-based silica glasses with particle sizes ranging from 1 to 2 µm, as well as SiO_2 or Si-based oxides with particle sizes of 10 to 500 nm. Figure 3 illustrates a scheme of the dispersed reinforcing phase within a polymeric matrix.[7]

inorganic glass filler (>50 wt%)

organic polymer matrix
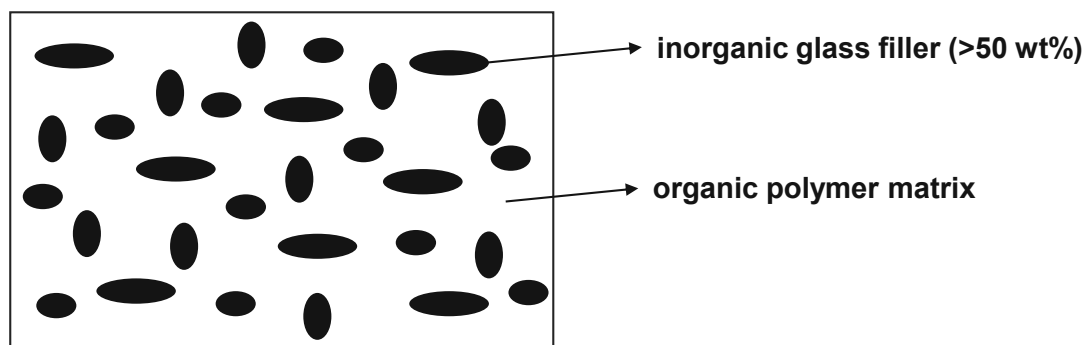
Figure 3: Schematic display of a dental composite structure showing the composition of filler material and matrix.[8]

13

Free-radical Polymerization

The most common technique to polymerize the organic matrix is via free-radical polymerization (FRP). In this type of polymerization, an initiator (I) is used to generate free radicals (I·). These radicals add to polymerizable, reactive monomers to form monomer radicals in the initiation (1) step. In the propagation (2) step, these monomer radicals proceed to add to more monomers and form polymer chains. This chain reaction is then terminated via either recombination of two radicals, or disproportion via hydrogen abstraction in the termination (4) step.[11-13] The scheme of the described free-radical polymerization reaction is depicted in Figure 4.
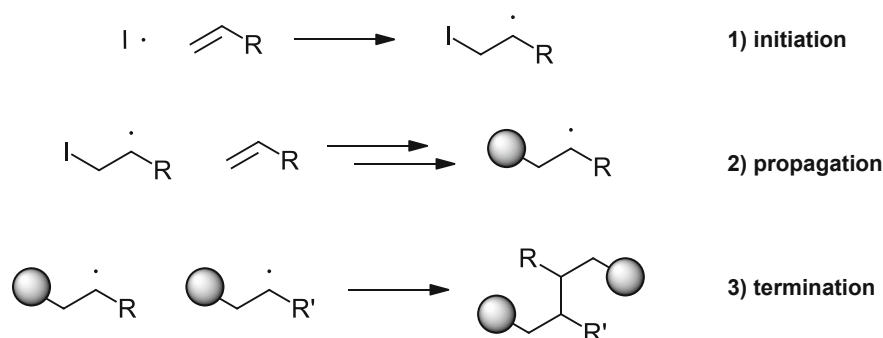
Figure 4: Scheme of the mechanism of free-radical polymerization, including the initiation by an initiator (I), the propagation of the radical on double bonds, and the termination via recombination of radicals.

This polymerization reaction proceeds very quickly, reaching the final molecular weight in a short time. However, when oxygen is present, the reaction is inhibited due to the formation of peroxy radicals, which exhibit significantly lower reactivity. The generation of these radicals is illustrated in Figure 5.
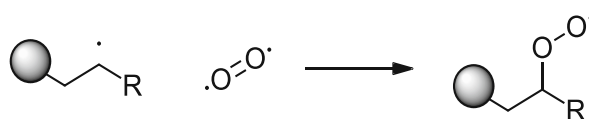
Figure 5: Scheme of the mechanism of oxygen inhibition in free radical polymerization, resulting in a poorly reactive peroxy radical.

One approach to addressing this problem involves the use of additives, such as co-initiators, oxygen barriers, optimized photoinitiators, or by creating an inert atmosphere. Nevertheless, oxygen inhibition primarily affects thin coatings because of their extensive surface exposure.[14]

Two-component (2K) Polymerization Systems

Dental composites mainly fall into two categories of materials: self-cure (SC) and dual-cure (DC) systems.[15] Herein we will focus on SC materials, where the initiation step of the polymerization is accomplished via two-component systems (2K systems). The most common method for 2K systems leading to radical polymerization is redox initiation.[16] To that end, an oxidizing agent is solubilized within a bulk monomer, referred to as the Ox-formulation, and a reducing agent is solubilized within a separate bulk monomer formulation, referred to as the Red-formulation (Figure 6).
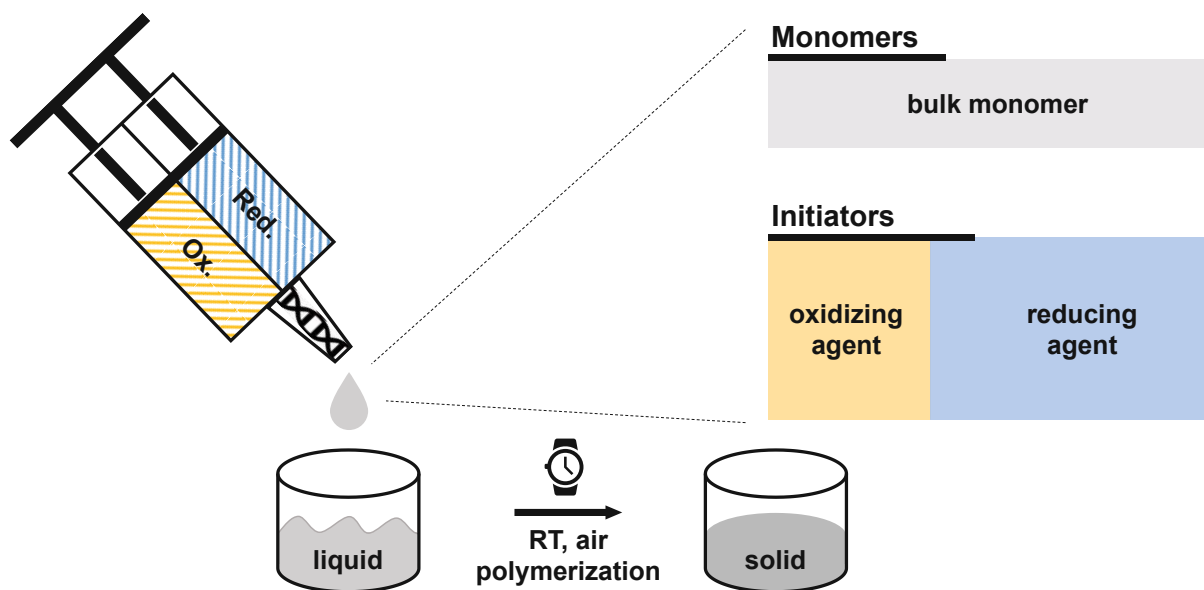
Figure 6: Schematic display of the principle of a 2K system. In one chamber, monomer and oxidizing agent is stored and, in another chamber, monomer and reducing agent is stored. Once mixed, the polymerization starts after a certain working time at room temperature and under air.

The advantage of such systems is their simplicity in handling. For application, the two separate formulations are mixed at the tip of the syringe and after a certain working time, depending on the reactivity of the formulation, the polymerization starts without any external trigger. These self-cure systems are especially valuable for the bulk curing of dental materials in the cavity of teeth. [15, 17-20] However, the main application for such 2K systems lies within adhesives industry where such initiation systems are by far the most common way to polymerize adhesives.[21] In this regard, 2K initiation systems have been developed fulfilling the needs of this industry. Despite this innovation, the requirements for 2K initiation system applied in the dental industry differ from adhesives and issues regarding stability, color and taste (including toxicity) are still to be addressed.[22-24]

2K Redox Initiation for Free Radical Polymerization

The generation of free radicals via a 2K system is possible using different approaches, however, the easiest would be through Fenton's reagent. This includes the reduction of a peroxide by a metal e.g., Fe^{2+}/H_2O_2.[25, 26] In this reaction, one electron is transferred from Fe(II) to the peroxide, which leads to a dissociation of the peroxide and the formation of Fe(III) (Figure 7 (1)). The hydroxyl radical can then initiate the polymerization by itself, or lead to a more reactive radical by hydrogen abstraction. However, one problem with this reaction is the reduction of the hydroxyl radical by Fe(II) (2). High concentrations of the initiation system lead to this unwanted side reaction, essentially destroying the formed radicals.[16] Furthermore, low reactive peroxy radicals will be formed by the reaction of the hydroxyl radical with residual hydroperoxide (3).

$$Fe^{2+} \;+\; HOOH \;\longrightarrow\; HO\cdot \;+\; HO^- \;+\; Fe^{3+} \qquad \textbf{(1)}$$

$$HO\cdot \;+\; Fe^{2+} \;\longrightarrow\; HO^- \;+\; Fe^{3+} \qquad \textbf{(2)}$$

$$HO\cdot \;+\; HOOH \;\longrightarrow\; HOO\cdot \;+\; H_2O \qquad \textbf{(3)}$$

Figure 7: Reaction scheme of the Fenton reaction. (1): reaction of Fe(II) with hydroperoxide, leading to a hydroxyl radical, a hydroxyl anion and oxidized Fe(III). (2): side reaction of the hydroxyl radical with Fe(II) leading to a hydroxyl anion and oxidized Fe(III). (3): side reaction of the hydroxyl radical with hydroperoxide leading to a low reactive peroxy radical and water.

Although it is difficult to get this reaction under control, elevated temperatures and low initiator concentrations proved to be helpful.[27, 28]

Other metals that are able to undergo a Fenton reaction with a peroxide include Rh(I), Cu(I), Mn(II), Co(II) and V(V).[29-32] Especially Cu(I) showed great potential and was investigated in great detail. The reversible reaction of the oxidation from Cu(I) to Cu(II), the reduction from Cu(II) to Cu(I) by an additional reducing agent enabled the development of catalytic initiation systems using only very low amounts of Cu(I) (Figure 8).[33, 34]
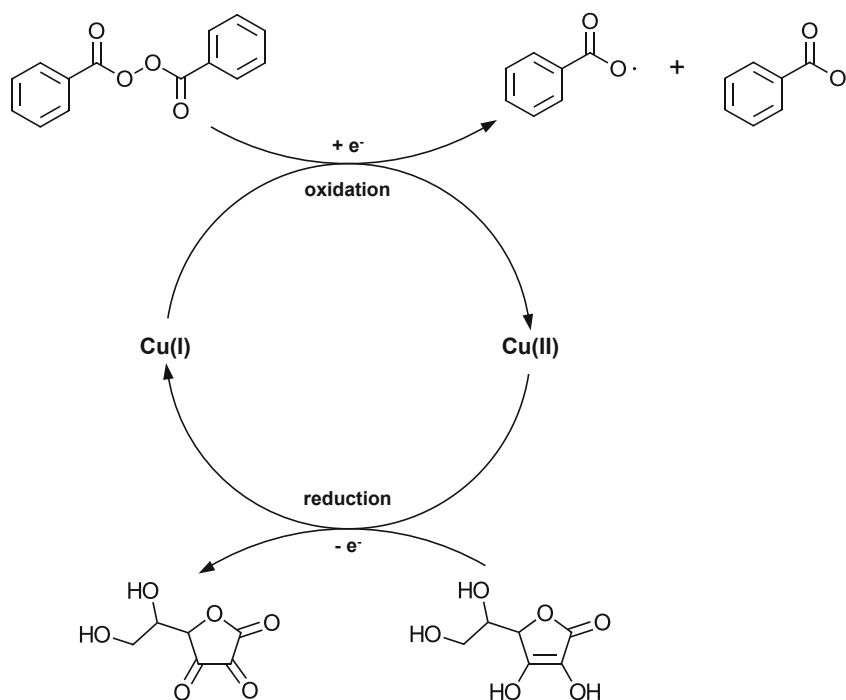
Figure 8: Scheme of the circular reaction of in a BPO/Cu(I)/VitC system. BPO is reduced by Cu(I), which is oxidized to Cu(II). Cu(II) can then be reduced by VitC to Cu(I) and close the cycle.

In these bulk polymerizations of organic monomers, the use of organic peroxides, such as dibenzoyl peroxide (BPO) are very common (Figure 8).[33]

Further advancements led to a redox system that comes without the use of metals as reducing agents. A tertiary aromatic amine, such as *N,N*-dimethylaniline, proved to be highly potent in reducing peroxides (Figure 9).[35]
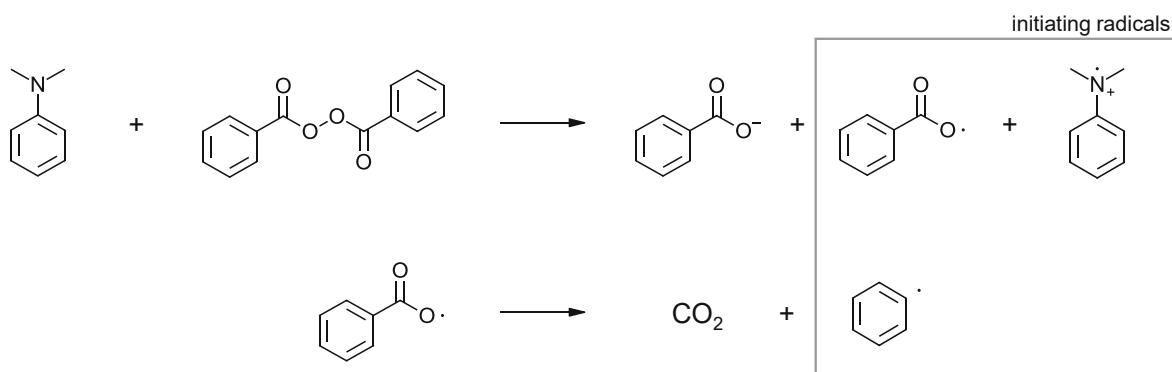
Figure 9: Reaction scheme of the reduction of dibenzoyl peroxide with NN-dimethylaniline. The dissociation of the peroxide leads to an anion and the benzoyl radical as well as the amine cation radical. The benzoyl radical can further eliminate CO_2 to form a phenyl radical.

The reduction of the peroxide leads to the dissociation likewise the Fenton reaction and a benzoyl anion as well as a benzoyl radical is formed. Additionally, an amino cation radical is formed that can also initiate the polymerization reaction. Recent studies showed, that the

benzoyl radical can readily eliminate CO_2 and form a phenyl radical.[24, 36] However, not only peroxy compounds can participate in Fenton reactions, also disulfides and disulfones as well as halides are reported to be reduced by Fe(II) and lead to the generation of free radicals (Figure 10).[37-40]

$$Fe^{2+} + RSSR \longrightarrow RS\bullet + RS^- + Fe^{3+} \qquad \textbf{(1)}$$

$$Fe^{2+} + {}^-O_3S\text{-}O\text{-}O\text{-}SO_3^- \longrightarrow SO_4^-\bullet + SO_4^- + Fe^{3+} \qquad \textbf{(2)}$$

$$Fe^{2+} + Br\text{-}Br \longrightarrow Br\bullet + Br^- + Fe^{3+} \qquad \textbf{(3)}$$

Figure 10: Scheme of Fenton like reaction between Fe(II) and a disulfide (1), a disulfone (2) and a halide (3) leading to the respective anions, radicals and Fe(III).

Classic Fenton reactions are limited regarding the choice of the reaction partners. To this end, other oxidation-reduction pairs were sought after. The development of the metal acetylacetonate-bidentate ligand interaction (MABLI) mechanism by Lalevée et al. was a major milestone in this regard.[41-43] The reaction occurring between the initiators of the 2K initiation system is a ligand exchange reaction leading to the formation of acetylacetonate radicals that can initiate the polymerization. Several metal acetylacetonates were investigated in this regard and it was found that Cu(II) and Mn(III) were the most promising candidates. As bidentate ligand, aromatic phosphines were used. The structures of the investigated compounds are depicted in Figure 11 and the mechanism of the reaction is depicted in Figure 12.[41]

2dppba   **2dppna**

Cu(acac)$_2$ **Mn(acac)$_3$**   **V(acac)$_3$**
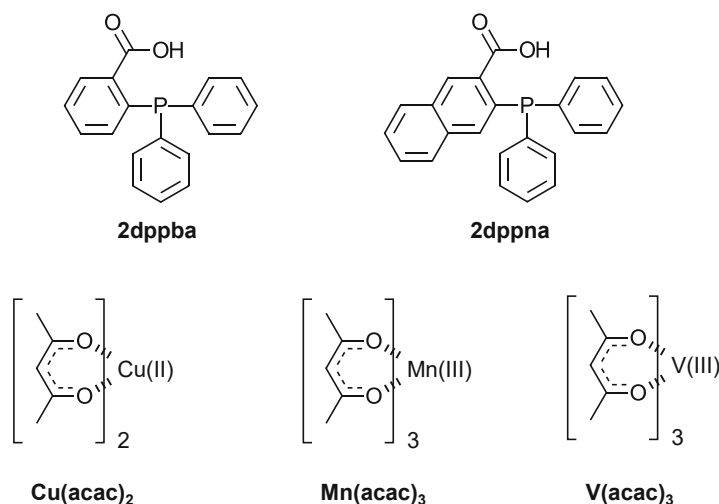
Figure 11: Chemical structure of some of the investigated bidentate ligands (2dppba and 2dppna) and metal acetylacetonates (Cu(acac)$_2$, Mn(acac)$_3$ and V(acac)$_3$ for MABLI reactions.[41]

initiating radicals

Mt(n)(acac)$_x$
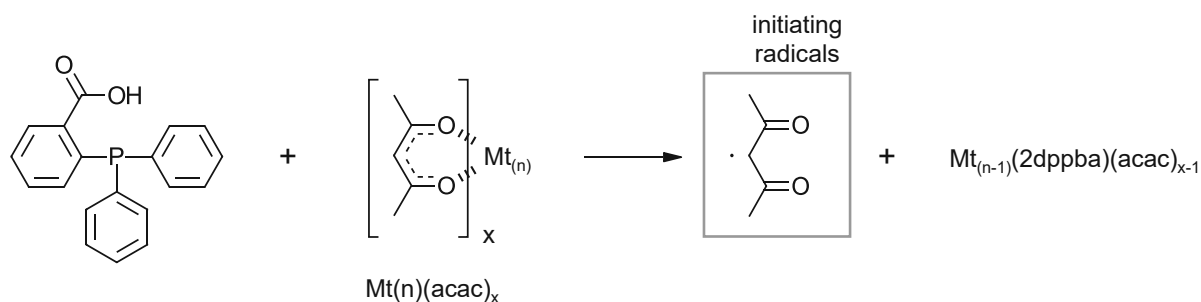
Figure 12: Reaction scheme for the MABLI reaction between a bidentate ligand and a metal acetylacetonate, leading to acetylacetonate radicals that can initiate polymerization.[41]

The drawback of such systems is the high amount of metal acetyl acetonate needed as the reaction is not catalytic but for every molecule of metal only one radical species is generated.[41] However, in several applications, including dental industry, high amounts of metal are not feasible.

To surpass these limitations, metal-free approaches beside the amine/peroxide system were investigated. Iodonium salts, used in as catalysts in cationic photopolymerization and frontal polymerization, proved to also show oxidizing properties.[44, 45]

These properties led to the development of redox initiation systems based on iodonium salts as oxidizing agents and silanes as reducing agents, which showed remarkable reactivity regarding the polymerization initiation of (meth)acrylic monomers.[46-49] Some of the studied compounds are depicted in Figure 13.[49]
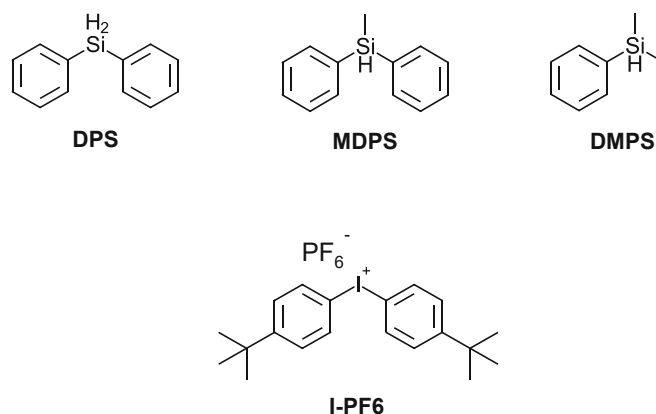
Figure 13: Chemical structure of silanes (diphenylsilane (DPS), methyldiphenylsilane (MDPS) and dimethylphenylsilane (DMPS)) used as reducing agents for redox initiation with an iodonium salt (IPF6).[49]

The initiation reaction between the iodonium salt and the silane is similar to a Fenton reaction, leading to the formation of aryl radicals that will initiate the polymerization. However, a drawback of this initiation system is the instability of silanes towards moisture and oxidation.[48] Especially when applied in dental composites, these limitations make such initiation systems not feasible anymore.

Summing up, 2K redox initiation shows great potential for the development of polymerization systems for bulk (meth)acrylates used in the dental industry. However, some limitations such as low stability and toxic compounds in the initiation systems have to be addressed for it to be applicable in dental composites.

Objective

In recent years the dental industry made progress in developing new restoratives based on dental composite materials. However, problems with self-cured (SC) materials based on 2K systems often lie within the initiation system. Low storage stability caused by instable silanes, high metal contents or explosive peroxides and toxic amines are just a few limitations. This work will attempt to overcome these limitations with two separate approaches.

In the first part of this work (Part A), a state-of-the-art initiation system consisting of a thiourea compound and a hydroperoxide should be **partially replaced**. Instead of the thiourea compound, a vitamin-C derivative should be synthesized and utilized. The vitamin-C derivative should show improved solubility in monomers compared to vitamin-C. Redox potentials should be determined of the new compound using cyclovoltammetry measurements. Thereafter, the reactivity of the optimized initiation system is to be investigated using polymerization temperature measurements and rheology/IR measurements. The thermomechanical properties and mechanical properties of cured polymer samples should be investigated using dynamical mechanical thermal analysis (DMTA) and tensile tests.

In the second part of this work (Part B), a state-of-the-art initiation system consisting of a thiourea compound and a hydroperoxide should be **fully replaced**. A new 2K radical polymerization system should be developed based on diboranes and copper compounds (diborane/Cu). The initial synthesis of new diborane compounds should broaden the scope of the investigated compounds. Electron paramagnetic resonance (EPR) spectroscopy and rheology/IR measurements should be utilized to investigate the mechanism of this new radical polymerization system. Detailed experiments with linear polymers should be conducted to understand important parameters of the diborane/Cu system.

Thereafter, the reactivity of the optimized initiation system should be investigated using polymerization temperature measurements and rheology/IR measurements. The thermomechanical properties and mechanical properties of cured polymer samples should be investigated using dynamical mechanical thermal analysis (DMTA) and tensile tests.

Part A: Vitamin C as a Reducing Agent in Redox Polymerization

1. State of the Art

Dimethacrylate-based two-component materials, commonly utilized in dentistry, comprise an organic matrix containing dimethacrylates, an initiator system, and various additives, alongside inorganic fillers like silanized glass, mixed oxides, and ytterbium fluoride.[50] These materials serve diverse dental applications, including self-adhesive resin cements, luting composites, dual-cure flowable composites, and temporary products.[15, 17-20]

They mainly fall into two categories: self-cure (SC) and dual-cure (DC). SC materials initiate polymerization through redox free-radical reactions when their two components are mixed. This reaction involves an oxidizing agent in the first component reacting with a reducing agent in the second component to generate radicals that initiate dimethacrylate polymerization.[15]

One commonly used initiator system for redox free-radical polymerization in two-component dental materials is the combination of benzoyl peroxide (BPO) and tertiary aromatic amine (Figure 14).[22, 23]

BPO   ***tert*-amine**
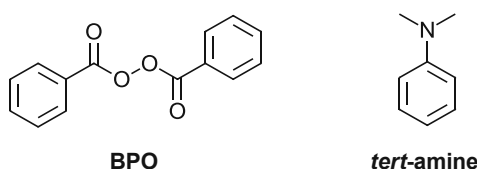
Figure 14: Structure of BPO and a tertiary amine used as 2K redox initiators.

However, this system has a significant drawback: the instability of BPO necessitates the storage of dental materials containing it in a refrigerator.[22-24] As a result, the dental industry actively sought out alternative redox initiator systems that would allow for the development of materials capable of being stored at room temperature. Hydroperoxides, such as cumene hydroperoxide (CHP) or amyl hydroperoxide, have now become the primary oxidizing agents used in SC dental materials. These hydroperoxides exhibit significantly improved stability when compared to dibenzoyl peroxide (BPO), making it feasible to store materials containing them at room temperature.[20] However, a challenge arose as hydroperoxides do not readily react with tertiary aromatic amines, necessitating the exploration of alternative reducing agents to facilitate the polymerization process.

1.1. Reference Substances and Mechanism

In this particular context, a broad spectrum of reducing agents has been examined regarding their applicability in dental materials. Investigative efforts have been focused on redox initiator systems that revolve around derivatives derived from barbituric acid, sulfinic acid, and thiourea and their derivatives (Figure 15).[51-55]

Barbituric acid   **Sulfinate**   **Thiourea**
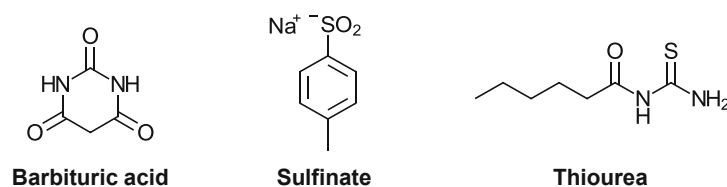
Figure 15: Exemplary structures of barbituric acid, a sulfinate and a thiourea compound.

Differently *N*-substituted barbituric acid derivatives are reported as reactive reducing agents with peroxide solutions via copper catalysis. They show good solubility in dental resins and depending on the applied concentration led to good working times of the investigated 2K systems.[56-58]

Furthermore, differently substituted sodium sulfonates are reported to act as effective reducing agents with copper and manganese acetates and acetylacetonates. They are highly reactive in difunctional methacrylate resins, however, they come with the drawback of necessitating high amounts of metal salts for a sufficient reactivity. Oftentimes, manganese acetylacetonate is used in concentrations up to 2 w%. Also, these initiation systems can lead to very strong discoloration of the final polymer to yellow or even dark brown.[59]

The mechanism of the reduction of barbituric acids with peroxides and sulfinates with metals are depicted below in Figure 16.

(1)

(2)

$$Ox \; + \; RSO_2^- \longrightarrow Ox^{\cdot -} \; + \; RSO_2^{\cdot}$$

Ox = Cu(II), Mn(III)
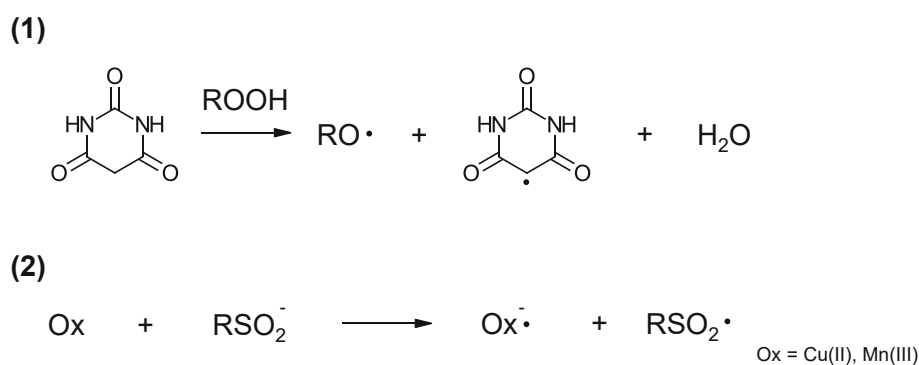
Figure 16: **(1):** Mechanism of the reduction of barbituric acid with a peroxide for the generation of radicals. **(2)** Mechanism of the reduction of a sulfinate with a metal (Cu(II) or Mn(III)) for the generation of radicals.[56, 59, 60]

As thiourea-based reducing agents are very oxygen stable and have very good reducing properties in the CHP based redox systems, they are under current investigation.[20] A thiourea based initiation system will be also used as reference system for all further experiments in this work.

It was found that the redox reaction between CHP and the reducing agent is highly facilitated by the addition of copper salts such as $Cu(acac)_2$ as a catalytic compound. This leads to the following mechanism shown in Figure 17. The Cu species and the thiourea compound are dissolved in the same formulation as they are safe to store together, even though a small amount of unreactive thiourea radicals as well as Cu(I) are formed during that reaction. As soon as the formulation is mixed with the CHP containing formulation the redox cycle closes and CHP oxidizes Cu(I) back to Cu(II) while forming a RO-radical that is reactive enough to start the polymerization.
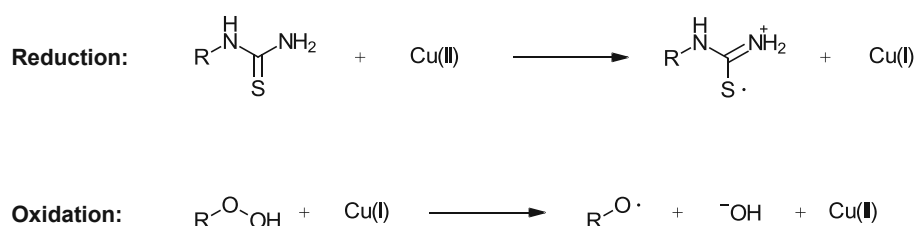
Figure 17: Reaction scheme of the redox reactions leading to initiating radicals. The reduction of Cu(II) to Cu(I) by the thiourea compound leads to unreactive thiourea radicals. The oxidation of Cu(I) to Cu(II) by CHP leads to reactive RO-radicals.

It was shown that thiourea compounds further react as a reducing agent with VO_2^+, Fe^{3+}, Ag^{3+} and other oxidants such as H_2O_2 and $S_2O_8^{2-}$. Similar redox initiation systems were used to produce polymers from acrylonitrile and vinyl monomers. [61, 62] The very convenient reducing properties of this compound class led to further investigations and acylthiourea compounds now find high demand in dental formulations.[63, 64] The success of such compounds further led to the development of oxidizing agents that can be applied with acylthioureas.[65]

Nonetheless, a significant drawback associated with this curing system is the undesirable bitter taste of the thiourea compound, which is unsuitable for dental purposes. Consequently, alternative reducing agents are being sought and studied.[20]

1.2.   Properties of Vitamin C

A potential substitute for thiourea compounds in this initiation system is vitamin C (VitC). Existing literature indicates that vitamin C can serve as a suitable reducing agent in redox initiation systems. These systems typically consist of a (hydro)peroxide, a copper catalyst, and vitamin C, which collectively facilitate the polymerization of methacrylates.[33, 66, 67] The structure of VitC is shown in Figure 18.
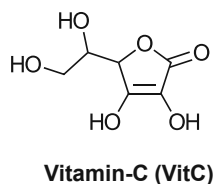
Vitamin-C (VitC)

Figure 18: Chemical structure of vitamin-C (VitC).

Nevertheless, the selection of monomers is constrained due to the highly polar nature of VitC. Typically, polar monomers like hydroxyethylmethacrylate (HEMA) are the preferred choices. One approach to circumvent this limitation is by incorporating water into the formulation, which helps improve the solubility of VitC in less polar monomers.[33]

The use of VitC is already reported for 2K systems applying a redox initiation mechanism with CHP as oxidizing agent, Cu(acac)$_2$ as catalyst and VitC as reducing agent (Figure 19). The reduction as well as the oxidation reaction occur in the same way as with thiourea compounds (Figure 17).[33]
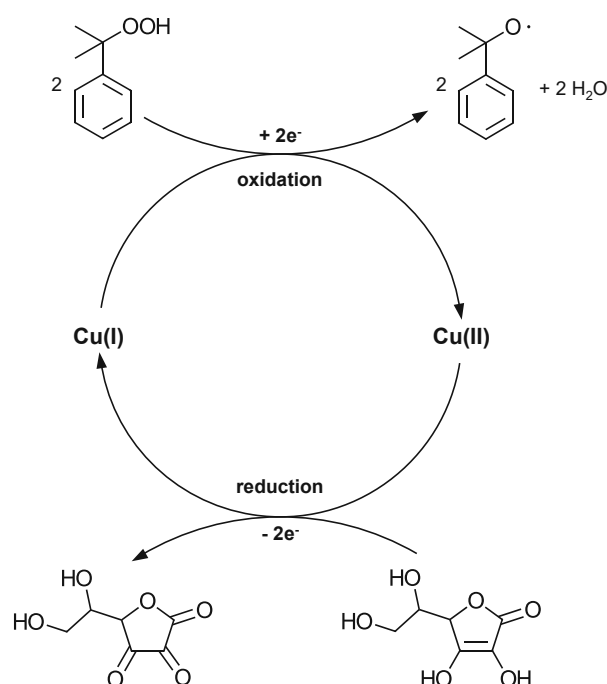
Figure 19: Redox initiation cycle using CHP (top) as the oxidizing agent, Cu(II) salts as the catalyst and vitamin C as the reducing agent.[33]

However, to achieve optimal polymer properties in the final product, it becomes essential to enhance the solubility of VitC in these specific monomers. Therefore, it is important to understand the mechanism of VitC reduction to not interfere with it during potential chemical modifications. Due to its resonance stabilized enediol next to the carbonyl it is a relatively strong acid with a pKa of 4.1. Furthermore, the hydroxy groups on the aliphatic sidechains can form a six-membered ring with the enediol hydroxy groups, further destabilizing them. These structural properties also lead to the ability to perform two single-electron transfers during reduction (Figure 20).[68]
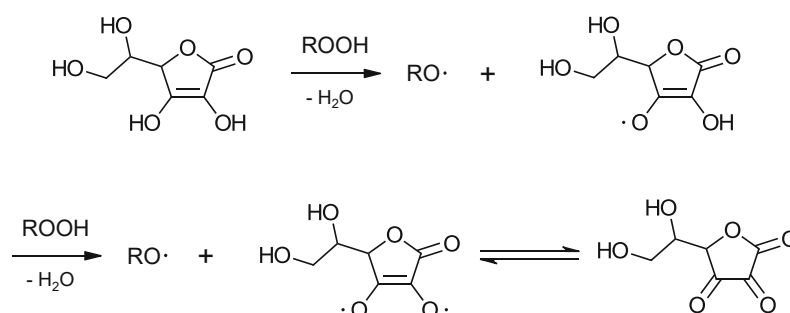
Figure 20: Mechanism of the reduction of VitC.[68]

As the aliphatic hydroxy groups are not participating in the reduction process, they are available for chemical reactions. There are commercial products such as ascorbyl stearate and

ascorbyl palmitate, however, the chains (C18, C16) are too long to facilitate the solubility in dental monomer mixtures and lead to more surfactant characteristics.[69]

2. Synthesis of VitC-1

For the purpose of a better solubility of vitamin C in apolar monomers, a modification of both aliphatic hydroxy groups via an esterification reaction will be attempted.
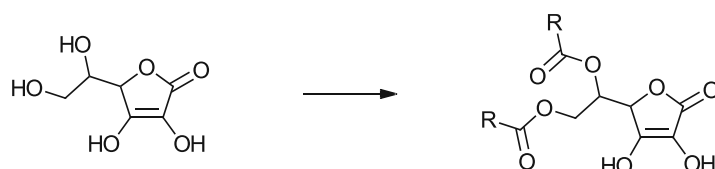
Figure 21: Scheme of the attempted modification of VitC that are conducted in this work.

The modified form of vitamin C will be subjected to examination in terms of its ability to dissolve in commonly used methacrylates, its effectiveness as reducing agent, the reactivity within a redox initiation system, and its impact on the (thermo)mechanical characteristics of the resulting polymer.

The synthesis of VitC-1 was planned in three steps: protection, esterification and deprotection. Literature reports the synthesis of similar structures following the same general synthetic pathway (Figure 22).[70]

Step 1: Protection
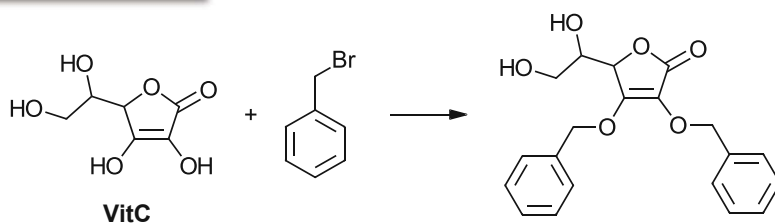
Step 2: Esterification
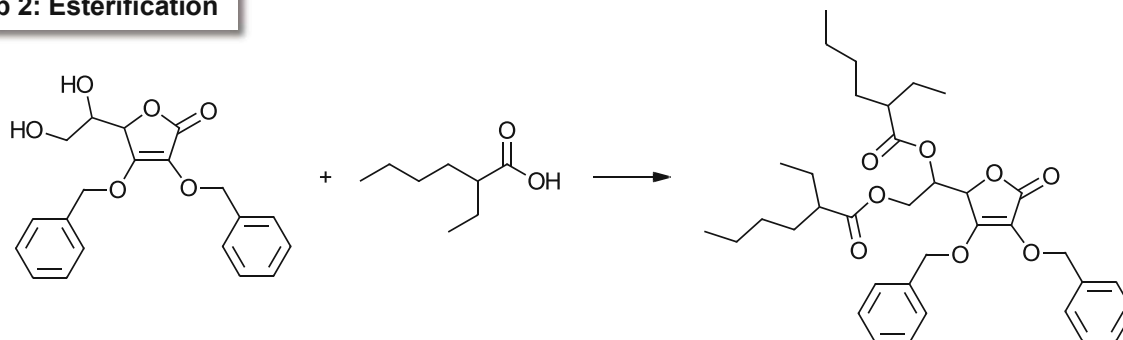
Step 3: Deprotection
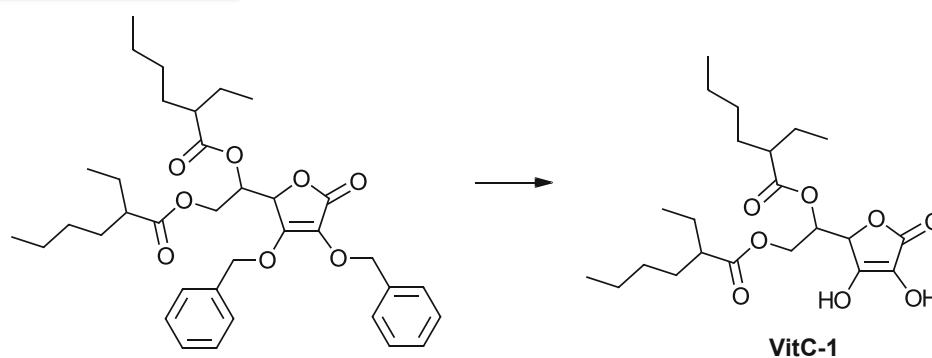
Figure 22: Synthetic pathway for the synthesis of VitC-1 starting with VitC. The first step involves a protection of the ene-diol hydroxygroups. The second step is an esterification reaction of the remaining aliphatic hydroxy groups. In the third step the benzyl ethers are removed selectively to yield the product compound VitC-1.

2.1. Synthesis of 3,4-bis(benzyloxy)-5-(1,2-dihydroxyethyl)-2,5-dihydrofuran-2-one (VitC-Bz)

The initial and very important first step in the modification of VitC is the selective protection of the hydroxy groups that are necessary for the reducing properties of vitamin-C. This was performed according to literature claiming the selective reaction of these hydroxy groups in basic conditions with benzylbromide (Figure 23).[71]
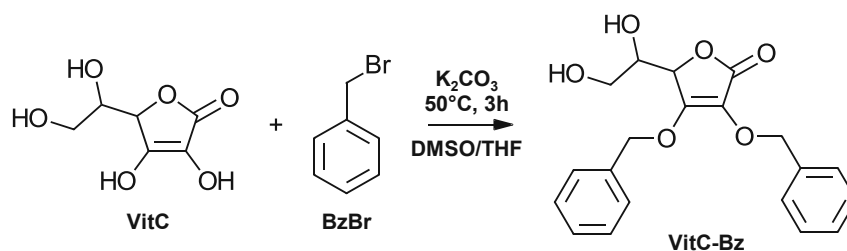
Figure 23: Reaction of VitC with benzylbromide to protect the ene-diol hydroxy groups selectively.

The weak base K_2CO_3 is enough to deprotonate the more acidic ring hydroxy groups and facilitate the selective substitution on the benzyl bromide resulting in the formed ether bond. The product was purified via column chromatography to ensure a pure product for the further reaction. The formation of the ether was confirmed via ^{1}H- and ^{13}C-NMR (Figure 24).

The loss in yield (yield: 60% of theory) is explained by less selectivity of the reaction than claimed in literature and the formation of mono-substituted side product, which was gotten rid of during column chromatography. The ^{1}H-NMR shows complete conversion of the hydroxy groups and the benzyl moiety that is present in VitC-Bz.
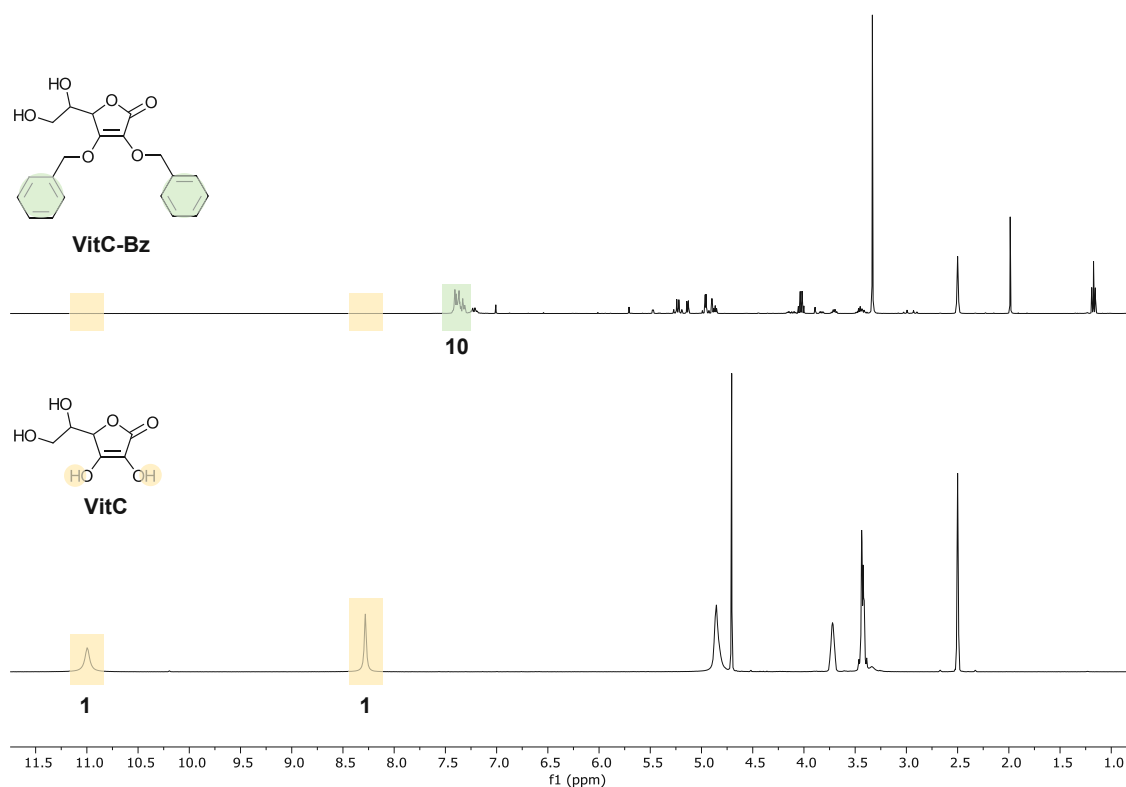
Figure 24: ^{1}H-NMR spectra of VitC starting material and the product VitC-Bz. The protected hydroxyl protons are highlighted as well as the benzyl protecting group.

2.2. Synthesis of 1-[3,4-bis(benzyloxy)-5-oxo-2,5-dihydro-2-furyl]-2-(1-ethylpentyl-carbonyloxy)ethyl-2-ethylhexanoate (VitC-Bz-M)

After the protection of the ring hydroxy groups, the next step was the esterification of the aliphatic hydroxy groups that were not protected in the first step. Therefore, 2-ethylhexylacid (EHA) was chosen as an ideal aliphatic acid with an ethylhexyl side chain to enhance the solubility of the final product in hydrophobic environments. A Steglich-esterification using EDC and DMAP was chosen as a convenient method to perform this reaction.[71]
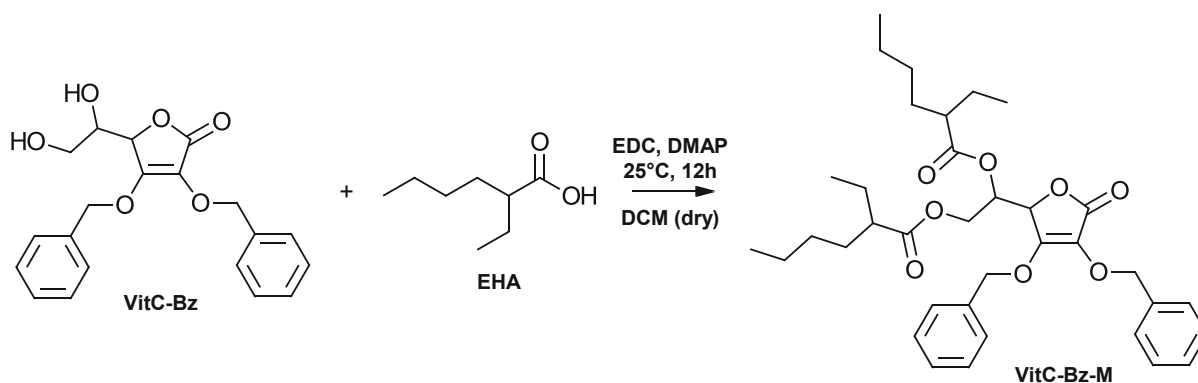
Figure 25: Steglich esterification of VitC-Bz with ethylhexylacid (EHA) to yield VitC-Bz-M.

31

First experiments showed that an enhancement of the yield was observed when 3 equivalents (instead of 2 according to literature[71]) of EHA and EDC were added to reaction and it was stirred at 0 °C to room temperature over the course of 12 h. A clear change in color from orange to yellow was seen during the reaction. The crude product was be purified via column chromatography. However, residual acid could not be removed in the column which led to further purification under high vacuum. The final product was obtained with a yield of 70% as a yellow oil and was confirmed via ^{1}H-NMR (Figure 26).
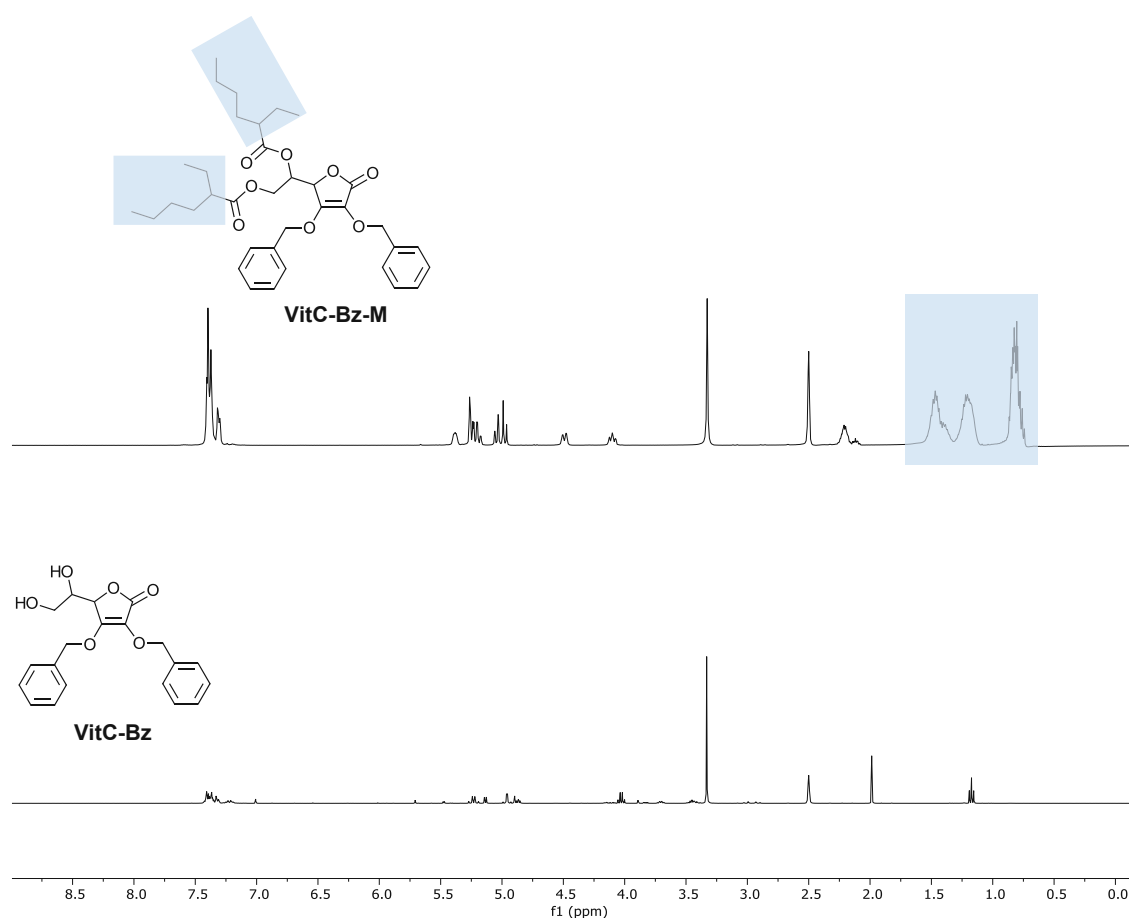
Figure 26: ^{1}H-NMR spectra of VitC-Bz starting material and the product VitC-Bz-M. The aliphatic protons of the ethylhexyl moiety are highlighted.

The purity of VitC-Bz-M was even higher than the starting material and was isolated in high yield. The highlighted sections show the aliphatic protons of the side chains, while no left-over acidic protons of residual EHA were visible anymore.

2.3. Synthesis of 1-(3,4-dihydroxy-2-oxo-5-furyl)-2-(1-ethylpentylcarbonyloxy)-ethyl-2-ethylhexanoate (VitC-1)

The final step of the modification of VitC is the selective deprotection of the benzyl ethers without cleaving the previously formed ester bonds. This reaction was performed according to literature, using an autoclave vessel with Pd/C and H_2 (Figure 27).[70]
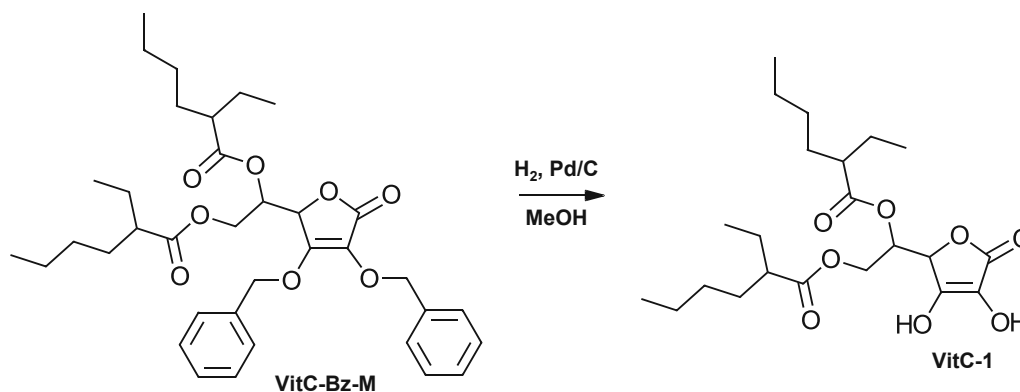
Figure 27: Catalytic hydration of the benzyl protecting groups on VitC-Bz-M, yielding the final product VitC-1.

Literature claims a selective reduction of the ethers without touching the ester using hydrogen gas with palladium on carbon as a catalyst. However, the optimum pressure of H_2-gas and also the reaction time in the autoclave vessel had to be determined. After optimization of these parameters with respect to the yield, a colorless oil was obtained after purification via column chromatography in 54% yield. The formation of the hydroxy groups was followed via ^{1}H-NMR (Figure 28).
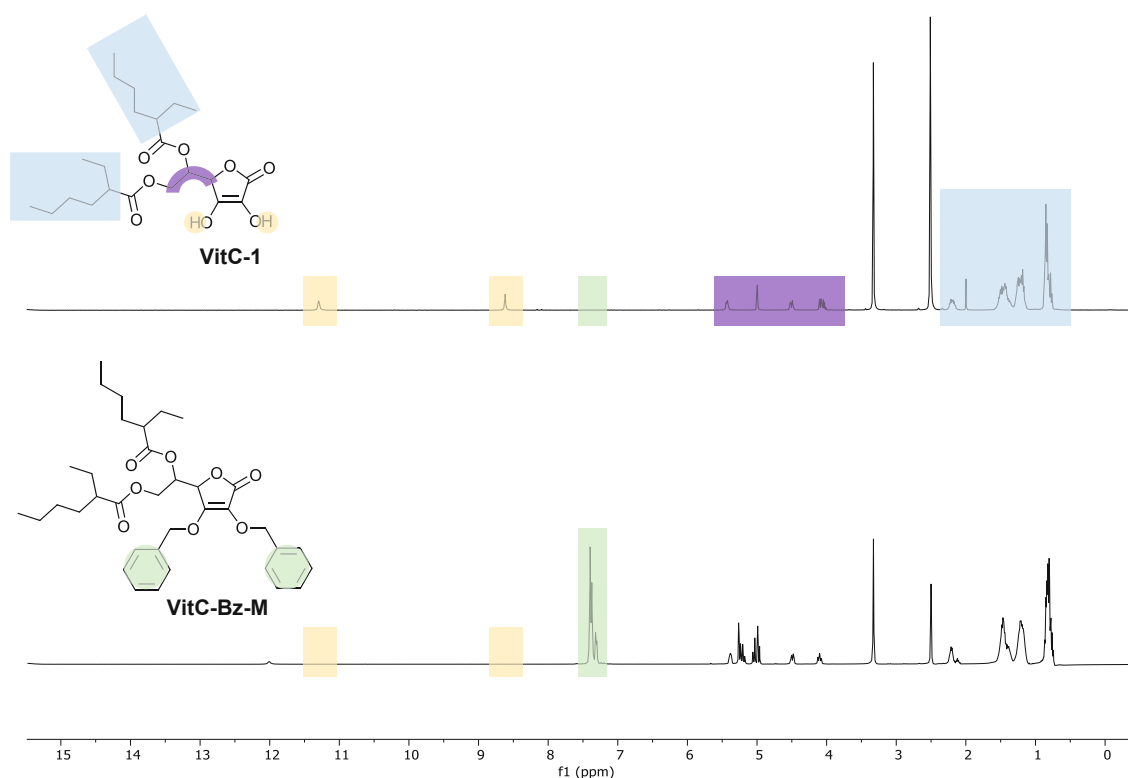
Figure 28: ¹H-NMR spectra of VitC-Bz-M starting material (bottom) and VitC-1 product (top). The vanishing of the benzyl protecting group (green) is clearly visible as well as the formation of the acidic hydroxyl protons of VitC-1 (yellow). Also, the aliphatic region of the product is marked in blue and the remaining proton signals in purple.

The final product shows all aliphatic peaks of the ethyl hexyl modification (blue), the aliphatic region of the VitC structure (purple) and the very important acidic protons (yellow). In green the benzyl protection groups are highlighted, and it can be seen that in the final product VitC-1, no benzyl moieties are present anymore. Furthermore, the molecular mass of the final product VitC-1 was confirmed via HPLC-MS with a m/z of 427 (Figure 29).
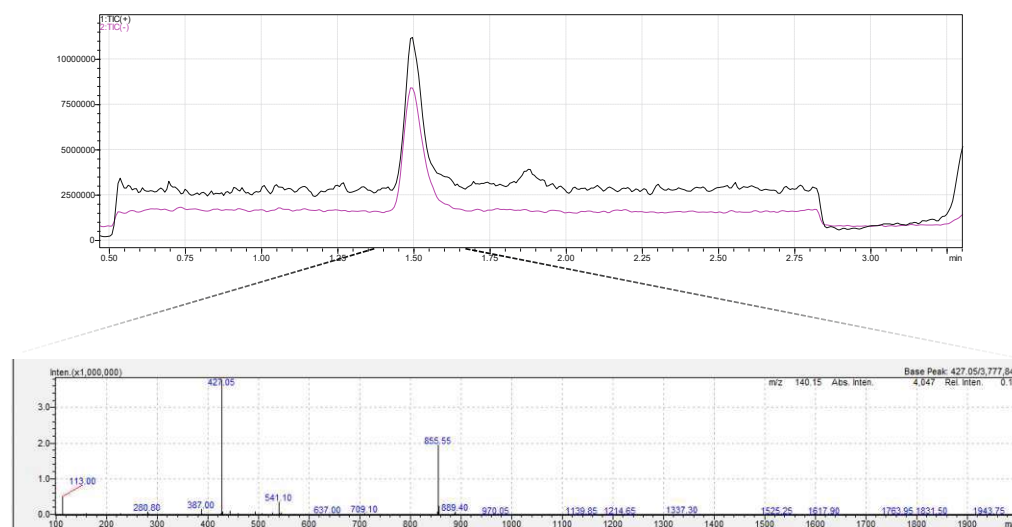
Figure 29: HPLC-MS measurement of VitC-1 showing one peak and an expected m/z of 427 and the x2 M peak at 855 m/z.

34

3. Cyclovoltammetry

A main characteristic of redox initiators is the redox potential of such, as the redox reaction that leads to the formation of radicals is highly dependent on it. To evaluate these electrochemical properties, cyclovoltammetry (CV) is a convenient tool. In this study, the newly synthesized VitC-1 as well as VitC were investigated. Furthermore, also oxidizing agents (hydroperoxides) and the catalyst ($Cu(acac)_2$) were evaluated.

In advance of each measurement, 5 mg of the analyte was weighed out and dissolved in dry acetonitrile (ACN) with 0.1 M tetra-butylammonium hexafluorophosphate as electrolyte. To evaluate the oxidation/reduction potential of the target molecule, a standard measurement was performed with ferrocene in advance. The standard potential (E_{0-exp}) of ferrocene was experimentally determined using Equation 4 and compared to a literature value.[72] The difference between the determined value and the literature value was added as a factor to all the other measurements as correction.

Equation 1: Determination of the experimentally found standard potential of ferrocene in ACN.

$$E_{0-exp} = \frac{E_{red} + E_{ox}}{2}$$

The values for E_{red} and E_{ox} can be retrieved from the respective measurement as shown in Figure 30. The potential at the positive peak when going from left to right marks the oxidation potential and the potential at the negative peak when going from right to left marks the reduction potential.
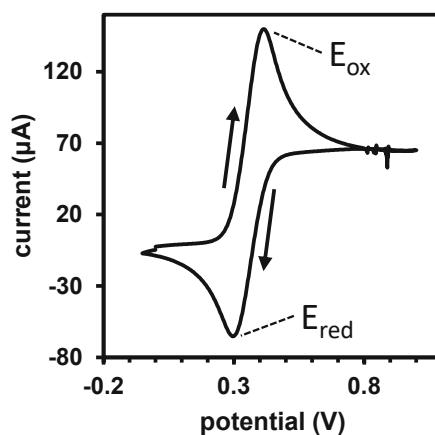
Figure 30: Voltammogram of ferrocene in ACN with marked oxidation potential (E_{ox}) and reduction potential (E_{red}) as well as the direction of the potential cycle.

The determination of the reduction potential as well as the oxidation potential was performed for every redox active compound used in the following chapter, including the reducing agents VitC, VitC-1, PalmVitC (no CV data due to poor solubility), a thiourea derivative (TU-Ref), the catalyst Cu(acac)$_2$ and the oxidation agents *tert*-butylhydroperoxide (*t*BuHP) and CHP. Some compounds do not show both potentials, since irreversible oxidations lead to the absence of a reduction potential and *vice versa*. In Figure 31 the cyclic voltammograms of VitC-1 and VitC are shown in a direct comparison to evaluate if the redox potentials of the compound have changed after the modification.
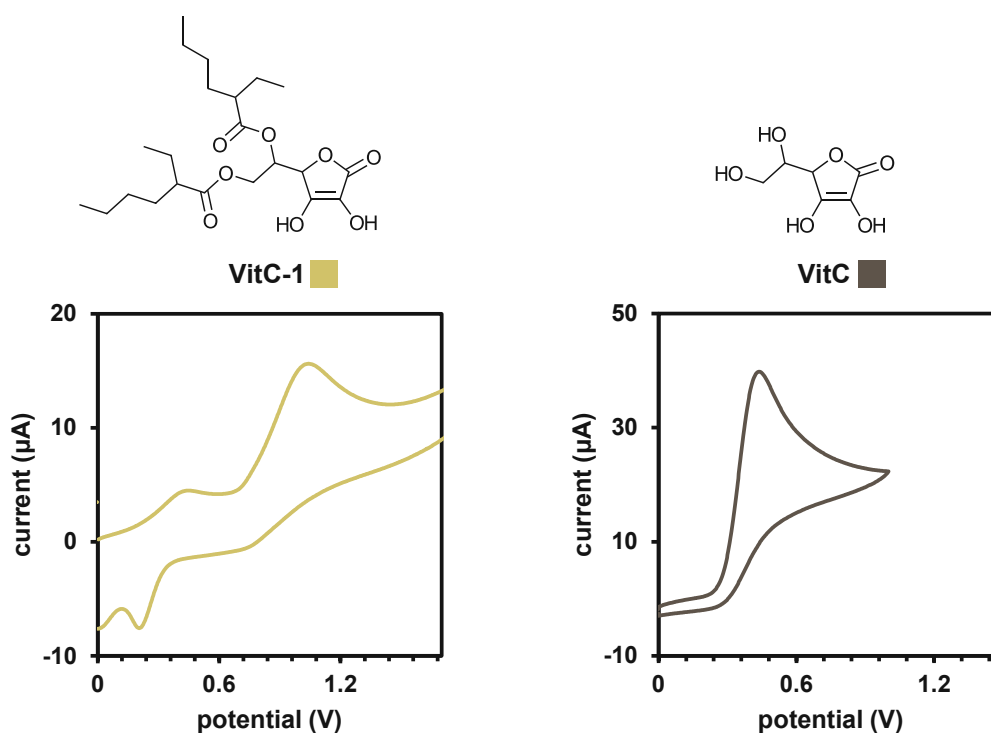
Figure 31: Chemical structures of VitC-1 (●) and VitC (●) in a side-by-side comparison as well as their cyclic voltammograms.

For the reducing agents VitC, VitC-1 as well as the reference reducing agent TU-Ref, the oxidation potential is the crucial parameter which determines the reactivity to undergo a redox reaction with an oxidizing agent. The oxidation potential marks the potential at which the respective compound is oxidized.

It is seen in the voltammogram of VitC that the oxidation of VitC is permanent and is not reversed in the measurement as no reduction potential is seen. Furthermore, it was shown that with every cycle the intensity of the peak decreases (the first cycle is shown in the diagram), indicating less available molecules for oxidation which is in good agreement with literature.[73] The same effect was shown for VitC-1 with the exception of a small peak at 0.2 V

which could indicate a reducing potential of VitC-1. Besides that, it is clearly seen that the oxidation potential of VitC-1 is shifted to higher potentials. The shift could be caused by an interaction of the newly formed ester bonds, facilitating the formation of hydrogen bridges (Figure 32).

hydrogen bonding
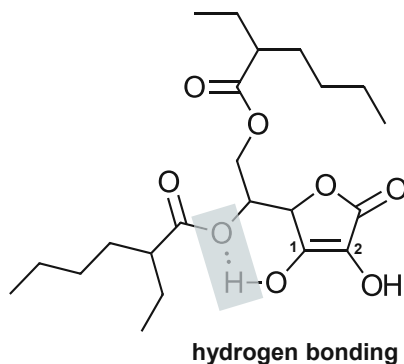
Figure 32: Possible interaction of the newly formed ester bonds with the hydroxygroups, causing a shift in the oxidation potential of VitC-1.

The proton on C1 is more acidic than on the hydroxy group bound to C2.[68] Now, that the C1 hydroxy proton can interact with the ester bond, a six-membered ring is formed, tending to stabilize the structure and therefore making it less prone to be oxidized. It can be seen in the voltammogram that there is a small peak at 0.49 V for VitC-1, indicating an oxidation of a VitC-like structure (E_{ox}=0.48 V), however, the main peak comes much later at 1.09 V (Table 1).[68]

Table 1: Oxidation potentials (E_{ox}) of VitC-1 and VitC determined via cyclovoltammetry.

VitC-1 E_{Ox} 1 (V)	0.49
VitC-1 E_{Ox} 2 (V)	1.09
VitC E_{Ox} (V)	0.48

Furthermore, the cyclic voltammograms of the oxidizing agents (CHP and tBuHP) as well as the catalyst (Cu(acac)$_2$) and the reference thiourea compound (TU-Ref) were measured and are depicted below in Figure 33.
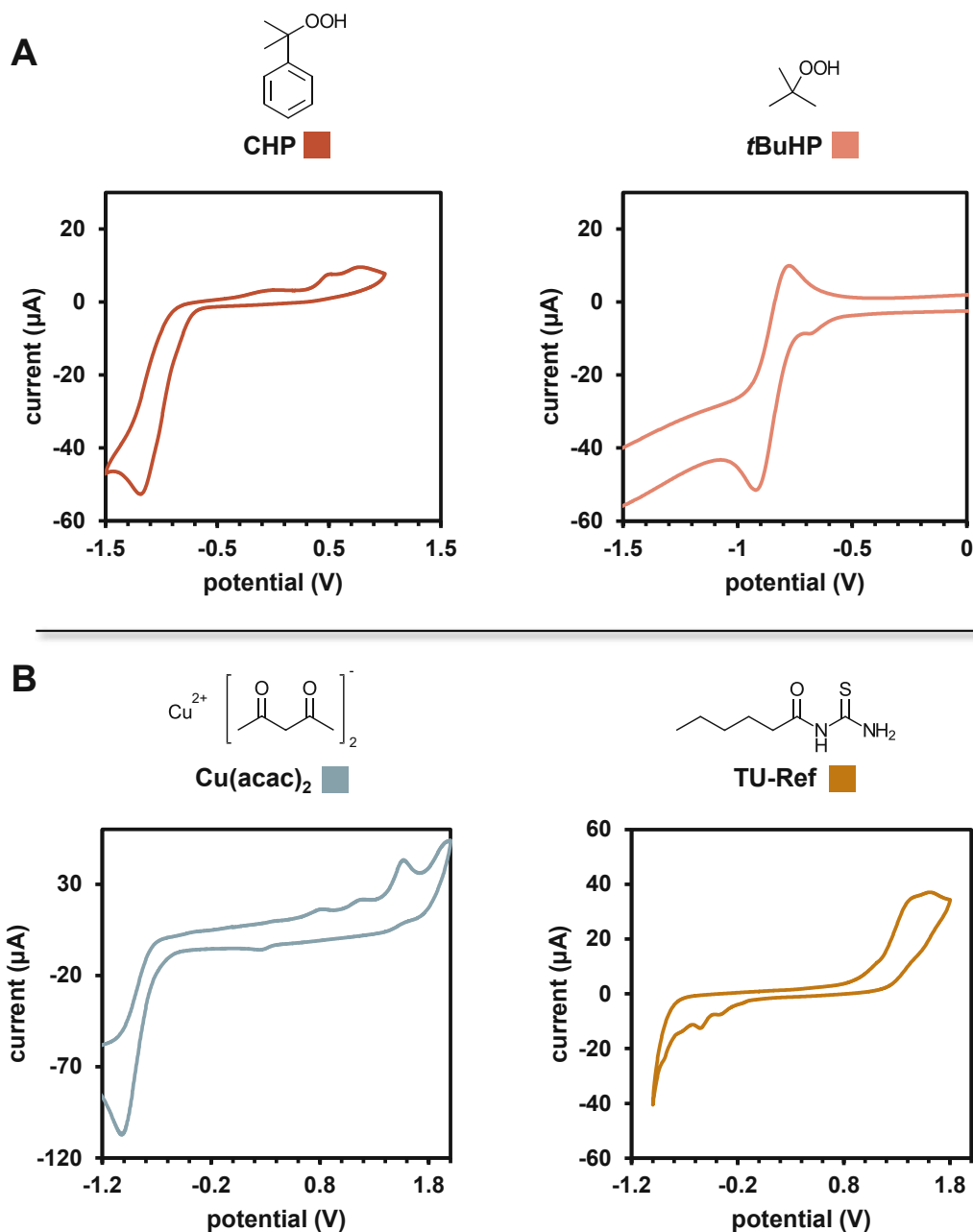
Figure 33: A: Chemical structures of the oxidizing agents CHP and *t*BuHP as well as their cyclic voltammograms. B: Chemical structures of the catalyst Cu(acac)$_2$ and the reference reducing agent TU-Ref as well as their cyclic voltammograms.

The evaluation of the shown voltammograms led to the calculation of all the reducing potentials (E_{Red}) and oxidation potentials (E_{Ox}) of the compounds that can be involved in a redox initiating cycle. Typically, the reducing agent is oxidized by reducing the Cu(acac)$_2$ catalyst, then the Cu(acac)$_2$ is reoxidized by the reduction of the oxidizing agent. For the reducing agents E_{Ox} is depicted and for the oxidizing agents E_{Red} is depicted in Table 2 calculated using Equation 1.

Table 2: Reduction potentials (E_{Red}) and oxidation potentials (E_{Ox}) for all reducing and oxidizing agents investigated in this study.

	E_{Red} (V)	E_{Ox} (V)
CHP	-1.15	-
*t*BuHP	-0.88	-
Cu(acac)$_2$	-0.97	1.62
TU-Ref	-	1.65
VitC-1	-	1.09
VitC	-	0.48

The bigger the gap between E_{Red} and E_{Ox} the likelier the electron transfer from the HOMO of the reducing agent to the LUMO of the oxidizing agent. The driving force for this thermodynamically favorable electron transfer is the difference in energy levels.[74] However, in some cases if the gap is too big, the electron transfer can be hindered, which is why the catalyst Cu(acac)$_2$ is so important in this redox cycle. According to the measured potentials, TU-Ref is slightly more reactive towards reducing Cu(II) to Cu(I) than VitC-1 and VitC. In the same way, CHP is more reactive towards oxidizing Cu(I) to Cu(II) than *t*BuHP.

It is shown that VitC-1 can readily reduce Cu(II) to Cu(I) with an E_{Ox} of 1.09 V and E_{Red} of -0.97 V. Cu(I) on the other hand is oxidized by CHP with E_{Ox} of 1.62 V and E_{Red} of -1.15 V. This redox cycle for the new reducing agent VitC-1 is depicted in Figure 34.

CHP

E_{red} = -1.15 V

E_{ox} = 1.62 V

Cu(I)

Cu(II)

E_{red} = -0.97 V

E_{ox} = 1.09 V
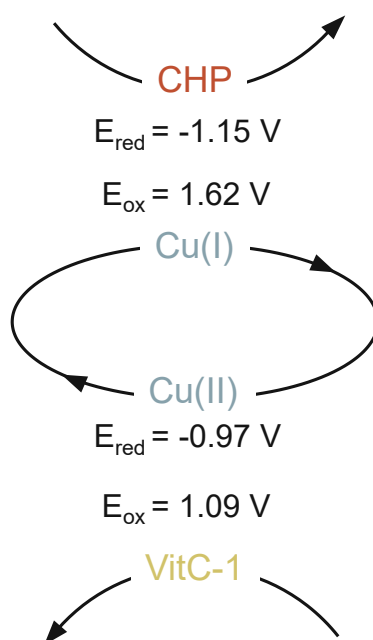
VitC-1

Figure 34: Complete redox initiation cycle applying the new VitC-1 reducing agent.

Summing up, these values are measured in solution and cannot be directly transferred to the situation in a monomer solution. However, the cyclic voltammograms give a very good estimation of the reactivity towards redox initiation for radical polymerization of the respective compounds. The observed data proved that the new VitC-1 reducing agent is suitable for application in such a redox initiation system and will be investigated in further chapters in detail.

4. Reactivity

The understanding of the reactivity of a redox initiation system is crucial in order to adjust important parameters in application such as the working time which is the time until the polymerization of the monomer mixture starts. In this study, the VitC-1 redox initiation system was characterized in the monomer mixture 3Mix, consisting of the monomers D3MA, UDMA and BisGMA (20:40:40wt%) (Figure 35).
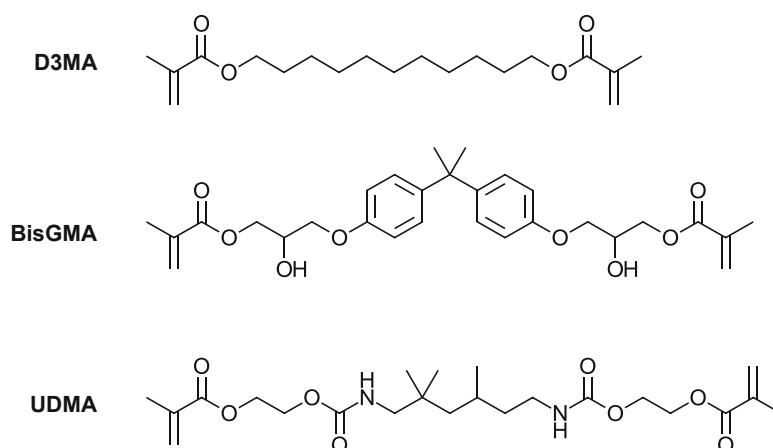
Figure 35: Chemical structure of the monomer mixture 3Mix (D3MA, BisGMA, UDMA)

4.1. Solubility

An important part of developing a new redox initiation system is the solubility of the newly synthesized reducing agent VitC-1 in the monomer mixture 3Mix. The solubility of VitC-1 in multiple concentrations was investigated and compared to similar compounds such as VitC and PalmVitC (Figure 36).
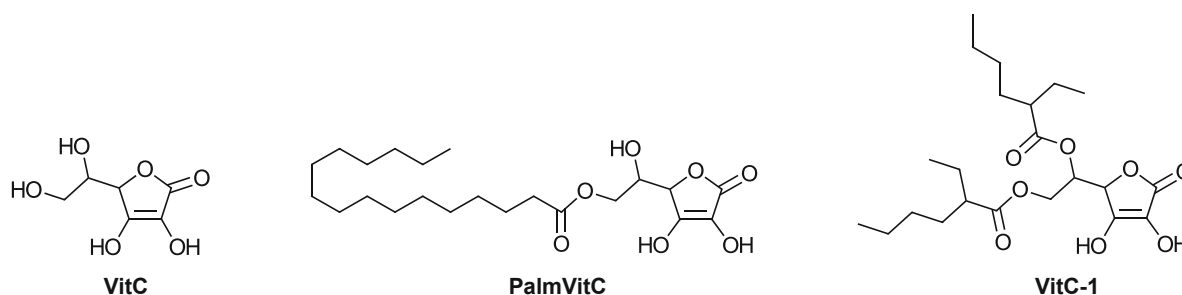
Figure 36: Chemical structures of VitC, PalmVitC and VitC-1. The compounds were investigated regarding their solubility in 3Mix.

VitC as it is a very polar structure does not show any solubility in the apolar monomer mixture 3Mix. However, even PalmVitC, exhibiting a C16 modification on one of the aliphatic hydroxy groups does only show limited solubility, leaving behind insoluble pieces even at low

concentrations (0.5 mol%). It could be shown that the ethylhexyl moieties of VitC-1 pushed the polarity into the perfect range for a good solubility in 3Mix and the new reducing agent is soluble in low concentrations (0.5 mol%) and up to 5 mol%.

4.2.   Polymerization Temperature Measurements

The quantification of the reactivity of the 2K system derived from VitC-1 and CHP was performed using polymerization temperature measurements to capture the amount of heat that is released during the polymerization reaction. However, reactivity is highly depending on the absolute amount of bulk formulation that is used in the experiment.[75, 76] In this study, 1.8 g of total formulation was used and the polymerization temperature was measured over time. The temperature recording in the bulk formulation starts directly after mixing the two formulations. In Figure 37 a schematic progression of such a measurement is depicted, highlighting all important characteristics.
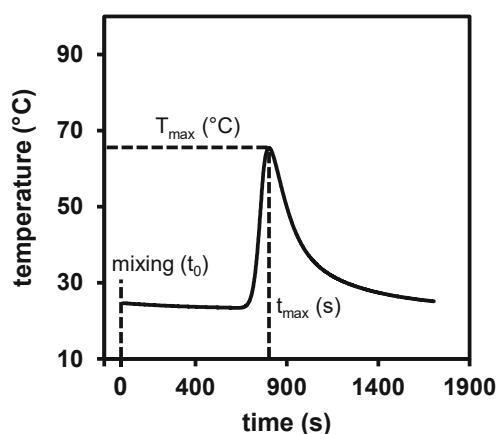
Figure 37: Schematic polymerization temperature measurement, highlighting important values T_{max} (highest temperature during polymerization and t_{max} (time until the highest temperature during polymerization is reached).

The most important values derived from these measurements are the highest temperature during polymerization (T_{max}) and the time until the highest temperature during polymerization is reached (t_{max}). T_{max} is a characteristic how many functional groups react at once and is therefore a value close to a polymerization rate. On the other hand, t_{max} is a very good indicator for the working time and reflects well how long the redox initiation system needs to yield enough reactive radicals to start the polymerization chain reaction.

4.2.1. VitC-1/Cu(acac)$_2$/CHP

In this basic study the new VitC-1 reducing agent was evaluated regarding its reactivity using polymerization temperature measurements. For each measurement, two separate formulations were prepared: a reducing formulation (F-red) and an oxidizing formulation (F-ox). The F-red contains the monomer mixture 3Mix as well as the catalyst Cu(acac)$_2$ and the reducing agent VitC-1. The oxidizing formulations contains 3Mix and the oxidizing agent CHP. After preparation of the formulations, the two formulations were mixed in a 1:1 w%:w% (0.9 g:0.9 g) ratio and the polymerization temperature measurement was started immediately. The structures of the respective compounds are shown in Figure 38.
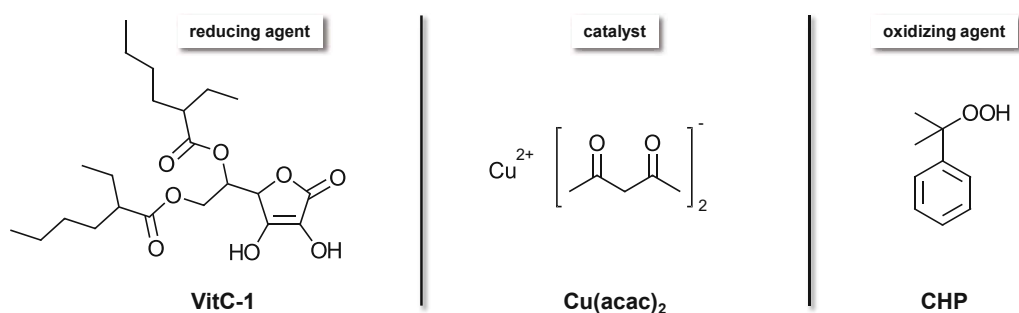
Figure 38: Chemical structure of the reducing agent VitC-1, the catalyst Cu(acac)$_2$ and the oxidizing agent CHP.

The formulations for the polymerization temperature measurements were prepared according to Table 3. The concentration of the copper catalyst Cu(acac)$_2$ was varied (0.1mol% and 0.01mol%).

Table 3: Formulations prepared for polymerization temperature measurements to characterize the reactivity of the polymerization reaction initiated by VitC-1, Cu(acac)$_2$ and CHP in 3Mix.

	F-red	F-ox
VitC-1 (mol%)	5	-
Cu(acac)$_2$ (mol%)	0.1 / 0.01	-
CHP (mol%)	-	11.5
3Mix (mol%)	94.9 / 94.99	88.5

The resulting polymerization temperature measurements are depicted below in Figure 39.

0.1 mol% Cu(acac)$_2$, CHP, VitC-1   **0.01 mol% Cu(acac)$_2$, CHP, VitC-1**

Figure 39: Polymerization temperature measurements of the polymerization of 3Mix, using VitC-1 as the reducing agent, and CHP as the oxidizing agent. The concentration of the catalyst Cu(acac)$_2$ was varied from 0.1 mol% (●) to 0.01 mol% (●).

The influence of the catalyst amount is clearly visible at the start of the polymerization. The higher catalyst amount, the faster the polymerization starts and also the more double bonds are polymerized in the same amount of time (higher T_{max}). With 0.1 mol% Cu(acac)$_2$ the polymerization starts almost immediately after mixing the formulations, which shows that even though Cu(acac)$_2$ reacts catalytically for the theoretical redox reaction, the absolute amount of the compound plays a crucial role in the bulk polymerization since the probability of meeting a redox partner is much higher, when using a higher amount of catalyst. In Table 4 the characteristic values for the polymerizations are shown. The evaluation of the double bond conversion was performed in a later chapter using the rheology/IR method.

Table 4: Characteristic values derived from the polymerization temperature measurement using 0.1 mol% or 0.01 mol% Cu(acac)$_2$ with CHP and VitC-1 in 3Mix.

	T_{max} (°C)	t_{max} (s)
0.1mol% Cu(acac)$_2$	83	20
0.01mol% Cu(acac)$_2$	64	54

With both Cu(acac)$_2$ concentrations the tail-out of the polymerization is quite long lasting up to 800 s. However, it is seen that the soluble VitC-1 reducing agent is able to reduce the Cu(II) catalyst effectively and participate in the redox reaction as it was expected, leading to a polymerization of 3Mix with $t_{max} < 60s$ for both catalyst concentrations.

4.2.2. VitC-1/Cu(acac)$_2$/CHP vs. State of the Art

In polymerization temperature measurements the reactivity of the newly synthesized reducing agent VitC-1 was compared to the state-of-the-art reducing agent (TU-Ref) used for similar formulations in industrial applications.[63, 64] Their structures are depicted below in Figure 40.
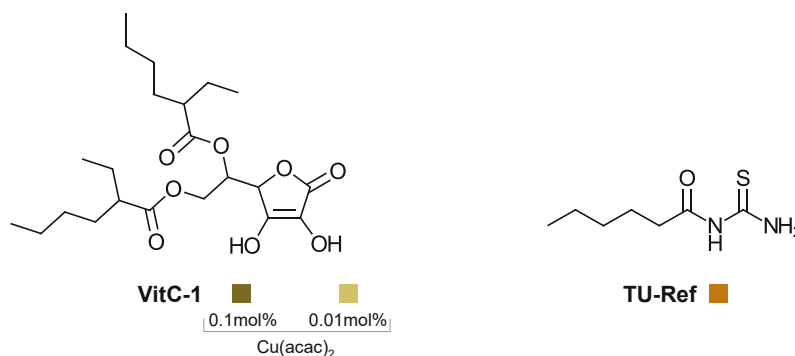
Figure 40: Chemical structure of VitC-1 and the state-of-the-art reducing agent TU-Ref. VitC-1 was investigated using two different concentrations of Cu(acac)$_2$ catalyst.

The formulations were prepared according to literature, using concentrations of the oxidizing agent, reducing agent and catalyst similar to industrial applications.[63, 64] (Table 5)

Table 5: Formulations prepared for polymerization temperature measurements to characterize the reactivity of the polymerization reaction initiated by VitC-1, Cu(acac)$_2$ and CHP in 3Mix and the reference TU-Ref.

	F-red (0.1)	F-red (0.01)	F-red (ref)	F-ox
VitC-1 (mol%)	5	5	-	-
TU-Ref (mol%)	-	-	5	-
Cu(acac)$_2$ (mol%)	0.1	0.01	0.01	-
CHP (mol%)	-	-	-	11.5
3Mix (mol%)	94.9	94.99	94.99	88.5

In the following Figure 41 the reactivity of the VitC-1 initiating system is compared with the reference initiation system using TU-Ref, Cu(acac)$_2$ and CHP.

0.1 mol% Cu(acac)$_2$, CHP, VitC-1   **0.01 mol% Cu(acac)$_2$, CHP, VitC-1**   **0.01 mol% Cu(acac)$_2$, CHP, TU-Ref**
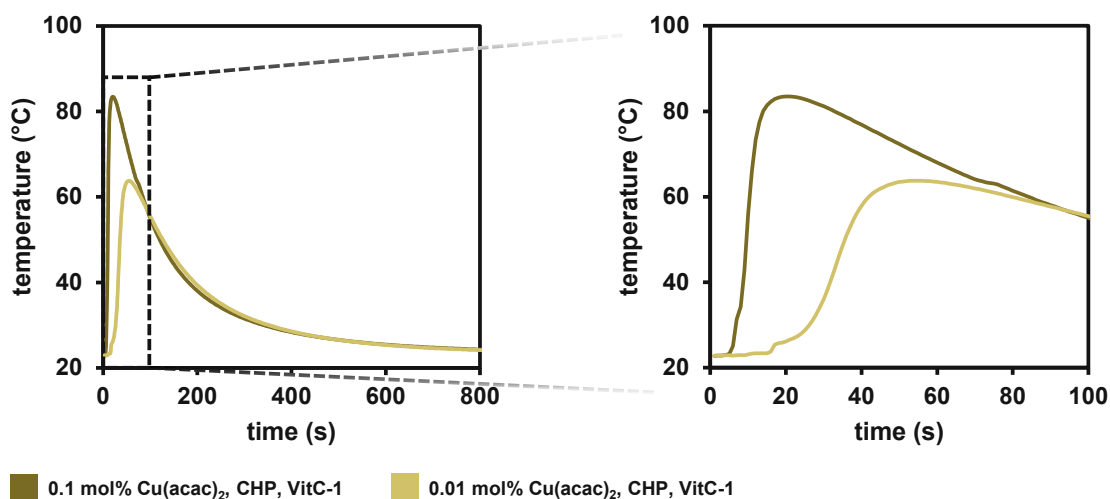
Figure 41: Polymerization temperature measurements of the polymerization of 3Mix, using VitC-1 as the reducing agent, and CHP as the oxidizing agent. The concentration of the catalyst Cu(acac)$_2$ was varied from 0.1 mol% (●) to 0.01 mol% (●). The reference initiation system using Cu(acac)$_2$, CHP and TU-Ref is depicted as well (●).

The polymerizations initiated with VitC-1 show a very high reactivity compared to the reference TU-Ref. The t_{max} is significantly shorter for both measurements with VitC-1 as reducing agent (Table 6). This indicates a very reactive nature of the reducing agent, leading to enough radicals very fast to start the polymerization. However, the maximum temperature is significantly higher for the reference TU-Ref. This may be explained by a possible oxygen inhibition reaction of the VitC-1 reducing agent. VitC-1 is highly reactive, which means it also reacts with any dissolved O$_2$ in the formulation and over time less radicals are generated in total because of the formation of unreactive peroxy radicals. Furthermore, the presence of the Cu(acac)$_2$ catalyst also catalyzes oxidation of VitC-1 with O$_2$, which is in good agreement with the observed reactivity compared to the thiourea reducing agent.[77, 78]

The reference TU-Ref however reacts slightly slower with the redox partner, however the generation of radicals is much more consistent in order to provide enough radicals for a polymerization temperature of 146 °C.

Table 6: Characteristic values derived from the polymerization temperature measurement using 0.1 mol% or 0.01 mol% Cu(acac)$_2$ with CHP and VitC-1 in 3Mix as well as the reference TU-Ref.

		T_{max} (°C)	t_{max} (s)
0.1mol%Cu(acac)$_2$	VitC-1	83	20
0.01mol%Cu(acac)$_2$	VitC-1	64	54
	TU-Ref	146	56

46

4.3. Rheology/IR

The reactivity of the newly developed initiation system based on VitC-1 was further investigated using the rheology/IR method. This characterization technique allows for simultaneous measurement of rheological data G' and G'', while measuring transmission MIR of the sample, tracking the double bond conversion via integration of the methacrylic C=C band at 6140 cm^{-1}. A total of 200 mg of formulation is used for the following measurements, having a 45 s mixing step in advance of the data recording to ensure a homogeneous mixture of the 2K system. Schematic measurements of G' and the DBC are shown in the following Figure 42 highlighting important characteristics G'$_{end}$, t$_{gel}$, DBC$_{end}$ and DBC$_{gel}$.
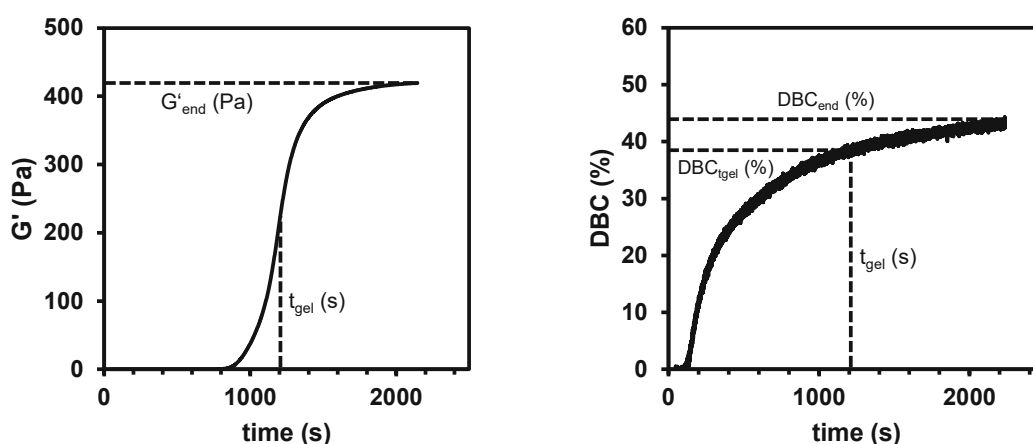
Figure 42: Schematic measurements of G' and the DBC are shown highlighting important characteristics G'$_{end}$, t$_{gel}$, DBC$_{end}$ and DBC$_{gel}$.

The information derived from the measurements of G' leads to evaluation of G'$_{end}$ referring to the mechanical strength of the polymer at the end of the polymerization. Another important value is t$_{gel}$ which is referred to as the gel time in these measurements. Often, the crosssection of G' and G'' are used to evaluate t$_{gel}$, however, for 2K systems it proved to be more reproducible to take the steepest increase of G' as a value for t$_{gel}$.[79] Furthermore, the DBC$_{gel}$ and DBC$_{end}$ derived from MIR measurements give information about the crosslinking density and the overall conversion at the gel point and at the end at a certain mechanical strength.

4.3.1. VitC-1/ Cu(acac)$_2$/CHP

In this basic study, the new VitC-1 reducing agent was evaluated regarding its reactivity towards polymerization of 3Mix using rheology/IR measurements. The chemical structures of the initiation system used are depicted below in Figure 43.
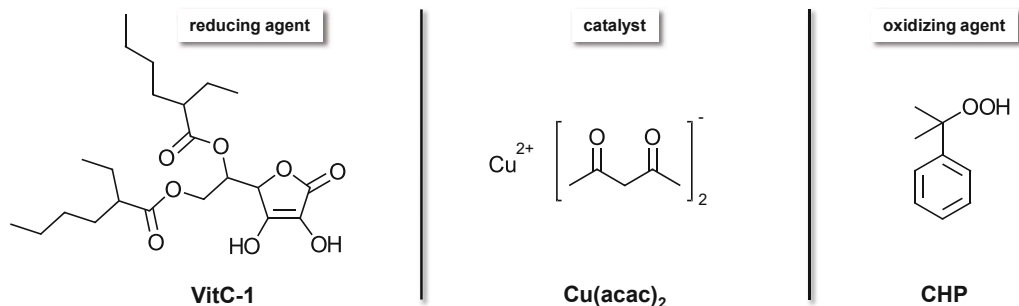
Figure 43: Chemical structure of the reducing agent VitC-1, the catalyst Cu(acac)$_2$ and the oxidizing agent CHP.

The formulations for the rheology/IR measurements were prepared according to Table 7. The concentration of the copper catalyst Cu(acac)$_2$ was varied in these measurements (0.1 mol% and 0.01 mol%)

Table 7: Formulations prepared for rheology/IR measurements to characterize the reactivity of the polymerization reaction initiated by VitC-1, Cu(acac)$_2$ and CHP in 3Mix.

	F-red	F-ox
VitC-1 (mol%)	5	-
Cu(acac)$_2$ (mol%)	0.1 / 0.01	-
CHP (mol%)	-	11.5
3Mix (mol%)	94.9 / 94.99	88.5

After homogenizing the 2K system for 45 s, G' and the DBC was recorded while the formulation starts to polymerize, depicted in Figure 44.

0.1 mol% Cu(acac)$_2$, CHP, VitC-1   0.01 mol% Cu(acac)$_2$, CHP, VitC-1
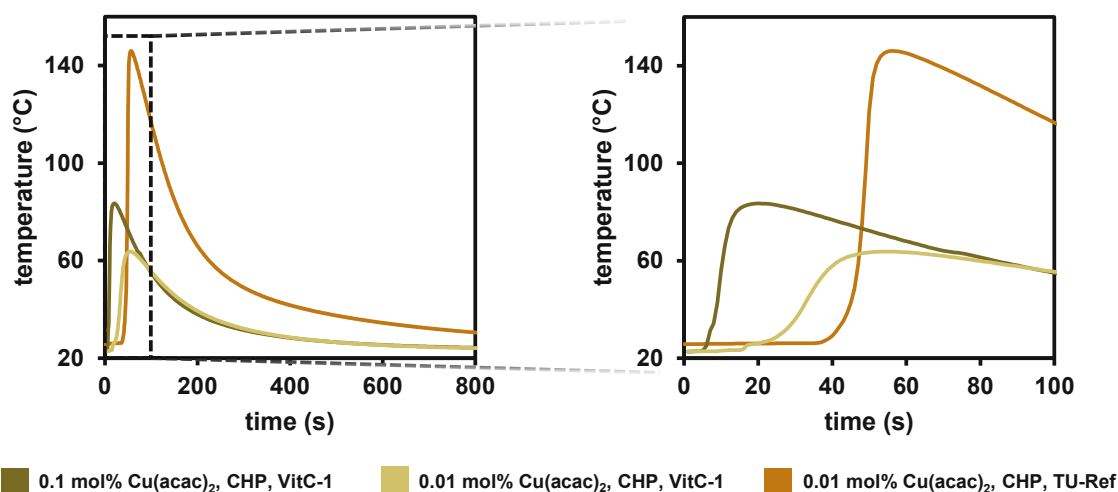
Figure 44: Rheology/IR measurements of the polymerization of 3Mix, using VitC-1 as the reducing agent, and CHP as the oxidizing agent. The concentration of the catalyst Cu(acac)$_2$ was varied from 0.1 mol% (●) to 0.01 mol% (●).

In the rheology measurements the progression of the storage modulus G' is shown for both concentrations of Cu(acac)$_2$. A higher concentration of Cu(acac)$_2$ leads to a significant improvement of the polymerization reaction itself due to higher probability of diffusion-caused meeting of the reaction partners, even though the initiation mechanism follows a cycle and Cu(acac)$_2$ is said to act as a catalytic species. The G' at the end of the measurement is significantly higher and also the progression follows a smoother path than with initiation using 0.01 mol% Cu(acac)$_2$. When looking at the t_{gel} it is clearly seen that the 0.1 mol% Cu(acac)$_2$ experiment showed a faster gelation (827 s), while 0.01 mol% Cu(acac)$_2$ has a t_{gel} almost double (1506 s). Furthermore, the DBC increase of the 0.01 mol% Cu(acac)$_2$ sample shows a lower rate, exhibiting less DBC$_{gel}$ (31.8% compared to 45.4%) and less DBC$_{end}$ (40.5% compared to 53.1%). The observed data is displayed in Table 8.

Table 8: Characteristic values derived from the rheology/IR measurement using 0.1 mol% or 0.01 mol% Cu(acac)$_2$ with CHP and VitC-1 in 3Mix, including G'$_{end}$, t_{gel}, DBC$_{end}$ and DBC$_{gel}$.

	G'$_{end}$ (kPa)	t_{gel} (s)	DBC$_{end}$ (%)	DBC$_{gel}$ (%)
0.1mol% Cu(acac)$_2$	549	827	53.1	45.4
0.01mol% Cu(acac)$_2$	333	1506	40.5	31.8

4.3.2. VitC-1/ Cu(acac)$_2$/CHP vs. State of the Art

The reactivity of the newly synthesized reducing agent VitC-1 was compared to the state-of-the-art reducing agent TU-Ref used for similar formulations in industrial applications using Rheology/IR measurements.[63, 64] The thiourea, TU-Ref, was used as represented in Table 9 and its structure is shown in Figure 45.

VitC-1   0.1mol%   0.01mol%
Cu(acac)$_2$
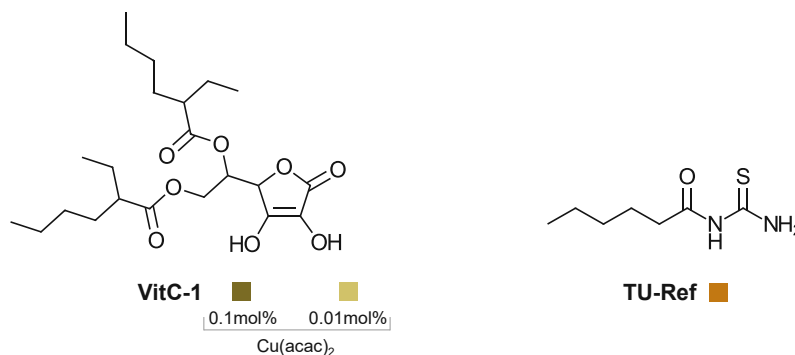
TU-Ref

Figure 45: Chemical structure of VitC-1 and the state-of-the-art reducing agent TU-Ref. VitC-1 was investigated using two different concentrations of Cu(acac)$_2$ catalyst.

All formulations compared in this study are shown in Table 9 below.

Table 9: Formulations prepared for rheology/IR measurements to characterize the reactivity of the polymerization reaction initiated by VitC-1, Cu(acac)$_2$ and CHP in 3Mix and the reference TU-Ref.

	F-red (0.1)	F-red (0.01)	F-red (ref)	F-ox
VitC-1 (mol%)	5	5	-	-
TU-Ref (mol%)	-	-	5	-
Cu(acac)$_2$ (mol%)	0.1	0.01	0.01	-
CHP (mol%)	-	-	-	11.5
3Mix (mol%)	94.9	94.99	94.99	88.5

In Figure 46 the VitC-1 based initiation system using two different concentrations of Cu(acac)$_2$ and the reference system using TU-Ref as reducing agent are compared regarding the polymerization reactivity.

0.1 mol% Cu(acac)₂, CHP, VitC-1 **0.01 mol% Cu(acac)₂, CHP, VitC-1** **0.01 mol% Cu(acac)₂, CHP, TU-Ref**
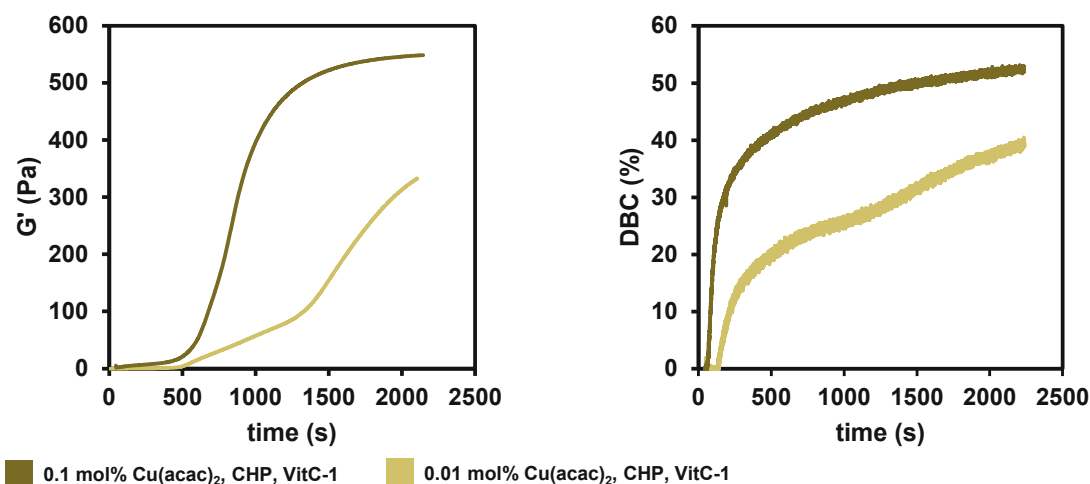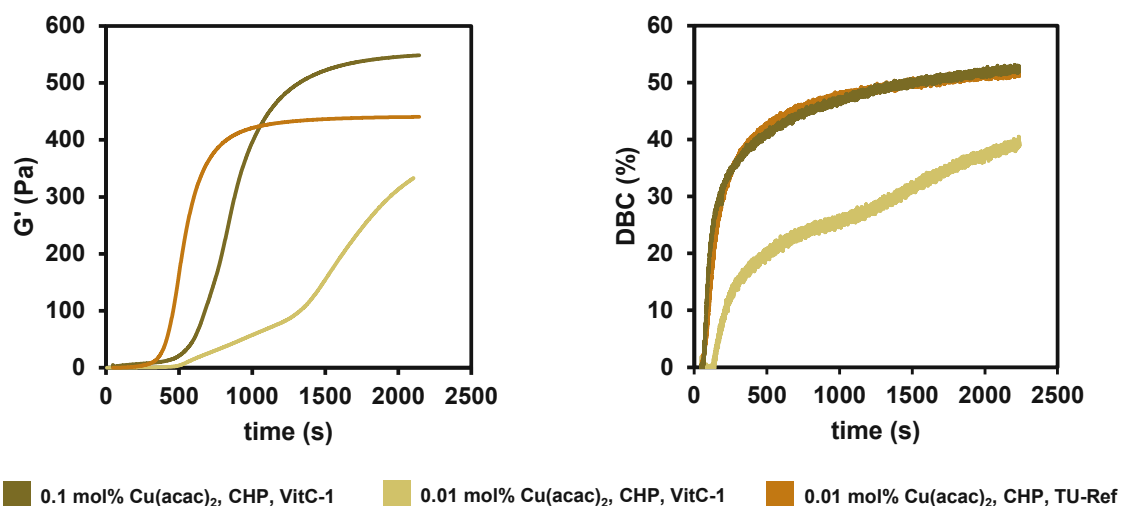
Figure 46: Rheology/IR measurements of the polymerization of 3Mix, using VitC-1 as the reducing agent, and CHP as the oxidizing agent. The concentration of the catalyst $Cu(acac)_2$ was varied from 0.1 mol% (●) to 0.01 mol% (●). The reference initiation system using $Cu(acac)_2$, CHP and TU-Ref is depicted as well (●).

The progression of G' using a higher concentration of $Cu(acac)_2$ of 0.1 mol% is similar to the reference system. However, even though with the reference a lower gel time is achieved, the final G' at the end is higher for the VitC-1 initiation system. It is remarkable in that regard that the progression of the DBC is almost congruent for these two measurements, however, resulting in different mechanical properties as well as showing different macroscopic reactivity represented by the gel time. It can be seen now very clearly that the sample using 0.01 mol% $Cu(acac)_2$ is outperformed by the state-of-the-art reference system. However, it could be shown that with higher concentrations of $Cu(acac)_2$ the reactivity can be tuned successfully to achieve results that are comparable to the state-of-the-art initiation system. (Table 10).

Table 10: Characteristic values derived from the rheology/IR measurement using 0.1 mol% or 0.01 mol% $Cu(acac)_2$ with CHP and VitC-1 in 3Mix as well as the reference TU-Ref, including G'_{end}, t_{gel}, DBC_{end} and DBC_{gel}.

		G'_{end} (kPa)	t_{gel} (s)	DBC_{end} (%)	DBC_{gel} (%)
0.1mol% Cu(acac)₂	VitC-1	549	827	53.1	45.4
0.01mol% Cu(acac)₂	VitC-1	333	1506	40.5	31.8
	TU-Ref	566	402	52.5	40.4

The slow polymerization reaction initiated by VitC-1 is mainly attributed to a strong oxygen inhibition. This can either be atmospheric oxygen in the air around the sample or dissolved oxygen in the monomer mixtures and the water they contain.

This theory is reflected by the optical appearance of the resulting polymer material that is obtained after the rheology/IR measurement (Figure 47).
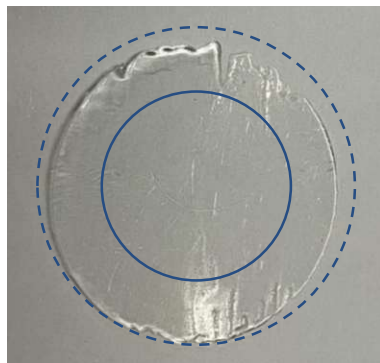
Figure 47: Polymer sample from the measurements shown using VitC-1 as reducing agent and 0.01 mol% Cu(acac)$_2$ as catalyst. Due to strong oxygen inhibition low double bond conversion in the outer layer is visible.

The outer layer of the platelet that is exposed to air during polymerization shows less polymerization than the inner layer of the polymer sample. A strong oxygen inhibition due to atmospheric oxygen is a plausible reason for this effect.[78]

4.3.3.   Stability of VitC-1

After determining the reactivity right after the preparation of the respective formulations (see Chapters Polymerization Temperature Measurements and Rheology/IR), the further stability of these formulations was investigated. The stability of VitC-1 in the monomer formulation is highly important for the application in 2K-systems. However, already after one week it could be shown that the formulation F-red (0.01) (see Table 9) was gelled at the bottom of the vial (Figure 48). The formulation F-red (0.1) was only stable for further processing for a couple of hours.
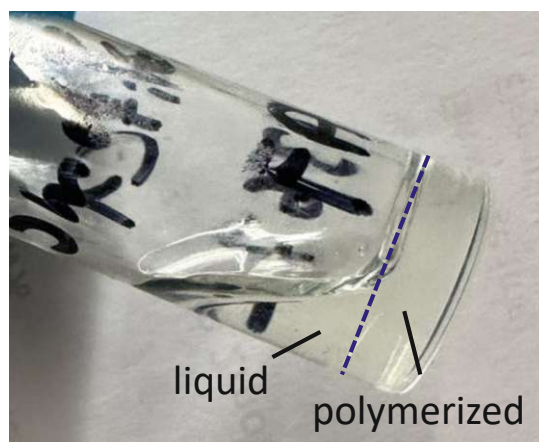
Figure 48: Formulation of 3Mix containing 5mol% VitC-1 and 0.01mol% Cu(acac)$_2$ after one week. The dashed line marks the border between the prematurely polymerized formulation and the still liquid formulation.

This indicates that VitC-1 is able to reduce $Cu(acac)_2$ very efficiently, leading to VitC-1 radicals that cause the formulation to polymerize prematurely as suggested in literature (Scheme 1).[33]

$$Cu(II) \ + \ VitC\text{-}1 \longrightarrow Cu(I) \ + \ {}^{+}_{\cdot}VitC\text{-}1$$
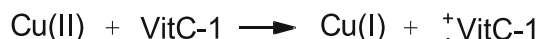
Scheme 1: Redox reaction between a Cu(II) compound and VitC-1 leading to Cu(I) and a positively charged VitC-1 radical.[33]

Rheology/IR measurements of supernatant liquid formulation after one week revealed a significant decrease in polymerization reactivity as well as DBC (Figure 49).

t₀ ▮ 0.01 mol% Cu(acac)₂, CHP, VitC-1   t₁week ▮ 0.01 mol% Cu(acac)₂, CHP, VitC-1
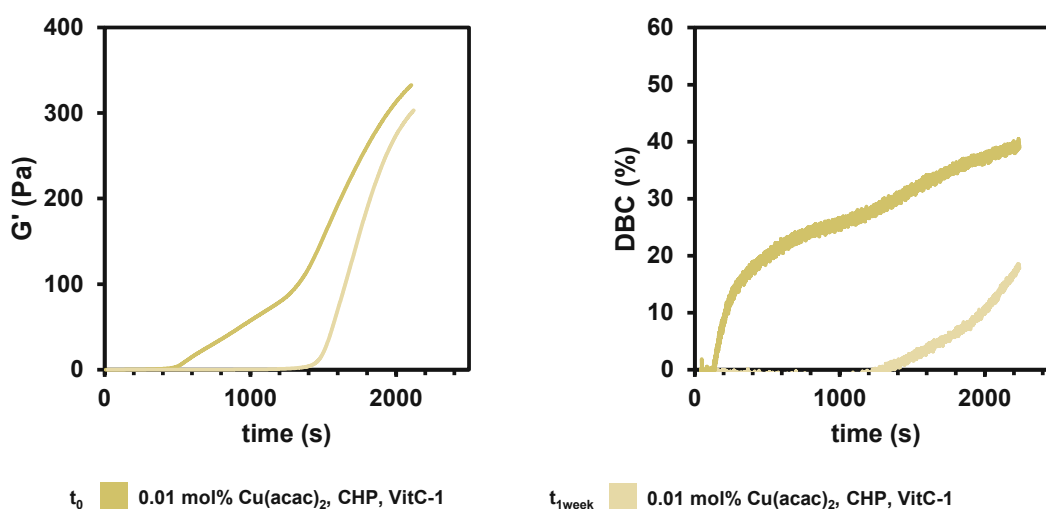
Figure 49: Rheology/IR measurements of the polymerization of 3Mix, using VitC-1 as the reducing agent, and CHP as the oxidizing agent. The concentration of the catalyst $Cu(acac)_2$ is 0.01 mol% and one sample was measured directly after making the formulations at t_0 (●) and the second measurement was performed after 1 week of storage in a fridge (t_{1week}) (●).

This decrease in reactivity seen in the figure shown above is easily explainable by already oxidized VitC-1 that is not further capable of reducing Cu(II) to Cu(I) effectively and therefore slowing down the initiation redox mechanism.

4.3.3.1. VitC-1/Cu(acac)$_2$/tBuHP

The previously discussed lack in stability led to the investigation of possible alternative compositions of the formulations, as it seems that VitC-1 is not stable in storage in a formulation together with Cu(acac)$_2$ in any of the tested concentrations. Following that reason, a less reactive aliphatic hydroperoxide oxidizing agent was used, which is stable in storage in a formulation together with Cu(acac)$_2$. Recent literature suggests the use of *tert*-butylhydroperoxide (*t*BuHP) in similar redox initiation systems.[80] The structure of the investigated oxidizing agent is depicted in Figure 50. This oxidizing agent allows for F-red to only contain VitC-1 without Cu(acac)$_2$, which could potentially increase the stability of the formulation.

CHP   ***t*BuHP**
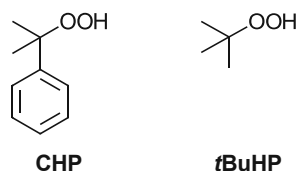
Figure 50: Chemical Structure of oxidizing agents CHP and *t*BuHP.

The formulations used for this study are shown in Table 11.

Table 11: Formulations prepared for rheology/IR measurements to characterize the reactivity of the polymerization reaction initiated by VitC-1, Cu(acac)$_2$ and CHP in 3Mix compared to the use of an alternative oxidizing agent *t*BuHP.

	F-red (CHP)	F-ox (CHP)	F-red (*t*BuHP)	F-ox (*t*BuHP)
VitC-1 (mol%)	5	-	5	-
Cu(acac)$_2$ (mol%)	0.01	-	-	0.01
CHP (mol%)	-	11.5	-	-
*t*BuHP (mol%)	-	-	-	11.5
3Mix (mol%)	94.99	88.5	95	88.49

It is seen in Figure 51 that even though the formulations using the aliphatic *t*BuHP are stable and allow for stable VitC-1 formulations without Cu(acac)$_2$, the reactivity is significantly decreased.

0.01 mol% Cu(acac)$_2$, CHP, VitC-1   0.01 mol% Cu(acac)$_2$, tBuHP, VitC-1
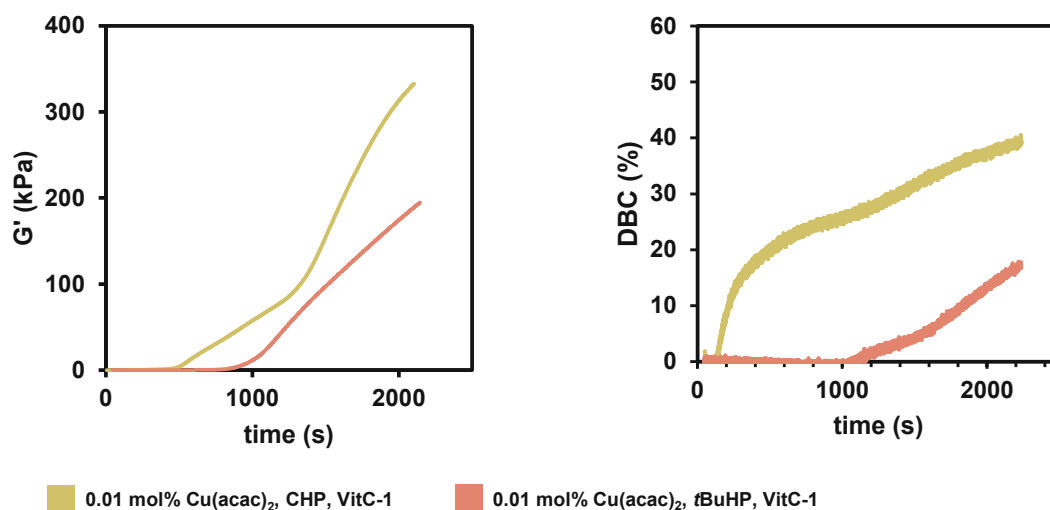
Figure 51: Rheology/IR measurements of the polymerization of 3Mix, using VitC-1 as the reducing agent, CHP (●) or tBuHP (●) as the oxidizing agent as well as the catalyst Cu(acac)$_2$ (0.01 mol).

The aliphatic oxidizing agent is significantly less reactive than the aromatic CHP, leaving the DBC very low over the whole measurement time. No gel time was evaluated since no gel point was observed at low DBC (Table 12). Even though the stability could be enhanced, the reactivity would suffer too much for this oxidizing agent to find application in this redox system.

Table 12: Characteristic values derived from the rheology/IR measurement using 0.01 mol% Cu(acac)$_2$ with CHP or tBuHP and VitC-1 in 3Mix, including G'_{end}, t_{gel}, DBC_{end} and DBC_{gel}.

	G'_{end} (kPa)	t_{gel} (s)	DBC_{end} (%)	DBC_{gel} (%)
CHP	333	1506	40.5	31.8
tBuHP	195	-	17.8	-

5. Polymer Properties

Looking at the previously discussed results concerning the reactivity, VitC-1 proved to be a highly reactive reducing agent with CHP and Cu(acac)$_2$ for the polymerization of 3Mix. However, not only reactivity is crucial for a 2K-system, also the final (thermo)mechanical properties of the polymer are of high importance. Due to the lack of stability of the unpolymerized formulations, all specimens discussed in this chapter were prepared right after the preparation of the formulations.

The properties of the final polymer material are highly dependent on the monomers used for the polymerization. However, in linear polymers as well as networks also the conversion of the reactive groups is crucial. In the case of methacrylates, the DBC significantly alters the properties of the polymer network. The overall DBC can be regulated and influenced among others by the choice of the initiation system. These effects of the initiation system on the properties are investigated in detail in the following chapter using DMTA and tensile tests.

5.1. DMTA

Dynamic mechanical thermal analysis (DMTA) is carried out to study the temperature dependency of the mechanical properties of polymers. Conclusions can be drawn regarding the network properties, T_g and temperature dependent post-curing effects.

A typical duromeric and highly crosslinked network exhibits a broad range of domain sizes and no distinct glass transition temperature is visible. Such a network will maintain its mechanical properties in the rubbery plateau until it degrades. However, a network with lower crosslinking density will show a decrease of storage modulus in the transition region. These effects are schematically displayed in a lower storage modulus at the rubber plateau (G'$_r$) and a narrow glass transition temperature range.[81]
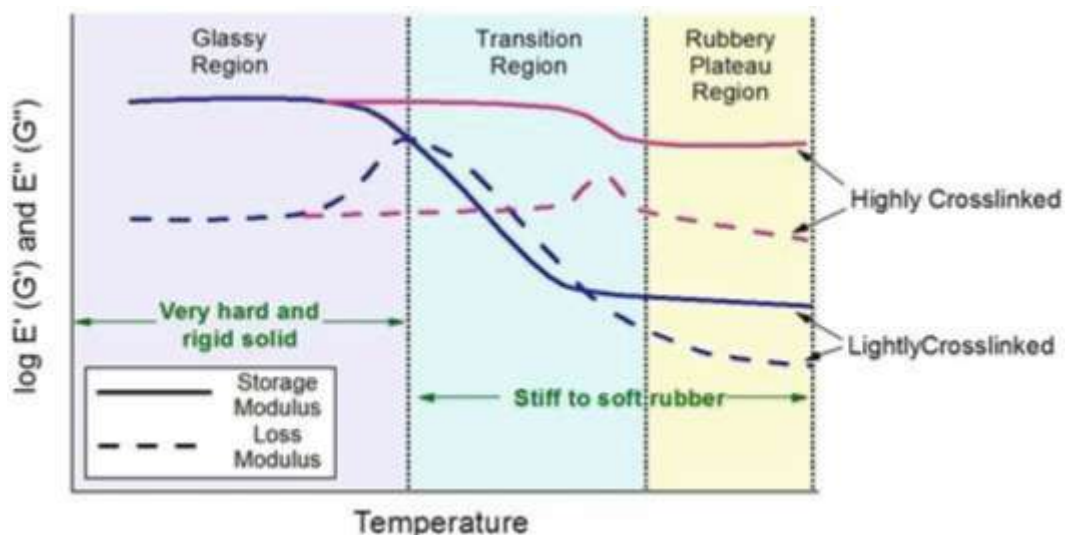
Figure 52: Schematic explanation of the influence of crosslink density on glass transition and storage modulus[81]

If polymer networks show an increase in double bond conversion and therefore crosslinking density after thermal treatment, post-curing is occurring. In DMTA measurements these post-curing phenomena can be observed, as G' increases with increasing temperature until a final more densely crosslinked rubber plateau is reached. As the T_g of the more crosslinked network is higher these effects are also reflected in the tanδ as a second peak. These effects are schematically shown in Figure 53.
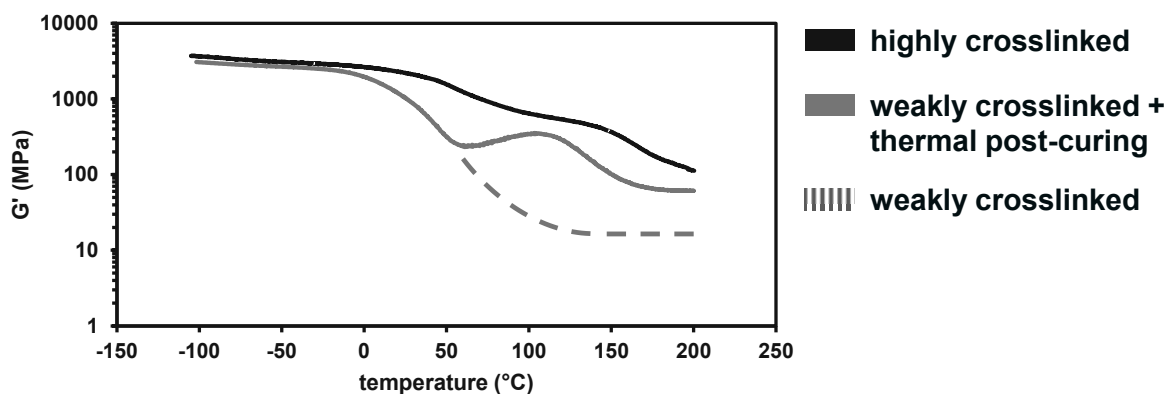
Figure 53: Schematic DMTA measurement of a highly crosslinked network (black), a weakly crosslinked network that shows thermal post-curing (grey) and a weakly crosslinked network that does not show thermal post-curing (grey dotted).

5.1.1. VitC-1/ Cu(acac)$_2$/CHP vs. State of the Art

The thermomechanical properties of polymerized 3Mix were evaluated, using the newly developed initiation system applying VitC-1 and TU-Ref as the reference reducing agent. The red-formulations and respective ox-formulation were mixed in w% 50:50 ratio and cured inside a mold for DMTA specimens at room temperature. Thereafter, the specimens were stored for 24 h at 37 °C and subsequently DMTA measurements were performed. The structures of the compounds used for initiation are depicted in the following Figure 54.
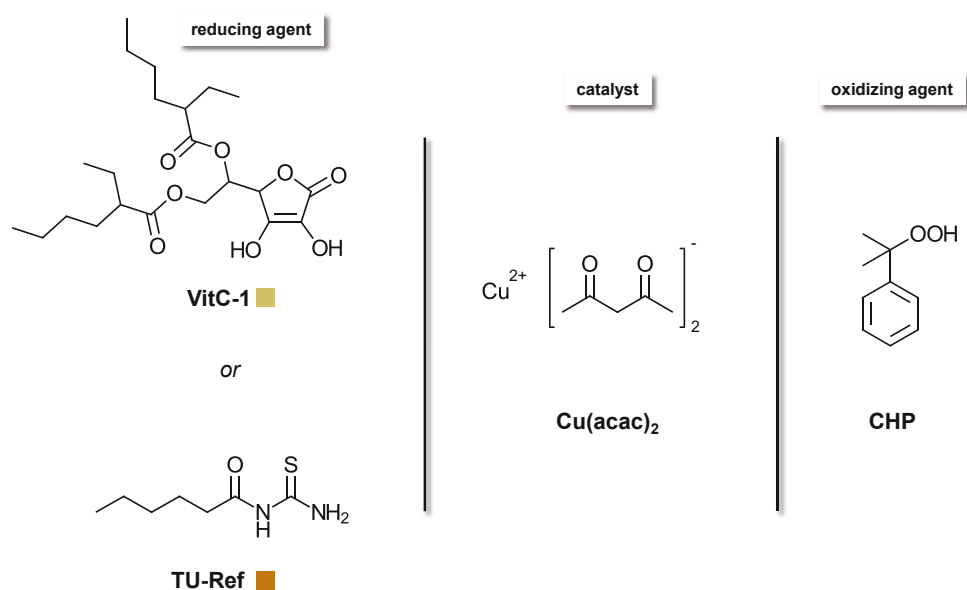
Figure 54: Chemical structure of the reducing agent VitC-1 and the reference reducing agent TU-Ref, the catalyst Cu(acac)$_2$ and the oxidizing agent CHP.

The concentration of Cu(acac)$_2$ was set to 0.01 mol% for a good comparison to the reference system. Furthermore, no specimen could be produced with higher concentrations of Cu(acac)$_2$, because the polymerization reaction was too fast to yield proper specimen in the molds. The exact formulations used in this study are shown in Table 13.

Table 13 Formulations prepared for DMTA measurements to characterize the thermomechanical properties of polymers derived from initiation by VitC-1, Cu(acac)$_2$ and CHP in 3Mix or the reference TU-Ref.

	F-red (VitC-1)	F-red (TU-Ref)	F-ox
VitC-1 (mol%)	5	-	-
TU-Ref (mol%)	-	5	-
Cu(acac)$_2$ (mol%)	0.01	0.01	-
CHP (mol%)	-	-	11.5
3Mix (mol%)	94.99	94.99	88.5

The storage modulus (G') of the respective specimens is plotted against the temperature increase from -100 °C to 200 °C. Another important parameter is the loss factor (tanδ) which is the quotient of G' and the loss modulus (G''). In the following Figure 55 G' and tanδ are depicted for samples applying VitC-1 and TU-Ref.

■ 0.01 mol% Cu(acac)$_2$, CHP, VitC-1   ■ 0.01 mol% Cu(acac)$_2$, CHP, TU-Ref
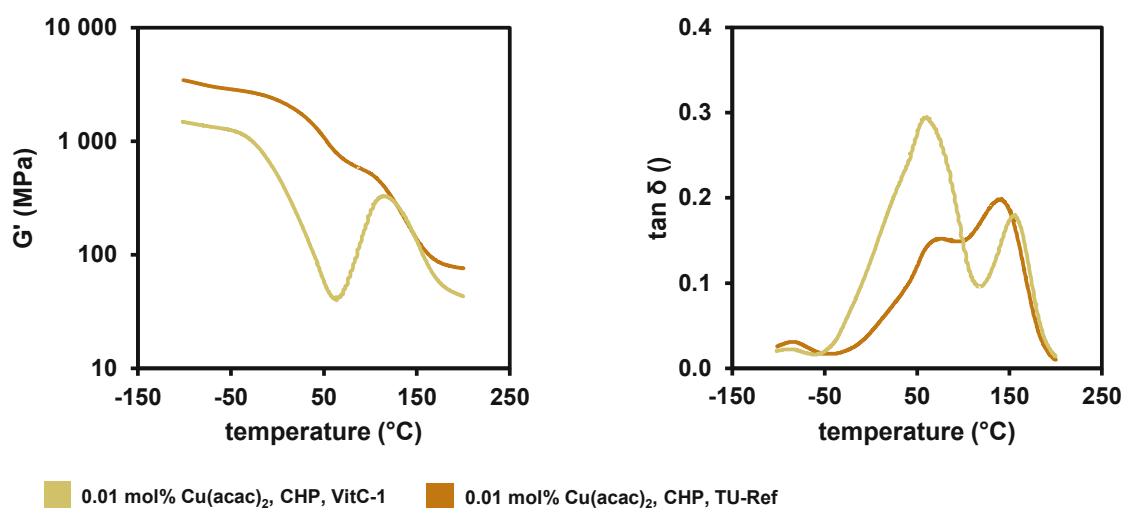
Figure 55: DMTA measurements of polymerized 3Mix via VitC-1 (●) or TU-Ref (●) as reducing agent. Left diagram shows the progression of G' and right diagram shows the progression of tanδ between -100 °C and 200 °C.

Figure 55 shows the DMTA measurement of the specimen applying VitC-1 as the reducing agent. The storage modulus G' shows a significant decrease around 0 °C, resulting in a very low T_g1 of 60 °C. This is the first sign for a very soft polymer, which is not really common for the 3Mix monomer mixture. However, when looking at the DBC measured via ATR-IR it is clear that the network density has to be very low with a DBC of 21.2 %. Furthermore, a thermal post-curing occurs from 50 °C upwards, which results in an increase in G' and a second T_g2 of the post-cured network of 156.3 °C. It is noted that the T_g2 of the VitC-1 sample is around 15 °C higher than the reference sample applying TU-Ref. The first formed low-density network results in an optimal backbone for the formation of a more homogeneous and higher crosslinked network through thermal post-curing. This post-curing process is also visible in the DBC after the thermal treatment (DBC$_{ATR-IR}$-therm), which shows a significant increase in the case of the VitC-1 sample (Table 14)

Table 14: Results of the DMTA measurements applying VitC-1 and TU-Ref as the reducing agents in 3Mix. G'$_{25°C}$, T_g1, T_g2, DBC$_{ATR-IR}$ and DBC$_{ATR-IR}$-therm are shown.

	G'$_{25°C}$ (MPa)	T_g1 (°C)	T_g2 (°C)	DBC$_{ATR-IR}$ (%)	DBC$_{ATR-IR}$-therm (%)
VitC-1	193	60.6	156.3	22	83
TU-Ref	1756	70.5	141.6	68	94

5.2.   Tensile Tests

Not only thermomechanical properties as obtained from DMTA measurements are necessary to characterize polymer specimen sufficiently. Tensile Tests give a great insight in the mechanical properties of the polymer, including stress at break (σ), elongation at break (ε) and Δσ/Δε, an approximate value for the Young's modulus.

To determine these important mechanical parameters tensile tests were conducted. They are a shock-free, quasi-static destructive method with a slow strain rate. Uniaxial loading is applied on the sample and steadily increased until the specimen ruptures. The resulting strain is monitored with increasing stress to obtain stress-strain curves.[82] The tensile stress σ (MPa) is calculated with Equation 2, while the strain ε (%) can be determined using Equation 3 and tensile toughness U_T (MJ/cm^3)was calculated as the integrated area under the curve.

Equation 2 Calculation of the stress in tensile testing. σ…tensile stress [MPa]; F…tensile force [N]; A_0…initial cross section [mm^2].

$$\sigma = \frac{F}{A_0}$$

Equation 3 Calculation of the strain in tensile testing. ε… tensile strain [%]; ΔL…elongation [mm]; L_0…initial length [mm].

$$\varepsilon = \frac{\Delta L}{L_0}$$
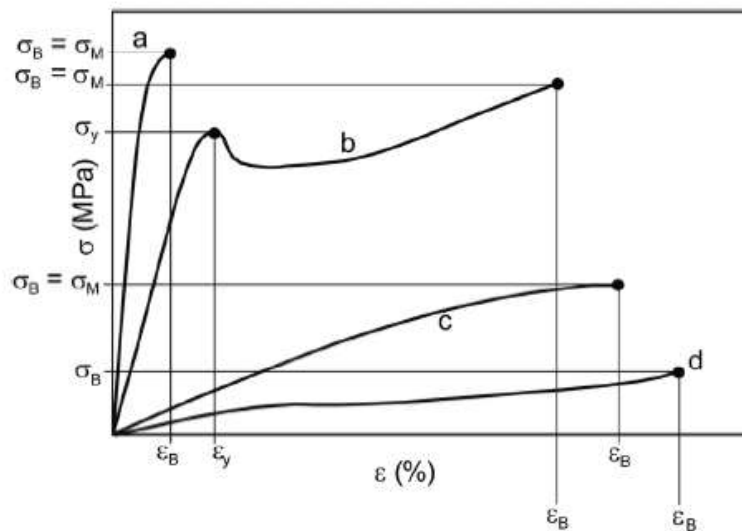
Figure 56: Scheme of typical stress-strain curves of polymer tensile testing.[82]

Figure 56 shows typical stress-strain curves of different materials. Initially, for all polymers, a linear behavior is observed. With increasing stress, a non-linear regime is exhibited, and a different behavior occurs. Highly crosslinked networks are very brittle and display very low ε_B and high σ_M (a). Furthermore, no yield point with a yield strength σ_y, as in curve b, is observed. If the crosslinking density is low, for example, in elastomers, high ε_B and low σ_M are exhibited (d).[82]

5.2.1. VitC-1/ Cu(acac)$_2$/CHP vs. State of the Art

The mechanical properties of polymerized 3Mix were evaluated via tensile testing using the newly developed initiation system applying VitC-1 and TU-Ref as the reference reducing agent. The red-formulations and respective ox-formulation were mixed in w% 50:50 ratio and cured inside a mold for bone shaped tensile test specimens at room temperature. Thereafter, the specimens were stored for 24 h at 37 °C and subsequently the tensile tests were performed. The structures of the compounds used for initiation are depicted in the following Figure 57.
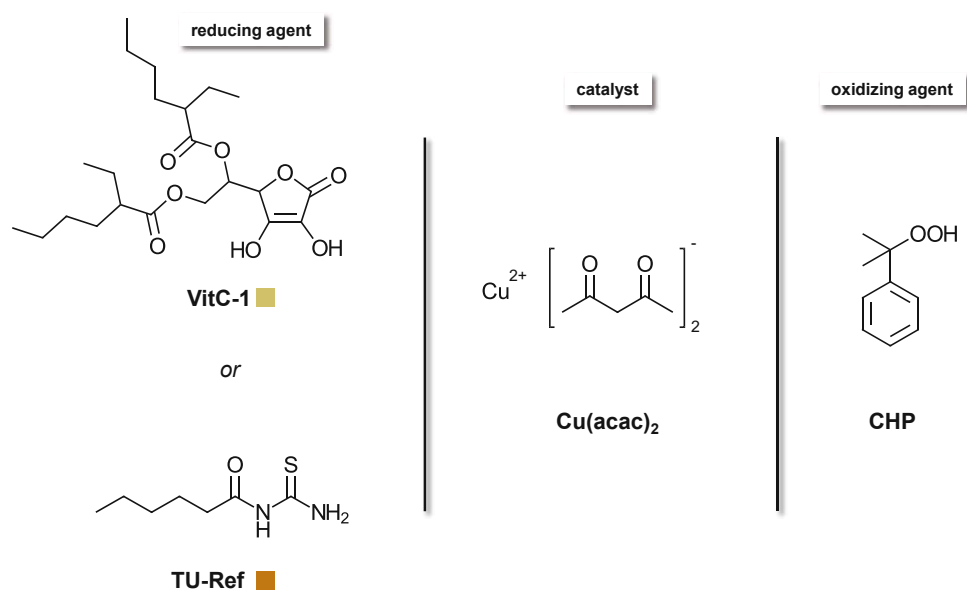
Figure 57: Chemical structure of the reducing agent VitC-1 and the reference reducing agent TU-Ref, the catalyst Cu(acac)$_2$ and the oxidizing agent CHP.

The concentration of Cu(acac)$_2$ was set to 0.01 mol% for a good comparison to the reference system. Furthermore, no specimen could be produced with higher concentrations of Cu(acac)$_2$, because the polymerization reaction was too fast to yield proper specimen in the molds. The exact formulations used in this study are shown in Table 15.

Table 15: Formulations prepared for tensile tests to characterize the mechanical properties of polymers derived from initiation by VitC-1, Cu(acac)$_2$ and CHP in 3Mix or the reference TU-Ref.

	F-red (VitC-1)	F-red (TU-Ref)	F-ox
VitC-1 (mol%)	5	-	-
TU-Ref (mol%)	-	5	-
Cu(acac)$_2$ (mol%)	0.01	0.01	-
CHP (mol%)	-	-	11.5
3Mix (mol%)	94.99	94.99	88.5

The previous results of the DMTA measurements lead to the conclusion that initiation via VitC-1 does not yield high double bond conversions and therefore a soft and low crosslinked network. This is also well reflected in the tensile tests compared to TU-Ref, shown in Figure 58.

■ 0.01 mol% Cu(acac)$_2$, CHP, VitC-1   ■ 0.01 mol% Cu(acac)$_2$, CHP, TU-Ref
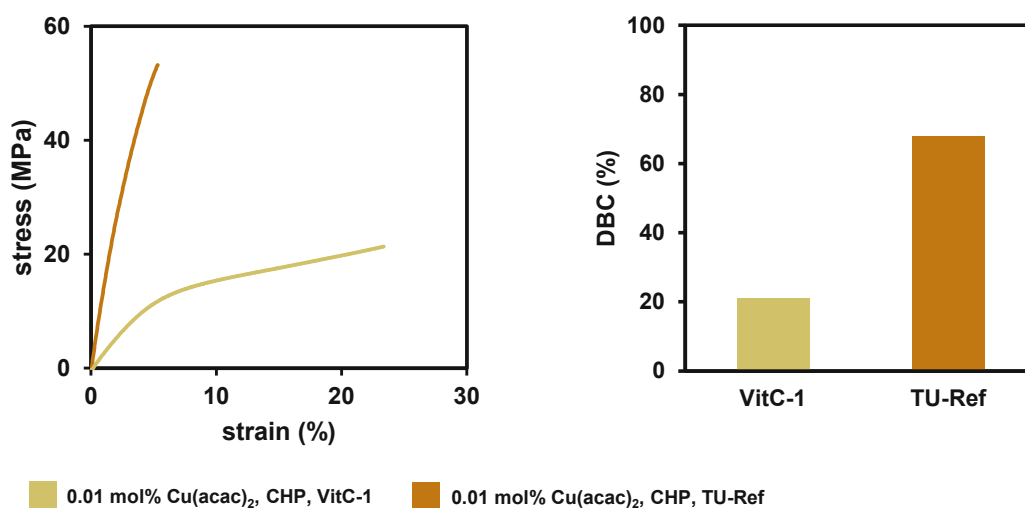
Figure 58: Left: Stress-strain diagrams of tensile tests of specimens derived from VitC-1 (●) and TU-Ref (●) in 3Mix. Right: Double bond conversion of the tested specimens.

In the figure above, the soft behavior of the VitC-1 sample is clearly visible as high elongations at break were reached with low stress values. Furthermore, a yield point is visible where permanent deformation occurs.

The results are also reflected in the data shown in Table 16. Especially $\Delta\sigma/\Delta\varepsilon$ is a good indicator for the brittleness of a material. It is clearly seen that this value correlates well to the DBC measured with ATR-IR, leading to the conclusion that the low double bond conversion leads to a loosely crosslinked polymer network that show rather elastic properties compared to the polymer derived from initiation with the reference system.

Table 16: Results of tensile tests of specimen derived from different VitC-1 and TU-Ref in 3Mix, including stress at break, elongation at break, $\Delta\sigma/\Delta\varepsilon$, DBC$_{ATR-IR}$ and the tensile toughness U$_t$.

	σ_M (MPa)	ε_M (%)	$\Delta\sigma/\Delta\varepsilon$ (MPa)	DBC$_{ATR-IR}$ (%)	U$_T$ (MJ/cm^3)
VitC-1	17.9 ± 2.7	18.9 ± 7.4	3.0	21.2	2,4±1,1
TU-Ref	46.3 ± 7.2	4.1 ± 1.1	14.5	67.7	1±0,5

6. Resumée

The synthesis of a VitC derivative with ethylhexyl ester groups (VitC-1) was successfully carried out. In three steps the product was obtained as a colorless oil in 50% yield. This oil proved to be highly soluble in the 3Mix monomer mixture, which highlights the effect of the apolar side chains (Figure 59).
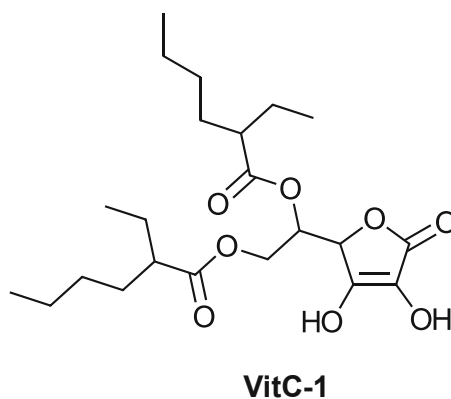
VitC-1

Figure 59: Chemical structure of the newly synthesized VitC derivative VitC-1.

Polymerization experiments with VitC-1/Cu(acac)$_2$/CHP were carried out in 3Mix and unfortunately very high oxygen inhibition was observed. The polymerization is slower and with less final DBC than the reference system containing the thiourea compound TU-Ref. Furthermore, instability of the formulations containing VitC-1 and Cu(acac)$_2$ was observed as they tend to be partly polymerized after one week. Therefore, polymerization experiments were carried out using a different oxidizing agent (*t*BuHP) which can be safely stored in the same formulation with Cu(acac)$_2$. However, the reactivity of this system was very low and led to only low double bond conversion. Due to the high oxygen inhibition, also the (thermo)mechanical properties of the final polymers revealed rather soft polymer networks with low DBC, compared to the reference system.

Part B: Diborane/Cu 2K System

Parts of this work are published by the author or are in the process of submission. See *https://doi.org/10.1039/D4PY00445K* for more information.

1. State of the Art - Diborane Chemistry

As stated in the objective, the aim of "Part B" is the development and investigation of a two-component radical polymerization system employing diboranes and copper compounds. In this regard, the state of the art of the chemistry of diboranes and their ability to add to double bonds will be examined in detail to evaluate their suitability as a central compound of the initiation system.

1.1. Borylation Reactions

The addition of diboranes e.g., B_2pin_2 and B_2neop_2 (Figure 60) to α, β-unsaturated carbonyl compounds is reported using a rhodium catalyst.
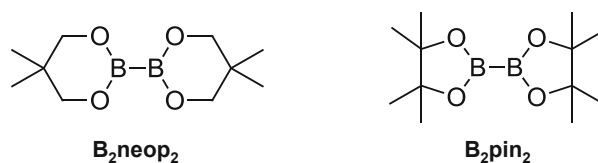
Figure 60: Chemical structure of diboranes B_2neop_2 and B_2pin_2.

The key step in this reaction is the oxidative addition of the diborane compound to the transition metal followed by coordination and insertion of the organic precursor and subsequent reductive elimination of the product.[83, 84] (Scheme 2)
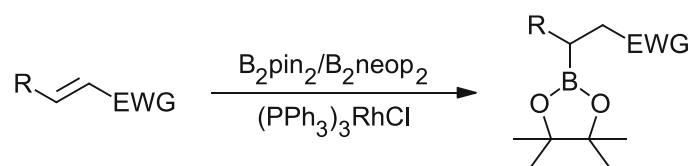
Scheme 2: Borylation of α, β-unsaturated carbonyl compounds with diboranes employing a rhodium catalyst[83, 84]

For such reactions radical pathways are suggested in the preparation of boronic esters from aryl amines using a methodology based on the Sandmeyer reaction, which usually transforms amines to the corresponding aryl halides. Borylation occurs by the addition of B_2pin_2 to the intermediate diazonium salt. It was found that benzylperoxide aided the reaction and radical scavengers retarded the reaction. Therefore, a radical mechanism involving a single electron transfer (SET) was proposed. This reaction comes without a metal catalyst.[85, 86]

It was shown that the addition of silver or copper salts increases the rate of transmetalation, as copper effects a more efficient pre-transmetalation with boron. $Cu(OAc)_2$ in combination with diethanol amine was found to substantially increase yields. A $Cu(DEA)_2$ species might be likely formed in the involved mechanism.[85]

Another report by Fernández et al. states that MeOH and the addition of base is a key parameter for the organo-borylation reactions. However, they present a method to replace the base by PR_3 to assist the β-borylation. The enhanced nucleophilicity of the Bpin moiety in the Cu/Rh-catalyzed and organocatalyzed versions that is responsible for the β-borylation on the α, β-unsaturated ester, ketone, amide and imide substrates is still intact with the new pathway.[87] (Scheme 3)
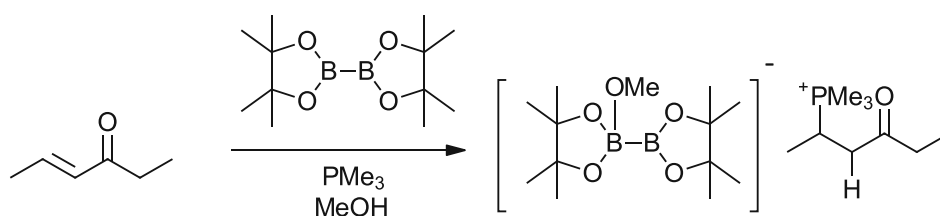
Scheme 3: Borylation via the formation of PR_3 catalyzed nucleophilic diboranes.[87]

1.2. Copper mediated Borylations

The addition reactions of diboranes such as B_2pin_2 and B_2neop_2 to α, β-unsaturated carbonyl compounds are reported to be especially effective if a copper catalyst is used. Those reactions will be discussed in the following.

The borylation of unsaturated compounds was reported in combination with Cu(I) catalysts and KOAc in DMF through the formation of a Cu-B Bond and a subsequent addition to the double bond. It is stated that the B-B bond is easily cleaved in an oxidative addition to the transition metal, allowing the catalyzed addition to the unsaturated organic substrates. They claim that through experimental data it was shown that a ionic species is likely formed through the addition of the OAc anion to B_2pin_2 resulting in a more nucleophilic Bpin moiety.[88] (Scheme 4)
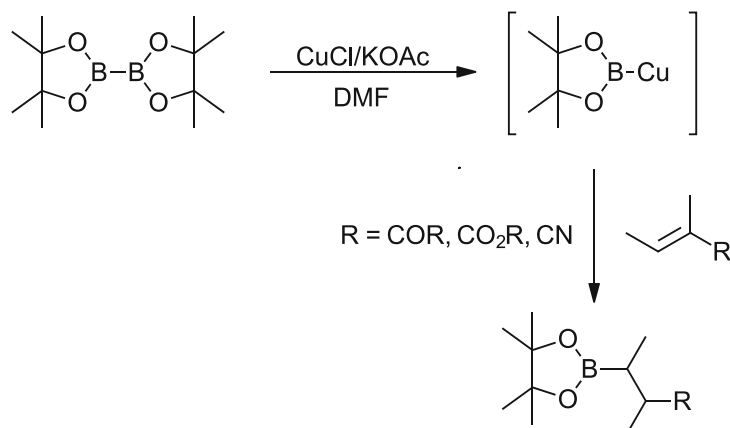
Scheme 4: Top: nucleophilic anionic species created from B_2pin_2 with Cu(I)OAc in DMF; Bottom: Reaction of these anionic species with α, β-unsaturated carbonyl compounds.[88]

Excellent yields of up to 98% were reached in the borylation of ethylacrylate and other α, β-unsaturated carbonyl compounds, using CuCl, DPEPhos and methanol. Both, the bidentate ligand as well as the alcohol were necessary for a high reactivity and not resulting in incomplete conversion.[89] (Scheme 5)
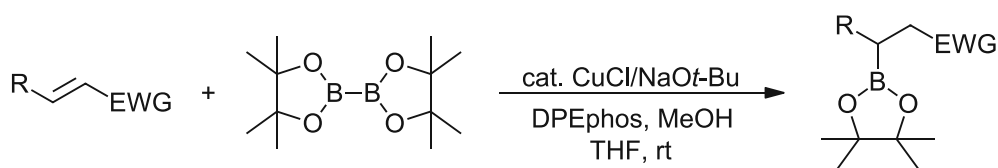
Scheme 5: Borylation of α, β-unsaturated carbonyl compounds with CuCl/DPEphos with MeOH.[89]

A mechanism for this reaction is proposed, in which the diborane species can add to the copper complex resulting in an organocopper species that adds to the unsaturated carbonyl compound.[89]

1.3.   Boranes as Initiators for FRP

The reactivity of diboranes towards addition to α, β-unsaturated carbonyl compounds is given under copper catalyzation. In addition, radical mechanisms are suggested in some cases. However, boranes are already reported to being utilized as radical initiators in several ways and proved to show high reactivity and low oxygen inhibition.[90]

Several amine borane complexes were investigated in this regard, used as initiators and co-initiators for radical polymerization of acrylates.[90, 91] (Figure 61)
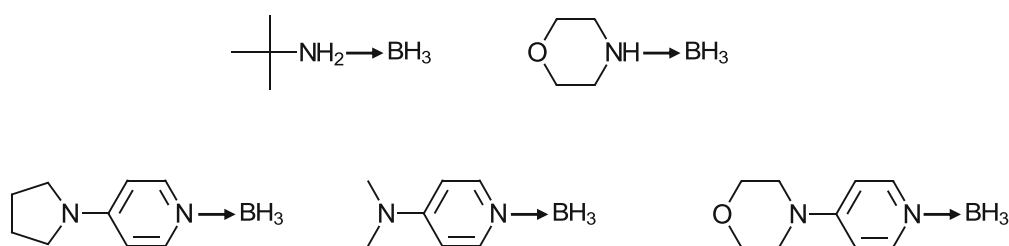
Figure 61: Chemical structures of amine borane complexes that are reported for (co)-initiation of radical polymerization of acrylates.[90, 91]

These complexes can exhibit high reactivity in co-initiation with amine/peroxide two-component redox radical initiation of acrylate polymerization. Furthermore, the amine borane complexes can be used as reducing agent for redox initiation systems, replacing the amine compound. In combination with phosphines or iodonium salts the generation of initiating radicals in reported. Also, extremely low oxygen inhibition of the polymerization is claimed, as a similar mechanism to phosphine catalysed oxygen capture is occuring.[90, 91]

Furthermore, photopolymerization of (meth)acrylates using N-heterocyclic carbene-borane complexes is reported with boryl radicals being the initiating species (Figure 62).[92]
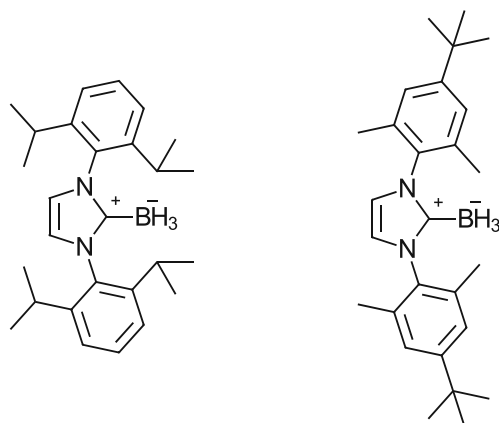
Figure 62: Chemical structure of photoactive N-heterocyclic carbene-borane complexes.[92]

2. Towards a Radical Polymerization System

The conducted analysis of the state-of-the-art literature showed that diboranes are used in various reactions with α, β-unsaturated carbonyl, catalyzed by different copper compounds. Furthermore, the initiation of radical polymerization using borane complexes is reported with boryl radicals as initiating species. However, the combination of diboranes and copper compounds, leading to radical polymerization is not investigated yet and has high potential as a new radical polymerization system.

Due to a good availability of commercial diboranes, multiple structurally different compounds were investigated. However, others, such as a dimethyl substituted six-membered ring diborane, or symmetrical diboranes with a B-N donating bond had to be synthesized (Figure 63).
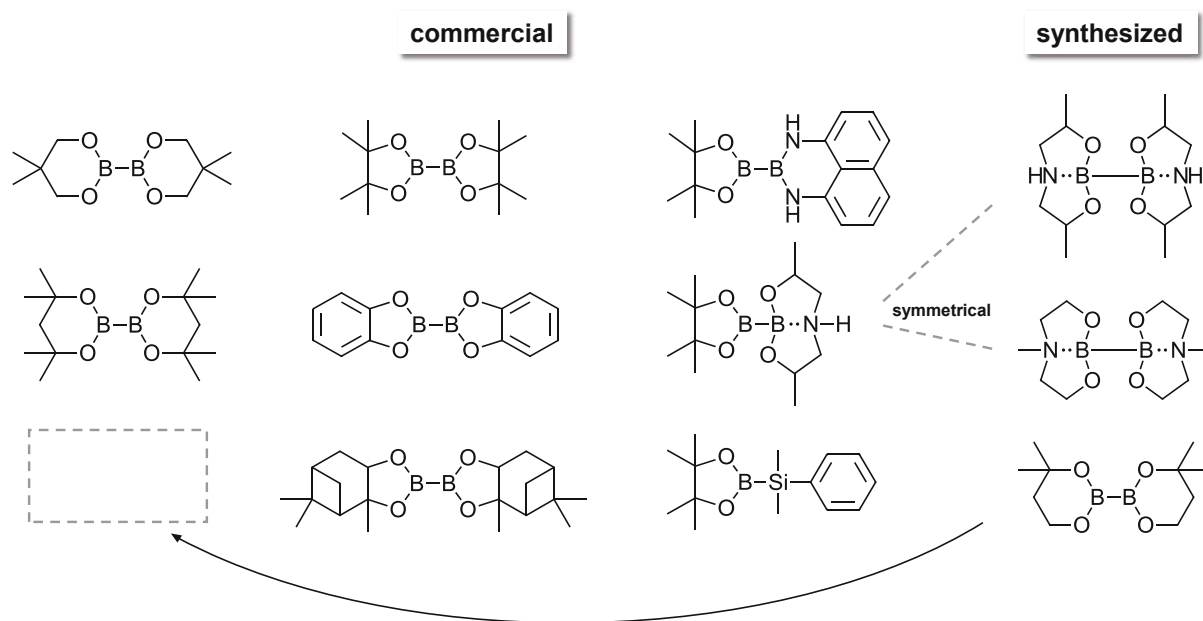
Figure 63: Chemical structures of diboranes that are commercially available or had to be synthesized.

2.1.   Synthesis of Diborane Initiators

Diborane compounds do find a lot of application in organic chemistry, especially metal catalysed reactions. For many reported reactions sp^2-sp^2 hybridized diboranes such as B_2pin_2 or B_2cat_2 are used.[83] However, sp^2-sp^3 hybridized diboranes show reactivity towards different functional groups and lead to more nucleophilic instead of electrophilic behaviour, which can be beneficial in the addition to methacrylic double bonds.[93, 94] Little is reported about sp^3-sp^3 hybridized diboranes, as they are extremely nucleophilic leading to properties that allow for

reduction of water.[95] In the following, attempts were made to synthesize two sp^3-sp^3 diboranes and a sp^2-sp^2 diborane.

2.1.1. Synthesis of BN-3

The synthesis of diborane compounds is a scarcely reported topic in organic synthesis due to the good commercial availability of compounds like B_2pin_2 and B_2neop_2. However, the majority of scientific reports and patents feature synthesis pathways starting from hypodiboronic acid and describe reactions with various diols.[96]

The objective was the investigation of syntheses leading to diborane compounds with a symmetrical structure and both borane centers in sp^3-hybridization (BN-3, Figure 64). This can be achieved using symmetrical diols with an amine moiety that can donate electrons into the B-B bond leading to the wanted hybridization in the target molecule.[97]

The commercially available BN-2 compound, being asymmetrically substituted with an amine-diol moiety, was the baseline of the synthesis pathway. The aim was to investigate the synthesis of a symmetrical diborane, namely BN-3 (Figure 64).

BN-2   **BN-3**
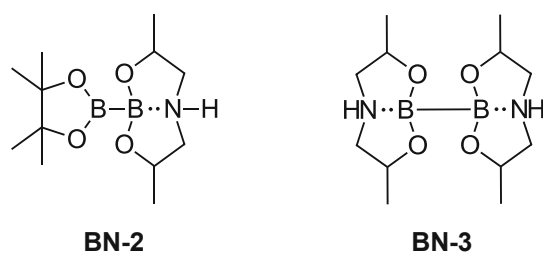
Figure 64: Chemical structure of the commercially available BN-2 and the target compound BN-3.

Following the reported synthetic pathway, the reaction of hypodiboric acid with diisopropanolamine was performed according to literature. The condensation reaction leads to the formation of 4 eq. water that has to be eliminated in order to shift the reaction equilibrium to the product side. In a first attempt, the addition of Na_2SO_4 was used to capture any moisture (Figure 65).[97]
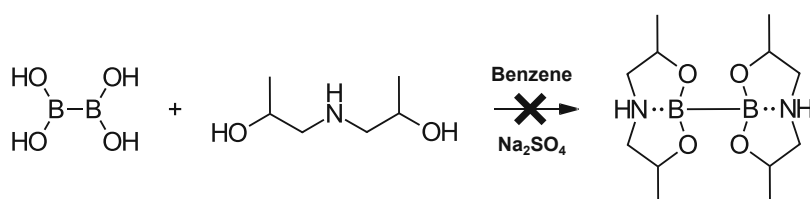
Figure 65: Reaction scheme of the condensation of hypodiboronic acid with an amine bearing diol, facilitated by the addition of Na_2SO_4, yielding the diboronic compound BN-3.

After 24 h the reaction was stopped, filtrated and the solvent was removed to yield colorless, hygroscopic crystalline solid. The product was analyzed *via* NMR spectroscopy using [1]H-, ^{11}B-, ^{13}C-, APT-, and HSQC-NMR. The analysis of the ^{11}B-NMR showed that a reaction took place, yielding a compound that shows one peak at 10.6 ppm (Figure 66).
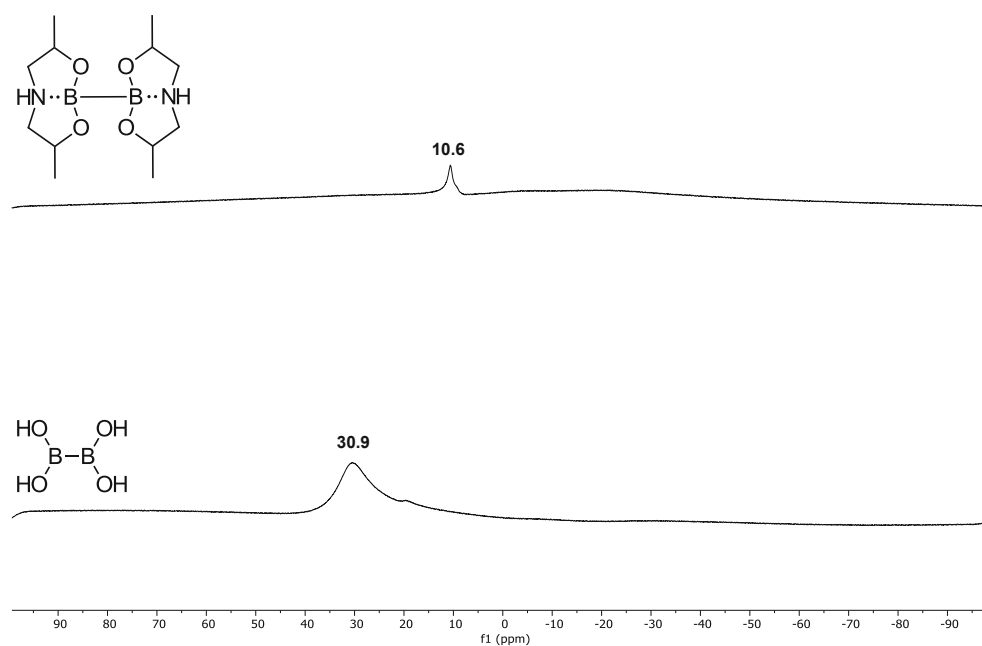
Figure 66: ^{11}B-NMR of the hypodiboronic acid starting material (bottom) and the product BN-3 (top) in DMSO.

This shift is very comparable to the shift of the sp^3-hybridized boron atom in BN-2 with 9.0 ppm.[98] However, the HSQC reveals that the wanted reaction did not take place and the side product SP-1 was synthesized instead (Figure 67).
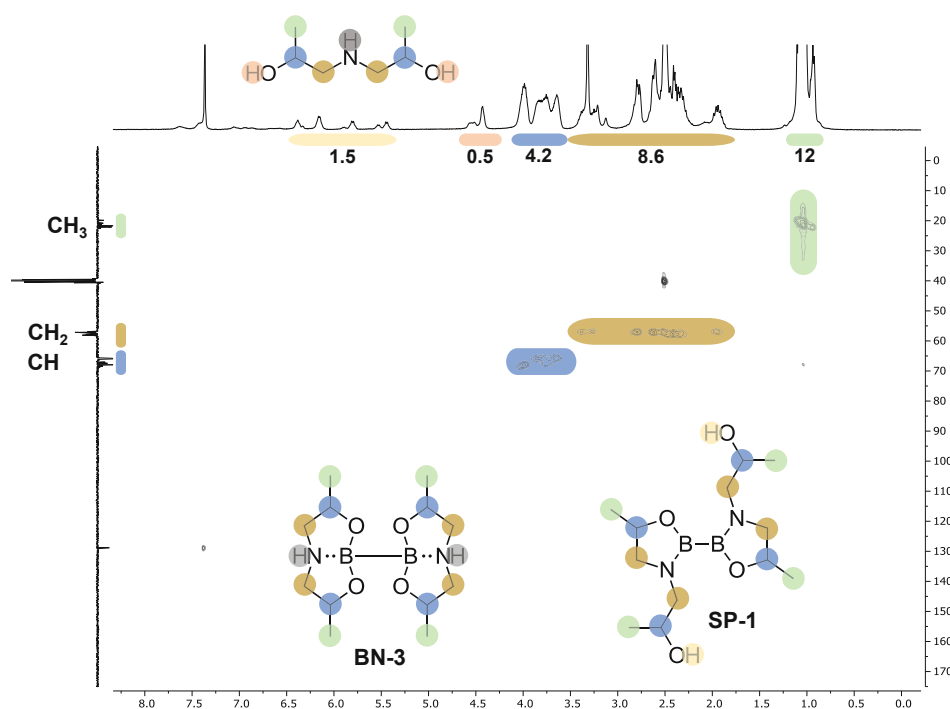
Figure 67: HSQC spectrum of an ^{1}H-NMR and an APT spectrum of the product BN-3 in DMSO.

The HSQC confirms the formation of SP-1 as the peaks from 5.5 ppm - 6.5 ppm correlate to hydroxyl protons that are not the diol starting material. Furthermore, the amine proton of the starting material is completely gone in the product, which strongly leads to the assumption that SP-1 was synthesized (Figure 68).
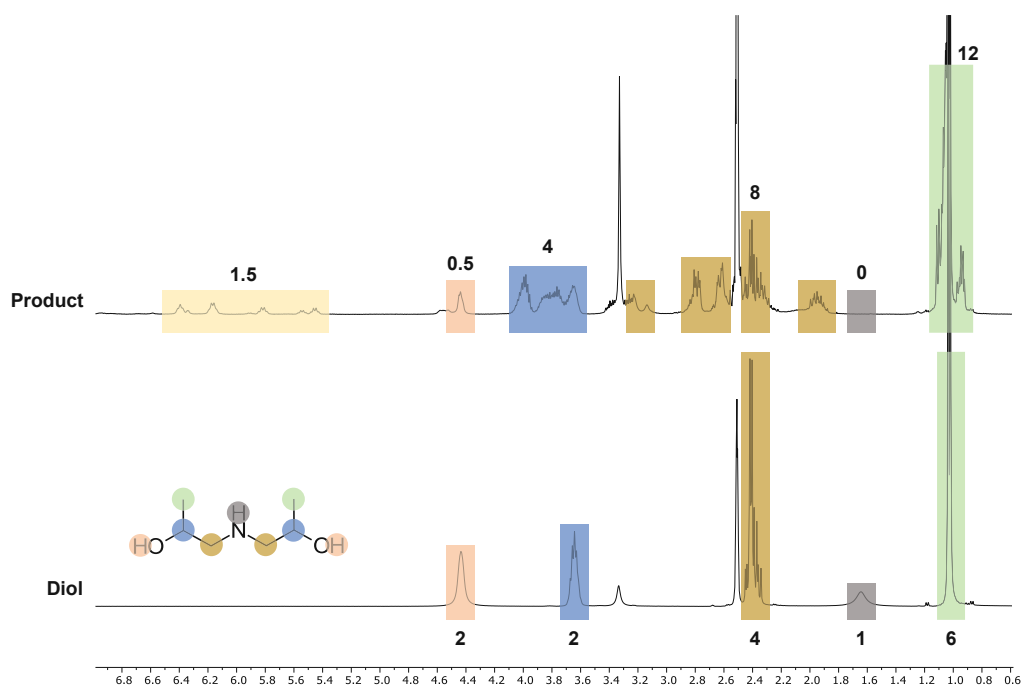
Figure 68: ^{1}H-NMR of the diol starting material (bottom) and the product (top) in DMSO.

The addition of Na_2SO_4 facilitates the condensation of the amine moiety to the hypodiboronic acid, which is why in another attempt, a Dean-Stark apparatus was used to perform the reaction. In this case also toluene instead of benzene was used (Figure 69).
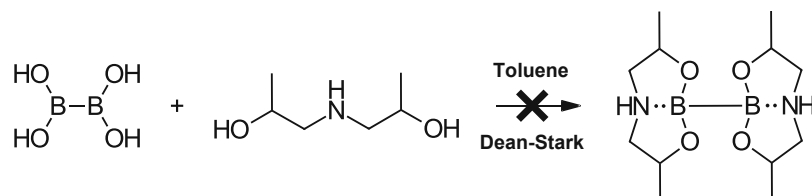
Figure 69: Reaction scheme of the condensation of hypodiboronic acid with a secondary amine bearing diol, using a Dean-Stark apparatus to capture the water, yielding the diboronic compound BN-3.

After 24 h the formation of 1.5 mL water was confirmed in the Dean-Stark apparatus, which corresponds to almost full conversion. However, after 5 more hours of reaction time the same amount of water was separated, which led to the conclusion that the reaction was complete. Unfortunately, the NMR spectra revealed also the formation of SP-1 instead of the desired product (Figure 70).
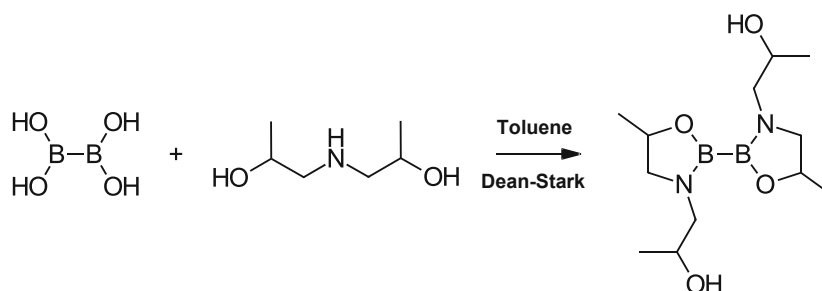
Figure 70: Reaction scheme of the formation of the side product SP-1.

2.1.2. Synthesis of BN-4

To avoid side reactions of secondary amine groups with the diol starting material, as previously discussed, a tertiary amine was used to investigate the synthesis of BN-4 in this chapter (Figure 71).
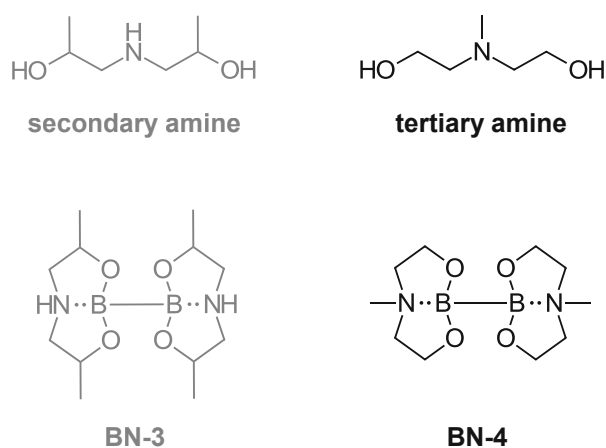
Figure 71: Chemical structure of BN-3 with a secondary amine moiety and BN-4 with a tertiary amine moiety.

The reaction was conducted according to available literature in similar fashion to the synthesis of BN-3, using a Dean-Stark apparatus to capture the water from the condensation reaction in toluene (Figure 72).[97]
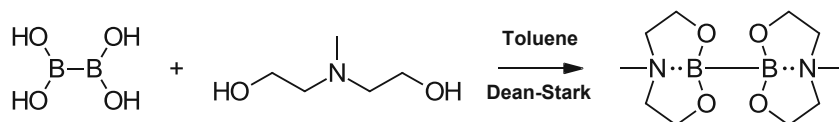
Figure 72: Reaction scheme of the condensation of hypodiboronic acid with a tertiary amine bearing diol, using a Dean-Stark apparatus to capture the water, yielding the diboronic compound BN-4.

As with the synthesis of BN-3, the ^{11}B-NMR showed a very clean peak at 10.5 ppm, which corresponds well to literature values for similar compounds. Also, it is to notice that the peak of the hypodiboronic acid starting material (30.9 ppm) is vanished in the product measurement (Figure 73).
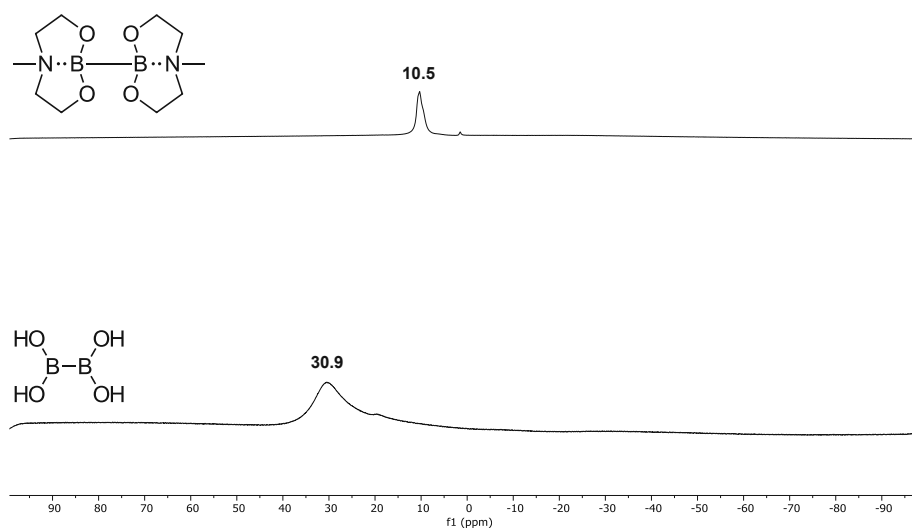
Figure 73: ^{11}B-NMR of the hypodiboronic acid starting material (bottom) and the product BN-4 (top) in DMSO.

The ^{1}H-NMR of the product indeed reveals the complete conversion of the alcohol as the hydroxy peak at 4.34 ppm is completely vanished (Figure 74). However, the CH$_2$-signals as well as the CH$_3$-signal are shifted in the product spectrum.
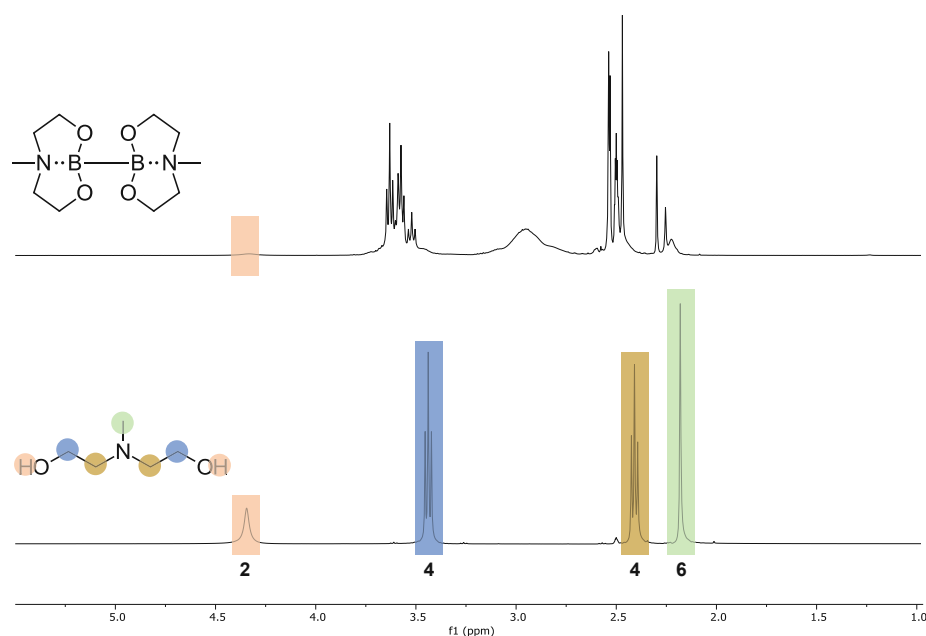
Figure 74: ^{1}H-NMR of the diol starting material (bottom) and the product BN-4 (top) in DMSO.

Furthermore, additional peaks can be observed as well as a strong broadening. Since diboranes are effective reducing agents, it can be argued that the NMR solvent DMSO is

oxidizing the product BN-4 in the NMR tube. Therefore, a change of the NMR solvent to D_2O was done.
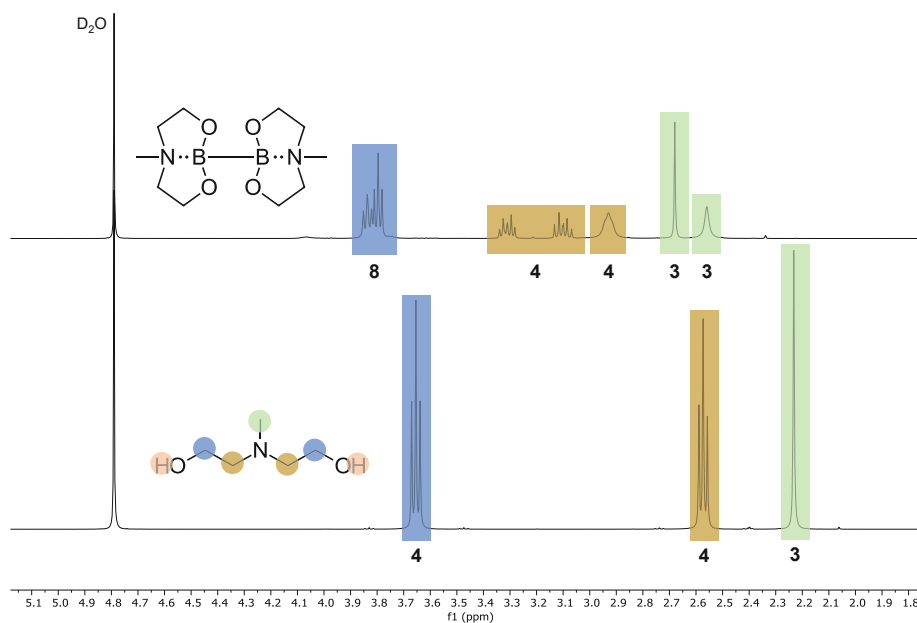
Figure 75: ^{1}H-NMR of the diol starting material (bottom) and the product BN-4 (top) in D_2O.

Indeed, it is shown that product formation has taken place as the integrals match perfectly with the suggested structure of BN-4, however, the compound proved to lack stability even in inert atmosphere and was not further used as an initiator.

It can be concluded that the addition of amine-diols to hypodiboronic acid is not as straight forward as it might seem at first glance. The addition of diols with secondary amine moieties did not work sufficiently and only side product was formed. The addition of a diol with a tertiary amine moiety proved to be challenging as well, however, BN-4 was synthesized successfully.

2.1.3. Synthesis of B6-2

Efforts were also made to synthesize a sp^2-sp^2 hybridized diborane. The commercially available diboranes depicted in Figure 76 can be categorized to the same family of diborane compounds as they are both solely aliphatic with a six-membered ring containing the respective boron centers. In order to complete the row of diborane compounds with increasing steric demand in proximity to the boron-boron bond, B6-3 was to be synthesized.
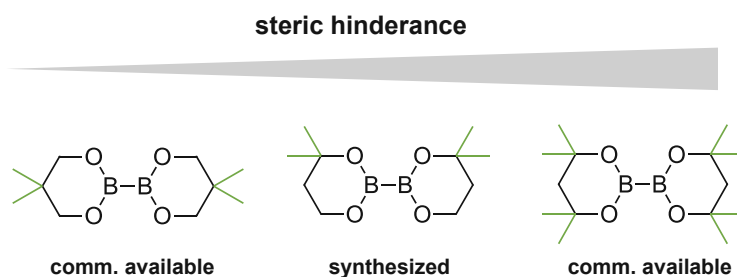
Figure 76: Diborane compounds B6-1, B6-2 and B6-3 having increased steric demand close to the boron-boron bond.[99]

It is reported that $B_2(NMe_2)_4$ undergoes similar condensation reactions with diols as hypodiboronic acid. Therefore, the highly reactive $B_2(NMe_2)_4$ was used to study the synthesis of B6-2 (Figure 77).[97]
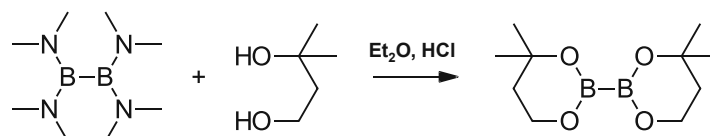
Figure 77: Reaction scheme for the synthesis of B6-2 from $B_2(NMe_2)_4$ and the corresponding diol.

The starting materials were stirred in dry Et_2O for 12 h at room temperature. Thereafter, 1M HCl in Et_2O was added and after 6 h hours of stirring at room temperature the mixture was filtrated, the solvents evaporated and the product recrystallized from *n*-hexane to yield white crystal needles with a melting point of 65 °C. The ^{11}B-NMR showed a clear shift of the peak of the starting material to the product, which is in perfect agreement with literature. (Figure 78).[100]
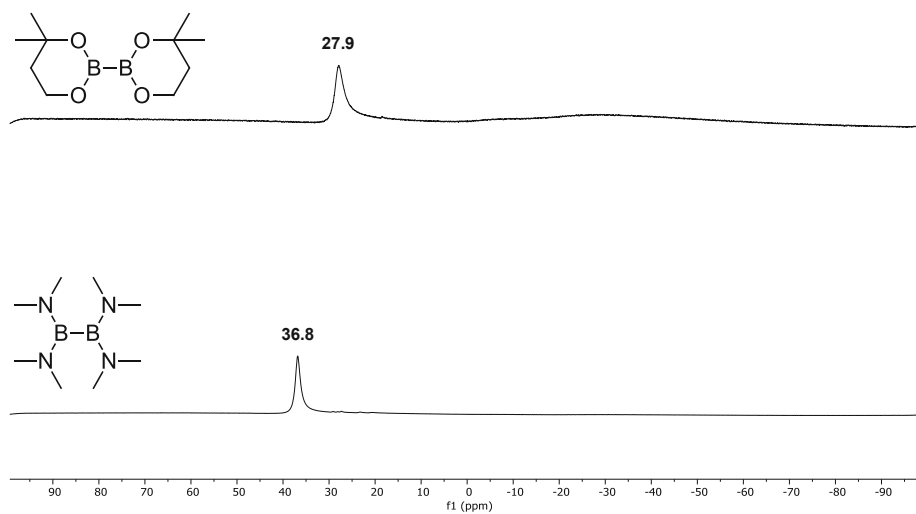
Figure 78: ^{11}B-NMR of the $B_2(NMe_2)_4$ starting material (bottom) and the product B6-2 (top) in DMSO.

The ^{1}H-NMR also showed perfect correlation of the peaks and integrals to the expected product (Figure 79).
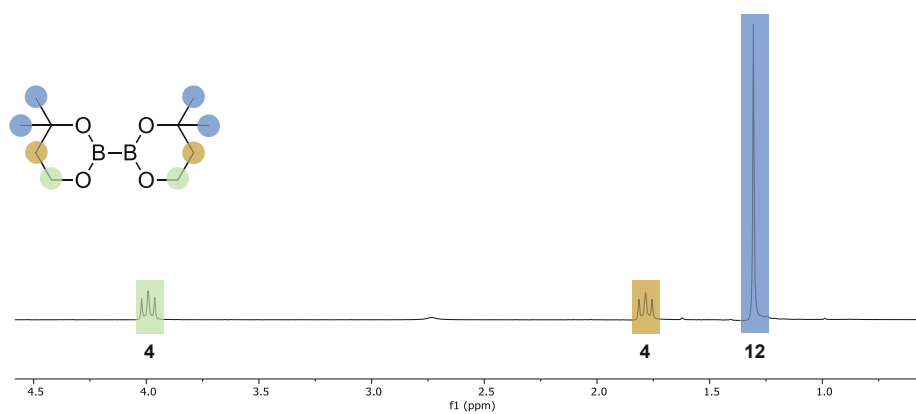
Figure 79: ^{1}H-NMR of B6-2 in CDCl$_3$.

The integrals and shifts are in perfect agreement to literature.[97]

2.2. Scope of the Radical Polymerization System

The successful synthesis of diboranes led to the investigation of the whole 2K initiation system that is intended to have a diborane in one component and a copper compound in the other component. Therefore, a study was performed, investigating various commercially available and synthesized diboranes and copper compounds for their ability to lead to an initiation of a radical polymerization of a methacrylate resin. Furthermore, also commercially available disilanes and digermanes will be evaluated.

The monomer mixture that was used in the following experiments is depicted in Figure 80. The mixture is referred to as 3Mix.
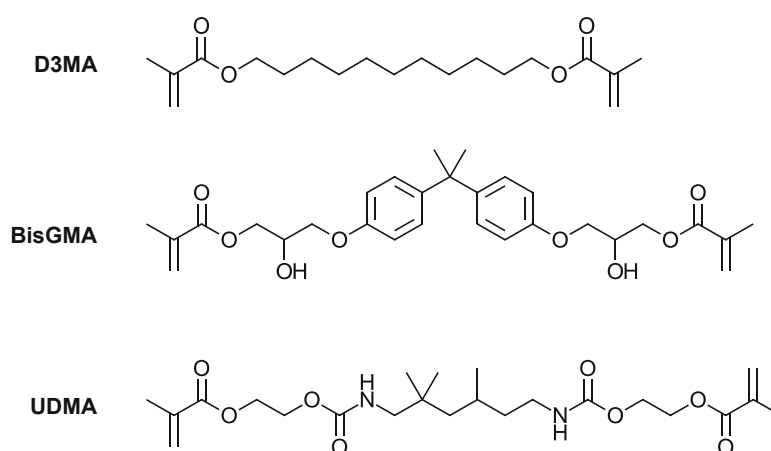
Figure 80: Chemical structure of the monomer mixture 3Mix, consisting of 20wt% D3MA, 40wt% BisGMA and 40wt% UDMA.

2.2.1. Screening of Diboranes

The investigated diborane compounds were categorized in four groups. The first two groups are referring to the ring size next to the B-B bond, 6-membered rings and 5-membered rings (Figure 81).

6-membered ring   **5-membered ring**

B6 -   **B5 -**

Figure 81: Schematic view of the ring size next to the boron-boron bond that led to categorizing of the diborane compounds.

Concerning the B6- category, different grades of steric hinderance were chosen for substituents on the ring (see Figure 82). B6-1 experiences very view steric demand in proximity of the B-B bond, B6-3 is more demanding as the two methyl groups shift from para to ortho

position. The highest steric hinderance shows B6-2, with four methyl groups in ortho position on each ring.
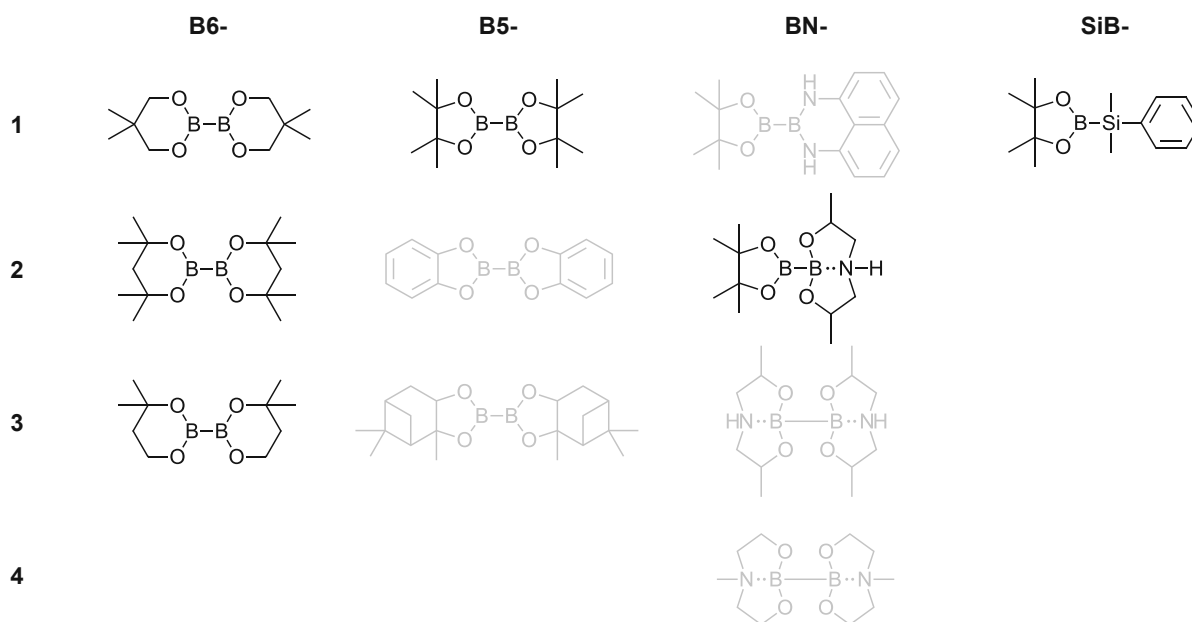
Figure 82: Chemical structures of the investigated diborane compounds and the silylborane compound. They are categorized in four categorys B6-, B5-, BN- and SiB-.

The B5- category contains the very common B_2pin_2 (here B5-1) and then increasing steric demand with different electrochemical effects. The phenyl moiety of B5-2 leads to very electron rich B-B bond and the aliphatic ring structure shows high steric demand with no significant electrochemical influences. In the BN- category, BN-1 exhibits a B-N bond next to the B-B bond, which leads to a very electron poor B-B bond and therefore should significantly stabilize this bond. On the other side, BN-2 has a donating nitrogen atom leading to a very electron rich B-B bond with high steric demand at the same time. The synthesized compounds BN-3 and BN-4 are symmetrical versions of BN-2. As for the SiB- category, SiB-1 was investigated as it is reported to be the most stable Si-B bond and frequently used in organic synthesis.[101] All mentioned boranes are depicted in Figure 82 and were investigated regarding their ability to initiate the polymerization of 3Mix, when combined with a formulation of 3Mix that is containing Cu(acac)$_2$. The respective experiments were performed at room temperature under air and it was observed, if a polymerization reaction would occur within 1 h.

The grayed-out compounds (Figure 82) did not successfully lead to a polymerization of 3Mix, however, the highlighted compounds led to a polymerization of 3Mix in combination with a formulation containing Cu(acac)$_2$. This leads to the conclusion that certain diboranes show

reactivity towards polymerization and therefore radical generation with Cu(acac)$_2$. However, the grayed-out diborane compounds were spared out from further experiments due to stability or reactivity problems. Compound B5-2 was unfortunately too reactive to be properly stabilized in 3Mix to perform reliable and reproducible experiments. Therefore, it was considered unsuitable as even high amounts of TEMPO were not enough to stabilize the formulation. Compound B5-3 on the other hand was too unreactive, caused by the bulky nature of the molecule. The same conclusion was drawn for BN-1, as it was too unreactive. In this case the nitrogen atoms next to the boron atoms stabilize the B-B bond and make it less reactive. Compound BN-3 could not be successfully synthesized and BN-4 is too unstable under atmospheric conditions and decomposes at room temperature.[95] For all further experiments, B6-1, B6-2, B6-3, B5-1, BN-2 and SiB-1 were considered as suitable initiators.[99]

2.2.2. Screening of Disilanes and Digermanes

In addition to the evaluated diboranes, different classes of compounds, including disilanes and digermanes depicted in Figure 83 were investigated regarding their ability to initiate radical polymerization after reacting with copper compounds.
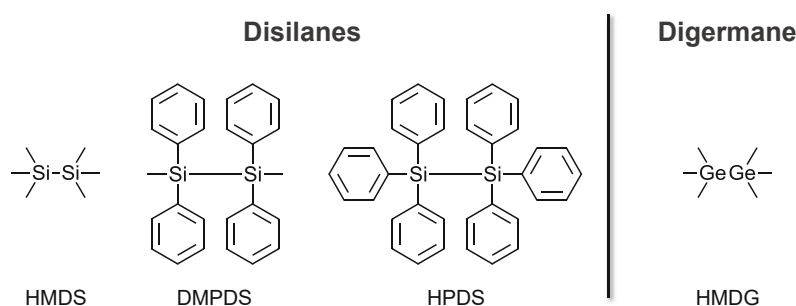
Figure 83: Chemical structures of disilanes HMDS, DMPDS and HPDS and the digermane HMDG that were investigated towards polymerization reactivity with the respective metal complexes.

It was shown that the phenyl substituted silanes were not sufficiently soluble in 3Mix, however, neither the HMDS nor the digermane showed polymerization reactivity in combination with formulations containing Cu(acac)$_2$. Therefore, this class of compounds was not investigated any further and the focus was set on diboranes.

2.2.3.   Screening of Metal Salts as Polymerization Catalysts

Previous experiments led to the conclusion that a variety of diborane compounds are suitable as initiators for polymerization of methacrylates when combined with Cu(acac)$_2$. However, it is also of interest to investigate other transition elements for this purpose. Therefore, a screening was conducted to study the reactivity of different metal complexes in combination with a highly reactive borane compound (SiB-1). Formulations of 3Mix (UDMA:BisGMA:D3MA = 2:2:1) with 0.2 mol% of the metal complex were prepared. Also, formulations of 3Mix containing 7 mol% SiB-1 were prepared and the two formulations were mixed (50wt%:50wt%). In the following Figure 84 an excerpt of the periodic table of elements is depicted, focusing on group 5-12 elements. The highlighted metal complexes were used in the screening.

Group 5 - 12 elements:

5	6	7	8	9	10	11	12
V(III)acac$_3$ V(IV)Oacac$_3$	Cr(III)acac$_3$	Mn(III)acac$_3$	Fe(III)acac$_3$	Co(II)acac$_2$ Co(III)acac$_3$	Ni(II)acac$_2$	Cu(II)acac$_2$ Cu(II)tfacac$_2$ Cu(II)hfacac$_2$ Cu(II)ac$_2$ Cu(I)ac	Zn
Nb	Mo	Tc	Ru	Rh(III)acac$_3$ Rh(I)(PPh$_3$Cl)	Pd(II)acac$_2$ Pd(II)ac$_2$ Pd(II)(PPhFc)Cl$_2$	Ag(I)ac	Cd(II)acac$_2$
			Os	Ir	Pt(II)acac$_2$	Au	Hg

Figure 84: Schematic excerpt of the periodic table with focus on period 4-6 and group 5-12. The investigated acetylacetonates, acetates or other salts of the respective elements are given. Spared out elements are greyed out. Vanadium- and manganese salts (highlighted in yellow) led to very little polymerization of 3Mix in combination with SiB-1 formulations. Cu(II) and Cu(I) salts (highlighted in green) led to fast polymerization of 3Mix when combined with SiB-1 formulations.

The testing of over 20 metal complexes showed that only copper salts are active catalysts for the generation of radicals for polymerization. Vanadium III & IV complexes and manganese II complexes led to minor polymerization. Interestingly, most of the investigated metals are described in literature together with SiB-1 or other diborane compounds for borylation reactions.[101] However, they seem to be unable to catalyze the cleavage of these compounds with the result of radical formation.[99]

3. Chemical Mechanism and Linear Polymers

To this date, the application of diboranes such as B_2pin_2 and B_2cat_2 are limited to borylations and similar reactions. They are catalyzed by transition metals (Pt, Pd, Rh, Cu) or organo-catalyzed by phosphines and e.g., Lewis bases. The molar ratio in those reactions is often very high with 1 equivalent reactant and 1.2 equivalents diborane with 10 mol% catalyst.[102]

Referring to the previous chapter, it was found that working in bulk methacrylates with diborane species and copper species as a two-component system (2K-system) in low molar concentrations (< 10 mol%) relative to the double bonds can lead to a polymerization of the respective monomers.

Since this diborane/Cu initiation system is completely new the mechanism has to be investigated first. Literature stated that the combination of diboranes and copper species in higher molar ratios lead to different products in organometallic synthesis than they do in this study with low molar concentrations. All that can be said to this point in time is that a radical polymerization mechanism is very likely because methacrylates are readily polymerized in a radical way (Scheme 6).[99]
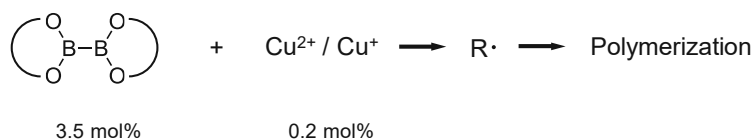
Scheme 6: A suggested scheme for the reaction between diborane and Cu species in low molar concentrations to yield radicals that can initiate the polymerization of the monomer.

To prove this hypothesis, several experiments are necessary concerning the initiation mechanism as well as the propagation mechanism.

3.1. Initiation

The work discussed in this chapter was performed by Konstantin Knaipp and Prof. Georg Gescheidt-Demner at TU Graz.

The initiation of the polymerization is a crucial part of the whole polymerization process. If the diborane/Cu initiated polymerization follows a radical polymerization mechanism, the reaction of a diborane with a copper salt has to lead to the generation of initiating radicals. With electron paramagnetic resonance (EPR) measurements including a spin-trapping (ST) agent, radicals can be detected and predictions about the nature of the radical can be made. This is particularly useful to investigate the diborane/Cu system and the radicals that are formed during the initiation reaction. Therefore, EPR-ST measurements were conducted with two different diboranes (B5-1 and B6-1) and two different copper species (Cu(acac)$_2$ and Cu(ac)$_2$ or Cu(OAc)$_2$), depicted in Figure 85.
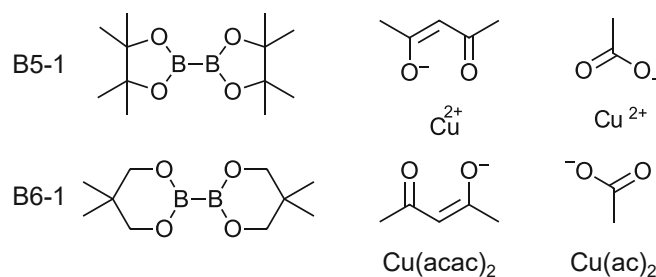
Figure 85: Diborane compounds (B5-1 and B6-1) and Cu species (Cu(acac)$_2$ and Cu(ac)$_2$) investigated in the EPR-ST measurements.

The formed radical species from the reaction of diborane with Cu was trapped with a trapping agent, 5.5-dimethyl-1-pyrrolin-N-oxide (DMPO). The adduct consisting of the trapped radical and DMPO can further be detected by the EPR measurement (Scheme 7).
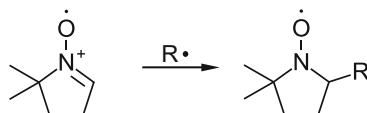
Scheme 7: DMPO forms a stable adduct with free radicals that reacts no further. This stable radical is then detectable by EPR measurements.

The best spectrum could be recorded for the B5-1/Cu(ac)$_2$ system 30 minutes after the start of the reaction. Because of the radical's good stability many spectra could be recorded, leading to a high signal/noise ratio.

At first glance the spectrum consists of four lines of similar intensity with equal spacing. Using the WinSIM program, the spectrum could be simulated using the following hyperfine coupling constants: a(N) = 1.39 mT and a(H) = 1.22 mT. While a spectrum containing one I = 1 and one I = 0.5 atom should contain six lines, the similar hyperfine coupling constants and large linewidths result in two lines being very poorly visible. Using a DPPH (2,2-diphenyl-1-picrylhydrazyl) reference the g-factor of the nitroxide radical adduct was determined to be g = 2.0069, which is within the expected range for a nitroxide.[2] A comparison of the recorded spectrum and its simulation is shown in Figure 86.
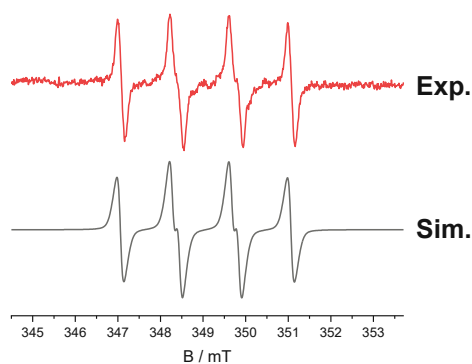
Figure 86: The EPR spectrum of the nitroxide radical adduct produced by the DMPO + B5-1 + Cu(ac)$_2$ system and a comparison to its simulation with a(N) = 1,39 mT and a(H) = 1,22 mT.

To confirm that the recorded spectrum is not the result of an artefact, several control experiments were conducted. The results of these experiments are shown in Figure 87. A pure solution of DMPO shows no signal, as does a solution of B5-1 and Cu(ac)$_2$ without the radical trap. Solutions of only the diborane or Cu(ac)$_2$ with DMPO are also EPR-silent.
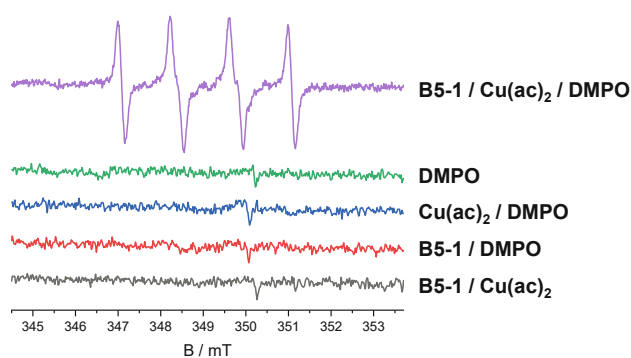
Figure 87: A comparison of the EPR spectra obtained during the control experiments. Only the combination of B$_2$pin$_2$ with Cu(ac)$_2$ as well as the radical trap DMPO shows a signal.

The fact that pure B5-1 with DMPO does not yield any detectable number of radicals is very good and speaks for its stability. Also, it proves that the radicals are really only formed when the reaction between the diborane and Cu species can occur.

The radicals produced by B6-1 and Cu species are very short lived and are detected much earlier (approx. 4 minutes after mixing) than the B5-1 radicals. This results in fewer spectra and therefore a poor signal/noise ratio of the measurement. The spectra recorded with $Cu(acac)_2$ as the Cu species do also have a poorer signal/noise ratio, which is because of the poor solubility of $Cu(acac)_2$ in acetonitrile. The compared spectra of all four diborane/Cu combinations are depicted in Figure 88.
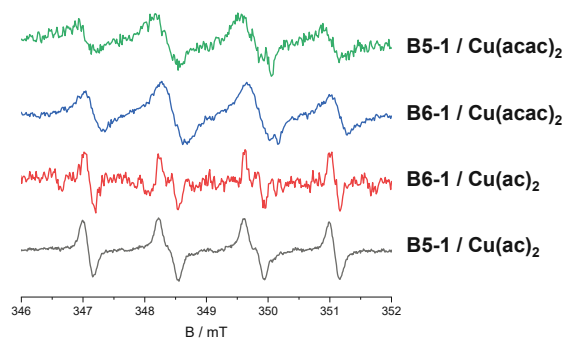
Figure 88: A comparison of the recorded EPR spectra of the 4 different copper salt/borane systems.

While the size of a(N) mostly depends on the polarity of the solvent and electron donating/withdrawing effects, a(H) is related to the dihedral angle between the p-orbital of the N-O group and the $C-H_\beta$ bond. This angle is influenced by the steric bulk of the trapped radical species. Since all nitroxide adducts have similar a(H), it can be inferred that all trapped radicals are of similar size.

These findings hint that boryl radicals are formed. The detection time of the occurring radicals depends only on the diborane species and the radicals are of similar size. If acetylacetonate radicals and acetate radicals would be formed they would differ highly in the size comparison.[99]

3.2. Propagation

After the initiation of the polymerization through the reaction of diborane and copper, leading to the formation of boryl radicals, the propagation of the radicals during the polymerization of the monomer follows. The boryl radicals react with the double bonds of the monomer mixture resulting in the generation of a polymer. The propagation might be inhibited by acidic species yielding H^+, if it was anionic; it might be inhibited by basic species yielding OH^-, if it was cationic; and it might be inhibited by stable radicals such as TEMPO if the propagation follows a radical mechanism. To investigate, whether the propagation step is anionic, cationic or radical, a study was performed with B6-1 and $Cu(acac)_2$ in 3Mix to see which of the respective species (H^+, OH^-, radicals) can inhibit the polymerization. The formulations prepared for this experiment are depicted in Table 17.

Table 17: Formulations prepared for Rheo/IR experiments to investigate the inhibition of the polymerization resulting from B6-1 and $Cu(acac)_2$ in 3Mix.

	B-formulation	Cu-formulation
B6-1 (mol%)	3.5	-
$Cu(acac)_2$ (mol%)	-	0.2
3Mix (mol%)	96.5	96.3
AcOH/Pyridine/TEMPO (mol%)	-	3.5

The polymerization reaction was followed by rheology/IR measurements tracking the storage modulus (G') and the double bond conversion (DBC) via transmission NIR during the polymerization. This characterization technique allows for simultaneous measurement of rheological data G' and G'', while measuring transmission MIR of the sample, tracking the double bond conversion via integration of the methacrylic C=C band at 6140 cm^{-1}. A total of 200 mg of formulation is used for the following measurements, having a 45 s mixing step in advance of the data recording to ensure a homogeneous mixture of the 2K system. Schematic measurements of G' and the DBC are shown in the following Figure 90 highlighting important characteristics G'_{end}, t_{gel} and DBC_{end}.
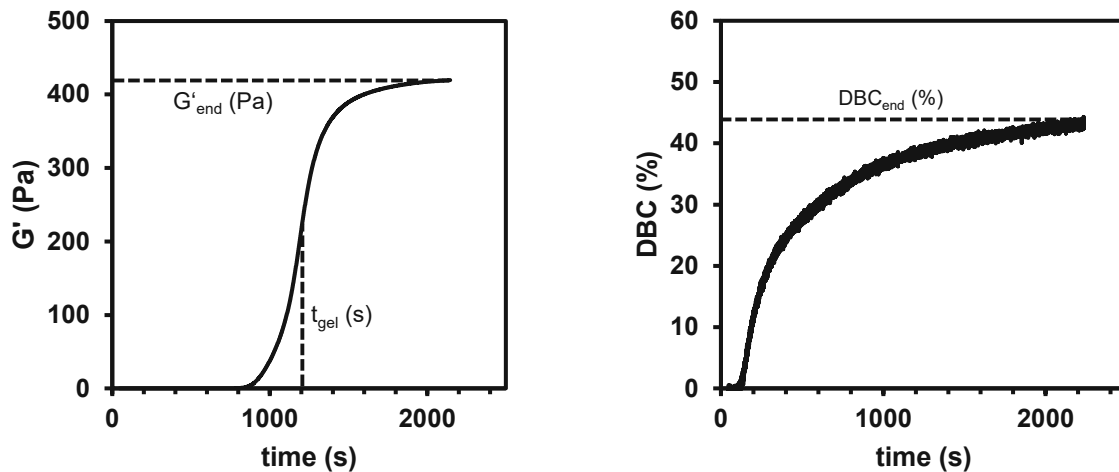
Figure 89: Schematic measurements of G' and the DBC are shown highlighting important characteristics G'$_{end}$, t$_{gel}$ and DBC$_{end}$.

The information derived from the measurements of G' are enormous, giving the analysis of G'$_{end}$ referring to the mechanical strength of the polymer at the end of the polymerization. Another important value is t$_{gel}$ which is referred to as the gel time in these measurements. Often, the cross section of G' and G'' are used to evaluate t$_{gel}$, however, for 2K systems it is much more reproducible to take the steepest increase of G' as t$_{gel}$.[79]

The measurements are depicted in Figure 90.
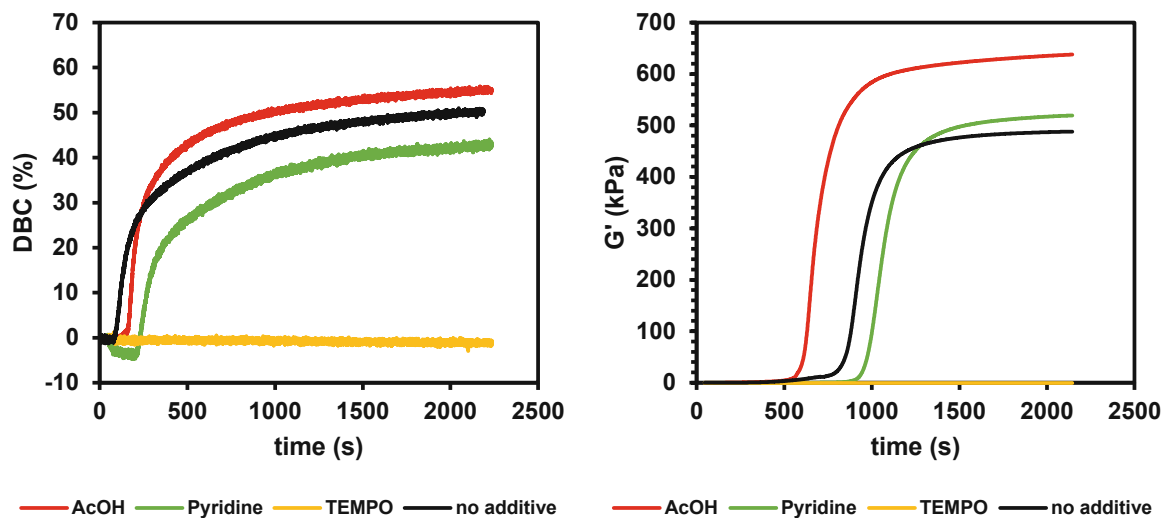
Figure 90: Left the DBC of the polymerization reaction is shown with each additive: AcOH, Pyridine, TEMPO and no additive. In the right graph the progess of the storage modulus of these reactions is shown.[99]

AcOH (H$^+$) clearly leads to a slight increase in reactivity, which can also be stated from Table 18. Furthermore, the DBC$_{end}$ is also slightly higher than without additives, which can lead to the conclusion that AcOH does not inhibit the polymerization, but even enhance it a little. In contrast, pyridine (OH$^-$) does only exhibit a small delay in the polymerization, but does not inhibit it either.

Table 18: The results of the Rheo/IR measurements including t_{gel}, G'_{end} and DBC_{end} are shown for each additive.

	t_{gel} (s)	G'_{end} (kPa)	DBC_{end} (%)
AcOH	646	638	55.0
Pyridine	1029	519	42.9
TEMPO	-	-	-
no additive	912	488	51.0

The addition of TEMPO (stable radical) on the other hand does completely stop the polymerization process. All the radicals generated during the initiation process are captured by TEMPO and cannot lead to a propagation. This confirms the radical nature of the initiation providing boryl radicals as well as the radical propagation step.[99]

3.3.   Proposed Mechanism

The previous studies of initiation and propagation of the polymerization of 3Mix initiated by the diborane/Cu 2K system led to deep insights into mechanistic details of the polymerization reaction.

In EPR-ST measurements with different diboranes and copper compounds it was found that boryl radicals are generated by the reaction of diborane with copper. This reaction is postulated to be catalyzed by the acac⁻ or ac⁻ ligand of the copper central atom (Figure 91).
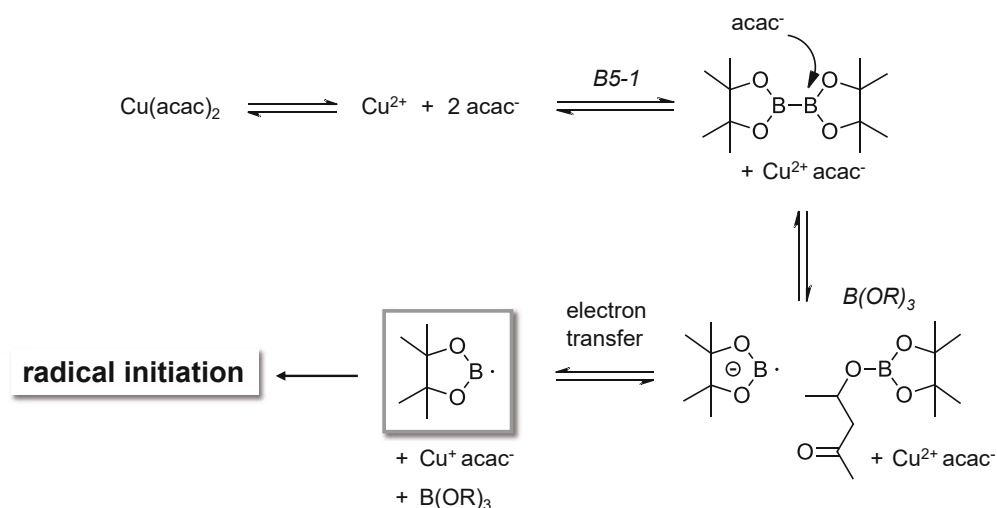
Figure 91: The proposed mechanism of the initiation reaction of the diborane/Cu 2K system is depicted. It includes the release of the acac⁻ ligands, then catalyzing the cleavage of the diborane, leading to a reduction of copper by the radical anion. The generated boryl radicals can then initiate the radical polymerization of methacrylates.

This catalyzed cleavage of the diborane bond leads to the formation of a highly reactive radical boryl anion. This species is able to readily reduce Cu^{2+} to Cu^+ and leave behind an uncharged boryl radical. This reaction can then even reoccur with Cu^+ being reduced to elemental Cu^0. The generated boryl radical is able to initiate the radical polymerization of methacrylic double bonds as found in rheology/IR measurements.[99]

3.4. Cyclovoltammetry

The proposed mechanism of the diborane/Cu 2K system initiation leads to the assumption of a redox reaction between the diborane and the copper compound, as Cu^{2+} is reduced to Cu^+ and further.

A main characteristic of redox initiators is the redox potentials of such, as the redox reaction that leads to the formation of radicals is highly dependent on it. To evaluate these electrochemical properties, cyclovoltammetry is a convenient tool. In this study, six diboranes and five copper compounds were investigated regarding their reduction and oxidation potentials.

In advance of the measurements, 5 mg of the analyte was weighed out and dissolved in dry acetonitrile (ACN) with 0.1 M tetra-butylammonium hexafluorophosphate as electrolyte. To evaluate the oxidation/reduction potential of the target molecule, a standard measurement was performed with ferrocene. The standard potential ($E_{0\text{-exp}}$) of ferrocene was experimentally determined using Equation 4 and compared to a literature value.[72] The difference between

the determined value and the literature value was added as a factor to all the other measurements as correction.

Equation 4: Determination of the experimentally found standard potential of ferrocene in ACN.

$$E_{0-exp} = \frac{E_{red} + E_{ox}}{2}$$

The values for E_{red} and E_{ox} can be retrieved from the respective measurement as shown in Figure 92. The potential at the positive peak when going from left to right marks the oxidation potential and the potential at the negative peak when going from right to left marks the reduction potential.
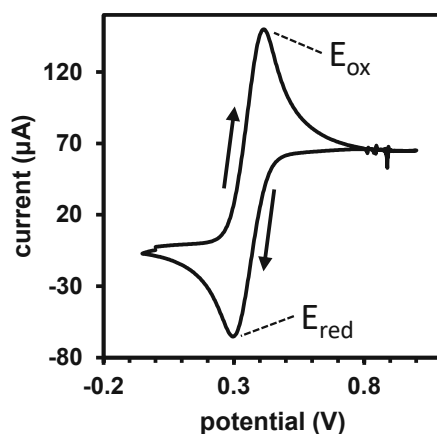
Figure 92: Voltammogram of ferrocene in ACN with marked oxidation potential (E_{ox}) and reduction potential (E_{red}) as well as the direction of the potential cycle.

The determination of the reduction potential as well as the oxidation potential was performed for every redox active compound used in the following chapter, including the six diboranes and five copper compounds.

3.4.1. Investigation of Cu Compounds

As the copper central atom is reduced during the initiation by the diborane it is of great importance to investigate the influence of the ligand onto this reduction, which can be done by cyclovoltammetry, evaluating the reduction and oxidation potential of the respective copper compound. The structures are depicted in Figure 93.
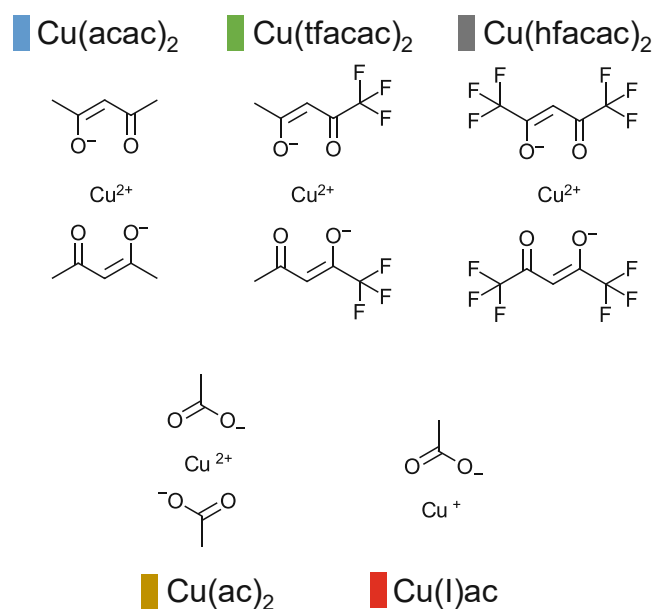
Figure 93: Structures of the investigated Cu compounds.

The respective voltammograms are depicted in Figure 94.
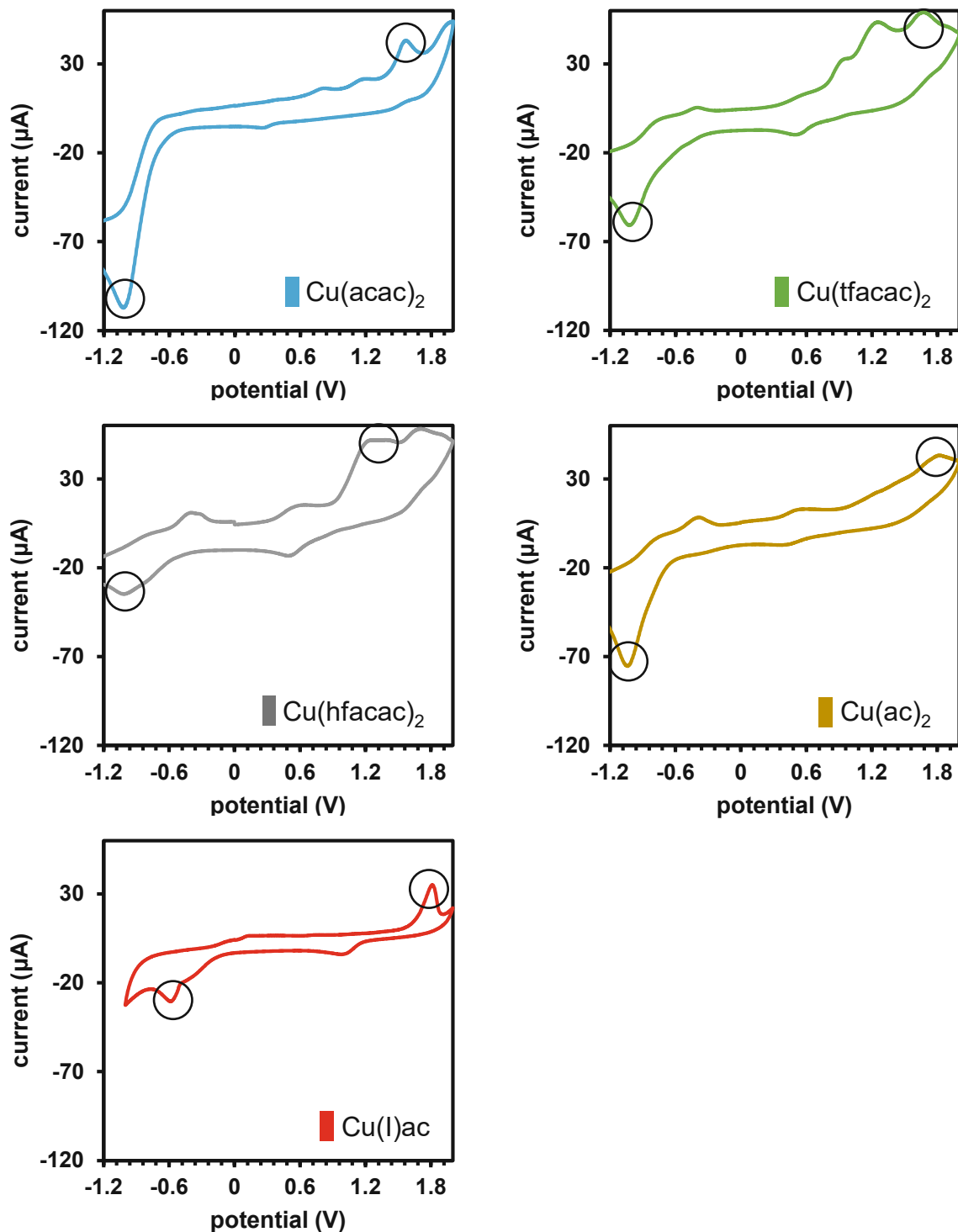
Figure 94: Cyclic voltammograms of the investigated Cu compounds between -1.2 V and 2 V (second cycle). The relevant signals are marked with black circles.

The first thing that is noticed is that although it is mostly Cu(II) compounds, the cyclic voltammograms do look very different for the respective species. The voltammogram of Cu(acac)$_2$ exhibits very clear peaks for reduction and oxidation. During the oxidation some minor peaks are visible that can be asserted to some irreversible oxidation processes,

however, the main peak with E_{Ox}=1.62 V of Cu(acac)$_2$ is clearly shown. The same is true for the reduction where a clear reduction potential with E_{Red}=-0.97 V is visible. It is noticed that neither the oxidation nor the reduction is truly reversible according to the cyclic voltammogram as they have no reduction or oxidation peak in a 0.57 V spacing.[74] This indicates that during the polymerization initiation reaction other Cu species are formed that can be reversibly reduced and oxidized.

For Cu(tfacac)$_2$ and Cu(hfacac)$_2$ only the first of the two visible oxidation potentials is relevant for this study. Also, for these compounds two reduction potentials can be distinguished, however, the first reduction seems very minor compared to the big reduction peak around -1 V. Interestingly, Cu(ac)$_2$ show a very late oxidation with an E_{Ox}=1.84 V. However, here a hint for a reversibility in the reduction is visible. Cu(I) also shows this very high oxidation potential and also a relatively high reduction potential with E_{Red}=-0.57 V. The values for the calculated oxidation potentials and reduction potentials are shown in Table 19.

Table 19: Values for the calculated oxidation potentials (E_{Ox}) and reduction potentials (E_{Red}).

	E_{Red} (V)	E_{Ox} (V)
Cu(acac)$_2$	-0.97	1.62
Cu(tfacac)$_2$	-0.98	1.30
Cu(hfacac)$_2$	-0.97	1.31
Cu(ac)$_2$	-0.99	1.84
Cu(I)ac	-0.57	1.86

It is clearly seen that the reduction of Cu(II) to Cu(I) is very reproducible for all Cu(II) compounds tested in this study. Also, the oxidation of Cu(I) to Cu(II) for the acetates is in very good agreement with one another.

3.4.2. Investigation of Diboranes

The respective diboranes are necessary for the reduction of the copper compounds, playing an important role in the polymerization initiation mechanism. In order to characterize their electrochemical properties, cyclovoltammetry measurements were conducted using B6-1, B6-2, B6-3, BN-2, B5-1 and SiB-1 (Figure 95).
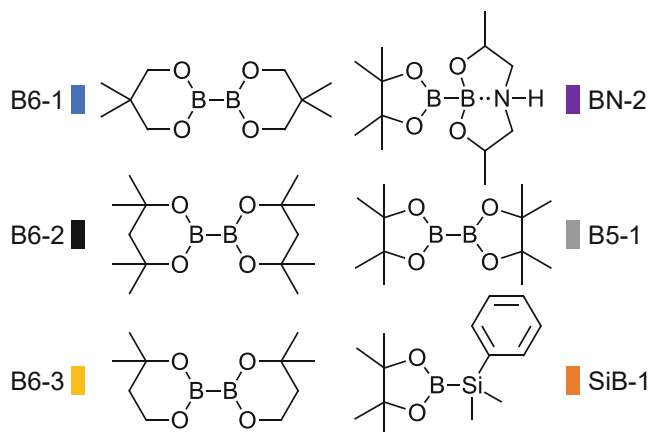
Figure 95: Structures of the investigated borane compounds.

The borane compounds investigated in this study are shown in Figure 95 and the respective cyclic voltammograms in Figure 96.
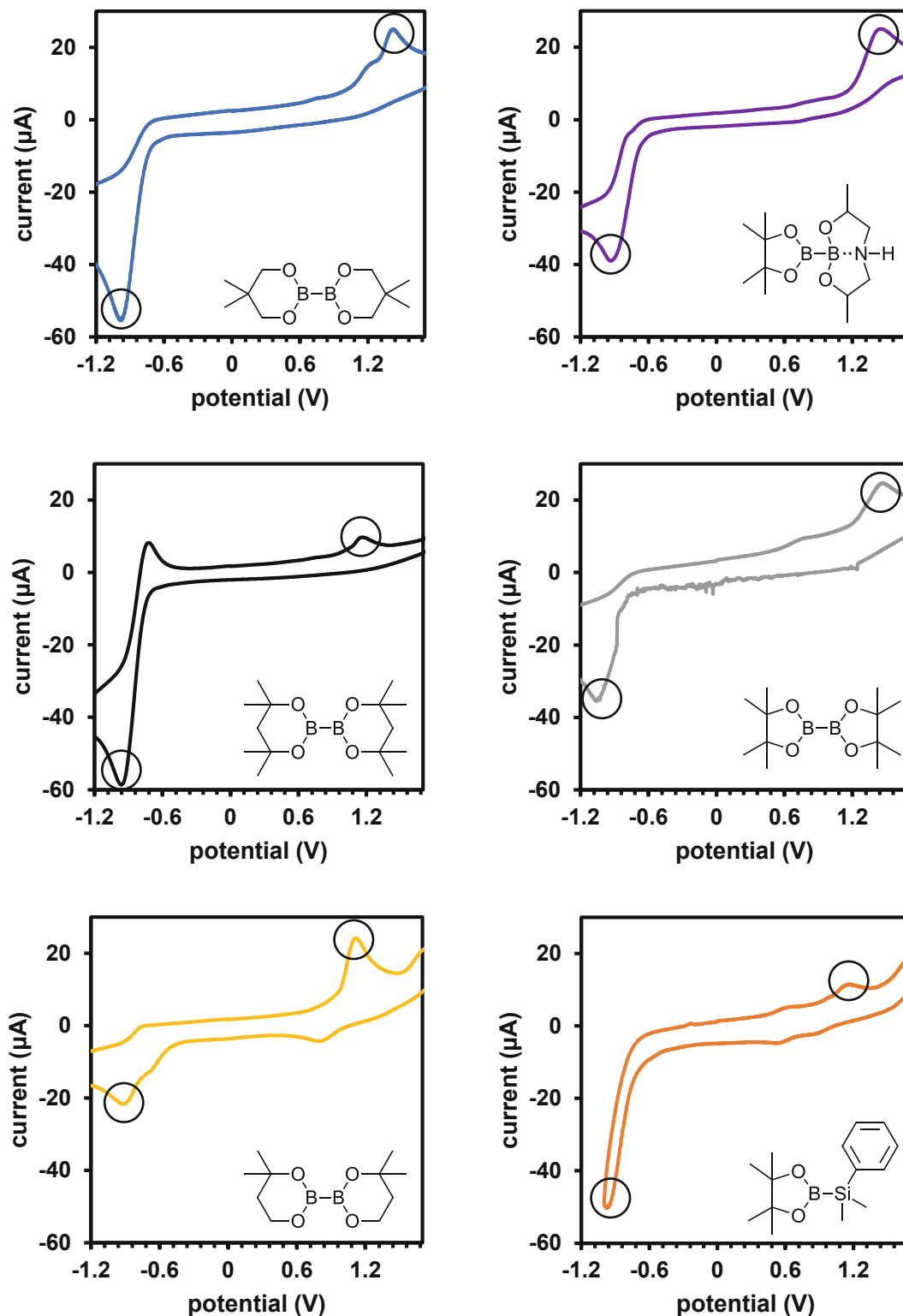
Figure 96: Cyclic voltammograms of the investigated borane compounds between -1.2 V and 1.4 V (second cycle).

The diborane compounds show very clean reduction and oxidation potentials, with an exception of SiB-1. Here, only a small oxidation at E_{Ox}=1.2 V is visible and a very intense reduction potential at E_{Red}=-0.97 V is shown. This indicates more oxidizing than reducing

properties of SiB-1. The compounds B6-1, BN-2, B5-1 and B6-3 exhibit clear irreversible oxidation and reduction potentials. A further exception is B6-2 which is the only investigated compound that shows a reversible reduction potential. The values for the calculated oxidation potentials and reduction potentials are shown in Table 20.

Table 20: Values for the calculated oxidation potentials (E_{Ox}) and reduction potentials (E_{Red}) of the investigated borane compounds.

	E_{Red} (V)	E_{Ox} (V)
B5-1	-1.02	1.50
B6-1	-0.94	1.47
B6-2	-0.92	1.21
B6-3	-0.87	1.16
BN-2	-0.89	1.50
SiB-1	-0.97	1.20

It is to notice that the investigated borane compounds show very similar reduction potentials, which implies that the substituents next to the B-B bond do not influence the electrochemical properties significantly. Although the oxidation potentials differ more, the same trend can be assigned to them. No trend or calculation for the reactivity of these compounds in a reaction with a Cu compound can be predicted from the electrochemical properties, as the initiator molecules show different behavior in monomer solution. However, the cyclovoltammetry measurements confirm a possible redox reaction between the respective copper compounds and diboranes.

3.5.   Linear Polymer Analysis

In order to better understand the polymerization behavior in bulk, experiments using monofunctional methacrylates were performed using the new diborane/Cu 2K radical initiation system. In this regard, focus was lain on rheology/IR measurements utilizing the simultaneous analysis of rheological and kinetic parameters during the polymerization reaction.

3.5.1.   Investigation of Diboranes

The polymerization of benzylmethacrylate (BzMA) (Figure 97) was investigated using a 2K system based on the copper catalyzed cleaving of diborane compounds that initiate radical polymerization without the use of peroxides or amines.[99] To this end, rheology/IR measurements tracking mechanical parameters such as G' and chemical parameters such as the DBC were conducted. Four diborane compounds depicted in Figure 97 were applied together with $Cu(acac)_2$ in respective formulations of BzMA containing 3.5 mol% diborane compound and formulations of BzMA containing 0.2 mol% $Cu(acac)_2$ with respect to the methacrylic double bond. The formulation compositions are shown in Table 21.
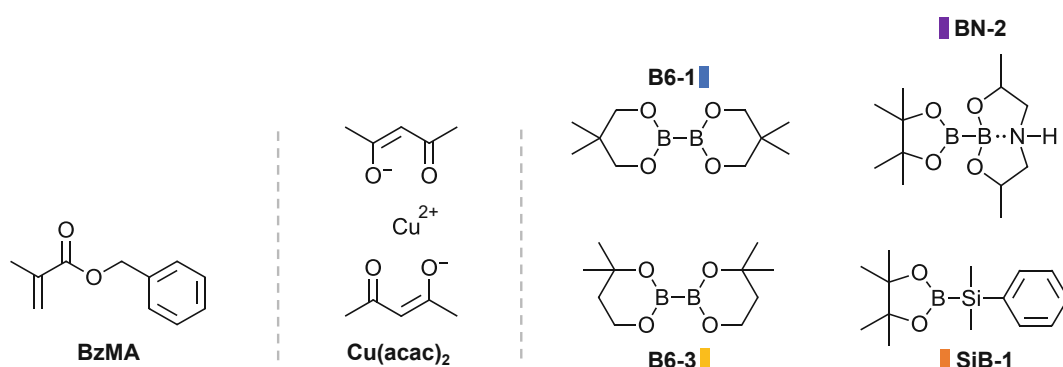
Figure 97: Chemical structures of the monomer benzylmethacrylate (BzMA), the copper catalyst $Cu(acac)_2$ and the diboranes B6-1, B6-3, BN-2 and SiB-1.

Table 21: Composition of the formulations used in this chapter. B-formulations contain diborane and monomer BzMA, while Cu-formulations contain $Cu(acac)_2$ and monomer BzMA.

	B-formulation	Cu-formulation
Diborane (mol%)	3.5	-
$Cu(acac)_2$ (mol%)	-	0.2
BzMA (mol%)	96.5	99.8

Looking at the results regarding the DBC, it is immediately seen that the choice of diborane initiator strongly influences the reactivity of the polymerization reaction (Figure 98). B6-1 and B6-3 seem structurally very similar, however, B6-3 bearing the methyl groups in close proximity to the boron-boron bond is less reactive due to a higher steric demand.[99] Diborane BN-2 showed almost no conversion due to very poor solubility in the monomer. However, silylborane SiB-1 led to more than 50% DBC, owing this to the higher reactive silyl radical.[101, 103] The highest DBC (96%) was achieved using B6-1 as the diborane initiator, observing also a very prominent increase of the slope of the DBC due to the Trommsdorff effect.
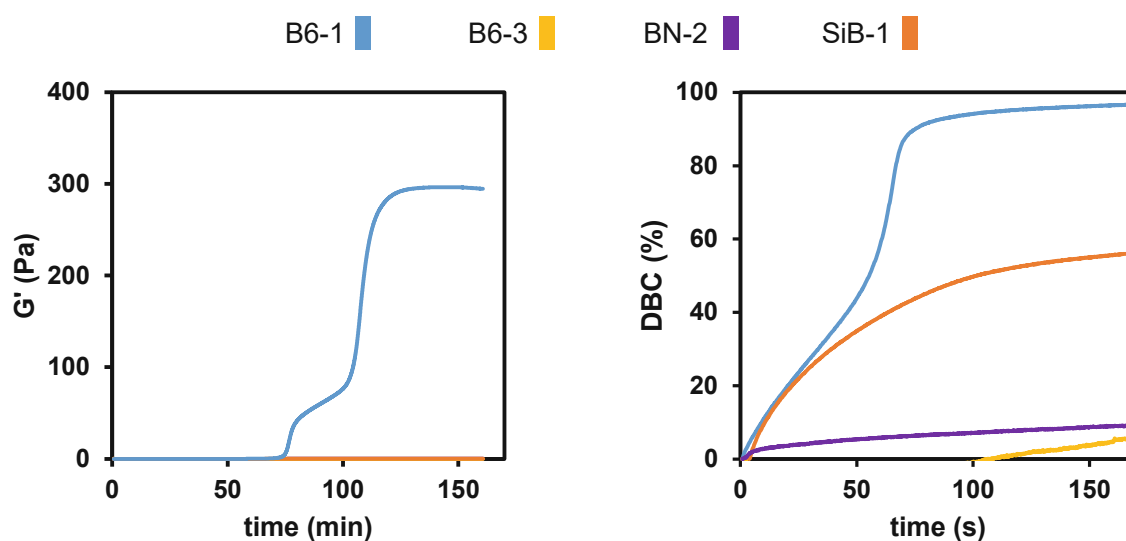
Figure 98: Left diagram: DBC resulting from rheology/IR measurements of the polymerization of BzMA using either 3.5 mol% B6-1, B6-3, BN-2 or SiB-1 and 0.2 mol% Cu(acac)$_2$. Right diagram: G' resulting from rheology/IR measurements of the polymerization of BzMA using either 3.5 mol% B6-1, B6-3, BN-2 or SiB-1 and 0.2 mol% Cu(acac)$_2$.

The rheology/IR method allows for further investigation of the progression of G' during the polymerization. Based on the progression of the DBC one might have thought that G' would follow a similar trend. However, monitoring both characteristic values simultaneously shows that only the polymer derived from B6-1 shows a significant increase in G' and a gel time (t_{gel} = 108 min). This is explained by an overall lesser conversion of the monomer using B6-3, BN-2 and SiB-1.

3.5.2. Bulk Kinetics of the Diborane/Cu System

A deep insight into the polymerization of BzMA with B6-1/Cu(acac)$_2$ (Figure 99) is presented using the coupling of rheology/IR with size exclusion chromatography (SEC). The polymerization using 3.5 mol% B6-1 and 0.2 mol% Cu(acac)$_2$ reaction during rheology/IR measurements was interrupted and was quenched at four different DBCs (27%, 59%, 91% and 97%) and SEC was measured of the respective polymer. This setup led to the diagram depicted in Figure 4 showing a direct comparison of DBC, G' and molecular weight.
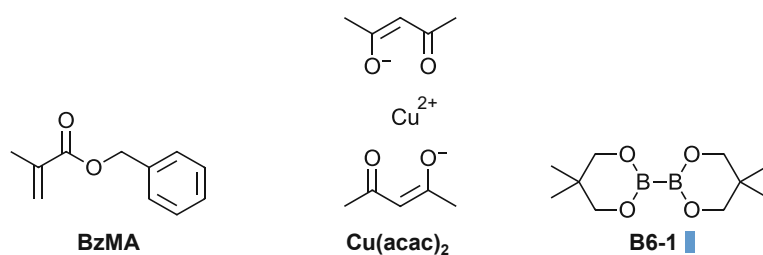
Figure 99: Chemical structures of benzylmethacrylate (BzMA), Cu(acac)$_2$ and B6-1.

The results show an interconnection between the three parameters DBC, G' and molecular weight (Figure 100). Going from low conversions to high conversions in Figure 100 (left), at 27% DBC the bulk formulation is still a liquid; however, the SEC shows the formation of polymer (M_n = 300 kDa). High molecular weight is reached very fast and at already low conversions, leading to few polymer chains dissolved in a lot of bulk monomers.
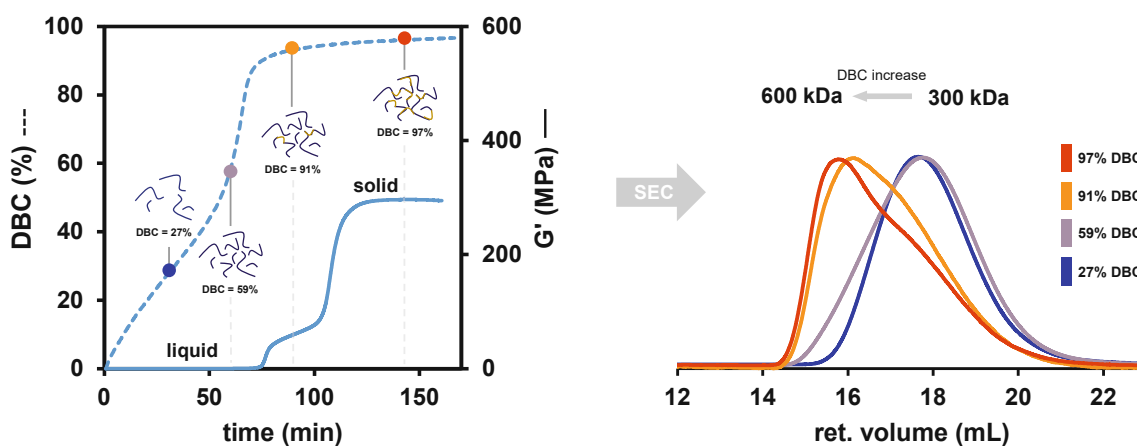
Figure 100: Rheology/IR measurement of the polymerization of BzMA using 3.5 mol% B6-1 and 0.2 mol% Cu(acac)$_2$. At 27% DBC, 59% DBC, 91% DBC and 97% DBC the measurement was interrupted and quenched to perform a SEC measurement. The information derived from the SEC in combination with the rheology/IR led to new conclusions about the formation of the solid polymer and its structure.

When looking at the data point at 59% DBC, the DBC starts to increase steeper due to the Trommsdorff effect, however, the formulation is still liquid (low G') and the molecular weight of the chains remained the same as with 27% DBC (Figure 100, right). This is interpreted as a higher quantity of polymer chains dissolved in less monomer (due to higher conversion).

At 91% DBC the measurement already surpassed the Trommsdorff effect phase and has reached a plateau-like progression of the DBC. Additionally, the first increase in G', which is a result of the Trommsdorff effect due to a high polymerization rate is already surpassed. This leads to very high molecular weight polymer chains with around 600 kDa, which caused the assumption that many of the chains that are present link together forming very high molecular weight chains. This is supported by the SEC trace (Figure 100 ,right; yellow) showing a remarkable shoulder leaning to lower molecular weights, which indicates a formation of 600 kDa polymer chains from 300 kDa chains.

At the last data point at 97% DBC the formulation is solid, having already surpassed its gel point (t_{gel} = 108 min). The SEC trace shows a less distinct shoulder, so it can be assumed that higher quantities of the very high molecular weight (M_n = 600 kDa) polymer chains are present in the gelled formulation.

It is remarkable, that using the rheology/IR and SEC coupling allowed us to show that 6% difference in DBC from 91% to 97% causes the formulation to gel. This is explained as the high molecular weight chains completely entangle and very little monomer is left in between them.

101

3.5.3. Testing of Various Monomers

Herein, the versatility of the presented initiation method using B6-1/Cu(acac)$_2$ as 2K initiation system shall be highlighted further. Rheology/IR was used to investigate the initiation reactivity towards radical polymerization of different monomer classes, including methacrylates, acrylates, acrylamides, acetonitrile, styrene and vinyl ethers ().
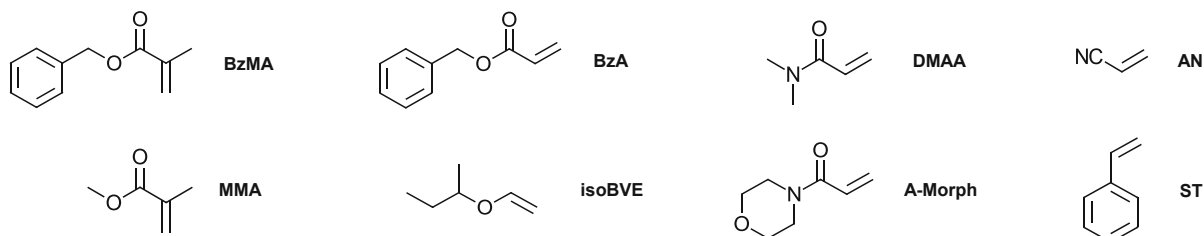
Figure 101: Chemical structure of various radically polymerizable monomers including benzylmethacrylate (BzMA), methylmethacrylate (MMA), benzylacrylate (BzA), isobutylvinylether (isoBVE), dimethylacrylamide (DMAA), acrylomorpholine (A-Morph), acrylonitrile (AN) and styrene (ST).

Formulations were prepared according to Table 22.

Table 22: Composition of the formulations used in this chapter. B-formulations contain diborane and monomer, while Cu-formulations contain Cu(acac)$_2$ and monomer.

	B-formulation	Cu-formulation
B6-1 (mol%)	3.5	-
Cu(acac)$_2$ (mol%)	-	0.2
Monomer (mol%)	96.5	99.8

The results show expectedly big differences depending on the type of monomer used for bulk polymerization (Figure 102). Interestingly, all the investigated monomers showed polymerization in the rheology/IR measurements. Especially high reactivity was observed for BzA, isoBVE and AN. Despite isoBVE was not expected to polymerize at all, the reactivity was very high, suggesting a possible formation of cations during the initiation that lead to the polymerization of isoBVE. The progression of the DBC does not develop any increase due to the Trommsdorff effect, as the formulations reach conversions over >99% in a comparatively short time.
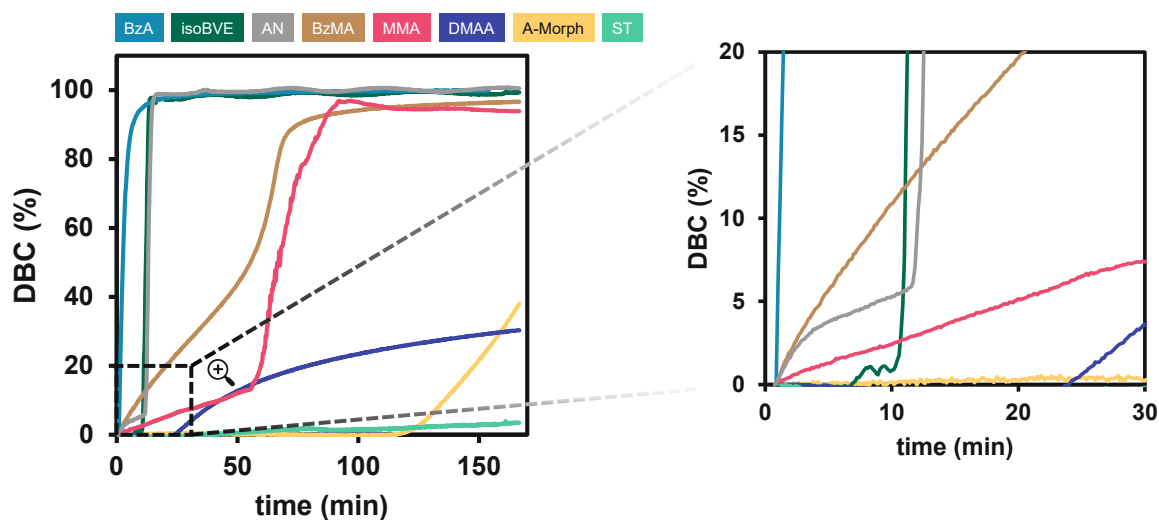
Figure 102: Rheology/IR measurement of the polymerization of BzA, isoBVE, AN, BzMA, MMA, DMAA, A-Morph and ST using 3.5 mol% B1 and 0.2 mol% Cu(acac)$_2$ as initiators. A close-up view gives a more detailed insight into the kinetics at the start of the polymerization reaction.

Interestingly, the acrylamides, which would be expected to be highly reactive, showed poor DBC with the B6-1/Cu(acac)$_2$ initiation system. In this regard, it was shown in previous work that amides might interact with the diborane compound, leading to side reactions, which could explain such a loss in reactivity.[99] Also, styrene would be expected to show high conversions, however, only up to 4% DBC were reached.

When looking at the start of the polymerization reaction in a close-up view (Figure 102, right), the different kinetics of polymerization of the monomers can be understood very clearly. The acrylate monomer showed very high conversion rates immediately after the mixing phase, while isoBVE and AN have a delay of about 10 min, after which high conversion rates are reached. The methacrylic monomers BzMA and MMA show low conversion rates right after mixing, however, increasing throughout the polymerization reaction. Overall, the reactivity increases from methacrylates to acrylates, vinyl ethers and acrylonitrile.

4. Stability of Formulations

The application of 2K systems for dental or adhesive purposes require a certain shelf life of the unpolymerized formulation containing monomers and initiators.[20, 63, 104] This stability of the respective Cu-formulations as well as B-formulations is an important factor for the application as a 2K system to provide reproducible polymerization. Therefore, the stability of certain formulations using 3Mix (Figure 103) was investigated regarding the thermal stability, the stability over time as well as the long-time reactivity of the formulations after storage over time.
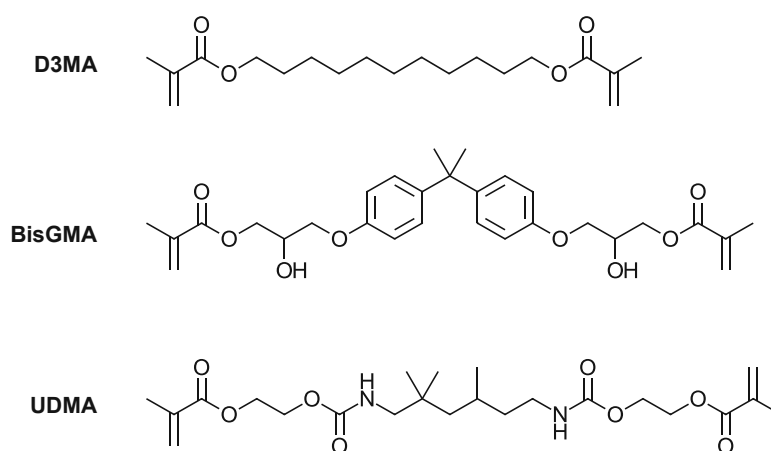
Figure 103: Chemical structure of the monomer mixture 3Mix, consisting of 20wt% D3MA, 40wt% BisGMA and 40wt% UDMA.

4.1. Thermal Stability

Thermal stability is a very important factor for storage conditions of 2K formulations. It is shown in literature that methacrylic and even acrylic formulations containing Cu compounds such as acetates and acetylacetonates are very stable and show no premature gelation or loss in reactivity over time.[105] However, diboranes are yet not investigated in this regard. The thermal stability was evaluated for the depicted diboranes in 3Mix (Figure 104) and formulations were prepared according to Table 23.
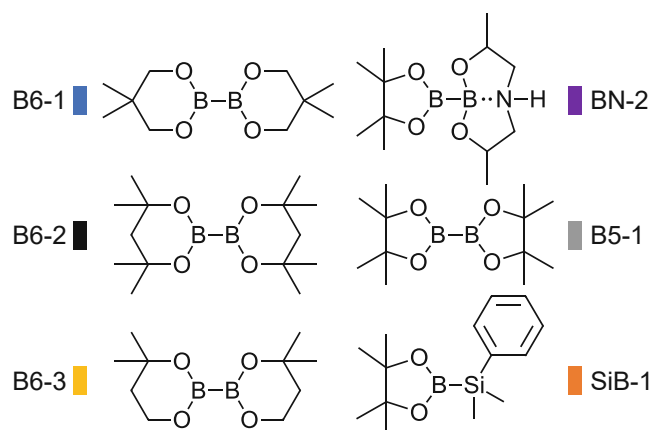
Figure 104: Structure of different diboranes (B6-1, B6-2, B6-3 obtain sixmembered rings. BN-2 obtains an electron donating nitrogen atom. B5-1 obtains fivemembered rings) and a silylborane SiB-1.

Table 23: Formulations for STA measurements to investigate the thermal stability of the formulations with B6-1, B6-2, B6-3, BN-2, B5-1 and SiB-1 in 3Mix.

	B-formulation
Diborane (mol%)	3.5
3Mix (mol%)	96.5

A temperature profile for DSC measurements (Figure 105) was selected, employing a heating step and then a second heating step. For the evaluation, the DSC-curves during the heating steps were subtracted to give the corrected values.
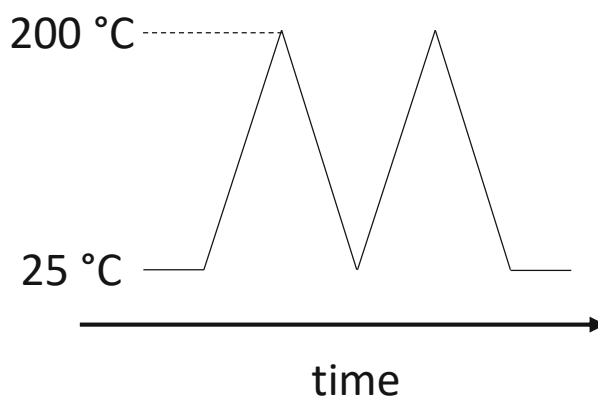
Figure 105: Temperature profile used for the STA measurements investigating thermal stability of different diboranes in 3Mix.

In the following Figure 106 the corrected DSC signal is shown as a function of the temperature. The DSC peak correlates to a thermally induced homolytic cleavage of the diborane bond and the subsequent radical polymerization of the monomer mixture 3Mix. It is seen, that the thermal stability is differing highly depending on the diborane. Thermally more stable

diboranes have a stronger B-B bond or are more sterically hindered and are not easily accessible.
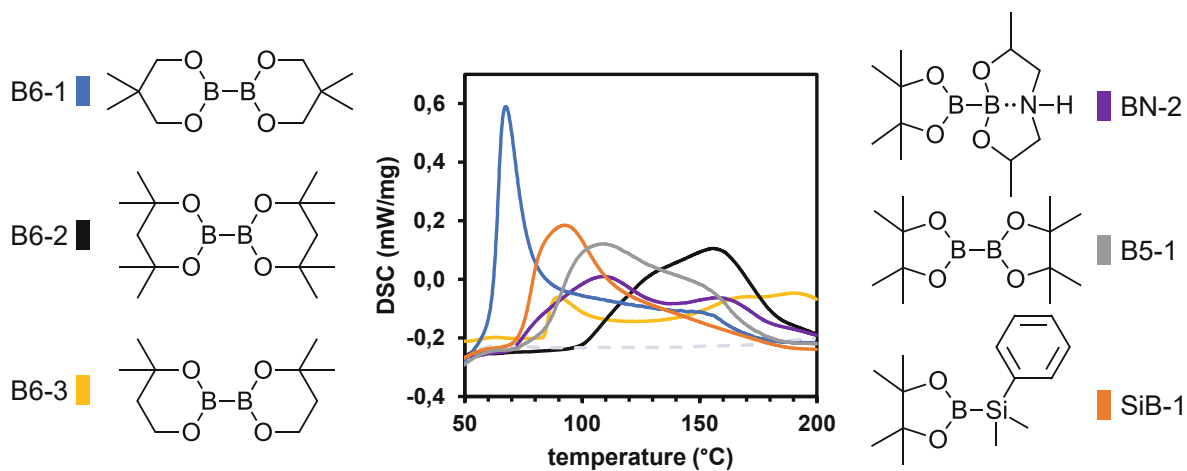
Figure 106: DSC-signal of the thermal polymerization of 3Mix, resulting from the thermally induced homolytic cleavage of the respective diborane. Dashed grey line: pure 3Mix.[99]

The shape of the curves is different for every diborane however the interesting value is only the onset of the thermal polymerization. This gives the temperature at which the formulation starts to polymerize. Figure 107 and Table 24 show the onset temperatures of the respective diboranes.
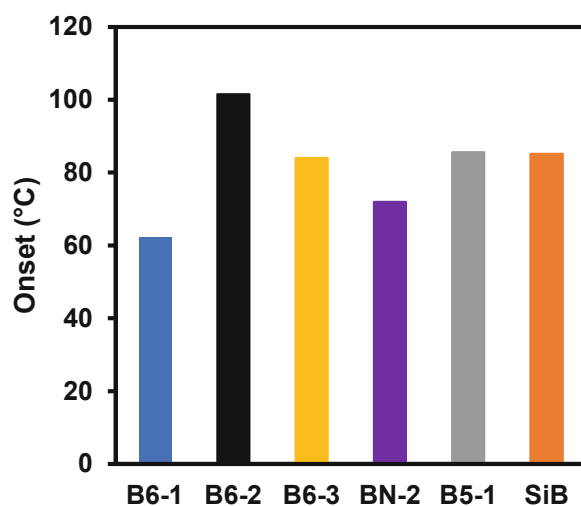
Figure 107: Onset temperature of the thermal polymerization of 3Mix, resulting from the thermally induced homolytic cleavage of the respective diborane.

Table 24: Onset temperature of the thermal polymerization of 3Mix, resulting from the thermally induced homolytic cleavage of the respective diborane.

	Onset (°C)
B6-1	62
B6-2	102
B6-3	84
BN-2	72
B5-1	86
SiB-1	85

It can be estimated that the bulkier B6-2 is more stable than the less bulky B6-3 and the even less bulky B6-1. The same conclusion can be drawn for B5-1. However, none of the shown diboranes are truly stable above 50 °C, as they all start a polymerization at relatively low temperatures. This leads to the conclusion that all the diborane formulations should ideally be stored at low temperatures in a fridge to ensure stability of the formulation.[99]

4.2.   Long Time Reactivity via Rheology

Long time stability is a very important factor for the application of 2K formulations. Not only do formulations have to be stable over time, they also have to stay reactive enough to polymerize in a reproducible way. This is already shown to be the case for copper salts in methacrylic and acrylic monomer solutions.[105] To investigate this long-time reactivity of diborane formulations, formulations were prepared according to Table 25 and stored in a fridge at 8 °C. Rheology measurements were performed regularly directly after mixing with the respective Cu-formulation, after 1 week, after 2 weeks and after 4 weeks of storage.

Table 25: Formulations prepared for long time reactivity studies consisting of Cu(acac)$_2$ and either BN-2, B6-1, SiB-1 or B6-3.

	B-formulation	Cu-formulation
Diborane (mol%)	3.5	-
Cu(acac)$_2$ (mol%)	-	0.2
Monomer (mol%)	96.5	99.8

4.2.1.   Stability in 3Mix

For this study, the stability of diboranes was investigated in 3Mix and focus was lain on the fast-polymerizing diborane species, since a possible decrease in t_{gel} would be visible best. Therefore, the respective formulations using 3Mix as monomer mixture were prepared with BN-2, B6-1, B6-3 and SiB-1. In Figure 108 the graphs of G' is displayed for the respective diboranes for t0 (right after preparing the formulations), after 1 week, after 2 weeks and after 4 weeks. In the case of SiB-1 there was no reactivity observed after 1 week of storage, which is why the respective graph is not shown here and SiB-1 formulations can be considered not stable after 1 week of storage at 8 °C.
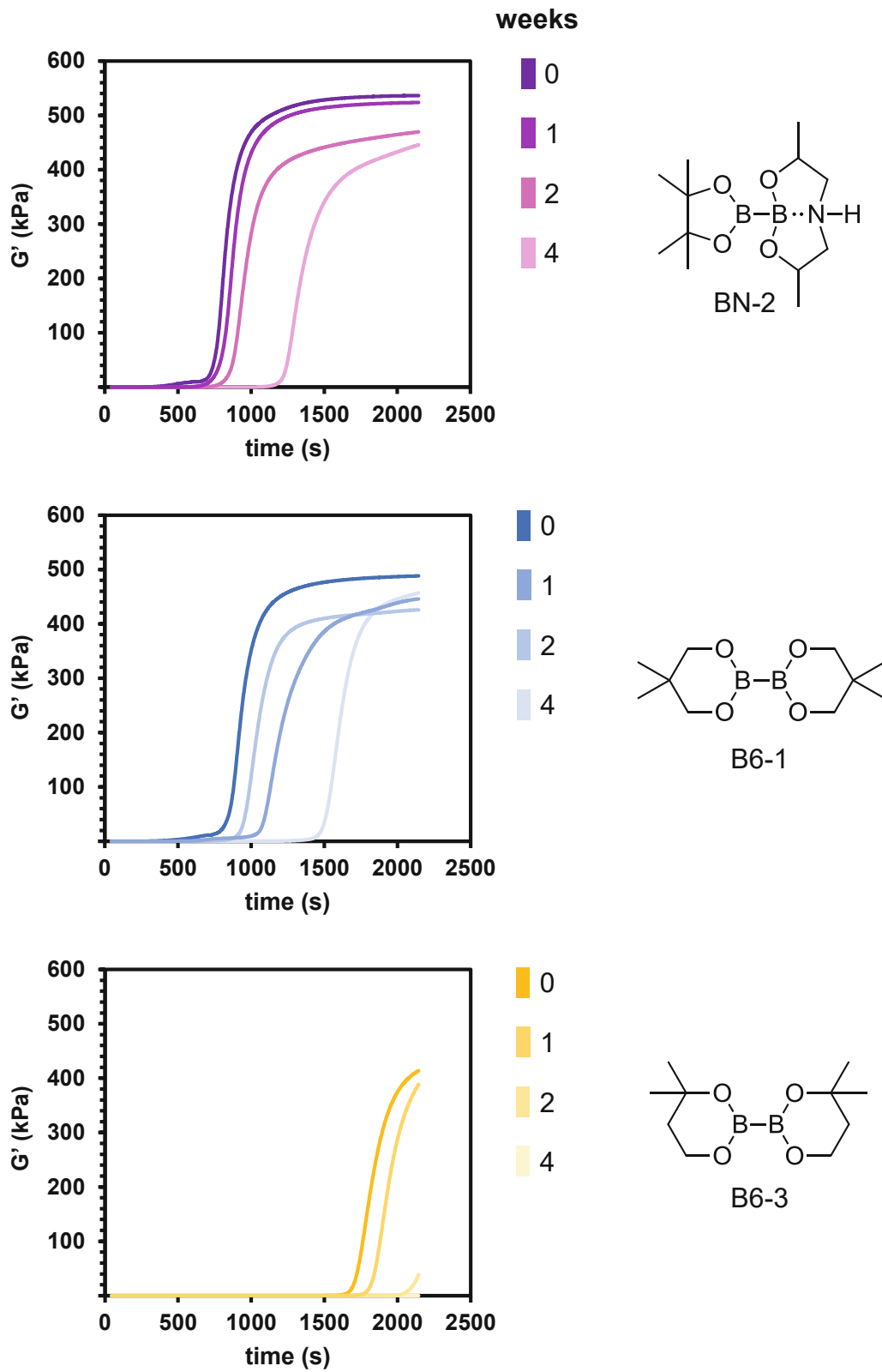
Figure 108: Storage modulus during the polymerization of 3Mix with Cu(acac)$_2$ and either BN-2, B6-1 or B6-3, after 0, 1, 2 and 4 weeks of storage.

All three investigated diboranes show a decrease in reactivity over time of storage which is reflected in higher t_{gel} value. All t_{gel} values for this study are shown in Table 26. For B6-3 the evaluation of t_{gel} was not possible after 2 weeks, for SiB-1 it was not possible after 1 week.

Table 26: t_{gel} of the polymerization of 3Mix with Cu(acac)$_2$ and either BN-2, B6-1, SiB-1 or B6-3, after 0, 1, 2 and 4 weeks of storage.

		t_{gel}(s)		
	t0	1week	2week	4week
BN-2	803	861	927	1287
B6-1	908	1143	1004	1576
B6-3	1774	1853	-	-
SiB-1	377	-	-	-

It is to be noted that the B6-3 formulations still show reactivity, the increase in G' was, however, outside the measurement window so that t_{gel} could not be evaluated. Overall, all formulations show sufficient reactivity to lead to a polymerization of 3Mix. Although there is a decrease in the polymerization speed, the reaction still works reproducibly. This result is very promising as it proves that these respective diborane formulations are relatively storage stable and still show sufficient reactivity even after storage of 4 weeks.

For the most stable diborane BN-2, it can be seen that the reactivity is decreasing a little over time, however, after two weeks the polymerization is delayed by only 60 s. Even after four weeks the reactivity is still sufficient which is very remarkable as no stabilizers are used in these formulations (Figure 109), as the transposed time/t_{gel} diagram shows.
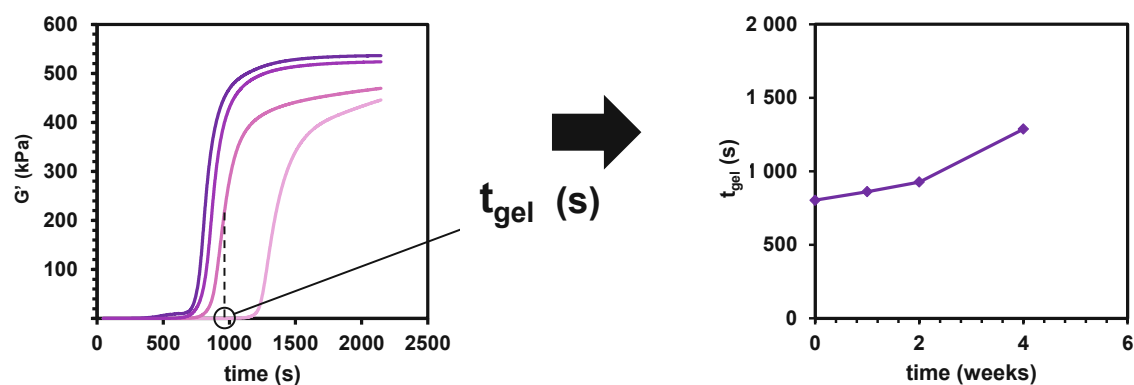
Figure 109: Left: Storage modulus G' during the polymerization of 3Mix with BN-2 and Cu(acac)$_2$ after storage of 0-4 weeks. The t$_{gel}$ value is marked as the time of maximum increase in storage modulus and transposed to time/t$_{gel}$ diagram shown on the right side.

A reason for the observed decrease in reactivity over time could be the degradation of the BN-2 compound, leading to a lower concentration compared to the starting concentration. Since 3Mix is a monomer mixture consisting of D3MA, UDMA and BisGMA the effects of the individual monomers on the long-time reactivity are to be investigated.[99]

4.2.2.   Stability in D3MA

The long-time reactivity and stability of 2K formulations is crucial for their application. Previous studies showed good reactivity after 2 weeks of storage in 3Mix for the diborane BN-2, however, a decrease in reactivity was observed thereafter. The influence of other monomers (D3MA) on the stability will be investigated in this study. Unfortunately, BN-2 is not soluble in D3MA, which is why B6-1 was chosen as the diborane compound due to comparable reactivities (Figure 110).
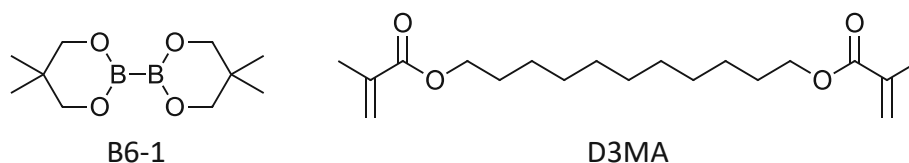
Figure 110: Structures of B6-1 and D3MA

Not only have the formulations to be stable over time, they also have to stay reactive enough to polymerize in a reproducible way. To this end, formulations were prepared according to Table 27 and stored in a fridge at 8 °C. Rheology measurements were performed regularly directly after mixing with the respective Cu-formulation, after 1 week, 2 weeks and 4 weeks of storage.

Table 27: Formulations prepared for long time reactivity studies consisting of Cu(acac)$_2$ and B6-1 in D3MA.

	B-formulation	Cu-formulation
B6-1 (mol%)	3.5	-
Cu(acac)$_2$ (mol%)	-	0.2
D3MA (mol%)	96.5	99.8

The measurements were evaluated and the respective t_{gel} values for 0, 1, 2 and 4 weeks of storage are displayed in Figure 111.
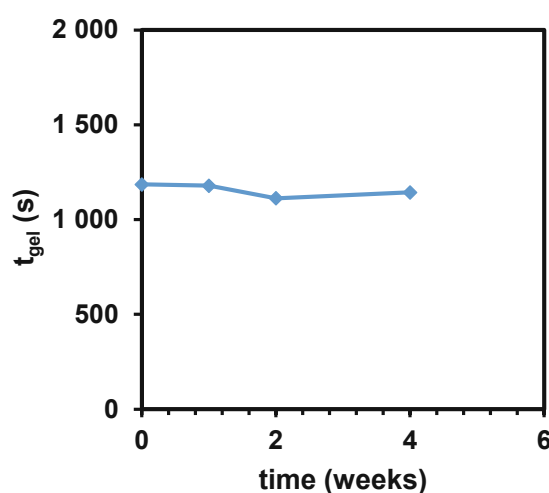
Figure 111: Long-term reactivity tests of diborane/Cu system with B6-1 in D3MA, after t0, 1 week, 2 weeks and 4 weeks, evaluating the t_{k-max} of the polymerization reaction in Rheo/IR measurements.[99]

It is shown that the reactivity stays constant over the course of at least four weeks of storage. This emphasizes the influence of the monomers on the stability of this 2K-system. The diborane formulation is highly stable when using the relatively inert monomer D3MA that has no functionalities besides the methacrylic end groups. This is also shown in Table 28.[99]

Table 28: Long-term reactivity tests of diborane/Cu system with B6-1 in D3MA, after t0, 1 week, 2 weeks and 4 weeks, evaluating the t_{gel} of the polymerization reaction in rheology measurements.

time (weeks)	t_{gel} (s)
0	1186
1	1179
2	1113
4	1144
	112

4.2.3. Stability in D3MA/BisGMA

In the previously discussed studies, the use of D3MA implicated a higher stability of the 2K initiation system due to less functional groups in the monomer mixture. However, D3MA alone leads to non-applicable materials due to the high brittleness of the resulting polymer. Therefore, a monomer mixture consisting of D3MA/BisGMA (50w%:50w%) was investigated in this study. The choice for this mixture was partly to increase to solubility properties with the addition of BisGMA, and also to see if the hydroxy groups of BisGMA show an influence on the long-time reactivity. BN-2 was soluble in this monomer mixture which is why the formulations using the compounds shown in Figure 112 were prepared.
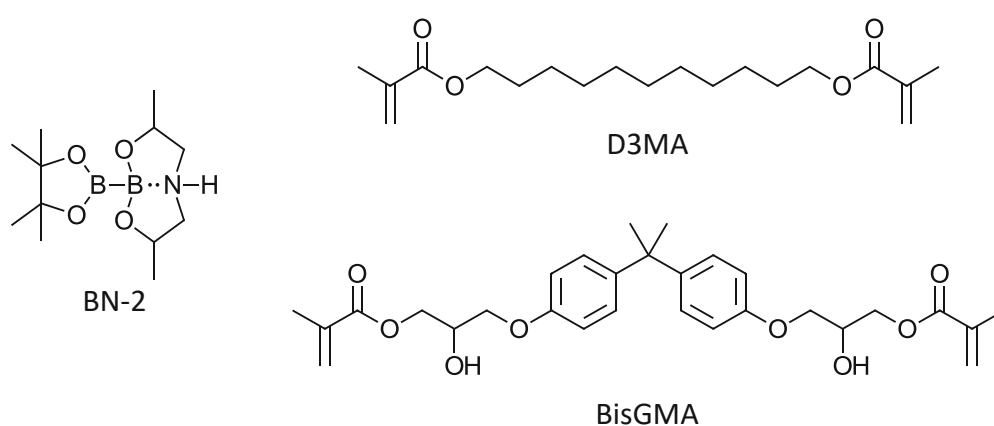
Figure 112: Structures of BN-2, D3MA and BisGMA

Formulations were prepared according to Table 29 and stored in a fridge at 8 °C. Rheology measurements were performed regularly directly after mixing, after, 3 weeks and 4 weeks.

Table 29: Formulations prepared for long time reactivity studies consisting of Cu(acac)$_2$ and BN-2 in D3MA and BisGMA.

	B-formulation	Cu-formulation
BN-2 (mol%)	3.5	-
Cu(acac)$_2$ (mol%)	-	0.2
D3MA (mol%)	96.5	99.8

The measurements were evaluated and the respective t_{gel} values for 0, 3 and 4 weeks of storage are displayed in Figure 113.
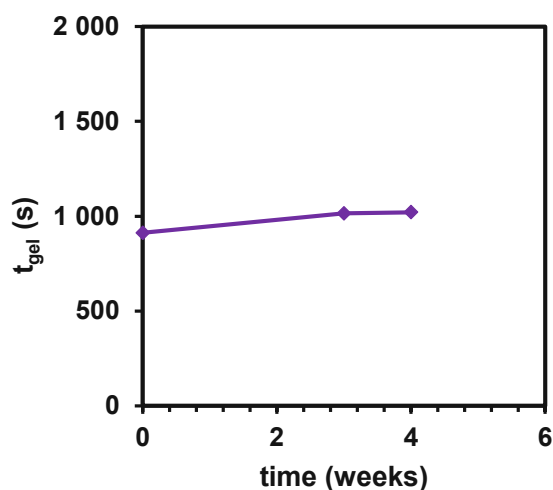
Figure 113: Long-term reactivity tests of diborane/Cu system with BN-2 in D3MA and BisGMA, after t0, 3 weeks and 4 weeks, evaluating the t_{gel} of the polymerization reaction in rheology measurements.[99]

It is shown that the reactivity stays almost constant over the course of at least four weeks of storage. This emphasizes the influence of the monomers on the stability of this 2K-system. Interestingly, the BN-2 formulation is highly stable when using the relatively inert monomer D3MA with BisGMA. This is also reflected in the data in Table 30.

Table 30: Long-term reactivity tests of diborane/Cu system with BN-2 in D3MA and BisGMA, after t0, 3 weeks and 4 weeks, evaluating the t_{k-max} of the polymerization reaction in Rheo/IR measurements.

time (weeks)	t_{gel} (s)
0	912
3	1015
4	1021

The hydroxy groups of BisGMA do not decrease the long-time reactivity significantly. It can be concluded that formulations with D3MA and BisGMA containing highly reactive diborane species such as BN-2 are suggested to be stable in terms of long-time reactivity under storage at 8 °C.

It was shown that the stability of the diborane/Cu(acac)$_2$ 2K-system can be greatly enhanced by a more suitable monomer choice. Even highly reactive diboranes such as BN-2 and B6-1 show good stability for at least four weeks of storage. However, the respective diboranes are all stable for at least 1 week in 3Mix, if stored in a fridge.[99]

5. Reactivity

The understanding of the reactivity of a redox initiation system is crucial in order to adjust important parameters in application such as the working time. This time until the polymerization of the monomer mixture starts is therefore a necessary value to evaluate during the characterization of the reactivity. In this work, the reactivity of the 2K initiation system based on diboranes in one component and copper compounds in the other component was characterized in the monomer mixture 3Mix, consisting of the monomers D3MA, UDMA and BisGMA (20:40:40wt%) (Figure 114).
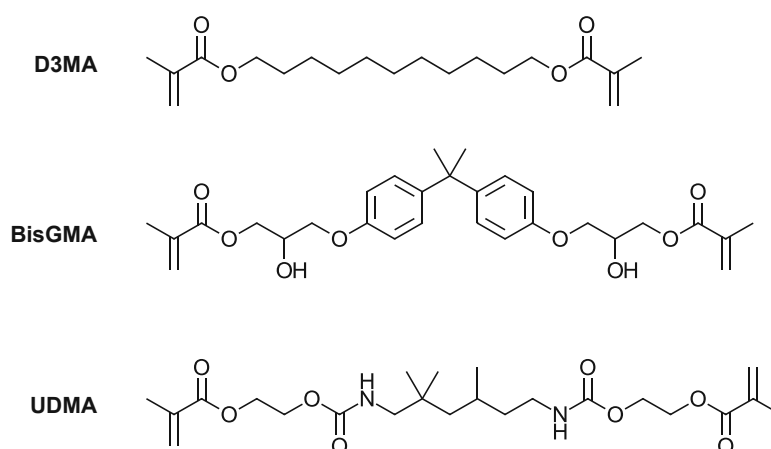
Figure 114: Chemical structure of the monomer mixture 3Mix (D3MA, BisGMA, UDMA)

5.1. Polymerization Temperature Measurements

The quantification of the reactivity of the 2K system derived from diboranes and copper compounds was performed using polymerization temperature measurements to capture the amount of heat that is released during the polymerization reaction. However, reactivity of 2K systems is highly depending on the absolute amount of bulk formulation that is used in the experiment.[75] Therefore, in this study, 1.8 g of total formulation was used and the polymerization temperature was measured over time. The temperature recording in the bulk formulation starts directly after mixing the two formulations. In Figure 115 a schematic progression of such a measurement is depicted, highlighting all important characteristics.[76]
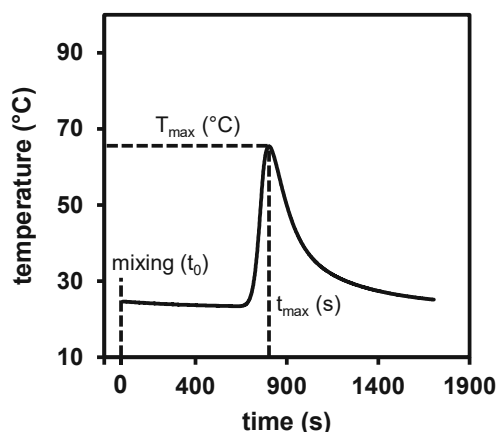
Figure 115: Schematic polymerization temperature measurement, highlighting important values T_{max} (highest temperature during polymerization and t_{max} (time until the highest temperature during polymerization is reached).

The most important values derived from these measurements are the highest temperature during polymerization (T_{max}) and the time until the highest temperature during polymerization is reached (t_{max}). The T_{max} is a characteristic how many functional groups react at once and is therefore a value close to a polymerization rate. On the other hand, t_{max} is a very good indicator for the working time and reflects well how long the redox initiation system needs to yield enough reactive radicals to start the polymerization chain reaction.

5.1.1. Investigation of Cu Compounds

In terms of characterization of the reactivity of 2K systems, particularly redox systems, the method of polymerization temperature measurements is frequently used in literature.[46] The experimental batch size of the produced polymer samples is close to a real application when applying 0.9 g of each respective formulation to a total mixed mass of 1.8 g. For this experimental setup a thermocouple was submerged into the liquid monomer mixture and the temperature of the bulk polymer is recorded as a function of time.

For the investigation of the reactivity of the diborane/Cu 2K system, different Cu compounds are compared with B6-1 as the diborane and the monomer mixture used is 3Mix (Figure 116). The general composition of the respective formulations is shown in Table 31.
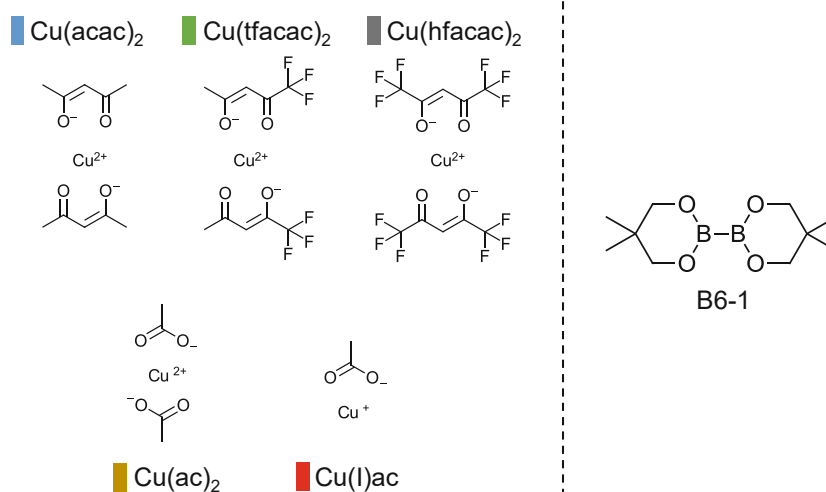
Figure 116: Left: Different Cu species ranging from differently substituted acetylacetonates, over acetate, to Cu(I) acetate. Right: B6-1, the diborane compound used in the following experiments.

Table 31: Formulations prepared for pyrometry experiments to investigate the reactivity of the polymerization reaction resulting from B6-1 and Cu(acac)$_2$, Cu(tfacac)$_2$, Cu(hfacac)$_2$, Cu(ac)$_2$ or Cu(I)ac in 3Mix. 0.9 g of each respective formulation were used for the experiments.

	B-formulation	Cu-formulation
B6-1 (mol%)	3.5	-
Cu compound (mol%)	-	0.2
3Mix (mol%)	96.5	99.8
	0.9 g	0.9 g

The thermocouple was submerged in the mixture immediately after homogenizing and the temperature is recorded. The measurements are performed inside a silicon mold under air at room temperature. All recorded temperature graphs are depicted in Figure 117.
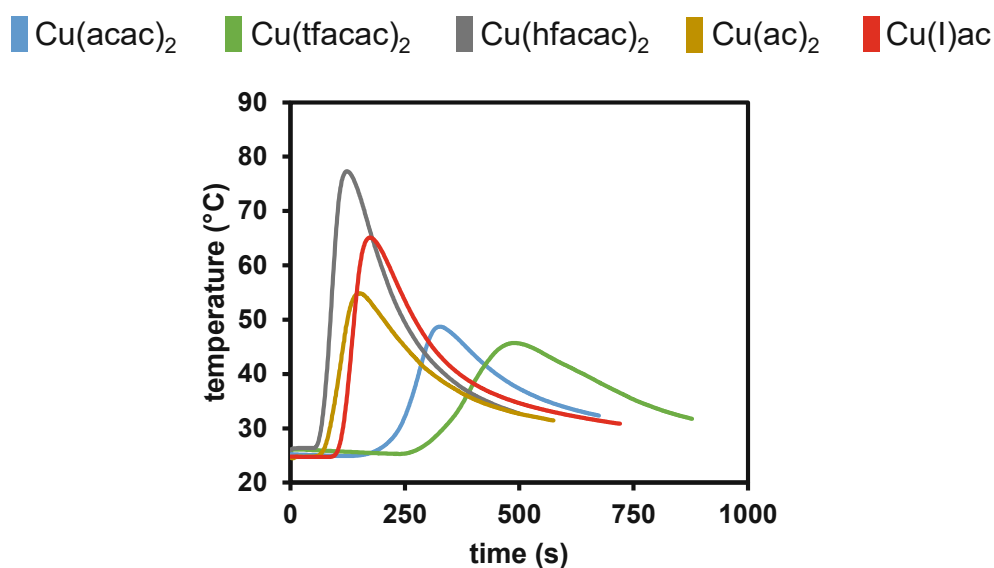
Figure 117: Temperature-time diagram during the polymerization reaction of different Cu compounds with B6-1 in 3Mix.[99]

In the depicted polymerization temperature measurements $Cu(hfacac)_2$, $Cu(ac)_2$ and $Cu(I)ac$ show very fast polymerization initiation with t_{max} (time until maximum temperature (T_{max}) is reached) below 180 s (Figure 117). Also, the maximum temperature is higher than for $Cu(acac)_2$ and $Cu(tfacac)_2$. They show a much slower polymerization with a very broad peak and a long tailing phase. In the case of $Cu(hfacac)_2$ the higher reactivity is explained by a better solubility due to the fluorination and therefore a higher diffusion in the monomer mixture. $Cu(ac)_2$ and $Cu(I)$ seem to be able to catalyze the diborane cleavage more effectively with the acetate anion and lead to a faster polymerization initiation. However, all copper compounds exhibit their peak maximum below 10 minutes.[99]

Table 32: Results of the polymerization temperature measurements of the polymerization of 3Mix with different Cu species and B6-1, including t_{max} and T_{max}.

	t_{max} (s)	T_{max} (°C)
$Cu(acac)_2$	326	48.7
$Cu(tfacac)_2$	488	45.7
$Cu(hfacac)_2$	124	77.3
$Cu(ac)_2$	151	54.9
$Cu(I)ac$	174	65.1

5.1.2. Investigation of Diboranes

The reactivity of the diborane/Cu 2K system was characterized using polymerization temperature measurements. In the previous study, various copper compounds and their ability to initiate the polymerization were compared. However, not only the influence of the copper compound onto the reactivity is of interest, also the diborane can have a significant impact. Therefore, different diborane compounds were examined for their reactivity in 3Mix with $Cu(acac)_2$ using polymerization temperature measurements. The general composition of the respective formulations is shown in Table 33.

Table 33: Formulations prepared for pyrometric experiments to investigate the reactivity of the polymerization reaction resulting from B6-1, B6-2, B6-3, BN-2, B5-1 and SiB-1 with $Cu(acac)_2$ in 3Mix. 0.9 g of each respective formulation were used for the experiments.

	B-formulation	Cu-formulation
Diborane (mol%)	3.5	-
$Cu(acac)_2$ (mol%)	-	0.2
3Mix (mol%)	96.5	99.8
	0.9 g	0.9 g

The thermocouple was submerged in the mixture immediately after homogenizing and the temperature is recorded. The measurements are performed inside a silicon mold under air at room temperature. The recorded temperature graphs as well as the chemical structures of the employed diboranes are depicted in Figure 118.
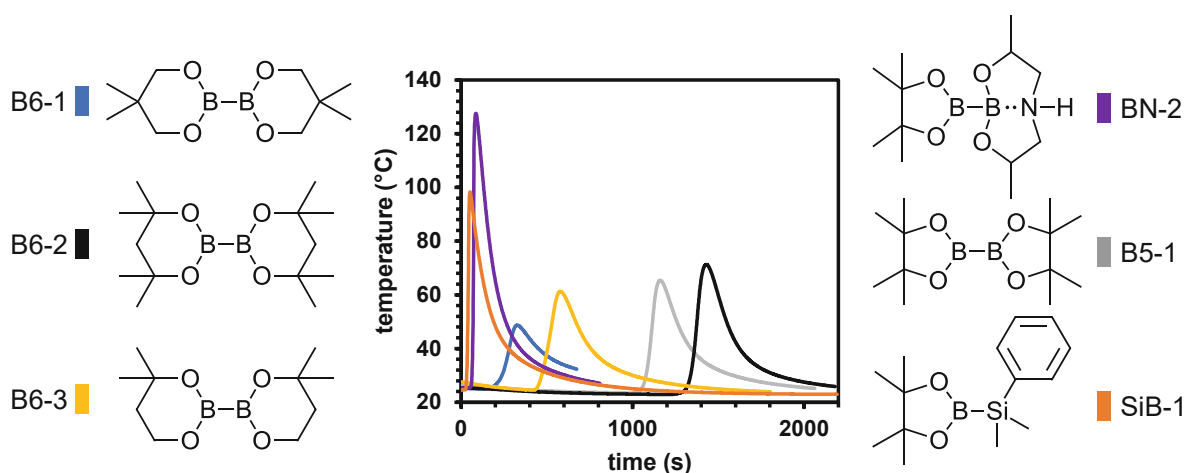
Figure 118: Temperature-time diagram during the polymerization reaction of different depicted diboranes with $Cu(acac)_2$ in 3Mix.[99]

As seen in the diagram above, SiB-1 and BN-2 exhibit a very fast polymerization with t_{max} under 90 s. They also reach extremely high temperatures, especially in the case of BN-2 with 127.6 °C (Table 34).

Table 34: Results of the pyrometry measurements of the polymerization of 3Mix with different diboranes with Cu(acac)$_2$, including t_{max} and T_{max}.

	t_{max} (s)	T_{max} (°C)
B6-1	326	48.7
B6-2	1430	71.3
B6-3	581	61.3
B5-1	1159	65.4
BN-2	86	127.6
SiB-1	51	98.4

The incredibly high reactivity of SiB-1 is most likely due to the formation of silyl radicals that are more reactive compared to boryl radicals.[101] The high reactivity of BN-2 is very likely due to the structural properties of the compound. The free electron pair of the spatially near nitrogen can donate to the boron resulting in a twisted structure and a weaker B-B bond compared to the other compounds. This weaker B-B bond can react faster with the Cu species resulting in a faster polymerization reaction.

Furthermore, the effect of the steric hinderance for the B6 compounds is seen clearly. The closer the methyl groups get to the B-B bond, the slower can polymerization occurs. This trend is depicted in following Figure 119. The B-B bond must be accessible for the reaction with the Cu species. This also true for the B5-1 compound where the four methyl groups are in close proximity to the B-B bond.[99]
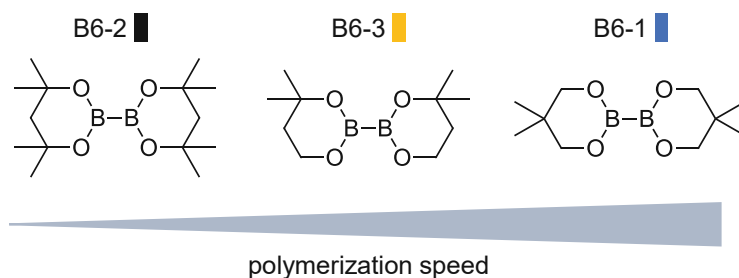
Figure 119: A schematic view of the polymerization speed increase with decreased steric hinderance from B6-2 to B6-1 being the fastest and least steric hindered diborane of the six-membered-ring series.[99]

5.2. Rheology/IR

The reactivity of the newly developed diborane/Cu 2K initiation system was further investigated using the rheology/IR method. This characterization technique allows for simultaneous measurement of rheological data G' and G'', while measuring transmission NIR of the sample, tracking the double bond conversion via integration of the methacrylic C=C band at 1636 cm^{-1}. A total of 200 mg of formulation is used for the following measurements, having a 45 s mixing step in advance of the data recording to ensure a homogeneous mixture of the 2K system. Schematic measurements of G' and the DBC are shown in the following Figure 120 highlighting important characteristics G'_{end}, t_{gel} and DBC_{end}.
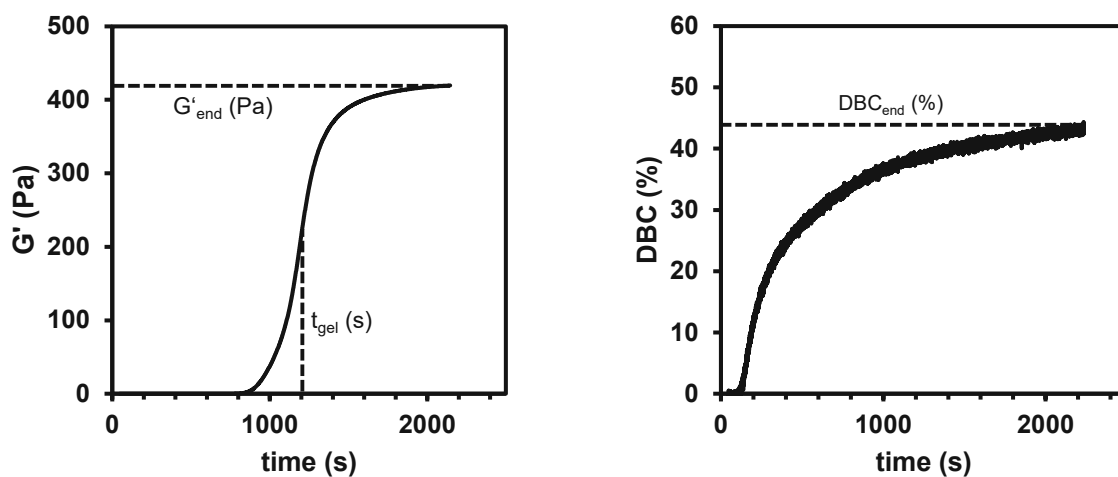
Figure 120: Schematic measurements of G' and the DBC are shown highlighting important characteristics G'_{end}, t_{gel} and DBC_{end}.

The information derived from the measurements of G' leads to evaluation of G'_{end} referring to the mechanical strength of the polymer at the end of the polymerization. Another important value is t_{gel} which is referred to as the gel time in these measurements. Often, the cross-section of G' and G'' are used to evaluate t_{gel}, however, for 2K systems it is much more reproducible to take the steepest increase of G' as t_{gel}.[79] Furthermore, the DBC_{tgel} gives information about

the crosslinking density and the overall conversion at the gel point and at the end at a certain mechanical strength.

5.2.1. Investigation of Cu Compounds

The diborane/Cu 2K system was characterized further in the following regarding the polymerization reactivity using rheology/IR measurements tracking mechanical parameters such as G' and chemical parameters such as the DBC. Different Cu species were examined in combination with a B6-1 to evaluate their influence on the polymerization speed and DBC. The respective compounds that were used in this study are depicted in Figure 121.
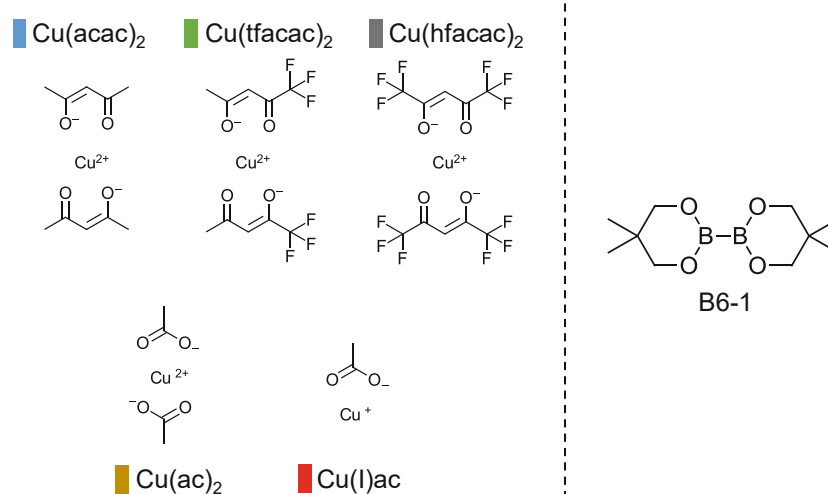
Figure 121: Left: Different Cu species ranging from differently substituted acetylacetonates, over acetate, to Cu(I) acetate. Right: B6-1, the diborane compound used in the following experiments.

The compositions of the formulations are shown in the following Table 35. For the measurement 100 mg of the respective Cu-formulation and B-formulation were applied to the rheometer with a gap size of 0.2 mm. Subsequently, a homogeneous mixture was ensured by rotation of the measuring stamp for 45 s after which the measurement started.

Table 35: Formulations prepared for Rheo/IR experiments to investigate the reactivity of the polymerization reaction resulting from B6-1 and Cu(acac)₂, Cu(tfacac)₂, Cu(hfacac)₂, Cu(ac)₂ or Cu(I)ac in 3Mix.

	B-formulation	Cu-formulation
B6-1 (mol%)	3.5	-
Cu compound (mol%)	-	0.2
3Mix (mol%)	96.5	99.8

During the rheology/IR measurements, G', F_N and the DBC were recorded as a function of time. Both parameters are shown for each formulation in Figure 122.
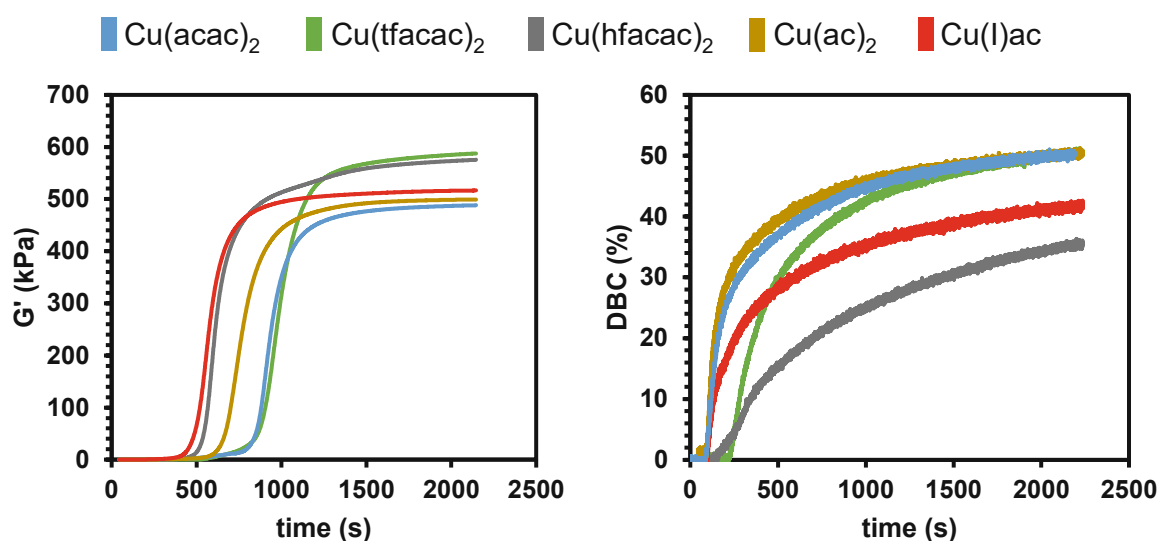
Figure 122: Left: Storage modulus G' of the polymerization reactions with all different Cu species and B6-1. Right: DBC of the polymerization reactions with all different Cu species and B6-1.[99]

The polymerization speed which is indicated by t_{gel}, is differing significantly with different Cu species. It is clearly seen that the cleavage of the diborane is highly dependent on the ligand of the copper compound. Interestingly, the fastest systems with Cu(I)ac and Cu(hfacac)$_2$ exhibit the lowest final DBC (Table 36). This likely due to a gelation of the formulation at low DBC and low diffusion due to subsequent high viscosity.

Table 36: The results of the Rheo/IR measurements including t_{gel}, G'_{end} and DBC_{end} are shown for each different Cu species with B6-1 in 3Mix.

	t_{gel} (s)	G'_{end} (kPa)	DBC_{end} (%)
Cu(acac)$_2$	908	488	51.0
Cu(tfacac)$_2$	951	587	51.2
Cu(hfacac)$_2$	588	575	36.3
Cu(ac)$_2$	732	499	50.4
Cu(I)ac	552	516	42.6

The formulation containing Cu(ac)$_2$, Cu(tfacac)$_2$ and Cu(acac)$_2$ do show a very fast increase in the DBC while the gelation of the mixture is relatively slow. Also, the final DBC is very high

123

with over 50% for all these respective Cu species. This behavior is explained by the formation of many low molecular weight chains that then connect and cause the mixture to gel at already high DBC. The shrinkage force F_N resulting from the polymerization reaction is plotted against the DBC in the following Figure 123.

Figure 123: The shrinkage force F_N is plotted against the DBC during the polymerization reaction using different Cu species and B6-1 in 3Mix.

It is clearly visible that the slower polymerizing samples also exhibit less shrinkage force. The similarity between Cu(acac)$_2$ and Cu(tfacac)$_2$ is shown as well. These two acetylacetonates as well as Cu(ac)$_2$ show almost no shrinkage force until around 25% DBC. This can be explained by the formation of many initiation centers that lead to many rather small network parts that can only connect later at higher DBC, causing the formulation to gel.[99]

Table 37: Final shrinkage force F_N of the polymers derived from the different Cu species with B6-1 in 3Mix.

	$F_{N\text{-}end}$ (N)
Cu(acac)$_2$	-8.8
Cu(tfacac)$_2$	-8.8
Cu(hfacac)$_2$	-17.4
Cu(ac)$_2$	-17.0
Cu(I)ac	-16.5

5.2.2. Investigation of Diboranes

The detailed characterization of the polymerization reactivity of the diborane/Cu 2K system was conducted not only looking at various copper compounds (previous chapter), but also by varying the diborane. The method of rheology/IR, tracking mechanical parameters such as G' and chemical parameters such as the DBC is ideal for the characterization of parameters such as G'_{end}, t_{gel} and DBC_{end}.

Various diboranes were examined for their reactivity in 3Mix with $Cu(acac)_2$. The structures of all employed compounds are depicted in Figure 124.
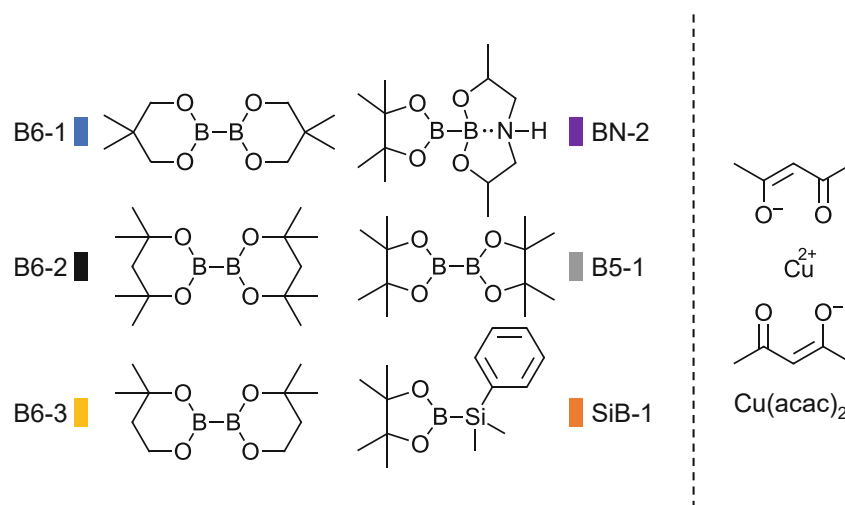
Figure 124: Left: Structure of different diboranes (B6-1, B6-2, B6-3 obtain sixmembered rings. BN-2 obtains an electron donating nitrogen atom. B5-1 obtains fivemembered rings) and a silylborane SiB-1. Right: Structure of $Cu(acac)_2$.

The compositions of the formulations are shown in the following Table 38. For the measurement 100 mg of the respective Cu-formulation and B-formulation were applied to the rheometer with a gap size of 0.2 mm. Subsequently, a homogeneous mixture was ensured by rotation of the measuring stamp for 45 s after which the measurement started.

Table 38: Formulations prepared for Rheo/IR experiments to investigate the reactivity of the polymerization reaction resulting from B6-1, B6-2, B6-3, BN-2, B5-1 and SiB-1 with $Cu(acac)_2$ in 3Mix.

	B-formulation	Cu-formulation
Diborane (mol%)	3.5	-
$Cu(acac)_2$ (mol%)	-	0.2
3Mix (mol%)	96.5	99.8

As seen in the following Figure 125, the polymerization is very dependent on the used diborane compound (Table 39). The silylborane compound SiB-1 shows the fastest reaction, reflected in the lowest t_{gel}. The formed silylradicals are very likely more reactive towards double bonds and result in a very fast polymerization. However, B6-1 and BN-2 exhibit very short polymerization times as well as very high double bond conversion over 50%. B6-2 and B5-1 show a very slow polymerization that is too slow for the measuring time window of 2100 s. In the DBC graph, the starting polymerization of B5-1 is recognized at around 2000 s, while B6-2 is slower.
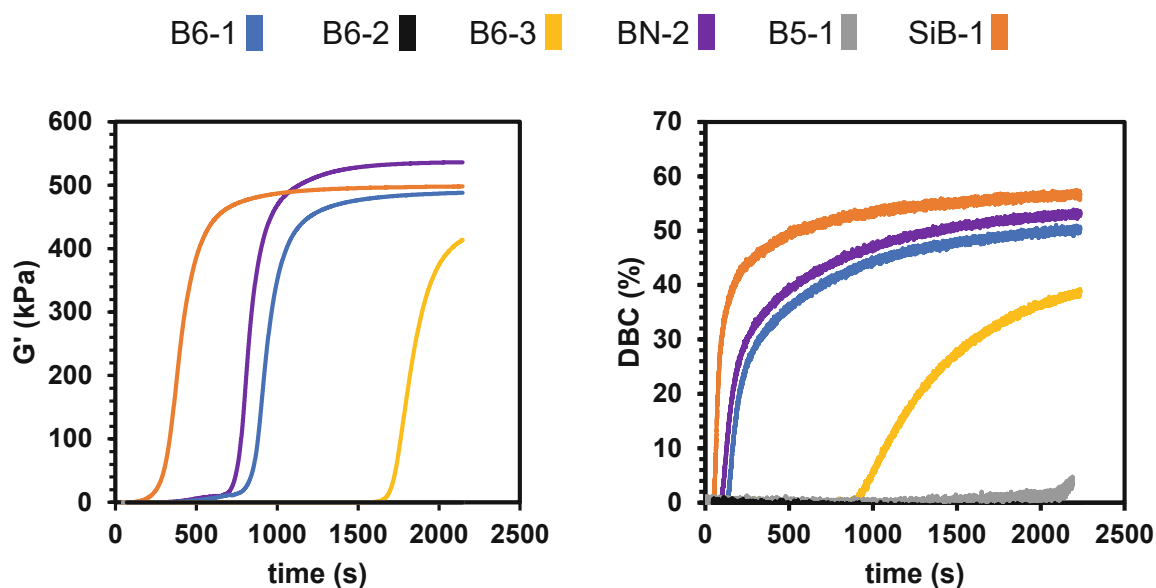
Figure 125: Left: Storage modulus G' during the polymerization reaction of 3Mix with the different diborane compounds and Cu(acac)$_2$. Right: DBC during the polymerization reaction of 3Mix with the different diborane compounds and Cu(acac)$_2$.[99]

Table 39: The results of the Rheo/IR measurements including t_{gel}, G'_{end} and DBC_{end} are shown for each different diborane compound with Cu(acac)$_2$ in 3Mix.

	t_{gel} (s)	G'_{end} (kPa)	DBC_{end} (%)
B6-1	908	488	51.0
B6-2	-	-	-
B6-3	1774	413.8	39.3
B5-1	-	-	-
BN-2	803	536	53.8
SiB-1	377	498	57.4

126

A clear trend can be identified between the six-membered ring diboranes (B6-1, B6-2, B6-3). The steric hinderance in the proximity of the B-B bond slows down the addition to the Cu species and therefore also slows down the overall polymerization. B6-1 has two methyl groups in para position to the B-B bond, which results in no hinderance and therefore a fast reaction. B6-3 has two methyl groups in ortho position to the B-B bond, causing a slightly hindered addition and therefore slower reaction times. The four methyl groups of B6-2 in ortho position highly hinder the addition reaction and therefore prolong the polymerization time.

Another interesting parameter to evaluate is the normal force (F_N) which corresponds to the shrinkage of the specimen during the polymerization. In Figure 126 the normal force is plotted against the respective double bond conversion of the measurements of SiB-1, B6-1, B6-3 and BN-2.
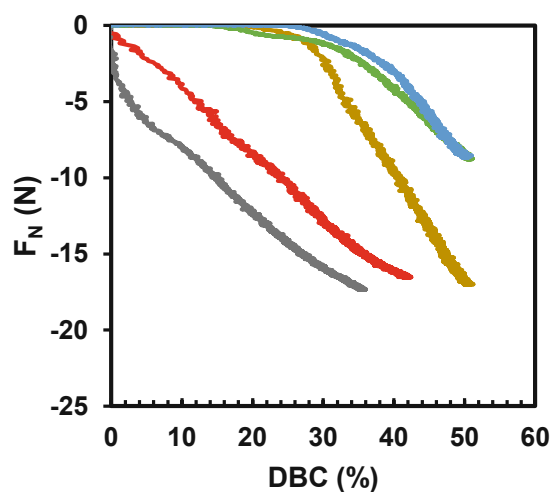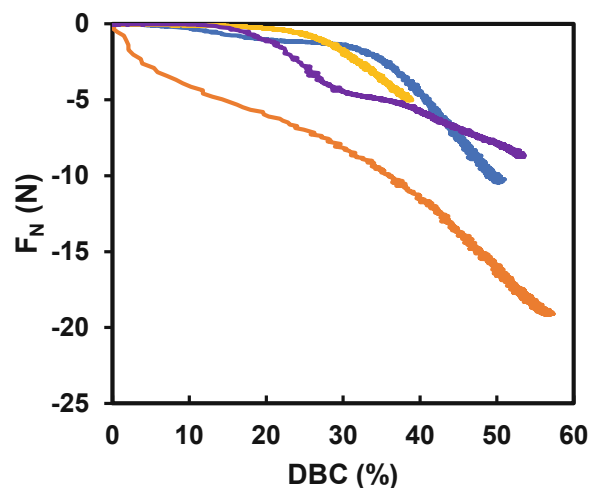

Figure 126: The shrinkage force F_N is plotted against the DBC during the polymerization reaction using different diborane compounds and Cu(acac)$_2$ in 3Mix.

It was noticed that the DBC at the gel point, which is interpreted as the DBC_{gel}, is relatively high for the tested diboranes (Table 40). Especially for BN-2 and B6-1 it is seen in Figure 125 in the DBC graph that the polymerization starts very fast as the double bond conversion increases. This is, however, not reflected in the G' as the maximum slope is at above 40% DBC. This is seen as a strong indication for the formation of lower molecular weight networks and the formation of a homogeneous network causing an increase in the DBC despite the low G'. When those preformed network parts then start to connect and form a dense network the G' rises and the formulation gels. When looking at Figure 126 this interpretation is supported by the very slow decrease of F_N until a DBC of 35%. The slow formation of lower molecular weight

127

chains does not cause the formulation to exhibit a strong normal force, however, when these chains connect this is also reflected in the normal force.[99]

Table 40: The normal force F_{N-end} at the end of the measurement as well as the DBC at t_{k-max} are displayed of the polymerization reaction of different diboranes with $Cu(acac)_2$ in 3Mix.

	DBC_{gel} (%)	F_{N-end} (N)
B6-1	43.6	-10.4
B6-3	33.4	-5.0
BN-2	44.5	-8.8
SiB-1	46.3	-19.1

5.2.3. Concentration Dependency of B6-1/$Cu(acac)_2$

The detailed characterization of the polymerization reactivity of the diborane/Cu 2K system was conducted employing various copper and diborane compounds and the most promising combination of diborane and copper compound was found to be B6-1 and $Cu(acac)_2$ (previous chapters). The method of rheology/IR, tracking mechanical parameters such as G' and chemical parameters such as the DBC is ideal for the characterization of parameters such as G'_{end}, t_{gel} and DBC_{end}.

To evaluate the limits and perspectives of the diborane/Cu 2K initiating system, different concentrations of diborane (B6-1) and $Cu(acac)_2$ were used in this study using 3Mix as monomers system.

B6-1   **Cu(acac)₂**
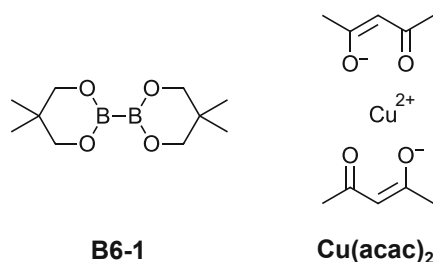
Figure 127: Chemical structure of B6-1 and $Cu(acac)_2$ that were investigated in this study.

The diborane concentration was varied between 0.5 mol% and 3.5 mol% while the $Cu(acac)_2$ concentration was varied between 0.05 mol% and 0.2 mol%. For both parts of the initiation system (B-formulation and Cu-formulation) it was shown that lower concentrations lead to a loss in initiation reactivity (Figure 128). This is reflected in a higher t_{gel} as well as lower G'_{end}.

The progression of the DBC during the polymerization clearly corresponds to these results as the polymerization starts later and ends with lower DBC_{end} with lower concentrations. However, it is remarkable that even catalytic amounts of Cu(acac)$_2$ (0.05 mol%) lead to a polymerization reaction with a DBC_{end} of over 30%. The diborane/Cu initiation system really shows its possibilities in initiation efficiency in this study as the reactivity can be tuned precisely via the concentration of the diborane or the Cu compound.[99]
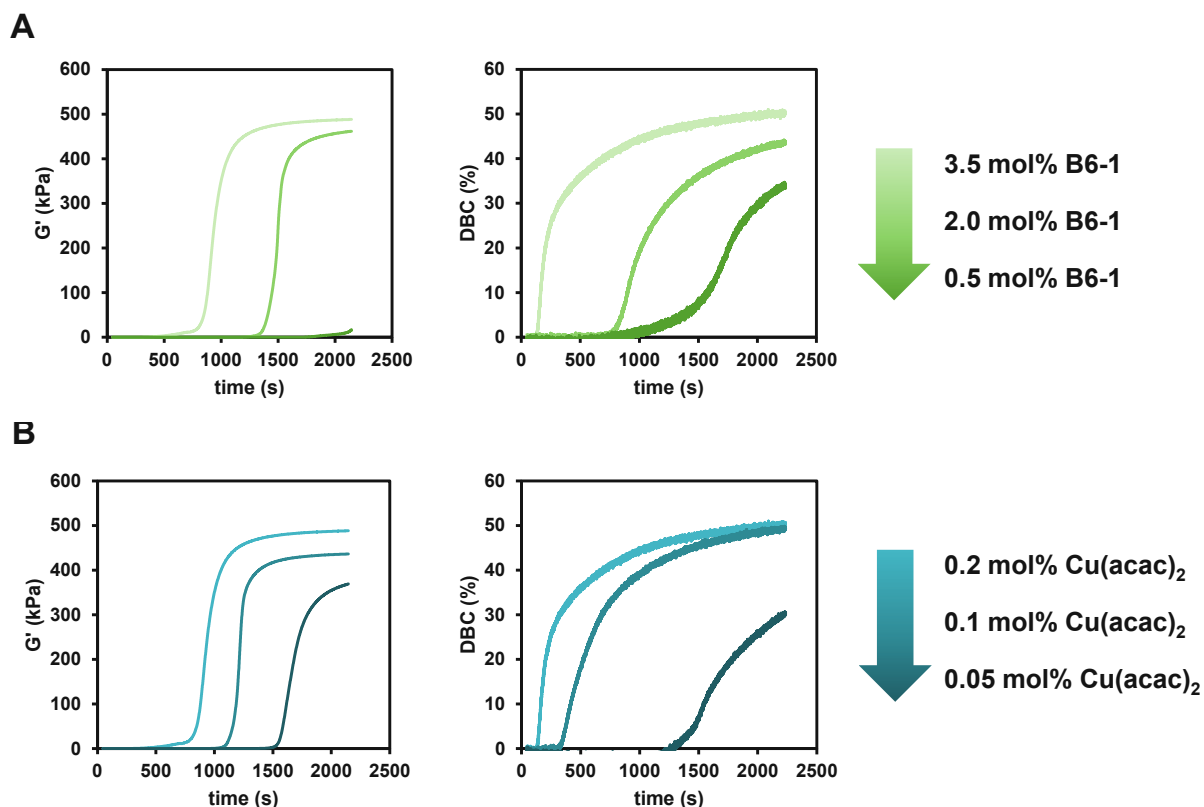
Figure 128: Rheology/IR measurements plotting G' and DBC as a function of the reaction time. 100 mg of formulations of Mix-3 containing 0.2 mol% copper salt were mixed with 100 mg formulation of Mix-3 containing 3.5 mol% (light green), 2.0 mol% (green) or 0.5 mol% (dark green) B6-1. B: Rheology/IR measurements plotting G' and DBC as a function of the reaction time. 100 mg of formulations of Mix-3 containing 0.2 mol% (light blue), 0.1 mol% (blue) or 0.05 mol% (dark blue) copper salt were mixed with 100 mg formulation of Mix-3 containing 3.5 mol% B6-1.[99]

5.3. Reactivity: Diborane/Cu vs. State of the Art

The reactivity of the diborane/Cu 2K initiation system was compared to the state-of-the-art 2K initiation system (Ref) used for similar formulations in industrial applications.[63, 64] Therefore, Rheology/IR measurements and polymerization temperature measurements in 3Mix were evaluated. The composition of the Ref formulations that was used in this study is shown in Table 41 and the structures of the compounds used are depicted in Figure 129.
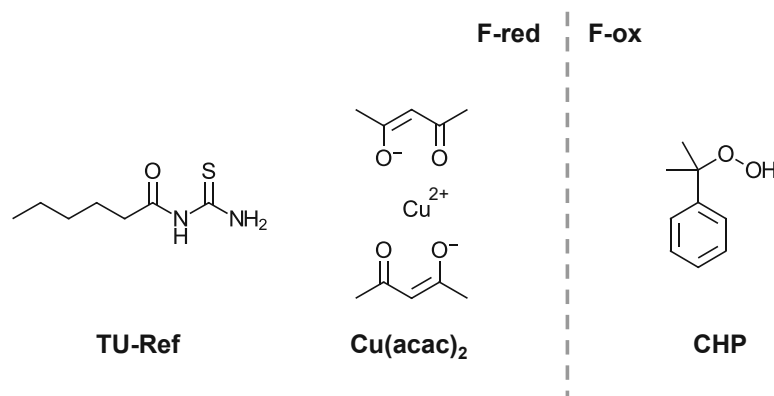
Figure 129: Chemical structures of the initiation system of the reference formulation (Ref).

Table 41: Composition of the reference formulation Ref.

	F-red	F-ox
TU-Ref (mol%)	5	-
Cu(acac)$_2$ (mol%)	0.01	-
CHP (mol%)	-	11.5
3Mix (mol%)	94.99	88.5

For the diborane/Cu 2K initiation system, the formulations were prepared as stated in the previous chapters. For the comparison of the copper compounds, B6-1 was used as the diborane and for the comparison of the diboranes, Cu(acac)$_2$ was used as the copper compound (Table 42).

The thermocouple was submerged in the mixture of F-red and F-ox or B-formulation and Cu-formulation respectively, immediately after homogenizing and the temperature was recorded. The measurements are performed inside a silicon mold under air at room temperature. All recorded temperature graphs are depicted together with the reference in Figure 131.

Table 42: Exemplary composition of the formulations used in this chapter. For B6-1 was used as diborane for the different copper comounds and Cu(acac)$_2$ was used as copper compound for the different diboranes.

	B-formulation	Cu-formulation
Diborane (mol%)	3.5	-
Cu compound (mol%)	-	0.2
3Mix (mol%)	96.5	99.8

The structures of the investigated Cu compounds and diboranes are depicted below in Figure 130.
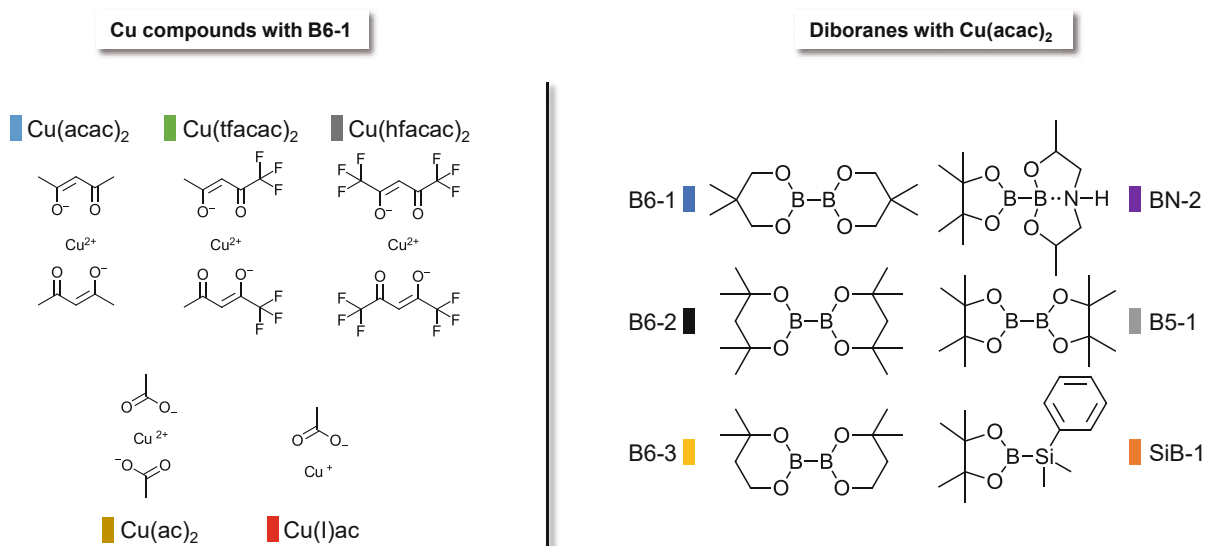
Figure 130: Chemical structures of the investigated Cu compounds and diboranes. For the comparison of the copper compounds, B6-1 was used as the diborane and for the comparison of the diboranes, Cu(acac)$_2$ was used as the copper compound.
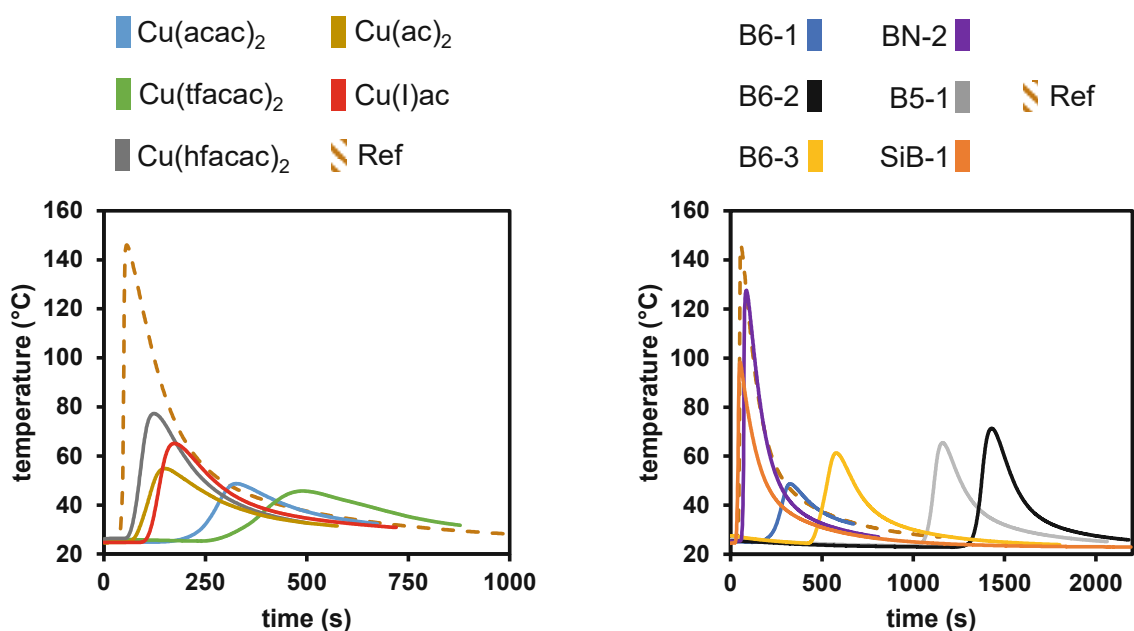
Figure 131: Summary of all polymerization temperature measurements that were discussed in chapter Reactivity, in comparison with the reference system Ref.

Although the diborane/Cu initiation system is sufficiently fast most of the discussed formulations are outperformed by the state-of-art reference system regarding t_{max} and T_{max}. However, two diboranes stand out regarding reactivity, BN-2 and SiB-1, as they lead to very fast polymerizations with t_{max} under 60 s. BN-2 can even compete to the reference system regarding the maximum temperature that is reached (Table 43 and

Table 44).

Table 43: Results of the polymerization temperature measurements of the polymerization of 3Mix with different Cu compounds and B6-1, including t_{max} and T_{max} as well as the reference system Ref.

	t_{max} (s)	T_{max} (°C)
Cu(acac)$_2$	326	48.7
Cu(tfacac)$_2$	488	45.7
Cu(hfacac)$_2$	124	77.3
Cu(ac)$_2$	151	54.9
Cu(I)ac	174	65.1
Ref	56	146.0

Table 44 Results of the polymerization temperature measurements of the polymerization of 3Mix with different diboranes and Cu(acac)$_2$, including t$_{max}$ and T$_{max}$ as well as the reference system Ref.

	t$_{max}$ (s)	T$_{max}$ (°C)
B6-1	326	48.7
B6-2	1430	71.3
B6-3	581	61.3
B5-1	1159	65.4
BN-2	86	127.6
SiB-1	51	98.4
Ref	56	146.0

The reactivity of the diborane/Cu 2K initiation system was studied further using rheology/IR measurements. In this chapter the previously discussed results are compared to the reference system Ref. In Figure 132 the summarized data in comparison to Ref is depicted.
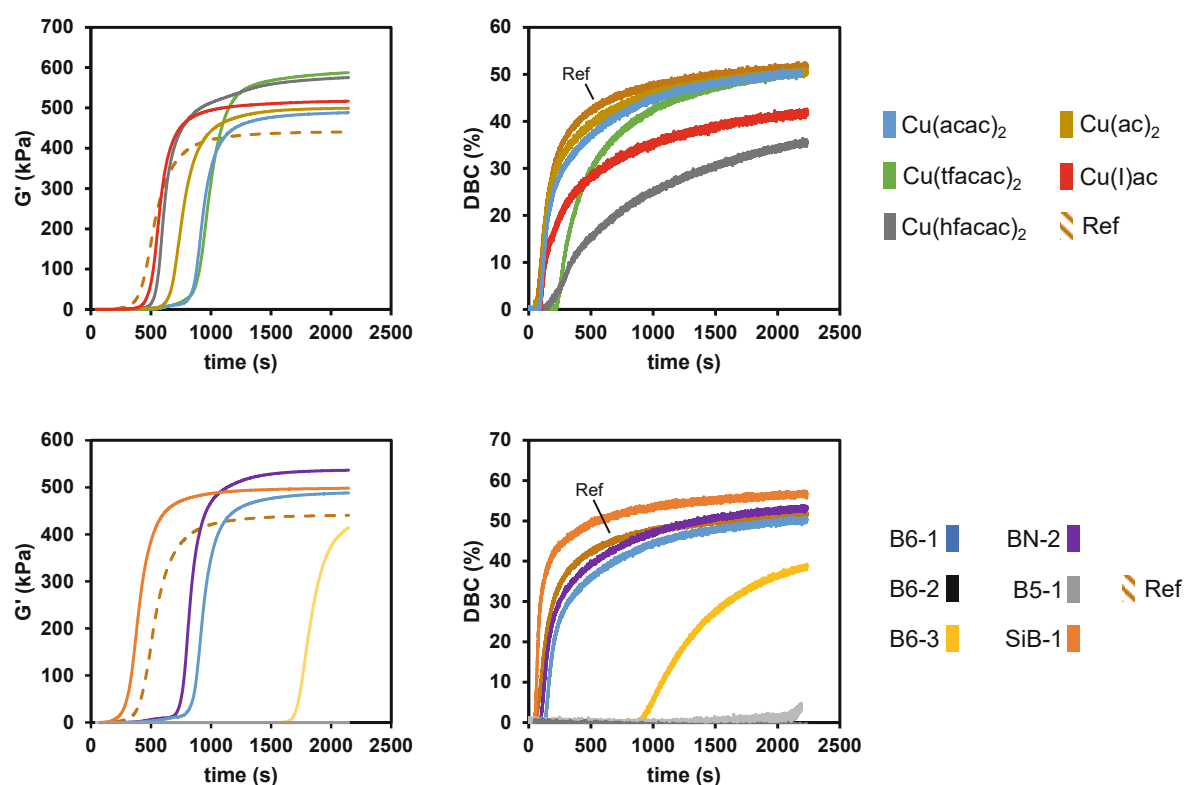
Figure 132: Top left: Storage modulus of samples that were polymerized using different Cu compounds and B6-1 and the reference (dashed). Top right: Double bond conversion of samples that were polymerized using different Cu compounds and B6-1 and the reference. Bottom left: Storage modulus of samples that were polymerized using different diboranes and Cu(acac)$_2$ and the reference (dashed). Double bond conversion of samples that were polymerized using different diboranes and Cu(acac)$_2$ and the reference.

As shown with the previously discussed polymerization temperature measurements, the rheology/IR show a very reactive reference system. Compared to B6-1 with different Cu compounds the DBC of the reference increases faster and higher, however, the mechanical properties expressed through G' are below what would be expected due to the very fast polymerization and the inhomogeneous network formation. On the other hand, as with the polymerization temperature measurements, BN-2 really stands out as it shows a higher conversion and also higher G'_{end} than the reference system (Table 45 and Table 46).

Table 45 Results of the rheology/IR measurements of the polymerization of 3Mix with different Cu compounds and B6-1, as well as the reference system Ref.

	t_{gel} (s)	G'_{end} (kPa)	DBC_{end} (%)
Cu(acac)$_2$	908	488	51.0
Cu(tfacac)$_2$	951	587	51.2
Cu(hfacac)$_2$	588	575	36.3
Cu(ac)$_2$	732	499	50.4
Cu(I)ac	552	516	42.6
Ref	566	402	52.5

Table 46: Results of the polymerization temperature measurements of the polymerization of 3Mix with different diboranes and Cu(acac)$_2$, as well as the reference system Ref.

	t_{gel} (s)	G'_{end} (kPa)	DBC_{end} (%)
B6-1	908	488	51.0
B6-2	-	-	-
B6-3	1774	413.8	39.3
B5-1	-	-	-
BN-2	803	536	53.8
SiB-1	377	498	57.4
Ref	566	402	52.5

6. Polymer Properties

The testing of mechanical and thermomechanical properties of cured polymer samples is highly important in regard of potential applications of polymer materials. Depending on the field, materials have different specifications to fulfill and these properties are also depending on the initiation systems. To this end, depending on the efficiency of the initiation system higher or lower double bond conversions are reached and network architecture is changed. These factors highly influence the mechanical and thermomechanical properties of the materials. Therefore, tensile tests and dynamical mechanical analysis (DMTA) is performed of polymer specimens with different combinations of the diborane/Cu initiation system in 3Mix. They give detailed insights in the influence on the diboranes, copper compounds, curing conditions and post-curing effects.

6.1. Tensile Tests

Tensile Tests give a great insight in the mechanical properties of the polymer, including stress at break (σ), elongation at break (ε) and Δσ/Δε, an approximate value for the Young's modulus. These tests are a shock-free, quasi-static destructive method with a slow strain rate. Uniaxial loading is applied on the sample and steadily increased until the specimen ruptures. The resulting strain is monitored with increasing stress to obtain stress-strain curves.[82] The tensile stress σ [MPa] is calculated with Equation 5, while the strain ε [%] can be determined with Equation 6 and tensile toughness U_T (MJ/cm^3)was calculated as the integrated area under the curve.

Equation 5: Calculation of the stress in tensile testing. σ…tensile stress [MPa]; F…tensile force [N]; A_0…initial cross section [mm^2].

$$\sigma = \frac{F}{A_0}$$

Equation 6: Calculation of the strain in tensile testing. ε… tensile strain [%]; ΔL…elongation [mm]; L_0…initial length [mm].

$$\varepsilon = \frac{\Delta L}{L_0}$$
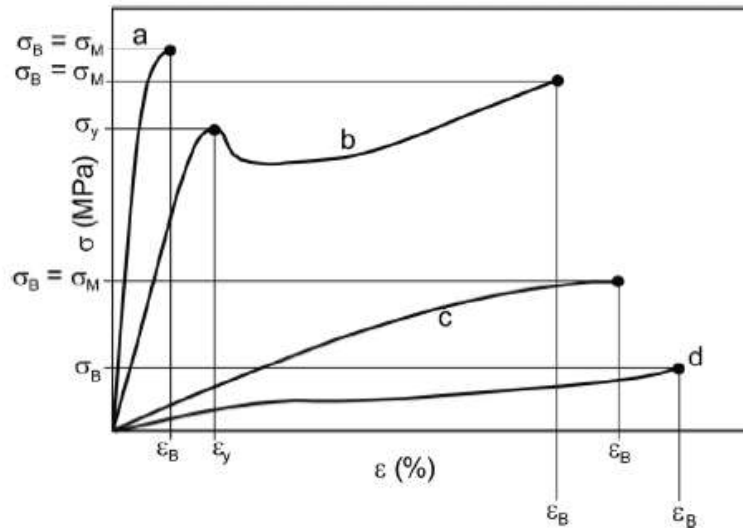
Figure 133: Scheme of typical stress-strain curves of polymer tensile testing.[82]

Figure 133 shows typical stress-strain curves of different materials. Initially, for all polymers, a linear behavior is observed. With increasing stress, a non-linear regime is exhibited, and a different behavior occurs. Highly crosslinked networks are very brittle and display very low ε_B and high σ_M (a). Furthermore, no yield point with a yield strength σ_y, as in curve b, is observed. If the crosslinking density is low, for example, in elastomers, high ε_B and low σ_M are exhibited (d).[82]

6.1.1. Post-Curing Efficiency

The time dependency of mechanical properties of a polymer material cured via a 2K system can be a problem for reproducibility. This is largely due to post-curing of polymers hours and days after the initial curing. To evaluate the optimum time for mechanical tests for the diborane/Cu 2K initiation system the post-curing efficiency was determined in this study. To this end, tensile test specimens were prepared and then measured after 1 hour, 1 day and 7 days of post-curing at 37 °C. In addition, the DBC of the cured specimen was determined via ATR-IR measurements at the respective times.

Therefore, formulations were prepared according to Table 47 and polymerized in a mold for tensile test specimen at room temperature under air. B6-1 was used as diborane, $Cu(acac)_2$ was used as copper compound and 3Mix was used as monomer mixture (Figure 134).
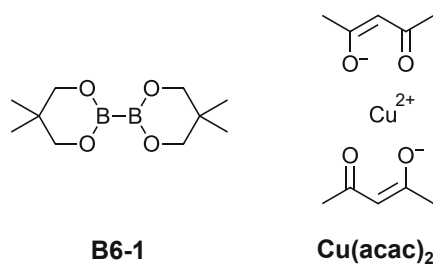
Figure 134: Chemical structure of diborane initiator B6-1 and copper catalyst Cu(acac)$_2$.

Table 47: Formulations prepared for tensile test specimens to investigate the mechanical properties of the polymer materials after 1h, 1d and 7d of post-curing at 37 °C. B6-1 was used as diborane, Cu(acac)$_2$ was used as the Cu compound and 3Mix was used as the monomer mixture.

	B-formulation	Cu-formulation
B6-1 (mol%)	3.5	-
Cu(acac)$_2$ (mol%)	-	0.2
3Mix (mol%)	96.5	99.8

The evaluated stress/strain diagrams as well as the corresponding DBCs are shown in the following Figure 135.
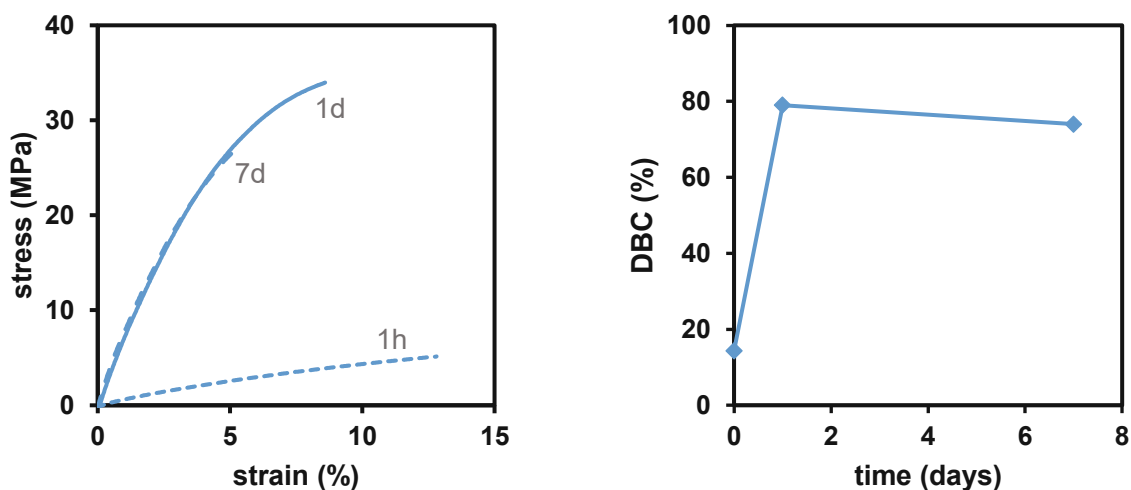
Figure 135: Left: Stress/strain diagram of the best-performing tensile test specimens at the respective times of 1h, 1d and 7d post-curing at 37 °C. Right: Double bond conversion of the respective tensile test specimens at the respective times of 1h, 1d and 7d of post-curing at 37 °C.

It is shown that post-curing plays a crucial role with the new diborane/Cu 2K initiation system as the specimens tested after 1h at 37 °C do exhibit only very little DBC of 14% and also low mechanical properties, resembling elastomeric properties with high elongations at break and low stress at break (Table 48). However, after only 1 day at 37 °C the specimens show an

increase of DBC of 65% to a total value of 79%, which results in a much denser crosslinked material. These properties are well reflected in a higher stress at break as well as a lower elongation at break. After 7 days of post-curing at 37 °C, however, the mechanical properties as well as the DBC do not increase further, marking an optimum of 1 day of post-curing. This is also well reflected in the tensile toughness U_T that is significantly higher after 1d, compared to 1h or 7d.

Table 48: Results of tensile tests of specimen derived from Cu(acac)$_2$ with B6-1 in 3Mix, including stress at break, elongation at break, Δσ/Δε, DBC$_{ATR-IR}$ and tensile toughness U_T after 1h, 1d and 7d of post-curing at 37 °C.

	stress at break (MPa)	elongation at break (%)	Δσ/Δε (MPa)	DBC$_{ATR-IR}$ (%)	U_T (MJ/cm^3)
1h	5.8±1.4	11.7±1	0.5	14	0,4±0,1
1d	27.6±4.1	6±1.6	8.5	79	1±0,5
7d	20.2±4.1	4.3±1	8.1	74	0,5±0,2

It can be concluded from this study that a post-curing time of 1 day at 37 °C is optimal for a sufficient curing of test specimens to provide reproducible results. In all further mechanical and thermomechanical tests, specimens were cured and then post-cured at 37 °C for 1 day.

6.1.2. Investigation of Cu Compounds

The choice of copper compound in the diborane/Cu 2K initiation system proved to influence the reactivity of the polymerization (see Chapter Reactivity). Since the polymerization reactivity and the progression of double bond conversion can highly influence the mechanical properties of the cured polymer material, tensile tests were performed using different copper compounds in the initiation system to evaluate these properties.

Therefore, five different Cu species were combined with two diboranes B6-1 and B5-1, to test the mechanical properties of the resulting polymers (Figure 138 and Figure 136).

6.1.2.1. B6-1/Cu Compounds

In this study, a highly reactive diborane (B6-1) was chosen as initiator in combination with five copper compounds and the mechanical properties of the cured polymers were evaluated using tensile tests.

Formulations in 3Mix were prepared according to Table 49 and mixed in a w% 50:50 ratio and transferred to a silicon mold for tensile test specimens. After polymerization the specimens were stored for 24 h at 37 °C, after which the measurements were performed.
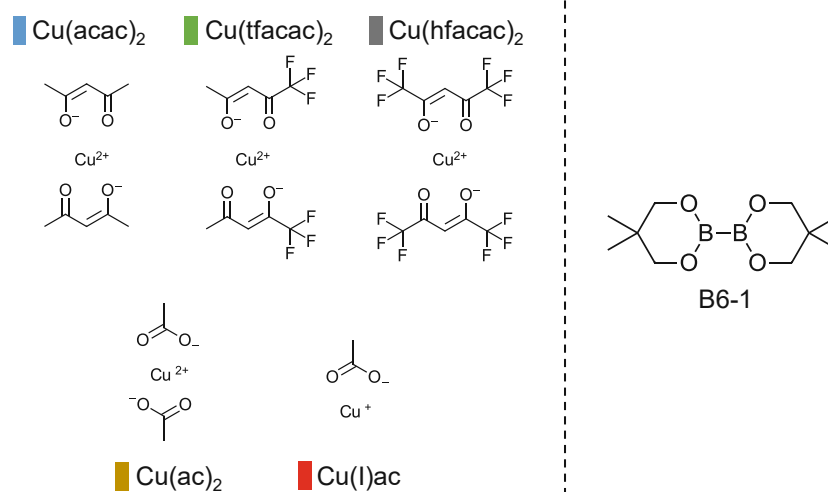
Figure 136: Left: Different Cu species ranging from differently substituted acetylacetonates, over acetate, to Cu(I) acetate. Right: B6-1, the diborane compound used in the following experiments.

Table 49: Formulations prepared for tensile test specimens to investigate the mechanical properties of the polymers derived from B6-1 and Cu(acac)$_2$, Cu(tfacac)$_2$, Cu(hfacac)$_2$, Cu(ac)$_2$ or Cu(I)ac in 3Mix.

	B-formulation	Cu-formulation
B6-1 (mol%)	3.5	-
Cu compound (mol%)	-	0.2
3Mix (mol%)	96.5	99.8

For the graphs shown in Figure 137 the trend of the mechanical properties of the polymers derived from initiation applying different Cu compound with B6-1 was expected. The slowest generated (see Chapter Reactivity) and therefore most regulated networks obtained from Cu(acac)$_2$ and Cu(tfacac)$_2$ show the best properties.
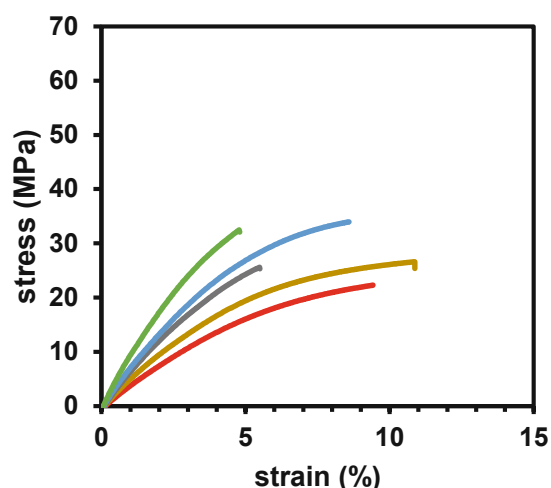
Figure 137: Stress-strain diagrams of tensile tests of specimen derived from different Cu species with B6-1 in 3Mix.[99]

The very homogeneous networks of the polymers derived from Cu(acac)$_2$ and Cu(tfacac)$_2$ prove to be the best performing regarding the mechanical properties. However, they are more brittle compared to Cu(ac)$_2$ and Cu(I)ac, which are very soft polymers. This is also reflected in the tensile toughness, as Cu(ac)$_2$ exhibits higher values compared to Cu(acac)$_2$ and Cu(tfacac)$_2$. Furthermore, it is shown that even though copper compounds like Cu(I)ac and Cu(ac)$_2$ show a high reactivity and fast growth in DBC, the mechanical properties are elastomer like due to a low resulting network density. The slower progressing DBCs initiated by Cu(acac)$_2$ and Cu(tfacac)$_2$ show a higher final DBC and therefore also a higher network density and lead to a stiffer polymer material.[99]

Table 50: Results of tensile tests of specimen derived from different Cu species with B6-1 in 3Mix, including stress at break, elongation at break, $\Delta\sigma/\Delta\varepsilon$, DBC$_{ATR-IR}$ and the tensile toughness U$_T$.

	stress at break (MPa)	elongation at break (%)	$\Delta\sigma/\Delta\varepsilon$ (MPa)	DBC$_{ATR-IR}$ (%)	U$_T$ (MJ/cm^3)
Cu(acac)$_2$	27.6±4.1	6±1.6	7.6	79	1±0,5
Cu(tfacac)$_2$	27.1±7.1	5.3±1.2	10.0	84	1,1±0,1
Cu(hfacac)$_2$	22.4±3	4.8±1.1	7.0	70	0,6±0,2
Cu(ac)$_2$	22.9±2.8	9±1.4	5.7	63	1,4±0,4
Cu(I)ac	19.3±2.2	8.6±2.2	4.4	44	1,1±0,4

6.1.2.2. B5-1/Cu Compounds

In this study, a slower reacting diborane (B5-1) was chosen as initiator in combination with five copper compounds and the mechanical properties of the cured polymers were evaluated using tensile tests. The aim is to highlight the effect of polymerization speed onto the mechanical properties of the polymer material.

Formulations in 3Mix were prepared according to Table 51 and mixed in a w% 50:50 ratio and transferred to a silicon mold for tensile test specimens. After polymerization the specimens were stored for 24 h at 37 °C, after which the measurements were performed.
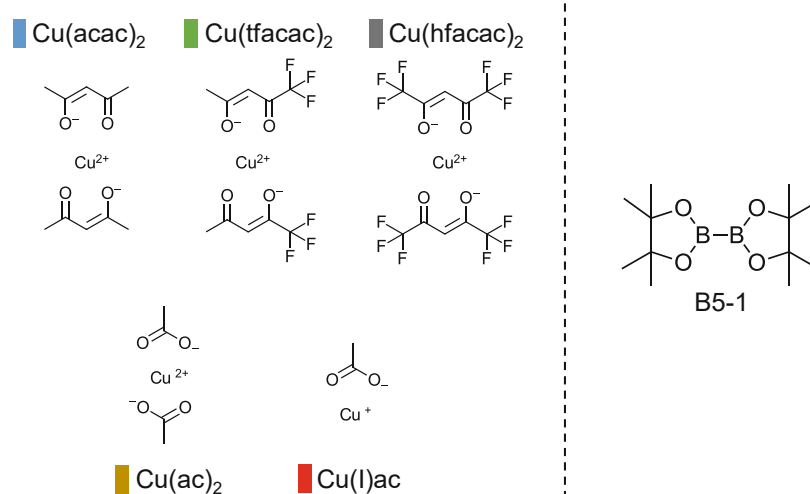
Figure 138: Left: Different Cu species ranging from differently substituted acetylacetonates, over acetate, to Cu(I) acetate. Right: B5-1, the diborane compound used in the following experiments.

Table 51: Formulations prepared for tensile test specimens to investigate the mechanical properties of the polymers derived from B5-1 and Cu(acac)$_2$, Cu(tfacac)$_2$, Cu(hfacac)$_2$, Cu(ac)$_2$ or Cu(I)ac in 3Mix.

	B-formulation	Cu-formulation
B5-1 (mol%)	3.5	-
Cu compound (mol%)	-	0.2
3Mix (mol%)	96.5	99.8

In previous studies, it was concluded that Cu(I)ac, Cu(ac)$_2$ and Cu(hfacac)$_2$ show a very fast polymerization with B6-1. However, as in this study B5-1 was used, which leads to rather slow polymerization, a more balanced polymerization observed. In Figure 139 the stress-strain diagram of the tensile tests of the investigated specimens is shown.
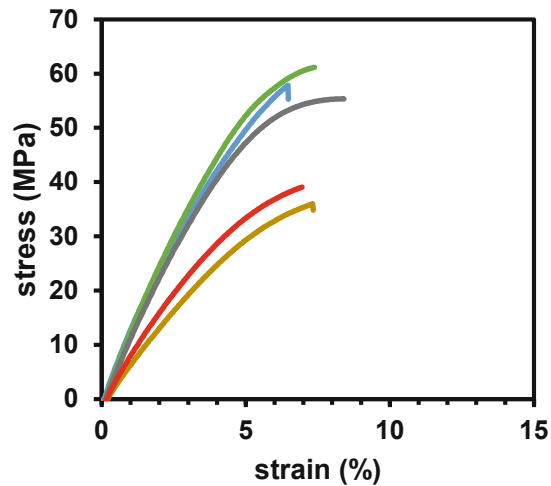
Figure 139: Stress-strain diagrams of tensile tests of specimen derived from different Cu species with B5-1 in 3Mix.

The very homogeneous networks of the polymers derived from Cu(acac)$_2$ and Cu(tfacac)$_2$ prove to be the best performing regarding the mechanical properties. They are a little more brittle compared to Cu(ac)$_2$ and Cu(I)ac, however, the stress at break is very high at over 50 MPa (Table 52). This highlights the effect of polymerization speed onto the mechanical properties, as all the specimens in which B5-1 was used as diborane outperform the specimens in which B6-1 was used. This is explained by the slow and more regular formation of the polymer network that is also much more homogeneous. Interestingly, Cu(acac)$_2$, Cu(tfacac)$_2$ and Cu(hfacac)$_2$ also show a higher tensile toughness compared to Cu(ac)$_2$ and Cu(I)ac, showing the superior mechanical properties of these polymers.

Table 52: Results of tensile tests of specimen derived from different Cu species with B5-1 in 3Mix, including stress at break, elongation at break, Δσ/Δε and DBC$_{ATR-IR}$ and the tensile toughness U$_T$.

	stress at break (MPa)	elongation at break (%)	Δσ/Δε (MPa)	DBC$_{ATR-IR}$ (%)	U$_T$ (MJ/cm^3)
Cu(acac)$_2$	55.1±3.2	6.4±0.4	13.9	>80	2±0,2
Cu(tfacac)$_2$	54.4±6.3	6.4±1.3	14.4	>80	2,1±0,7
Cu(hfacac)$_2$	51.7±3.4	6.8±1.3	13.2	>80	2±1
Cu(ac)$_2$	32.2±3.5	7.2±1.1	8.1	83	1,4±0,4
Cu(I)ac	33.7±3.3	7.2±1.9	9.8	63	1,6±0,6

6.1.3. Investigation of Diboranes

The previous chapters discussed the influence of various copper compounds in the diborane/Cu 2K initiation system onto the mechanical properties of the cured polymer material in combination with two selected diboranes. Not only the copper part of the 2K initiation system can affect the resulting mechanical properties, but also the diboranes can influence these parameters. The following chapters will discuss the influence of the diborane onto the mechanical properties evaluated with tensile tests and also the diborane concentration dependency of these properties.

6.1.3.1. Cu(acac)$_2$/Diboranes

The mechanical properties of polymer networks using 3Mix as monomer mixture were evaluated with different diboranes as the diborane part of the diborane/Cu 2K initiation system and Cu(acac)$_2$ as the copper compound (Figure 140) using tensile tests. Formulations were prepared according to Table 53 and mixed in a w% 50:50 ratio and transferred to a silicon mold for tensile test specimens. After polymerization the specimens were stored for 24 h at 37 °C, after which the measurements were performed.
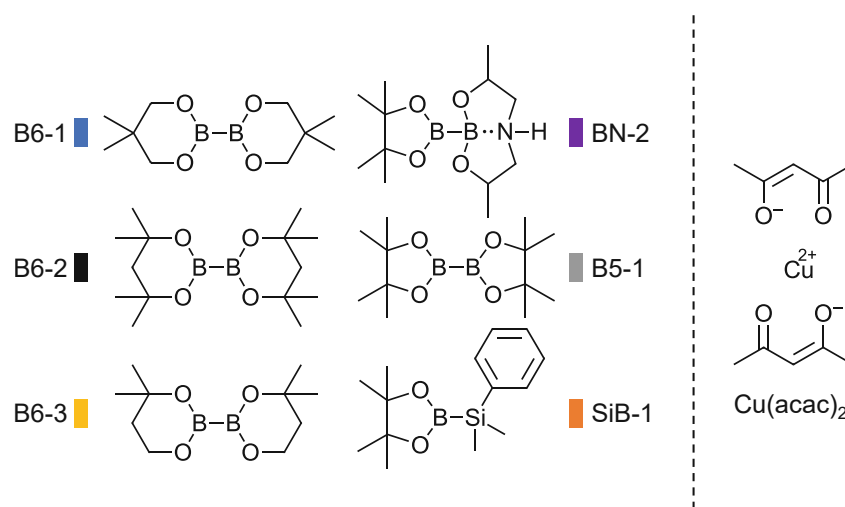

Figure 140: Left: Structure of different diboranes (B6-1, B6-2, B6-3 obtain sixmembered rings. BN-2 obtains an electron donating nitrogen atom. B5-1 obtains fivemembered rings) and a silylborane SiB-1. Right: Structure of Cu(acac)$_2$.

Table 53: Formulations for tensile test specimens to investigate the mechanical properties of the polymers derived from B6-1, B6-2, B6-3, BN-2, B5-1 and SiB-1 with Cu(acac)$_2$ in 3Mix.

	B-formulation	Cu-formulation
Diborane (mol%)	3.5	-
Cu(acac)$_2$ (mol%)	-	0.2
3Mix (mol%)	96.5	99.8

The mechanical properties of the polymers derived from initiation of different diboranes differ very much. It is to notice that with the exception of BN-2, the polymerization speed measured in polymerization temperature measurements (see Chapter Reactivity) correlates extremely well to the final mechanical properties. The slower polymerizing diboranes lead to more organized networks and the mechanical properties of those polymers are very promising. Especially, B6-2, B6-3, B5-1 and BN-2 lead to a very high stress at break with a $\Delta\sigma/\Delta\varepsilon > 10$ (Figure 141).

Figure 141: Stress-strain diagrams of tensile tests of specimen derived from different diborane compounds with Cu(acac)$_2$ in 3Mix.[99]

The specimens polymerized using SiB-1 show extremely high elongation at break with the least stress at break compared to the other diboranes (Table 54). The very fast polymerization leads to a relatively fast gel point with the consequence of a low DBC. The slower the polymerization is getting the more time have the polymer chains and initiating system compounds to regulate the network and delay the gel point. These samples have higher DBC when reaching the gel point and therefore show very good mechanical properties.[99] The tensile toughness, however,

144

shows that the polymer polymerized with SiB-1 is tougher compared to BN-2 and B6-1. The best performing initiator B6-2, however, also exhibits the highest tensile toughness.

Table 54: Results of tensile tests of specimen derived from different diborane compounds with Cu(acac)$_2$ in 3Mix, including stress at break, elongation at break, Δσ/Δε and DBC$_{ATR-IR}$ and the tensile toughness U$_T$.

	stress at break (MPa)	elongation at break (%)	Δσ/Δε (MPa)	DBC$_{ATR-IR}$ (%)	U$_T$ (MJ/cm^3)
B6-1	27.6±4.1	6±1.6	7.6	79	1±0,5
B6-2	64.1±2.1	7.2±0.9	15.2	79	2,2±0,8
B6-3	49.8±3.2	5.7±0.5	13.7	72	1,3±0,4
B5-1	55.1±3.2	6.4±0.4	13.9	>80	2,1±0,9
BN-2	47.9±0.7	4.8±0.3	13.5	58	0,9±0,4
SiB-1	17.6±4.9	7.7±3.1	5.1	46	1,4±0,5

6.1.3.2. Concentration Dependency of B6-1/Cu(acac)2

The detailed characterization of the mechanical properties of polymers polymerized with the diborane/Cu 2K system was conducted employing various copper and diborane compounds in the previous chapters. However, not only the choice of diborane or copper compound is important, but also the concentration of such. To evaluate the limits and perspectives of the diborane/Cu 2K initiating system, different concentrations of diborane (B6-1) were used in this study using 3Mix as monomers system.

B6-1   **Cu(acac)$_2$**
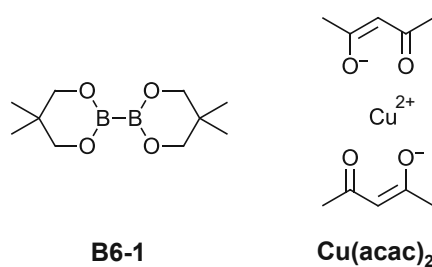
Figure 142: Chemical structure of B6-1 and Cu(acac)$_2$ that were investigated in this study.

The diborane concentration was varied between 1.8 mol%, 3.5 mol% and 7 mol% and the concentration of Cu(acac)$_2$ was set to 0.2 mol%. The concentration of the copper compound above 0.2 mol% could not be reliable varied due to solubility issues at higher concentrations and extremely low performance polymers at lower concentrations. Therefore, the optimum for copper concentration was set to 0.2 mol%. Formulations were prepared according to Table 55.

Table 55: Formulations for tensile test specimens to investigate the mechanical properties of the polymers derived from B6-1 and Cu(acac)$_2$ in 3Mix at different concentrations of the diborane.

	B-formulation	Cu-formulation
B6-1 (mol%)	1.8 / 3.5 / 7	-
Cu(acac)$_2$ (mol%)	-	0.2
3Mix (mol%)	98.2 / 96.5 / 93	99.8

The formulations were mixed in a w% 50:50 ratio and transferred to a silicon mold for tensile test specimens. After polymerization the specimens were stored for 24 h at 37 °C, after which the measurements were performed (Figure 143).
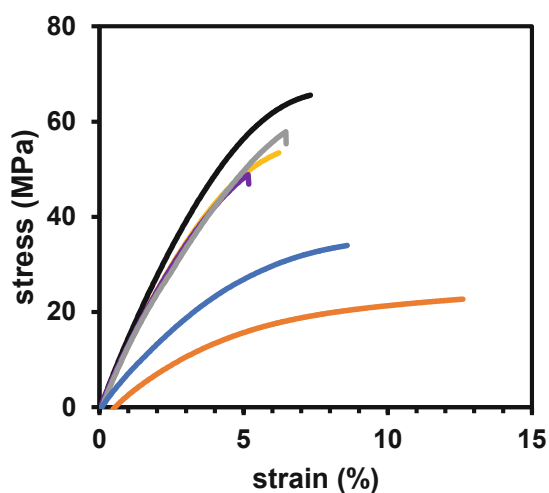

Figure 143: Stress-strain diagrams of best performing tensile tests of specimens derived from initiation with different concentrations of B6-1 (1.8 mol%, 3.5 mol%, 7 mol%) and Cu(acac)$_2$ (0.2 mol%) in 3Mix.

The tensile test specimens that were polymerized using only 1.8 mol% B6-1 as diborane do show a significant decrease in DBC and result in a loss of mechanical properties concerning both, the stress at break and the elongation at break. However, the benefit of exceeding 3.5 mol%, using 7 mol%, is not massive as the Young's modulus is increasing slightly, but stress at break and elongation at break decrease compared to the 3.5 mol% sample. Also, the tensile toughness shows very comparable values for 3.5 mol% B6-1 and 7 mol% B6-1.

Table 56: Results of tensile tests of specimen derived from initiation with different concentrations of B6-1 and $Cu(acac)_2$ in 3Mix, including stress at break, elongation at break, $\Delta\sigma/\Delta\varepsilon$ and DBC_{ATR-IR} and the tensile toughness U_T.

mol% B6-1	stress at break (MPa)	elongation at break (%)	$\Delta\sigma/\Delta\varepsilon$ (MPa)	DBC_{ATR-IR} (%)	U_T (MJ/cm^3)
1.8	23.9±6.4	7.8±3.9	5.7	33	0,4±0,2
3.5	27.6±4.1	6±1.6	7.6	79	1±0,5
7	29±4.4	5.6±1.2	11.3	73	1±0,4

Regarding the previous results it can be concluded that 3.5 mol% diborane is already an optimum condition for the polymerization and the resulting mechanical properties.

6.1.4. Tensile Tests: Diborane/Cu vs. State of the Art

The mechanical properties of specimen that were polymerized using the diborane/Cu 2K initiation system in 3Mix were compared to the state-of-the-art 2K initiation system (Ref) used for similar formulations in industrial applications.[63, 64] Therefore, tensile tests were evaluated. The composition of the Ref formulations that was used in this study is shown in Table 57 and the structures of the compounds used are depicted Figure 147.
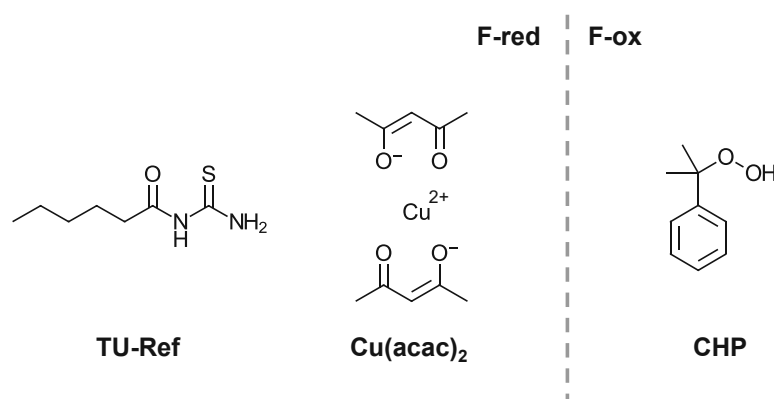
Figure 144: Chemical structures of the initiation system of the reference formulation (Ref).

Table 57: Composition of the reference formulation.

	F-red	F-ox
TU-Ref (mol%)	5	-
$Cu(acac)_2$ (mol%)	0.01	-
CHP (mol%)	-	11.5
3Mix (mol%)	94.99	88.5

For the diborane/Cu 2K initiation system, the formulations were prepared as stated in the previous chapters. For the comparison of the copper compounds, B6-1 and B5-1 were used as the diboranes and for the comparison of the diboranes, $Cu(acac)_2$ was used as the copper compound (Table 58). All recorded stress/strain diagrams are depicted together with the reference in Figure 146.

Table 58: Exemplary composition of the formulations used in this chapter. B6-1 was used as diborane for the different copper comounds and $Cu(acac)_2$ was used as copper compound for the different diboranes.

	B-formulation	Cu-formulation
Diborane (mol%)	3.5	-
Cu compound (mol%)	-	0.2
3Mix (mol%)	96.5	99.8

The structures of the investigated Cu compounds and diboranes are depicted below in Figure 148.
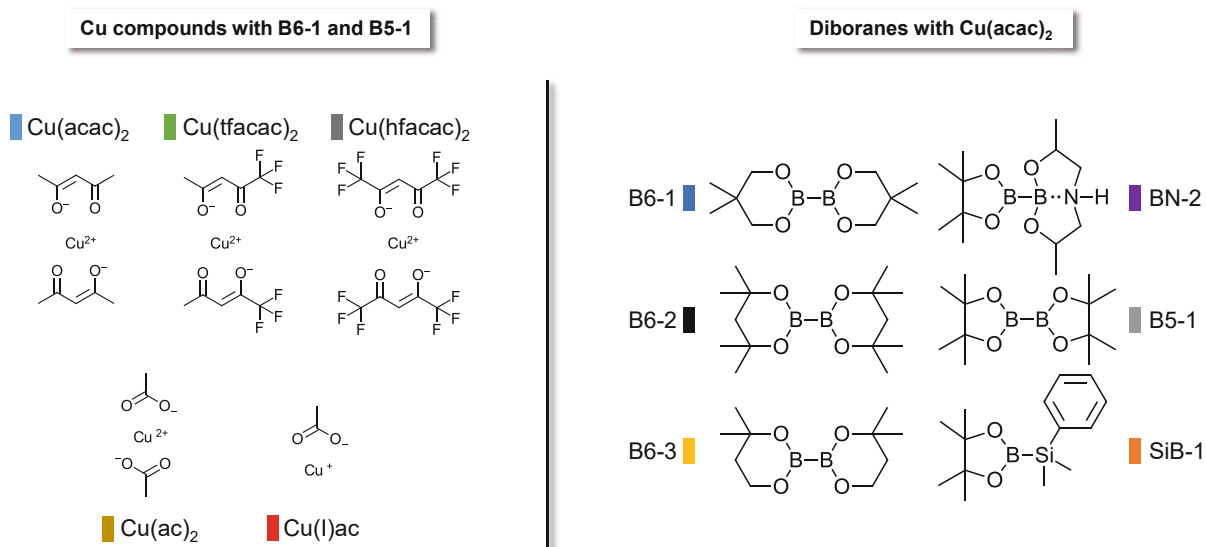
Figure 145: Chemical structures of the investigated Cu compounds and diboranes. B6-1 and B5-1 were used as the diboranes for the comparison of the Cu compounds. $Cu(acac)_2$ was used as the copper compound for the comparison of the diboranes.
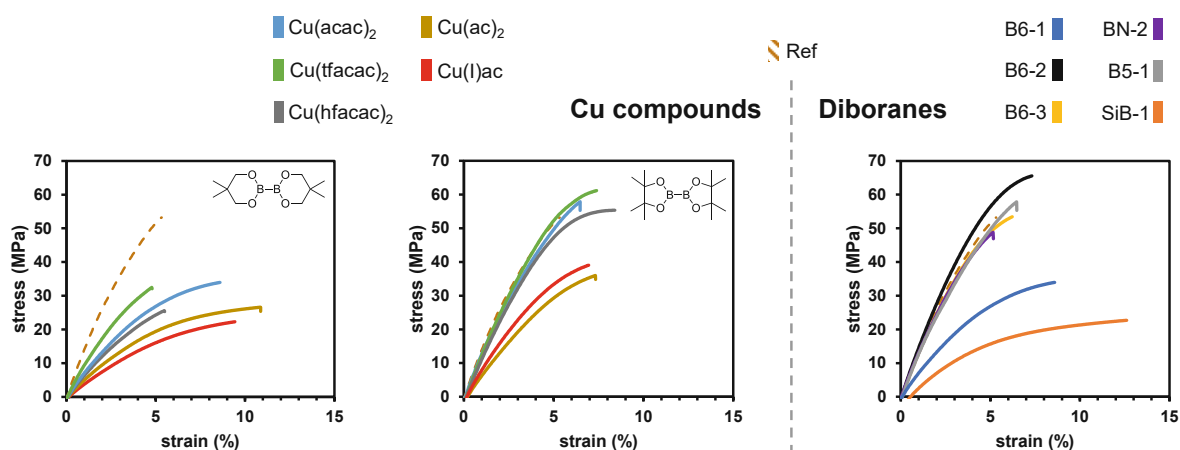
Figure 146: Left: Tensile tests of specimen polymerized using B6-1 and different Cu compounds in 3Mix including Ref. Middle: Tensile tests of specimen polymerized using B5-1 and different Cu compounds in 3Mix including Ref. Right: Tensile tests of specimen polymerized using Cu(acac)$_2$ and different diboranes in 3Mix including Ref.

The polymer derived from the polymerization using B6-1 and different Cu compounds in the initiation system show more elastic behaviour than the reference which is rather stiff and brittle. When looking at the results from using B5-1 as the diborane instead, it clearly shows that Cu(acac)$_2$, Cu(tfacac)$_2$ and Cu(hfacac)$_2$ led to very stiff and brittle polymer networks that are comparable to the ones derived from the reference initiation system. From the comparison of different diboranes with Cu(acac)$_2$ to the reference, we see that B6-2, B5-1, B6-3 and BN-2 lead to very comparable mechanical properties of the polymers. In this regard especially BN-2 stands out, as this diborane also shows high reactivity. The full comparison of the presented data is further shown in Table 59.

Table 59: Summarized data of tensile tests using B6-1 with different Cu compounds, B5-1 with different Cu compounds and Cu(acac)$_2$ with different diboranes in 3Mix, compared to Ref.

		stress at break (MPa)	elongation at break (%)	$\Delta\sigma/\Delta\varepsilon$ (MPa)	DBC$_{ATR-IR}$ (%)	U$_T$ (MJ/cm^3)
B6-1	Cu(acac)$_2$	27.6±4.1	6±1.6	7.6	79	1±0,5
	Cu(tfacac)$_2$	27.1±7.1	5.3±1.2	10.0	84	1,1±0,1
	Cu(hfacac)$_2$	22.4±3	4.8±1.1	7.0	70	0,6±0,2
	Cu(ac)$_2$	22.9±2.8	9±1.4	5.7	63	1,4±0,4
	Cu(I)ac	19.3±2.2	8.6±2.2	4.4	44	1,1±0,4
B5-1	Cu(acac)$_2$	55.1±3.2	6.4±0.4	13.9	>80	2±0,2
	Cu(tfacac)$_2$	54.4±6.3	6.4±1.3	14.4	>80	2,1±0,7
	Cu(hfacac)$_2$	51.7±3.4	6.8±1.3	13.2	>80	2±1
	Cu(ac)$_2$	32.2±3.5	7.2±1.1	8.1	83	1,4±0,4
	Cu(I)ac	33.7±3.3	7.2±1.9	9.8	63	1,6±0,6
Cu(acac)$_2$	B6-1	27.6±4.1	6±1.6	7.6	79	1±0,5
	B6-2	64.1±2.1	7.2±0.9	15.2	79	2,2±0,8
	B6-3	49.8±3.2	5.7±0.5	13.7	72	1,3±0,4
	B5-1	55.1±3.2	6.4±0.4	13.9	>80	2,1±0,9
	BN-2	47.9±0.7	4.8±0.3	13.5	58	0,9±0,4
	SiB-1	17.6±4.9	7.7±3.1	5.1	46	1,4±0,5
	Ref	46.3±6.2	4.4±0.9	14.5	68	1±0,5

6.2. DMTA

Dynamic mechanical thermal analysis (DMTA) is carried out to study the temperature dependency of the mechanical properties of the polymers. Conclusions can be drawn regarding the network properties, the T_g and post-curing effects.

A typical duromeric and highly crosslinked network exhibits a broad range of domain sizes and no distinct glass transition temperature is visible. Such a network will maintain its mechanical properties in the rubbery plateau until it degrades. However, a network with lower crosslinking density will show a decrease of storage modulus in the transition region. These effects are schematically displayed in a lower storage modulus at the rubber plateau (G'_r) and a narrow glass transition temperature range.[81]

Figure 147: Schematic explanation of the influence of crosslink density on glass transition and storage modulus[81]

If polymer networks show an increase in double bond conversion and therefore crosslinking density after thermal treatment, post-curing is occurring. In DMTA measurements these post-curing phenomena can be observed, as G' increases with increasing temperature until a final more densely crosslinked rubber plateau is reached. As the T_g of the more crosslinked network is higher these effects are also reflected in the tanδ as a second peak. These effects are schematically shown in Figure 148.
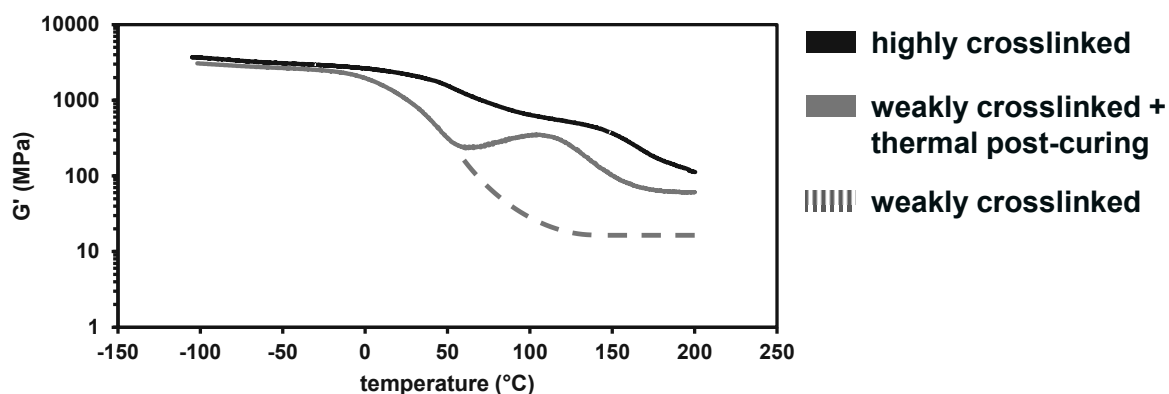
Figure 148: Schematic DMTA measurement of a highly crosslinked network (brown), a weakly crosslinked network that shows thermal post-curing (purple) and a weakly crosslinked network that does not show thermal post-curing (purple dotted).

6.2.1. Investigation of Cu Compounds

The choice of copper compound in the diborane/Cu 2K initiation system proved to influence the reactivity of the polymerization (see Chapter Reactivity) and the mechanical properties of the cured polymer (see Chapter Tensile Tests). Since the polymerization reactivity and the progression of double bond conversion can also influence the thermomechanical properties of the cured polymer material, DMTA measurements were performed using different copper compounds in the initiation system to evaluate these properties.

Therefore, five different Cu species were combined with two diboranes B6-1 and B5-1, to investigate the thermomechanical properties of the resulting polymers.

6.2.1.1. B6-1/Cu Compounds

In this study, a highly reactive diborane (B6-1) was chosen as initiator in combination with five copper compounds and the thermomechanical properties of the cured polymers were evaluated (Figure 149).

Formulations in 3Mix were prepared according to Table 60and mixed in a w% 50:50 ratio and transferred to a silicon mold for DMTA specimens. After polymerization the specimens were stored for 24 h at 37 °C, after which the measurements were performed.
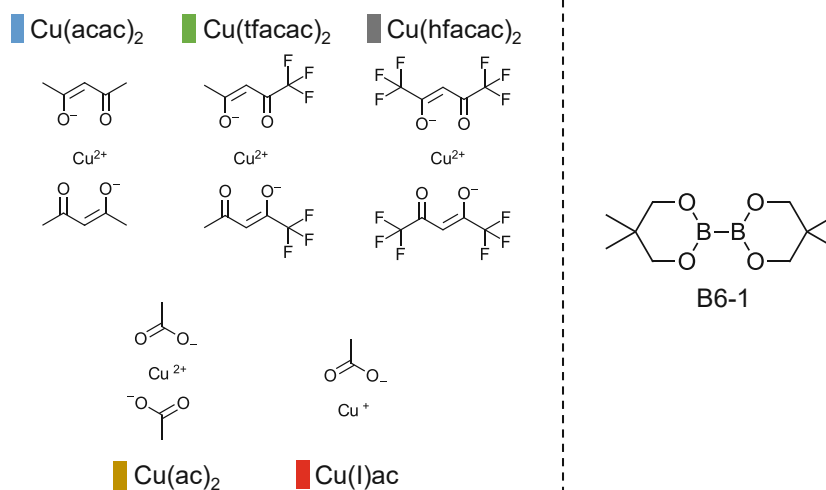
Figure 149: Left: Different Cu species ranging from differently substituted acetylacetonates, over acetate, to Cu(I) acetate. Right: B6-1, the diborane compound used in the following experiments.

Table 60: Formulations prepared for DMTA specimens to investigate the thermomechanical properties of the polymers derived from B6-1 and Cu(acac)₂, Cu(tfacac)₂, Cu(hfacac)₂, Cu(ac)₂ or Cu(I)ac in 3Mix.

	B-formulation	Cu-formulation
B6-1 (mol%)	3.5	-
Cu compound (mol%)	-	0.2
3Mix (mol%)	96.5	99.8

The storage modulus (G') of the respective specimens is plotted against the temperature increase from -100 °C to 200 °C. Another important parameter is the loss factor (tanδ) which is the quotient of G' and the loss modulus (G''). In the following Figure 150 G' and tanδ are depicted for different Cu compounds after polymerization with B6-1.

Figure 150: DMTA curves with G' (fully drawn) and tanδ (dashed line) of samples derived from $Cu(acac)_2$, $Cu(tfacac)_2$, $Cu(hfacac)_2$, $Cu(ac)_2$ or $Cu(I)ac$ with B6-1 in 3Mix.

The polymers derived from the polymerization with different Cu compounds and B6-1 do show different properties depending on the Cu compound. Especially in the case of $Cu(ac)_2$ and $Cu(I)ac$ the decrease in G' is significant. The T_g is for all samples at around 50 °C, however in the case of $Cu(acac)_2$, $Cu(tfacac)_2$ and $Cu(hfacac)_2$ a shoulder towards a higher T_g is visible (Figure 151).

154
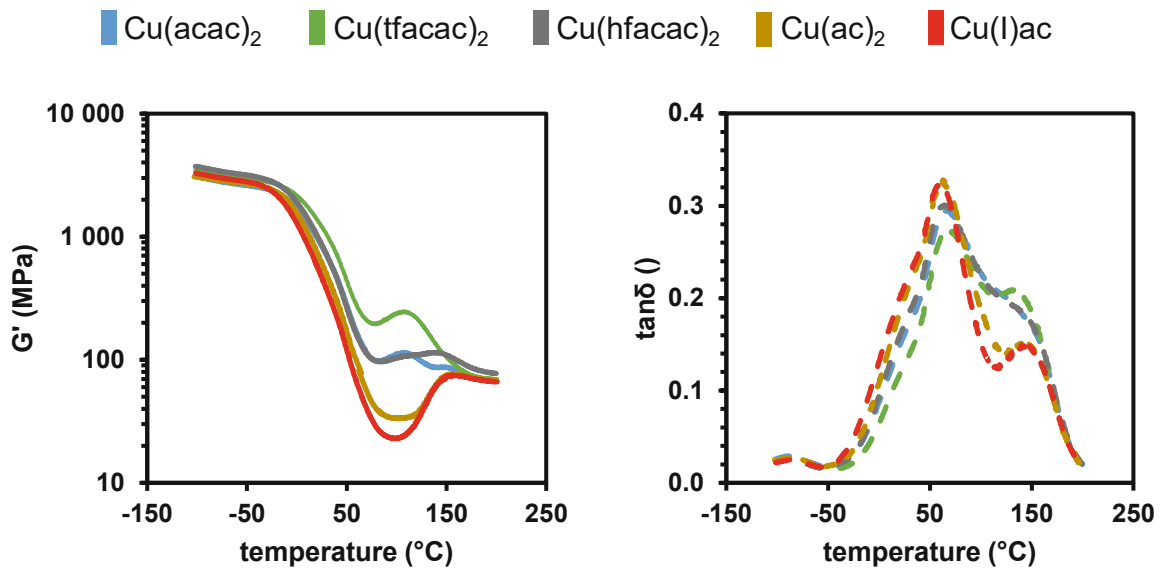
Figure 151: Left: Storage modulus of all DMTA measurements compared. Right: tanδ of all DMTA measurements compared.[99]

The networks formed with Cu(acac)$_2$ and Cu(tfacac)$_2$ are the most homogeneous and lead to the fewest post-curing. When looking at reactivity of the different Cu compounds in this context it can be seen that Cu(acac)$_2$ and Cu(tfacac)$_2$ exhibit the slowest polymerization, however also show the least decrease in G'. This shows that the reactivity towards polymerization is influencing not only the mechanical properties (see Tensile Tests) but also influence the thermomechanical properties. The slower reacting Cu compounds tend to form more homogeneous networks with a less steep drop in G' and less thermal post-curing.[99]

6.2.1.2.   B5-1/Cu Compounds

In this study, a slow reacting diborane (B5-1) was chosen as initiator in combination with five copper compounds and the thermomechanical properties of the cured polymers were evaluated (Figure 152) using DMTA. The aim is to highlight the effect of polymerization speed onto the thermomechanical properties of the polymer material.

Formulations in 3Mix were prepared according to Table 61 and mixed in a w% 50:50 ratio and transferred to a silicon mold for DMTA specimens. After polymerization the specimens were stored for 24 h at 37 °C, after which the measurements were performed.

155
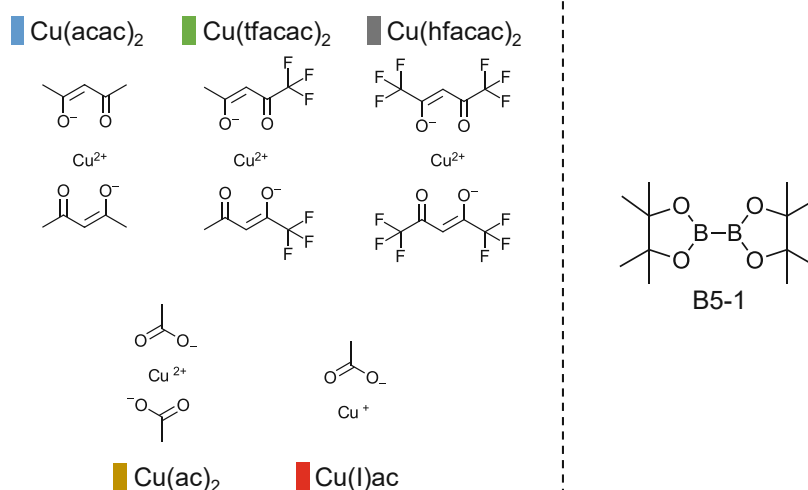
Figure 152: Left: Different Cu species ranging from differently substituted acetylacetonates, over acetate, to Cu(I) acetate. Right: B5-1, the diborane compound used in the following experiments.

Table 61: Formulations prepared for DMTA specimens to investigate the thermomechanical properties of the polymers derived from B5-1 and Cu(acac)$_2$, Cu(tfacac)$_2$, Cu(hfacac)$_2$, Cu(ac)$_2$ or Cu(I)ac in 3Mix.

	B-formulation	Cu-formulation
B5-1 (mol%)	3.5	-
Cu (mol%)	-	0.2
3Mix (mol%)	96.5	99.8

The storage modulus (G') of the respective specimens is plotted against the temperature increase from -100 °C to 200 °C. Another important parameter is the loss factor (tanδ) which is the quotient of G' and the loss modulus (G''). In the following Figure 153 G' and tanδ are depicted for different Cu compounds after polymerization with B5-1.
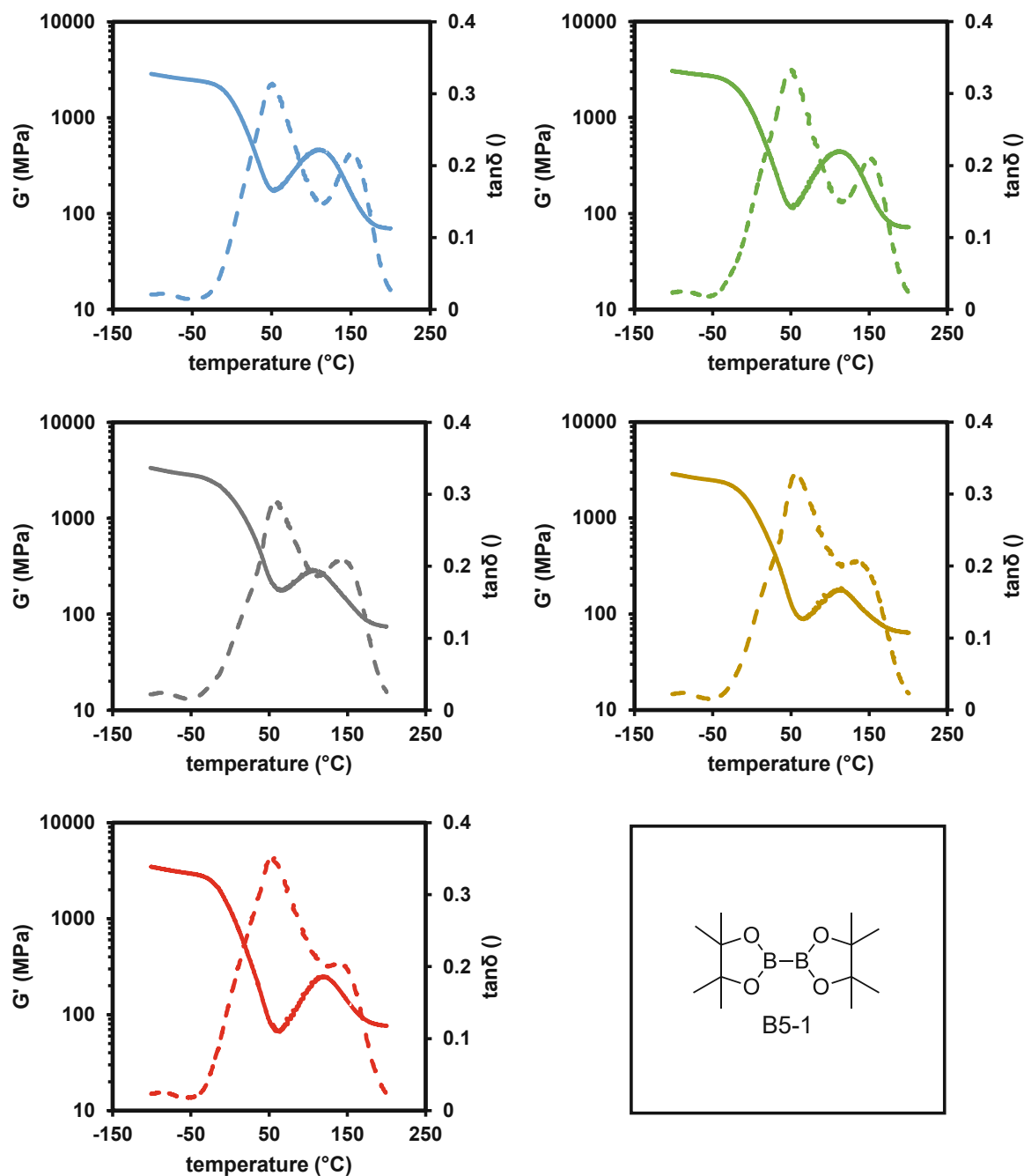
Figure 153: DMTA curves with G' (fully drawn) and tanδ (dashed line) of samples derived from Cu(acac)$_2$, Cu(tfacac)$_2$, Cu(hfacac)$_2$, Cu(ac)$_2$ or Cu(I)ac with B5-1 in 3Mix.

The choice of the Cu compound makes a significant difference in the thermomechanical properties of the resulting polymers. Since also the reactivity of the polymerization depends a lot on the Cu compound it is an obvious conclusion that this also influences other properties of the polymer. For all investigated polymers, two peaks are visible in the tanδ, which correspond to the glass transition temperature (T_g). The first observed T_g is at 50 °C and is due to the rapid decrease of G'. A very important feature of the peak is its shape as it is quite high and also very narrow with a full width half maximum of about 50 °C for every investigated

formulation. However, it is shown that in the case of Cu(ac)$_2$ and Cu(I)ac, and partly Cu(hfacac)$_2$, the first peak tails towards high temperatures into a shoulder and not a distinct second peak (Figure 154). This is the result of severe loss in storage modulus at 50 °C and a less distinct post-curing effect at higher temperatures. The Cu compounds that lead to a faster polymerization also lead to rather irregular networks in comparison to Cu(acac)$_2$ and Cu(tfacac)$_2$. This is also reflected in the tanδ of those specimens as the peak is more distinct and also the post-curing leads to a distinct second peak at 150 °C.

Figure 154: Left: Storage modulus of all DMTA measurements compared. Right: tanδ of all DMTA measurements compared.

The post-curing that is seen in these measurements is likely to occur due to unreacted diborane species that are trapped in the network. With temperature increase, the B-B bond can cleave and lead to a polymerization of 3Mix (see Chapter Thermal Stability). This is especially true if the specimen is already past its gel point and the network is flexible. In the case of Cu(hfacac)$_2$, Cu(ac)$_2$ and Cu(I), this is an indication that in those specimens, more diborane is left unreacted, therefore the post-curing process starts earlier, leading towards a broadening of the peak towards higher temperatures.

6.2.2. Investigation of Diboranes

The previous chapters discussed the influence of various copper compounds in the diborane/Cu 2K initiation system onto the thermomechanical properties of the cured polymer material in combination with two selected diboranes (B6-1 and B5-1). Not only the copper part of the 2K initiation system can affect the resulting thermomechanical properties, but also the diboranes can influence these parameters. The following chapters will discuss the influence of the diborane onto the thermomechanical properties evaluated via DMTA measurements and also the diborane concentration dependency of these properties.

6.2.2.1. Cu(acac)$_2$/Diboranes

In this study, the thermomechanical properties of polymer networks using 3Mix as monomer mixture were evaluated using different diboranes as the diborane part of the diborane/Cu 2K initiation system and Cu(acac)$_2$ as the copper compound (Figure 140) using DMTA. Formulations were prepared according to Table 53 and mixed in a w% 50:50 ratio and transferred to a silicon mold for tensile test specimens. After polymerization the specimens were stored for 24 h at 37 °C, after which the measurements were performed.

The chemical structure of the respective compounds is displayed in Figure 155, while in Table 62 the composition of the formulations used is shown. The Cu-formulations and respective B-formulation were mixed in w% 50:50 ratio and cured inside a mold for DMTA specimens. Thereafter, the specimens were stored for 24 h at 37 °C and subsequently the measurements were performed.
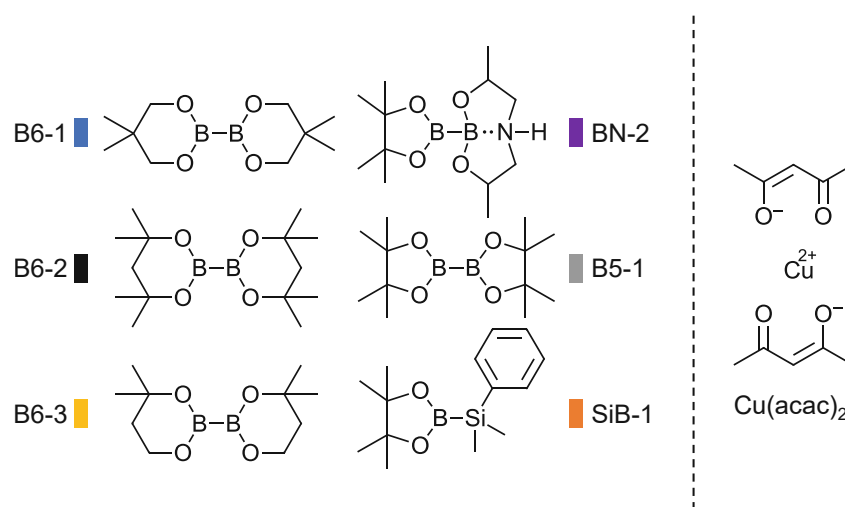
Figure 155: Left: Structure of different diboranes (B6-1, B6-2, B6-3 obtain sixmembered rings. BN-2 obtains an electron donating nitrogen atom. B5-1 obtains fivemembered rings) and a silylborane SiB-1. Right: Structure of Cu(acac)$_2$.

Table 62: Formulations for DMTA specimens to investigate the thermomechanical properties of the polymers derived from B6-1, B6-2, B6-3, BN-2, B5-1 and SiB-1 with $Cu(acac)_2$ in 3Mix.

	B-formulation	Cu-formulation
Diborane (mol%)	3.5	-
$Cu(acac)_2$ (mol%)	-	0.2
3Mix (mol%)	96.5	99.8

The storage modulus (G') of the respective specimens is plotted against the temperature increase from -100 °C to 200 °C. The important parameter is the loss factor (tanδ) which is the quotient of G' and the loss modulus (G''). In the following Figure 156 G' and tanδ are depicted for all respective diboranes after polymerization with $Cu(acac)_2$.
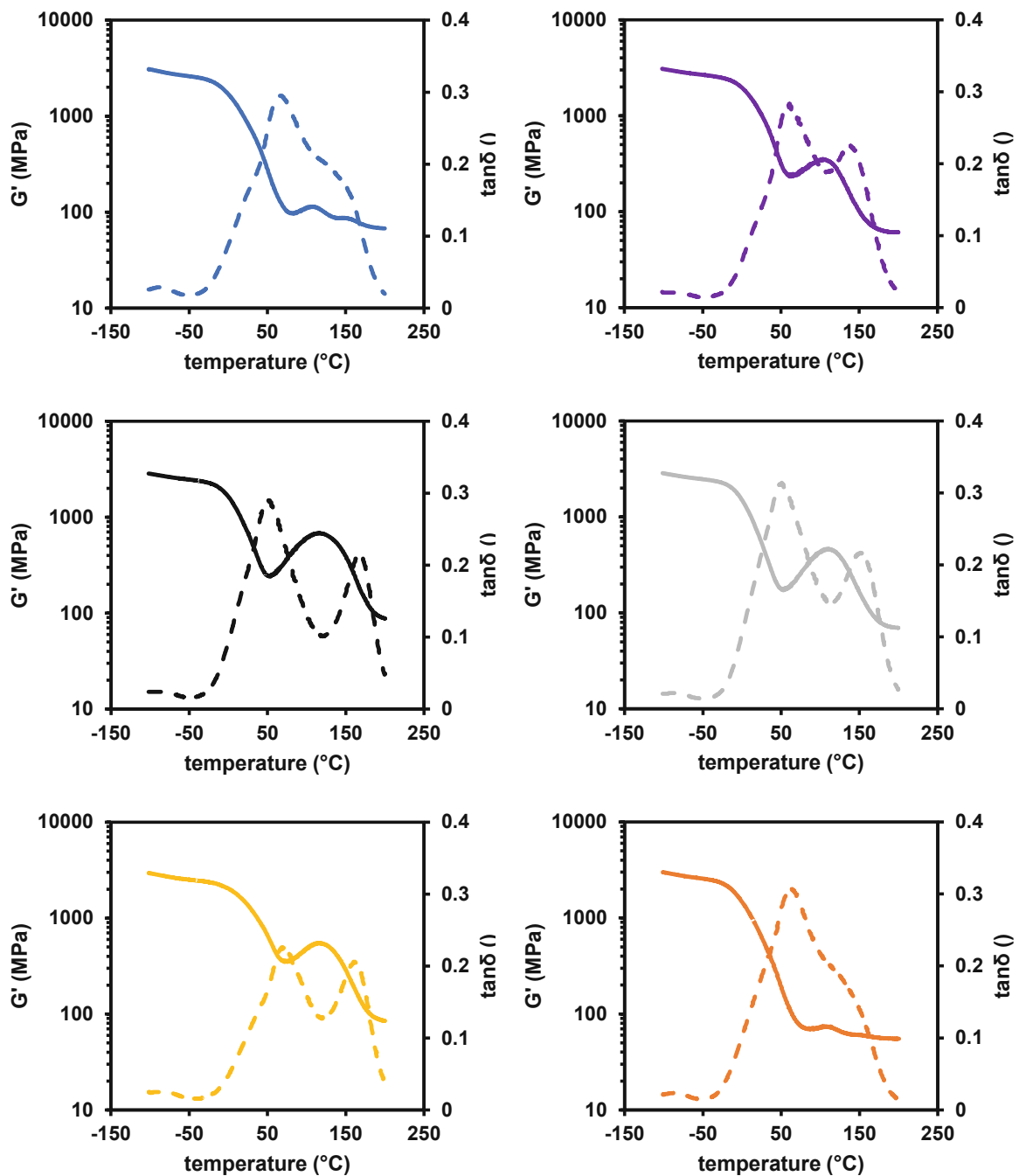
Figure 156: DMTA curves with G' (fully drawn) and tanδ (dashed line) of samples derived from B6-1, B6-2, B6-3, BN-2 B5-1 or SiB-1 with Cu(acac)$_2$ in 3Mix.

The shown graphs for the thermomechanical properties of the polymers derived from different diboranes show very distinctive differences. Interestingly, again B6-1 and SiB-1 leading to the fastest polymerization, yielding a very broad peak in tanδ, which is a sign for a more irregular network structure. This is explained by the fast polymerization of the respective formulations and the formation of an irregular network that has no possibility to properly reinforce itself at higher temperatures.

Despite the high polymerization reactivity of BN-2, the thermomechanical properties are more similar to the very slow diboranes. In the case of B6-2 and B6-3, the second peak at above 150 °C is very distinctly visible, which also reflects in the little decrease of G'.
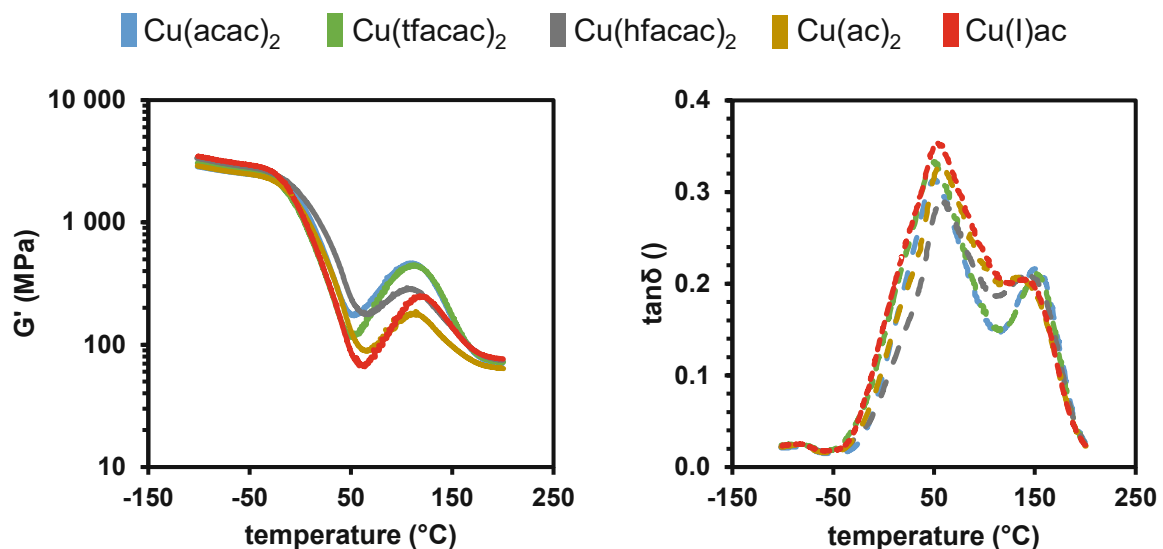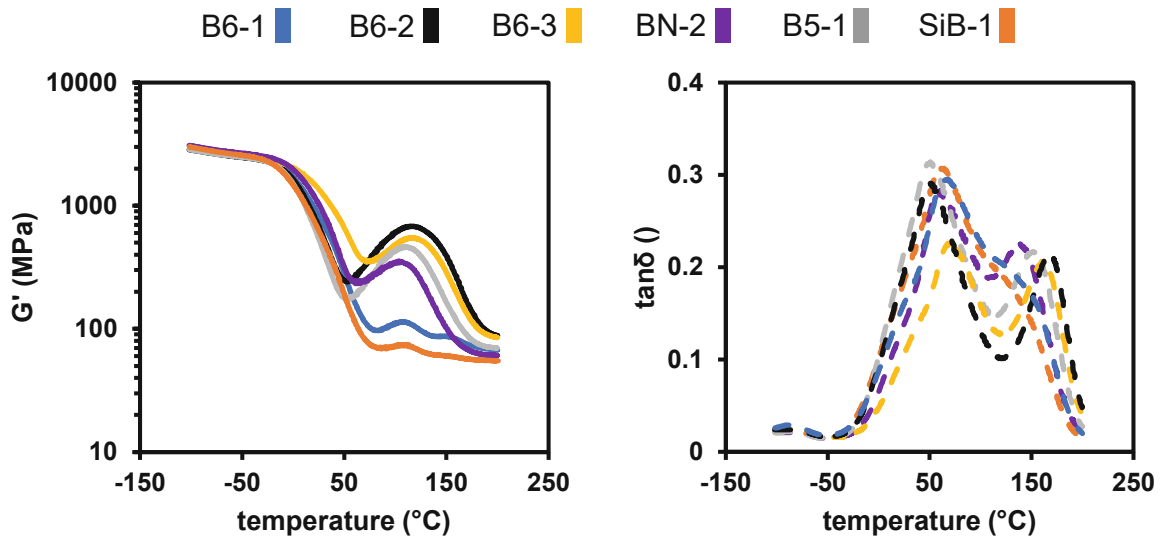

Figure 157: Left: Storage modulus of all DMTA measurements compared. Right: tanδ of all DMTA measurements compared.[99]

Overall, for B6-1 and SiB-1 no post-curing can be observed at higher temperatures, which would be the case if the G' increased again. For the other diboranes B6-2, B6-3, BN-2 and B5-1 a post-curing reaction starts at around 50 °C. This indicates that B6-1 and SiB-1 fully react during the polymerization and no further B-B and B-Si bonds are left to induce a post curing. B6-2, B6-3, BN-2 and B5-1 on the other hand would not fully react during the polymerization, since leftover B-B bonds will cleave at higher temperatures and induce the post-curing due to the network's flexibility above its T_g.

Due to the very distinct bimodal peak in tanδ of the B6-2 polymer, the network of the post-cured sample was investigated as well. Therefore, the DMTA specimen that was already measured and heated to 200 °C, was re-measured. The second measurement together with the first measurement of the B6-3 specimen is depicted in Figure 158.
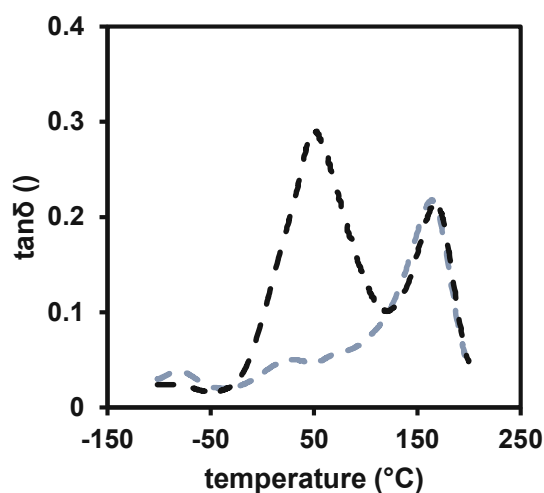
Figure 158: Black dashed: tanδ of B6-2 first measurement. Blue-grey dashed: tanδ of B6-2 second measurement.[99]

In the tanδ of the second measurement only one T_g is observable at high temperatures over 150 °C. The first T_g of the non-post-cured is completely transformed in the second measurement and is not detectable anymore.

It is concluded that a homogeneous network is formed in the polymerization of 3Mix via diboranes, especially B6-2, B6-3, BN-2 and B5-1 in combination with Cu(acac)$_2$. These networks still contain unreacted amount of diborane. During the thermal treatment of the DMTA measurement, the T_g is reached and the network get more flexible. In the same temperature range of the T_g, also the B-B bonds of the unreacted diborane can cleave thermally and lead to a post-curing of the network. This strengthening effect leads to a more crosslinked network with a higher T_g.[99]

6.2.2.2. Concentration Dependency of B6-1/Cu(acac)$_2$

The detailed characterization of the thermomechanical properties of polymers polymerized with the diborane/Cu 2K system was conducted employing various copper and diborane compounds in the previous chapters using DMTA. However, not only the choice of diborane or copper compound is important, but also the concentration of such. To evaluate the limits and perspectives of the diborane/Cu 2K initiating system, different concentrations of diborane (B6-1) were used in this study using 3Mix as monomers system.

B6-1   **Cu(acac)₂**
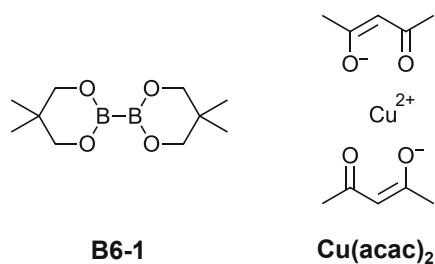
Figure 159: Chemical structure of B6-1 and Cu(acac)₂ that were investigated in this study.

The diborane concentration was varied between 1.8 mol%, 3.5 mol% and 7 mol% and the concentration of Cu(acac)₂ was set to 0.2 mol%. The concentration of the copper compound above 0.2 mol% could not be reliable varied due to solubility issues at higher concentrations and extremely low performance polymers at lower concentrations. Therefore, the optimum for copper concentration was set to 0.2 mol%. Formulations were prepared according to Table 63.

Table 63: Formulations for tensile test specimens to investigate the mechanical properties of the polymers derived from B6-1 and Cu(acac)₂ in 3Mix at different concentrations of the diborane.

	B-formulation	Cu-formulation
B6-1 (mol%)	1.8 / 3.5 / 7	-
Cu(acac)₂ (mol%)	-	0.2
3Mix (mol%)	98.2 / 96.5 / 93	99.8

The formulations were mixed in a w% 50:50 ratio and transferred to a silicon mold for DMTA specimens. After polymerization the specimens were stored for 24 h at 37 °C, after which the measurements were performed (Figure 160).

1.8mol% 3.5mol% 7mol%

Figure 160: Left: Storage modulus G' as a function of temperature of specimen that were polymerized using different concentrations of diborane B6-1 and 0.2 mol% Cu(acac)$_2$. Right: tanδ as a function of temperature of specimen that were polymerized using different concentrations of diborane B6-1 and 0.2 mol% Cu(acac)$_2$.

It is shown that the thermal behaviour of the polymers also depends on the concentration of diborane that is used in the initiation. The lower the concentration gets, the more extreme is the decrease of G' with an increase of temperature, and the less thermal post-curing is visible. This is due to less unreacted diborane initiator that can also thermally cleave at above 50 °C. In the case of the 7 mol% sample, it is nicely visible that residual B6-1 cleaves and leads to a post-curing as the G' increase from 50 °C – 100 °C. Also, the formation of a strong second T_g is visible in the right diagram at around 150 °C. This is due to the formation of a more densely crosslinked network.

6.2.3. DMTA: Diborane/Cu vs. State of the Art

The thermomechanical properties of specimens that were polymerized using the diborane/Cu 2K initiation system in 3Mix were compared to the state-of-the-art 2K initiation system (Ref) used for similar formulations in industrial applications.[63, 64] Therefore, DMTA measurements were evaluated. The composition of the Ref formulations that was used in this study is shown in Table 64 and the structures of the compounds used are depicted Figure 161.
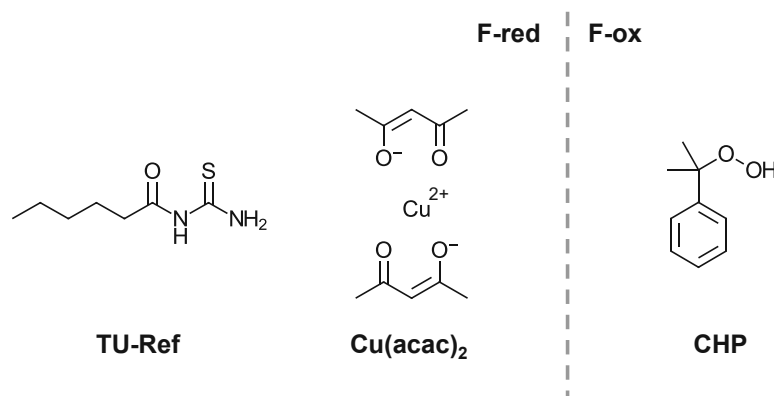
Figure 161: Chemical structures of the initiation system of the reference formulation (Ref).

Table 64: Composition of the reference formulation.

	F-red	F-ox
TU-Ref (mol%)	5	-
Cu(acac)$_2$ (mol%)	0.01	-
CHP (mol%)	-	11.5
3Mix (mol%)	94.99	88.5

For the diborane/Cu 2K initiation system, the formulations were prepared as stated in the previous chapters (DMTA). For the comparison of the copper compounds, B6-1 and B5-1 were used as the diboranes and for the comparison of the diboranes, Cu(acac)$_2$ was used as the copper compound (Table 65). All recorded stress/strain diagrams are depicted together with the reference in Figure 163.

Table 65: Exemplary composition of the formulations used in this chapter. For B6-1 was used as diborane for the different copper comounds and Cu(acac)$_2$ was used as copper compound for the different diboranes.

	B-formulation	Cu-formulation
Diborane (mol%)	3.5	-
Cu compound (mol%)	-	0.2
3Mix (mol%)	96.5	99.8

The structures of the investigated Cu compounds and diboranes are depicted below in Figure 162.
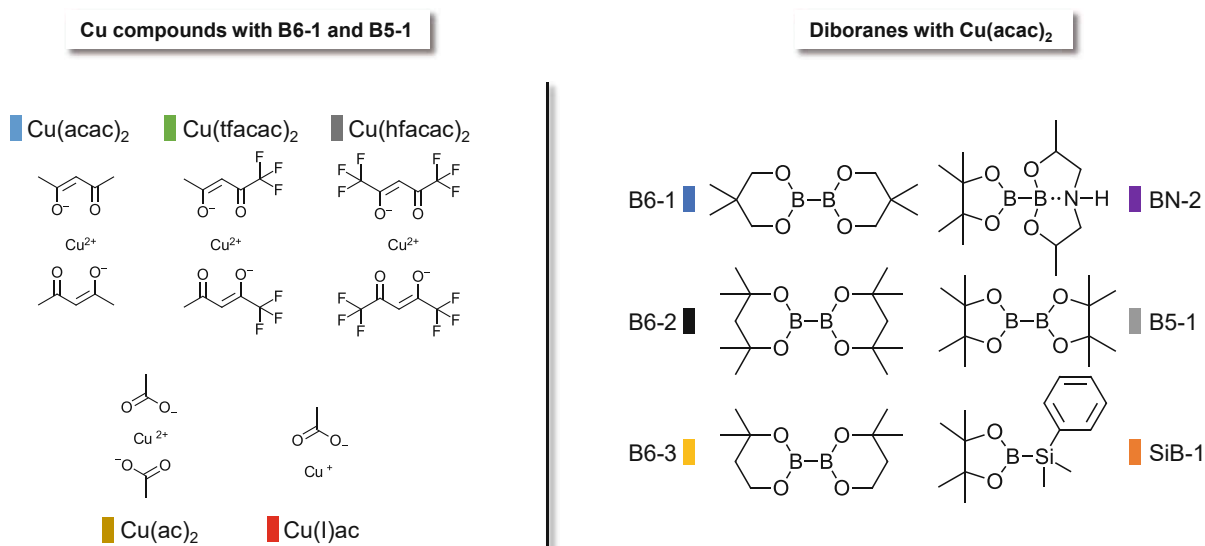
Figure 162: Chemical structures of the investigated Cu compounds and diboranes. B6-1 and B5-1 were used as the diboranes for the comparison of the Cu compounds. Cu(acac)$_2$ was used as the copper compound for the comparison of the diboranes.

The results depicted in the diagrams below summarize the previously discussed data of the DMTA measurements, now in comparison to the reference system. It is shown that the reference system does not show a strong decrease in storage modulus over the temperature range, which all of the samples polymerized with the diborane/Cu system do show. Therefore, also the first T$_g$ at 50 °C is not very prominent for the reference system and the higher T$_g$ at 150 °C is much more distinguished. However, it is shown that the reference does not exhibit very narrow T$_g$ compared to some diborane/Cu samples. As with BN-2 or B6-2 as the diborane initiator, the T$_g$ at 150 °C is very narrow and does show a much more homogeneous network structure than the reference system.
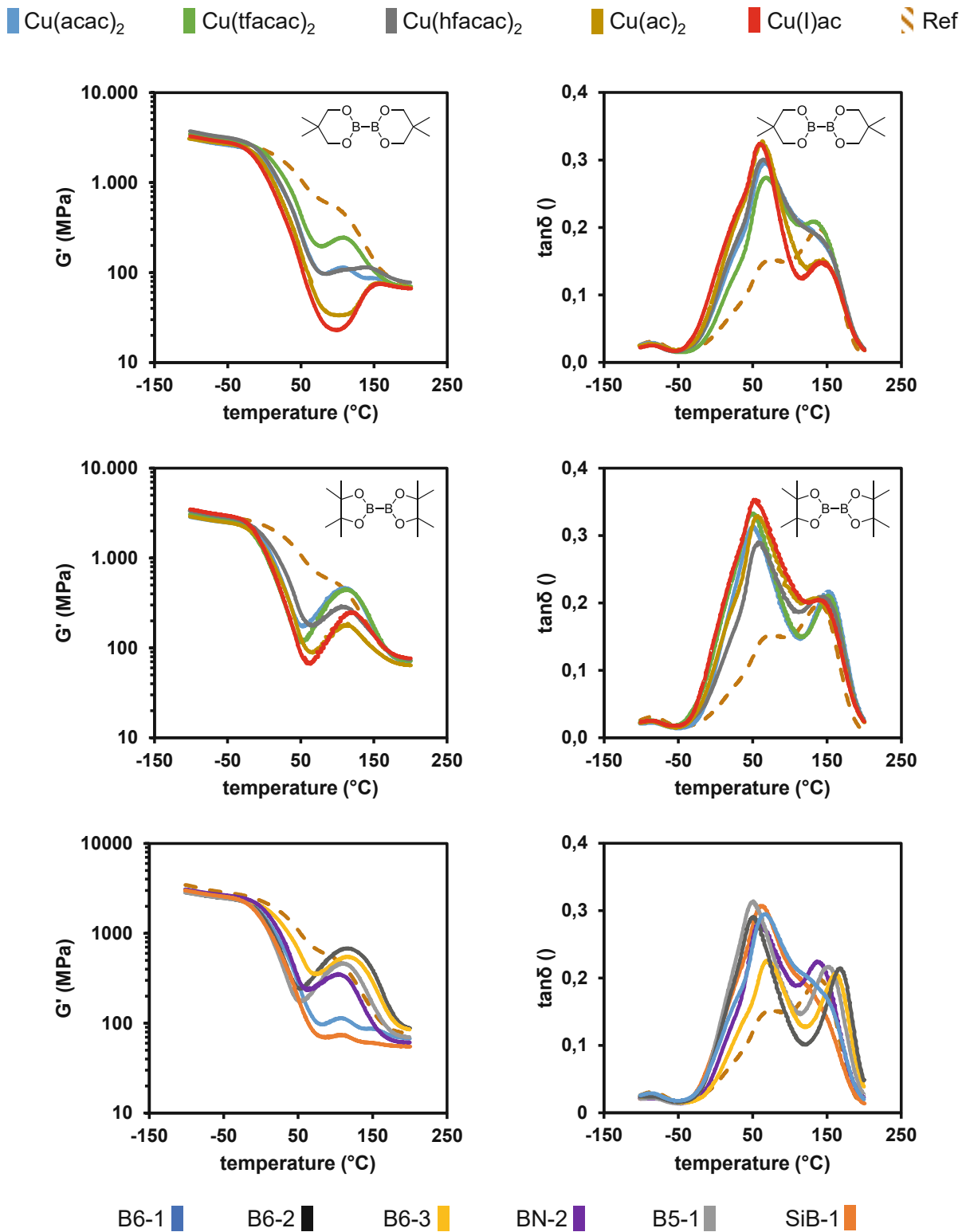
Figure 163: Top: DMTA measurements of specimen polymerized using B6-1 and different Cu compounds in 3Mix including Ref. Middle: DMTA measurements of specimen polymerized using B5-1 and different Cu compounds in 3Mix including Ref. Bottom: DMTA measurements of specimen polymerized using Cu(acac)₂ and different diboranes in 3Mix including Ref.

Summary

In recent years the dental industry made progress in developing new restoratives based on dental composite materials. However, problems with self-cured materials based on two-component (2K) systems often lie within the initiation system. Low storage stability caused by instable silanes, high metal contents or explosive peroxides and toxic amines are just a few limitations. This work attempts to overcome these limitations with two separate approaches. In the first approach (Part A) the implementation of a new vitamin C derivative that is soluble in organic monomer formulations as a reducing agent for redox initiated radical polymerization was discussed. In the second approach (Part B), a new 2K system was developed based on the copper catalysed cleavage of diboranes and the subsequent formation of radicals that can initiate radical polymerization.

1. Part A: VitC Derivative

A vitamin-C (VitC) derivative was synthesized with the goal of enhancing the solubility of the reducing agent in the methacrylic monomer mixture 3Mix. The analysis of the reducing mechanism of VitC showed that modifications on the aliphatic hydroxy groups would not interfere with the properties of the compound. The synthesis of VitC-1 was performed according to similar literature known synthesis routes, starting with a protection of the hydroxy groups on ring. After a Steglich esterification of the remaining hydroxy groups, a Pd-catalyzed removal of the protecting groups yielded the wanted structure VitC-1 (Figure 164).

Step 1: Protection
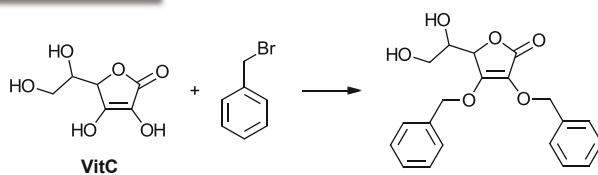
VitC

Step 2: Esterification
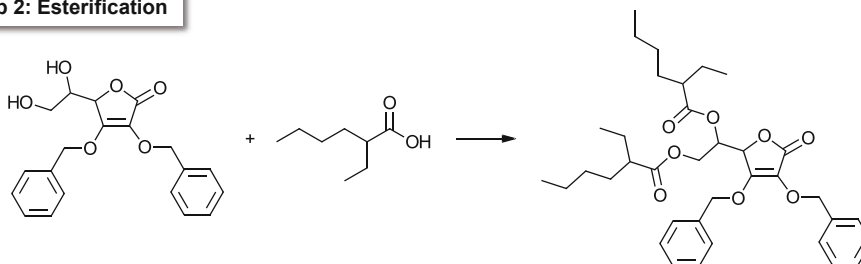
Step 3: Deprotection
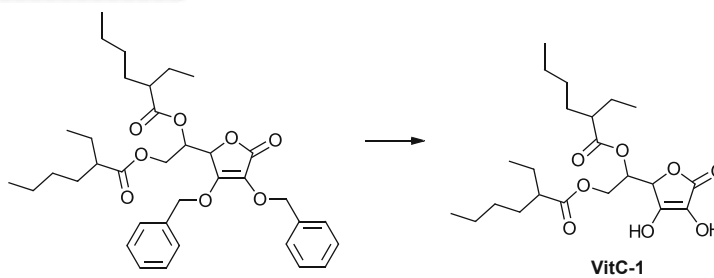
VitC-1

Figure 164: Synthetic pathway for the synthesis of VitC-1 starting with VitC. The first step involves a protection of the ene-diol hydroxygroups. The second step is an esterification reaction of the remaining aliphatic hydroxy groups. In the third step the benzyl ethers are removed selectively to yield the product compound VitC-1.

Since the solubility of the newly synthesized reducing agent VitC-1 proved to be very good in the monomer mixture, the reactivity of the initiation system was to be evaluated. Therefore, a state-of-the-art initiation system for similar application was picked as the ideal reference, however, the reducing agent TU-Ref was changed to VitC-1.

The formulations and compounds used are summarized in Figure 165 and Table 66.
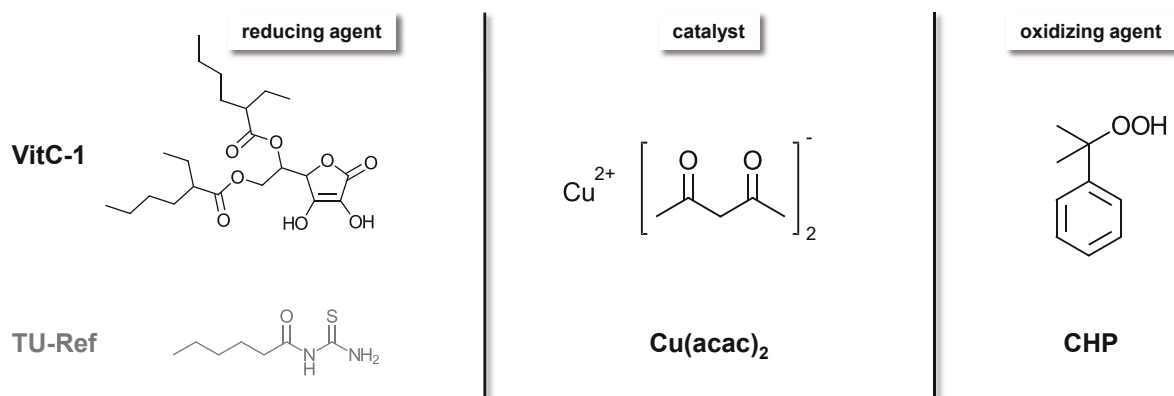
Figure 165: Chemical structure of the reducing agent VitC-1 and the reference reducing agent TU-Ref, the catalyst Cu(acac)$_2$ and the oxidizing agent CHP.

Table 66: Formulations prepared for polymerization temperature measurements and rheology/IR measurements to characterize the reactivity of the polymerization reaction initiated by VitC-1, Cu(acac)$_2$ and CHP in 3Mix and the reference TU-Ref.

	F-red (0.1)	F-red (0.01)	F-red (ref)	F-ox
VitC-1 (mol%)	5	5	-	-
TU-Ref (mol%)	-	-	5	-
Cu(acac)$_2$ (mol%)	0.1	0.01	0.01	-
CHP (mol%)	-	-	-	11.5
3Mix (mol%)	94.9	94.99	94.99	88.5

Reactivity was evaluated using polymerization temperature measurements and rheology/IR measurements, yielding valuable information about working time of large-scale bulk formulations (t_{max} and T_{max}) as well as double bond conversions (DBC) and mechanical properties during the polymerization process (t_{gel}). The following Figure 166 shows the summarized results of the respective measurements (A: polymerization temperature measurements; B: rheology/IR measurements).
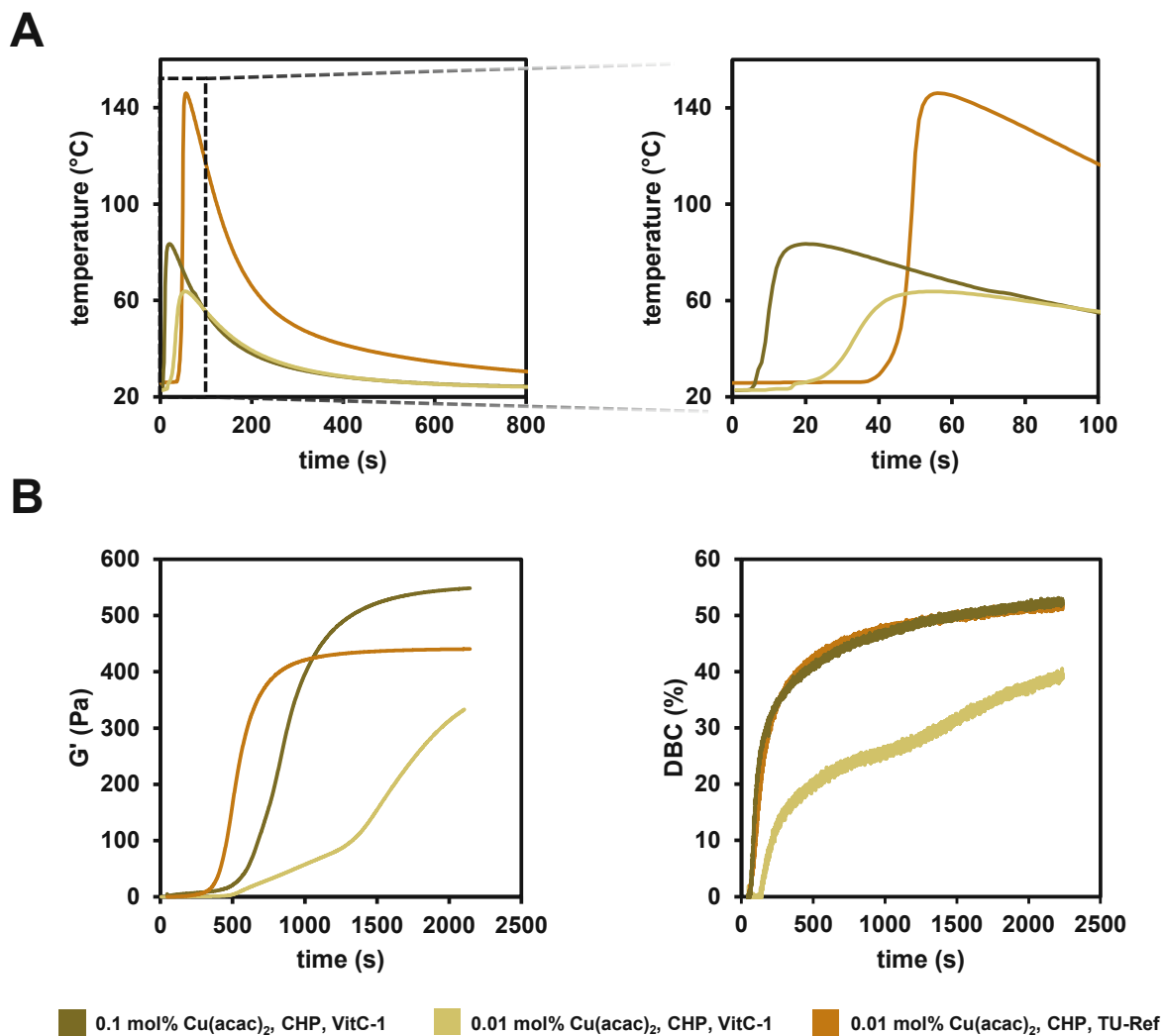
Figure 166: **A:** Polymerization temperature measurements of the polymerization of 3Mix, using VitC-1 as the reducing agent, and CHP as the oxidizing agent. The concentration of the catalyst Cu(acac)$_2$ was varied from 0.1 mol% (●) to 0.01 mol% (●). The reference initiation system using Cu(acac)$_2$, CHP and TU-Ref is depicted as well (●). **B:** Rheology/IR measurements of the polymerization of 3Mix, using VitC-1 as the reducing agent, and CHP as the oxidizing agent. The concentration of the catalyst Cu(acac)$_2$ was varied from 0.1 mol% (●) to 0.01 mol% (●). The reference initiation system using Cu(acac)$_2$, CHP and TU-Ref is depicted as well (●).

The new reducing agent VitC-1 proved to lead to a very fast polymerization of 3Mix (A) in low (0.01 mol%) and higher (0.1 mol%) concentrations of the catalyst Cu(acac)$_2$ compared to the reference system. However, the maximum temperature of the polymerizing formulation was significantly lower in comparison with the reference, which is an indicator for a lower double bond conversion. Indeed, rheology/IR measurements (B) verified the polymerization speed and showed, that a higher concentration of Cu(acac)$_2$ (0.1 mol%) leads to a high double bond conversion that is comparable to the state-of-the-art.

Furthermore, thermomechanical and mechanical properties of the yielded polymer networks were characterized using DMTA measurements and tensile tests, as well as ATR-IR measurements to evaluate the double bond conversions of the evaluated specimens. The summarized results are depicted in Figure 167.
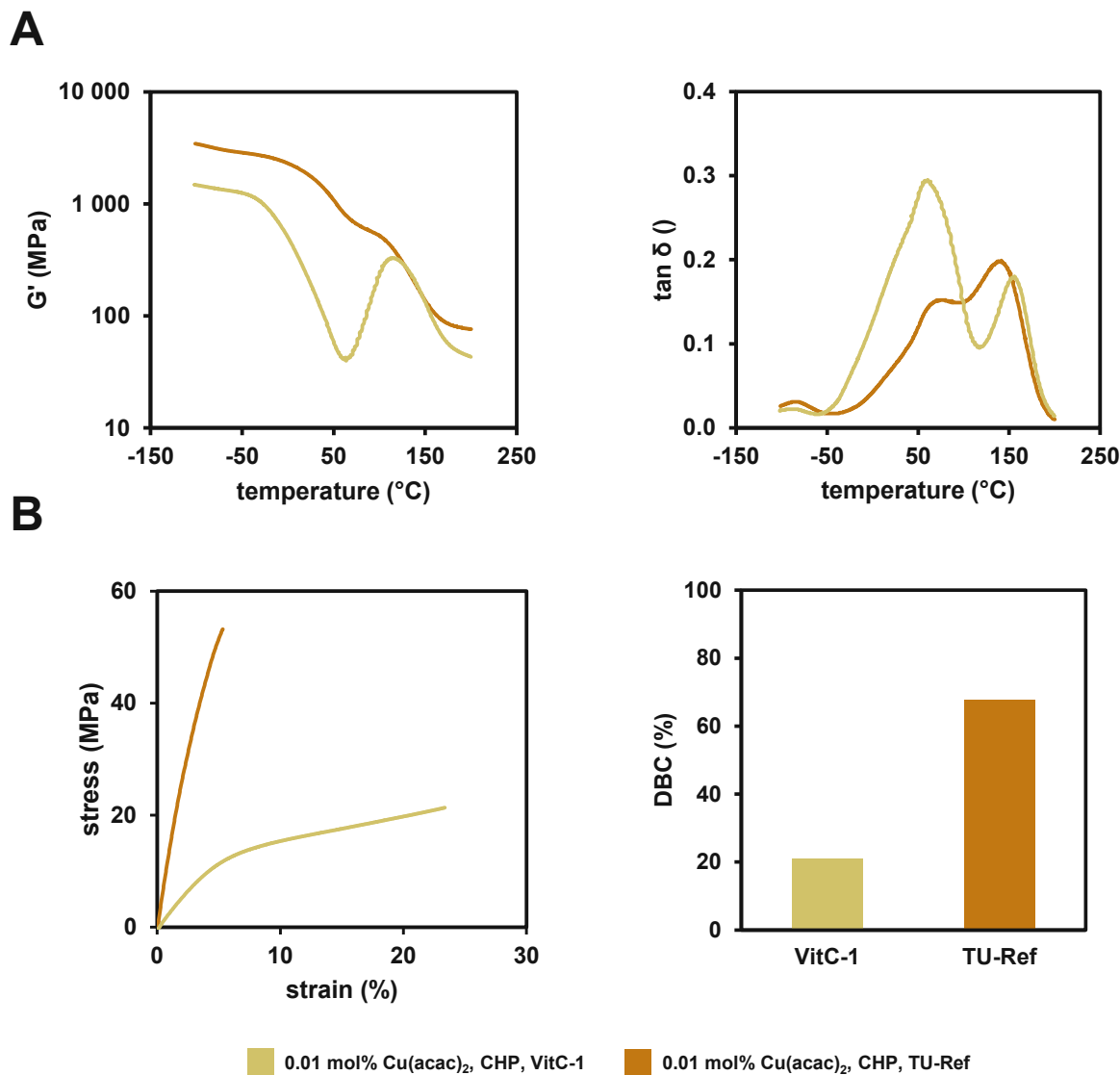
Figure 167: **A:** DMTA measurements of polymerized 3Mix via VitC-1 (●) or TU-Ref (●) as reducing agent. Left diagram shows the progression of G' and right diagram shows the progression of tanδ between -100 °C and 200 °C. **B:** Left: Stress-strain diagrams of tensile tests of specimens derived from VitC-1 (●) and TU-Ref (●) in 3Mix. Right: Double bond conversion of the tested specimens.

The low double bond conversion of the VitC-1 system seen in rheology/IR measurements is also reappearing in the (thermo)mechanical characterization. The DMTA measurements (A) show a significantly lower G' and also signs of a post-curing due to a temperature increase. This indicates that the network formed by initiation with VitC-1 is not as densely crosslinked compared to the reference initiation system. The lower network density leads to a decrease

173

in mechanical properties as the polymer material shows a higher elasticity, but less strain at break (B).

Summarizing the presented results, it can be concluded that VitC-1 is a perfect proof of concept that VitC derivatives show a high reactivity with improved solubility in apolar organic monomers. However, instability of the formulations as well as low DBC of the final polymer materials leave room for further improvements of such initiation systems.

2. Part B: Diborane/Cu System

A completely new 2K radical polymerization system was developed in Part B of this work. It is based on the copper catalyzed cleavage of boron-boron bonds that lead to the generation of radicals, which can initiate free radical polymerization. After an initial screening of multiple metal compounds and diboranes, disilanes and digermanes the following compounds proved to lead to a reliable polymerization of the monomer mixture 3Mix (Figure 168).
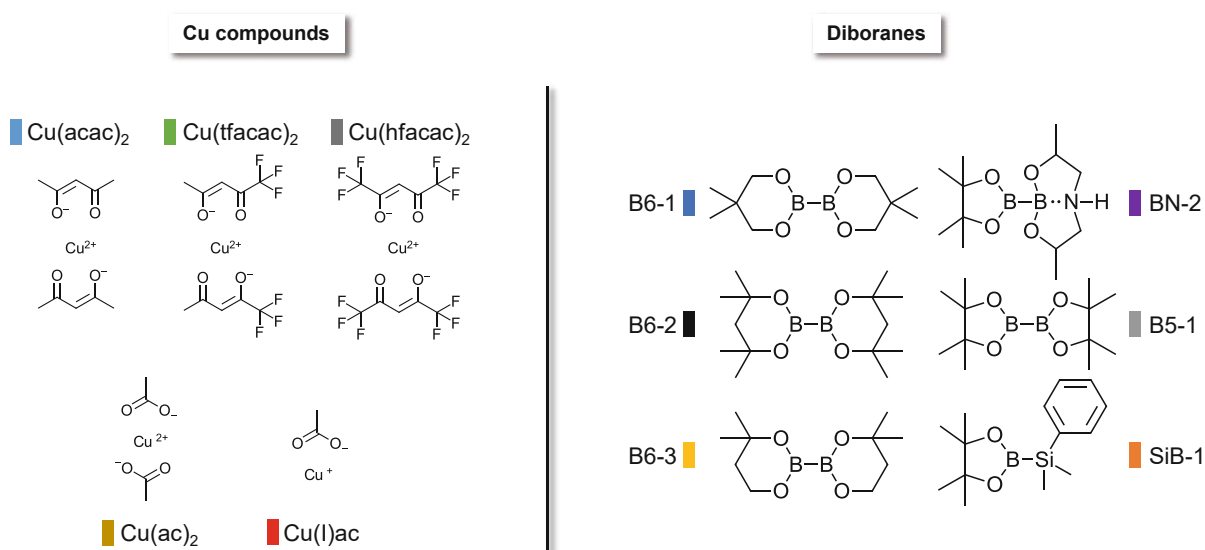
Figure 168: Chemical structures of the investigated Cu compounds (left) and diboranes (right).

Mechanistic details were investigated first, as such an initiation system was not known to literature to the best of our knowledge. Rheology/IR and EPR-ST measurements lead to the proposal of a possible mechanism of the initiation reactions between the copper compound and the diborane (Figure 169).
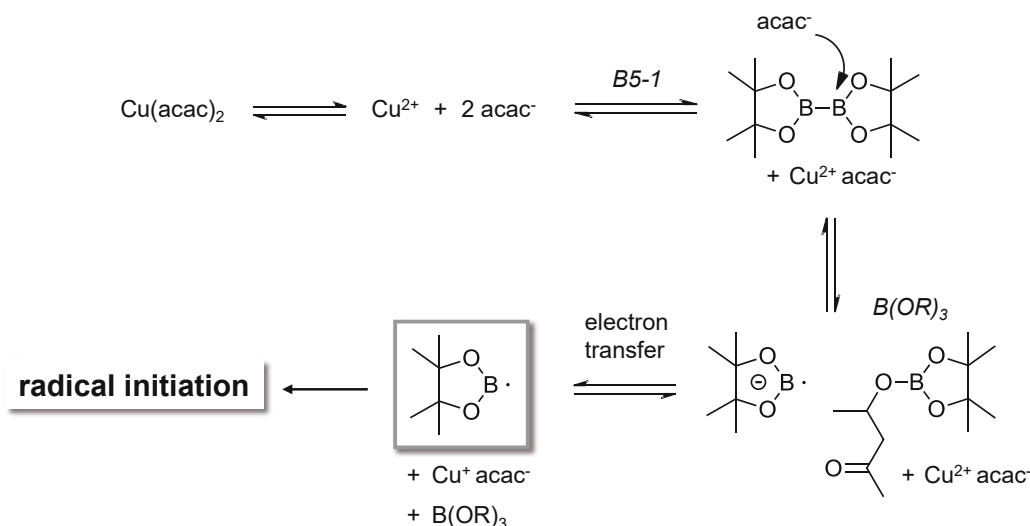
Figure 169: The proposed mechanism of the initiation reaction of the diborane/Cu 2K system is depicted. It includes the release of the acac⁻ ligands, then catalyzing the cleavage of the diborane, leading to a reduction of copper by the radical anion. The generated boryl radicals can then initiate the radical polymerization of methacrylates.

The catalyzed cleavage of the diborane bond leads to the formation of a highly reactive radical boryl anion. This species is able to readily reduce Cu^{2+} to Cu^+ and leave behind an uncharged boryl radical. This reaction can then even reoccur with Cu^+ being reduced to elemental Cu^0. The generated boryl radical is able to initiate the radical polymerization of methacrylic double bonds as found in rheology/IR measurements.

The investigated formulations showed overall good stability in the monomer mixture, which led to further testing of reactivity of this new 2K initiation system. The overall composition of the investigated formulations is displayed in Table 67.

Table 67: Exemplary composition of the formulations used in this work.

	B-formulation	Cu-formulation
Diborane (mol%)	3.5	-
Cu compound (mol%)	-	0.2
3Mix (mol%)	96.5	99.8

Polymerization temperature measurements and rheology/IR measurements were performed and compared to a state-of-the-art 2K initiation system (Ref) consisting of a thiourea compound (TU-Ref), $Cu(acac)_2$ and cumylhydroperoxide. The summarized results are depicted in Figure 170.
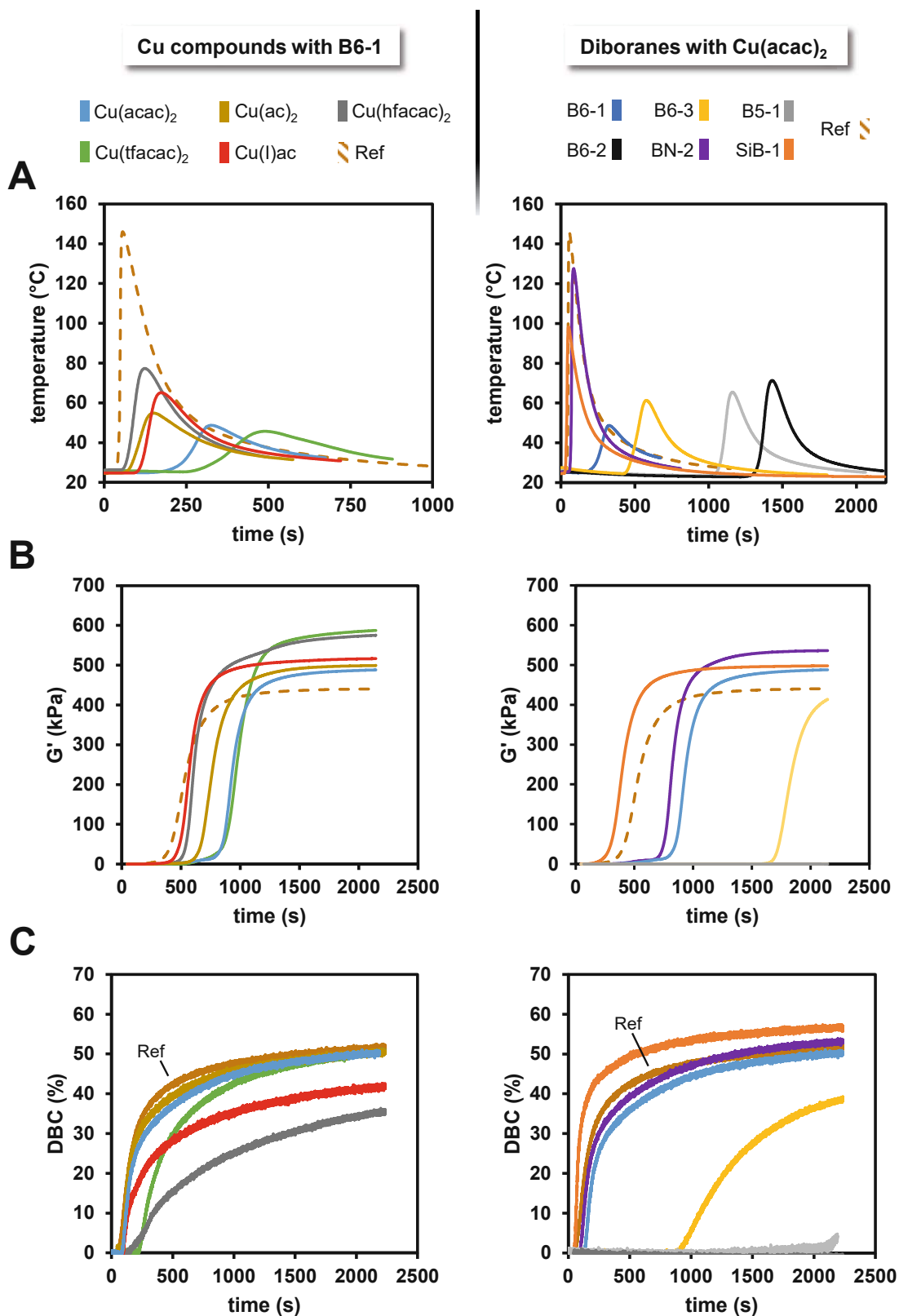
Figure 170: **A:** Polymerization temperature measurements of all investigated Cu compounds with B6-1 (left) and all investigated diboranes with Cu(acac)$_2$. **B:** Rheology/IR measurements displaying G' of all investigated Cu compounds with B6-1 (left) and all investigated diboranes with Cu(acac)$_2$. **C:** Rheology/IR measurements displaying the DBC G' of all investigated Cu compounds with B6-1 (left) and all investigated diboranes with Cu(acac)$_2$.

The polymerization temperature measurements (A) showed that the reactivity of the initiation system is depending on the type of Cu compound, which is due to different properties of the investigated ligands. Also, the choice of diborane can significantly influence the working time of the polymerization reaction, as BN-2 leads to a very fast polymerization, B6-2 however, to a very slow polymerization. In addition, the steric hinderance in proximity to the boron-boron bond influences the reactivity, as B6-2 leads to the slowest polymerization, B6-3 to a faster polymerization and B6-1 to the fastest. The same trends were observed in rheology/IR measurements (B&C). Overall, it could be concluded that depending on the Cu compound and the diborane, the initiation system performed similar to the state-of-the-art reference system, leading to high double bond conversions in a short amount of time.

The mechanical and thermomechanical properties of the resulting polymer networks were characterized using tensile testing and DMTA measurements. Multiple Cu compounds were investigated using two diboranes, B6-1 or B5-1. On the other hand, various diboranes were characterized with Cu(acac)$_2$ (Figure 171).
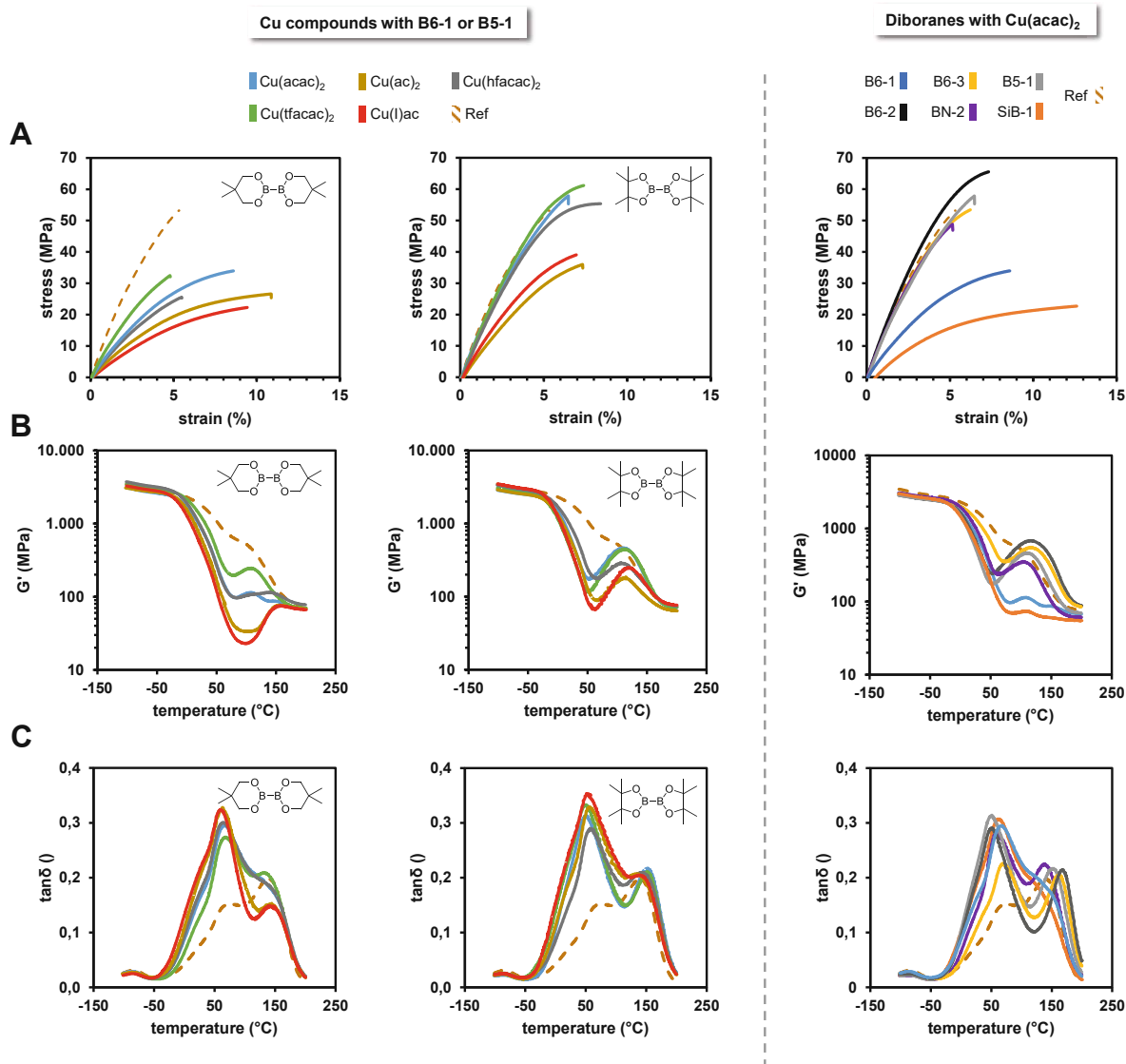
Figure 171: **A:** Tensile tests using multiple Cu compounds with B6-1 (left) and B5-1 (middle), and using multiple diboranes with Cu(acac)$_2$ (right). **B:** DMTA measurements displaying G' using multiple Cu compounds with B6-1 (left) and B5-1 (middle), and using multiple diboranes with Cu(acac)$_2$ (right). **C:** DMTA measurements displaying tanδ using multiple Cu compounds with B6-1 (left) and B5-1 (middle), and using multiple diboranes with Cu(acac)$_2$ (right).

It could be shown that faster reacting Cu compounds or diboranes lead to more elastic materials with less crosslinking density displayed in the tensile tests (A). The DMTA revealed an interesting post-curing behavior of all tested specimens seen in the progression of the G' and tanδ (B&C), that leads to highly homogeneous networks after thermal treatment. However, depending on the choice of Cu compound and diborane compound, the new diborane/Cu initiation system is performing very comparable to the state-of-the-art initiation system regarding reactivity as well as properties of the polymers.

Experimental Part

Experimental Part: Part A: Vitamin C as a Reducing Agent in Redox Polymerization

2. Synthesis of VitC-1

2.1.   Synthesis of 3,4-bis(benzyloxy)-5-(1,2-dihydroxyethyl)-2,5-dihydrofuran-2-one (VitC-Bz)
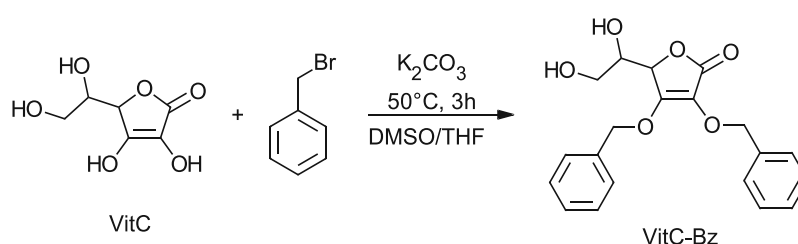
The synthesis of VitC-Bz was performed analogue to literature.[71] In a three-necked flask VitC (1 eq., 9.34 mmol) and K_2CO_3 (3 eq., 28.01 mmol) were dissolved in 40 mL DMSO/THF (2:1 vol%). Benzylbromide (2.4 eq., 22.41 mmol) were dissolved in 20 mL DMSO/THF (2:1 vol%) separately and added to the reaction mixture over time. The mixture was stirred at 50 °C for 3 h. Thereafter, the reaction mixture was filtrated and extracted with ethyl acetate, washed with brine, dried over Na_2SO_4, and all solvents were evaporated in vacuo. After column chromatography (PE:EA) the product was obtained as a yellow/brown oil.[71]

Yield: 60% of theory

R_f-value (PE:EE=1:2) = 0.5

^{1}H NMR (400 MHz, DMSO-d_6) δ 7.45 − 7.29 (m, 8H), 7.26 − 7.18 (m, 2H), 5.29 − 5.18 (m, 2H), 5.14 (d, J = 6.3 Hz, 1H), 5.00 − 4.92 (m, 2H), 4.91 − 4.83 (m, 2H), 3.71 (dtd, J = 7.7, 6.2, 1.4 Hz, 1H), 3.51 − 3.38 (m, 1H).

2.2. Synthesis of 1-[3,4-Bis(benzyloxy)-5-oxo-2,5-dihydro-2-furyl]-2-(1-ethylpentyl-carbonyloxy)ethyl-2-ethylhexanoate (VitC-1-Bz-M)
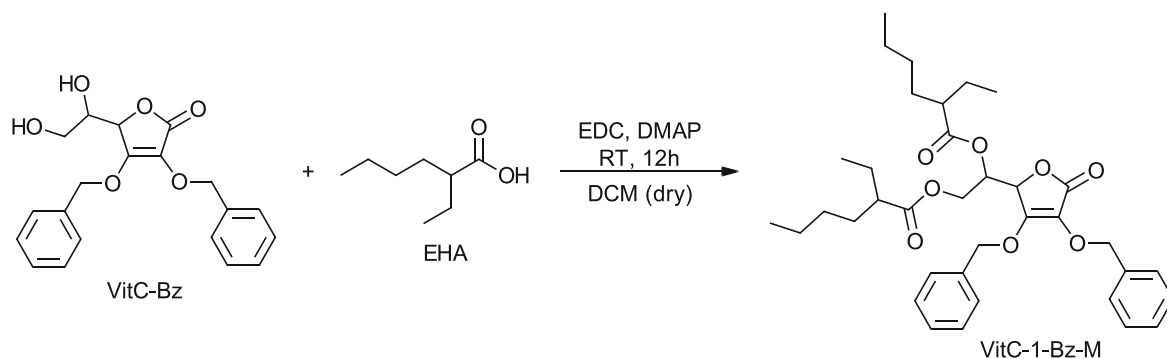
The synthesis was performed analogue to literature.[71] In a dry three-necked flaks under argon VitC-Bz (1 eq., 5.44 mmol) was dissolved in 30 mL dry DCM. DMAP (0.27 eq., 1.48 mmol) and EHA (3.26 eq., 17.73 mmol) were dissolved in 10 mL dry DCM and added. The mixture was cooled to -20 °C (ice:salt 3:1) and EDC (3.25 eq., 17.71 mmol) was dissolved in 10 mL dry DCM and added dropwise to the cooled reaction mixture. The reaction mixture was allowed to get to room temperature while stirring for 12 h. Thereafter, the mixture was filtered and the solvent was evaporated. After column chromatography (PE:EA) the product was obtained as an orange oil.[71]

Yield: 70% of theory

R_f-value (PE:EE=4:1) = 0.5

^{1}H NMR (400 MHz, DMSO-d_6) δ 7.43 – 7.35 (m, 8H), 7.31 (dd, J = 7.2, 2.3 Hz, 2H), 5.38 (ddt, J = 7.9, 5.8, 3.5 Hz, 1H), 5.22 (ddd, J = 23.7, 11.2, 2.5 Hz, 3H), 5.09 – 4.94 (m, 2H), 4.49 (dd, J = 11.7, 2.9 Hz, 1H), 4.15 – 4.03 (m, 1H), 2.28 – 2.16 (m, 2H), 1.56 – 1.33 (m, 8H), 1.30 – 1.12 (m, 8H), 0.90 – 0.71 (m, 12H).

HPLC-MS (ESI-MS) *m/z*: calc: 608.752; found: 608.71 ([M$^-$] detected).

2.3. Synthesis of 1-(3,4-Dihydroxy-2-oxo-5-furyl)-2-(1-ethylpentylcarbonyloxy)-ethyl-2-ethylhexanoate (VitC-1)
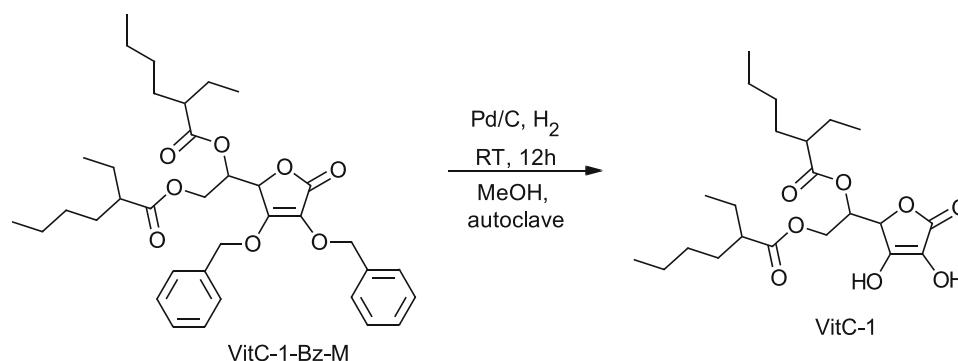
VitC-1-Bz-M

The synthesis of VitC-1 was performed analogue to literature.[70] In an autoclave vessel 1.29 g (2.12 mmol) VitC-1-Bz-M were dissolved in 20 mL methanol and Pd/C 10% (0.2193 g) were added. The reaction was stirred under H_2-pressure of 7 bar for 12 h. The reaction mixture was filtered and the solvent was evaporated. After column chromatography (PE:EA) the product was obtained as a colorless oil.[70]

Yield: 54% of theory

R_f (PE:EE=1:5): 0.75

^{1}H NMR (400 MHz, DMSO-d_6) δ 11.30 (s, 1H), 8.62 (s, 1H), 5.52 – 5.35 (m, 1H), 5.00 (d, J = 2.1 Hz, 1H), 4.51 (dt, J = 11.8, 2.7 Hz, 1H), 4.08 (dd, J = 11.8, 8.5 Hz, 1H), 2.29 – 2.13 (m, 2H), 1.58 – 1.34 (m, 8H), 1.32 – 1.14 (m, 8H), 0.92 – 0.72 (m, 12H).

HPLC-MS (ESI-MS) m/z: calc: 427.508; found: 427.05 ([M$^-$] detected).

3. Cyclovoltammetry

Cyclovoltammetry is a useful electrochemical technique to determine redox potentials of target molecules. For redox initiation systems, it can be a valuable tool to assess the performance of specific redox pairs. A scheme of the used setup is depicted in Figure 172. An Ag/AgCl reference electrode, a glassy carbon working electrode as well as a Pt counter electrode was used. The potentiostat used was a Metrohm Autolab PGStat302N with the Nova 2.1.4 software. The potential was varied between -1500 mV and 2200 mV with a rate of 50 mV/s.
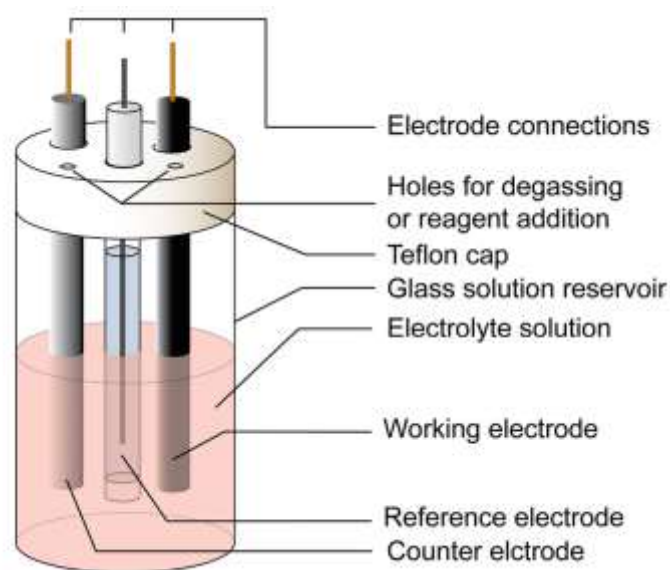
Figure 172 Scheme of the experimental setup of the cyclovoltammetry measurements[74]

In advance of the measurements, 5 mg of the analyte was weighed out and dissolved in dry acetonitrile with 0.1 M tetra-butylammonium hexafluorophosphate as electrolyte. To evaluate the oxidation/reduction potential of the target molecule, a standard measurement had to be performed with ferrocene. The standard potential of ferrocene was experimentally determined and compared to a literature value.[72] The difference between the determined value and the literature value was added as a factor to all the other measurements as correction.

4. Reactivity

4.1. Solubility

In glass vials, the solubility in 3Mix monomer mixture of reducing agents (two VitC derivatices, VitC-1 and PalmVitC as well as vitamin C) was tested. Therefore, concentrations of 0.5 mol%, 2 mol%, 3.5 mol% and 5 mol% of the reducing agent was tried to dissolve in 3Mix at room temperature using a vortex mixer. The solubility was determined by eye, as either a clear solution formed, or a white dispersion formed that indicates no, or little solubility in the monomer.

4.2. Polymerization Temperature Measurements

For the polymerization temperature measurements, 0.9 g of each of the respective 2K formulations (F-red and F-ox) were weighed out and mixed in a silicon mold (15 x 15 x 15 mm) under air at room temperature. During the curing of the formulation the temperature was measured with a thermocouple (type K) submerged into the formulation and processed with a Picolog 6.2.6 software.

4.2.1. VitC-1/Cu(acac)$_2$/CHP

See procedure described in 4.2.

4.2.2. VitC-1/Cu(acac)$_2$/CHP vs. State of the Art

See procedure described in 4.2.

4.3. Rheology/IR

Rheology measurements were performed with a real time-near infrared rheometer consisting of an Anton Paar MCR 302 WESP with a P-PTD 200/GL Peltier glass plate and a PP25 measuring system coupled with a Bruker Vertex 80 FTIR spectrometer. An external mirror was used to guide the IR beam from the spectrometer through the glass plate and the sample to the rheology plate, which reflected the beam. The beam was detected with an external MCT detector.

100 mg of each respective 2K-formulation (F-red and F-ox) was placed at the center of the glass plate, which was covered with a PE tape and the measurements were conducted at 25 °C with an Anton Paar H-PTD 200 furnace and a gap of 200 μm. The shear strain was set to 1 % and a frequency of 1 Hz.

4.3.1.   VitC-1/ Cu(acac)$_2$/CHP

See procedure described in 4.3.

4.3.2.   VitC-1/ Cu(acac)$_2$/CHP vs. State of the Art

See procedure described in 4.3.

4.3.3.   Stability of VitC-1

See procedure described in 4.3.

4.3.3.1.   VitC-1/Cu(acac)$_2$/tBuHP

See procedure described in 4.3.

5. Polymer Properties

5.1.   DMTA

For the DMTA measurements, polymer specimens were fabricated by pouring a 50wt%:50wt% mixture of the two respective formulations (F-red and F-ox) into a silicone mold (sticks, 5 × 2 × 40 mm) and letting it polymerize under air at room temperature. Subsequently, the specimens were post-cured for 24 h at 37 °C. Thereafter, the specimens were sanded until uniform dimensions (< ± 0.1 mm) were reached.

DMTA measurements were performed with an Anton Paar MCR 301 with a CTD 450 oven and an SRF 12 measuring system. Polymer specimens were tested in torsion mode with a frequency of 1 Hz and strain of 0.1%. The temperature was increased from -100 °C to 200 °C with a heating rate of 2 °C min^{-1}. The storage modulus and the loss factor of the polymer samples was recorded with the software Rheoplus/32 V3.40 from Anton Paar.

ATR-IR experiments of the specimens were performed on a PerkinElmer Spectrum 65 FT-IR Spectrometer, using a Specac MKII Golden Gate Single Reflection ATR System and evaluated with PerkinElmer Spectrum 10.03.07.0112. Therefore, the uncured monomer formulation was measured and the ration between the integral of the double bond band and the carbonyl band was calculated. This ratio was then also measured for cured samples and the conversion of double bonds was calculated.

5.1.1.   VitC-1/ Cu(acac)$_2$/CHP vs. State of the Art

See procedure described in 5.1.

5.2. Tensile Tests

Tensile test specimens were prepared in accordance to DMTA (see 5.1) specimen. The dog chew bone-shaped samples met the requirements for ISO 527 test specimen 5b (total length of 35 mm and a parallel region dimension of 2 × 2 × 12 mm). Five specimens were tested per sample. The tests themselves were performed on a Zwick Z050 with a maximum test force of 50 kN. The specimens were fixed between two clamps and strained with a traverse speed of 5 mm min^{-1}. A stress–strain plot was recorded simultaneously.

ATR-IR experiments of the specimens were performed on a PerkinElmer Spectrum 65 FT-IR Spectrometer, using a Specac MKII Golden Gate Single Reflection ATR System and evaluated with PerkinElmer Spectrum 10.03.07.0112. Therefore, the uncured monomer formulation was measured and the ration between the integral of the double bond band and the carbonyl band was calculated. This ratio was then also measured for cured samples and the conversion of double bonds was calculated.

5.2.1. VitC-1/ Cu(acac)$_2$/CHP vs. State of the Art

See procedure described in 5.2.

Experimental: Part B: Diborane/Cu 2K System

2.1.2. Synthesis of BN-4
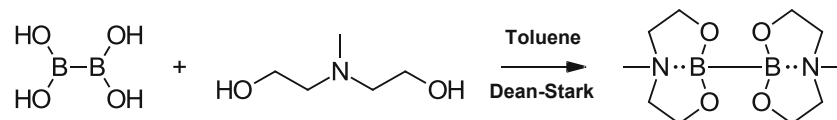
The synthesis of BN-4 was performed analogue to literature.[106] In a round bottom flask, hypodiboronic acid (1 eq.; 5 mmol) and isopropylalcocoldiamine (2.5 eq. 12.5 mmol) were weighed in. 20 mL of distilled toluene and a stirring bar were added. Then, the flask was connected to the dean-stark apparatus. While stirring, the mixture was heated up to 130 °C for 3h. Thereafter, the solvent was removed by evaporation. White crystals were obtained in 67% yield.[106]

Yield: 67% of theory

m.p. could not be determined due to instability

^{11}B NMR (128 MHz, D$_2$O) δ 9.18 (m).

^{1}H NMR (400 MHz, D$_2$O) δ 3.76 (t, 8H), 3.68 (t, 8H), 3.27 (m, 2H), 3.03 (m, 2H), 2.73 (s, 4H), 2.60 (s, 3H), 2.37 (s, 3H).

2.1.3. Synthesis of B6-3
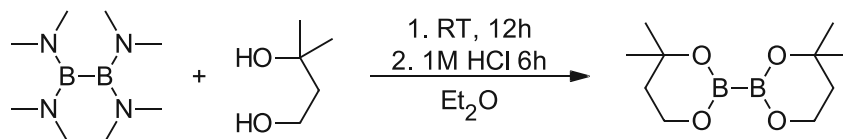
The synthesis of B6-3 was performed analogue to literature.[107] A solution of $B_2(NMe_2)_4$ (1 eq., 4.64 mmol) in dry Et_2O (20 mL) was prepared inside a glovebox. 3-methylbutane-1,3-diol (2.22 eq., 10.3 mmol) in another 20 mL dry Et_2O were added under Argon atmosphere. The reaction mixture was stirred at room temperature for 12 h. Thereafter, a 1 M solution of HCl in Et_2O (4 eq.) was added and the mixture was stirred for another 6 h at room temperature. The reaction mixture was filtered and all volatiles were removed in vacuo. The product was recrystallized from n-hexane to yield 370 mg white solid needles.[97, 107]

Yield: 35% of theory

m.p. 65 °C (no literature m.p. available)[97]

^{11}B NMR (128 MHz, Chloroform-d) δ 27.87.

^{1}H NMR (200 MHz, Chloroform-d) δ 4.06 – 3.93 (m, 1H), 1.85 – 1.72 (m, 1H), 1.31 (s, 3H).

2.2.   Scope of the Radical Polymerization System

2.2.1.   Screening of Diboranes

Formulations were prepared according to Table 68.

Table 68: Composition of formulations that were used to screen various diborane compounds with Cu(acac)$_2$ and their polymerization reactivity in 3Mix.

	B-formulation	Cu-formulation
Diborane (mol%)	3.5	-
Cu(acac)$_2$ (mol%)	-	0.2
3Mix (mol%)	96.5	99.8

B-formulation and Cu-formulation were mixed in a 50wt%:50wt% ratio under air at room temperature in a glass vial. Subsequently, it was observed by eye if the mixture would polymerize within 1h.

2.2.2.   Screening of Disilanes and Digermanes

Formulations were prepared according to Table 69.

Table 69: Composition of formulations that were used to screen various disilane and digermane compounds with Cu(acac)$_2$ and their polymerization reactivity in 3Mix.

	Si/Ge-formulation	Cu-formulation
Disilane/Digermane (mol%)	3.5	-
Cu(acac)$_2$ (mol%)	-	0.2
3Mix (mol%)	96.5	99.8

B-formulation and Cu-formulation were mixed in a 50wt%:50wt% ratio under air at room temperature in a glass vial. Subsequently, it was observed by eye if the mixture would polymerize within 1h.

2.2.3. Screening of Metal Salts as Polymerization Catalysts

Formulations were prepared according to Table 70.

Table 70: Composition of formulations that were used to screen various transition metal salts with SiB-1 and their polymerization reactivity in 3Mix.

	B-formulation	M-formulation
SiB-1 (mol%)	7	-
transition metal salt (mol%)	-	0.2
3Mix (mol%)	93	99.8

B-formulation and M-formulation were mixed in a 50wt%:50wt% ratio under air at room temperature in a glass vial. Subsequently, it was observed by eye if the mixture would polymerize within 1h.

3. Chemical Mechanism and Linear Polymers

3.1. Initiation

Stock solutions of the copper salts and the boron compounds in acetonitrile were prepared. The stock solutions were combined with a spin trap (DMPO; 5,5-dimethyl-1-pyrrolin-Noxide). The final concentrations were: 0.57 mM Cu-salt, 10 mM boron compound and 50 mM spin trap. The mixture was filled into a capillary and EPR spectra were recorded on a Bruker EMX spectrometer. For simulations the WinSIM software was used.

3.2. Propagation

Rheology measurements were performed with a real time-near infrared rheometer consisting of an Anton Paar MCR 302 WESP with a P-PTD 200/GL Peltier glass plate and a PP25 measuring system coupled with a Bruker Vertex 80 FTIR spectrometer. An external mirror was used to guide the IR beam from the spectrometer through the glass plate and the sample to the rheology plate, which reflected the beam. The beam was detected with an external MCT detector.

100 mg of each respective 2K-formulation (B-formulation and Cu-formulation) was placed at the center of the glass plate, which was covered with a PE tape and the measurements were conducted at 25 °C with an Anton Paar H-PTD 200 furnace and a gap of 200 µm. The shear strain was set to 1 % and a frequency of 1 Hz.

3.3. Proposed Mechanism

No experimental procedures were performed in this chapter.

3.4. Cyclovoltammetry

Cyclovoltammetry is a useful electrochemical technique to determine redox potentials of target molecules. For redox initiation systems, it can be a valuable tool to assess the performance of specific redox pairs. A scheme of the used setup is depicted in Figure 172. An Ag/AgCl reference electrode, a glassy carbon working electrode as well as a Pt counter electrode was used. The potentiostat used was a Metrohm Autolab PGStat302N with the Nova 2.1.4 software. The potential was varied between -1500 mV and 2200 mV with a rate of 50 mV/s.
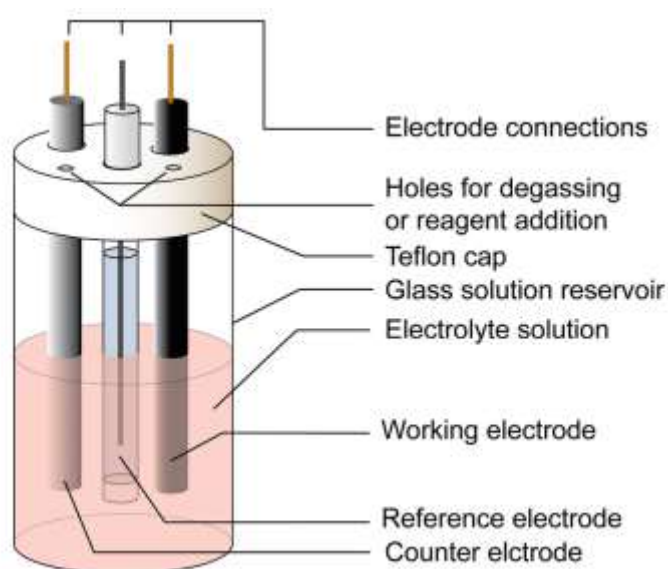
Figure 173 Scheme of the experimental setup of the cyclovoltammetry measurements[74]

In advance of the measurements, 5 mg of the analyte was weighed out and dissolved in dry acetonitrile with 0.1 M tetra-butylammonium hexafluorophosphate as electrolyte. To evaluate the oxidation/reduction potential of the target molecule, a standard measurement had to be performed with ferrocene. The standard potential of ferrocene was experimentally determined and compared to a literature value.[72] The difference between the determined value and the literature value was added as a factor to all the other measurements as correction.

3.4.1. Cu Compounds

See procedure described in 3.4.

3.4.2. Diboranes

See procedure described in 3.4.

3.5. Linear Polymer Analysis

3.5.1. Investigation of Diboranes

Rheology measurements were performed with a real time-near infrared rheometer consisting of an Anton Paar MCR 302 WESP with a P-PTD 200/GL Peltier glass plate and a PP25 measuring system coupled with a Bruker Vertex 80 FTIR spectrometer. An external mirror was used to guide the IR beam from the spectrometer through the glass plate and the sample to the rheology plate, which reflected the beam. The beam was detected with an external MCT detector.

100 mg of each respective 2K-formulation (B-formulation and Cu-formulation) was placed at the center of the glass plate, which was covered with a PE tape and the measurements were conducted at 25 °C with an Anton Paar H-PTD 200 furnace and a gap of 200 μm. The shear strain was set to 1 % and a frequency of 1 Hz.

3.5.2. Bulk Kinetics of the Diborane/Cu System

See procedure described in 3.5.1.

After the respective times described in the chapter, the measurement was interrupted and the sample was put into a vial and was quenched with 15 mg TEMPO in 2 mL THF. Afterwards, the dissolved sample was filtered and SEC measurements were conducted. SEC measurements were carried out on a Waters GPC using 3 columns (Styragel HR 0.5, Styragel HR 3 and Styragel HR 4) and a Waters 2410 RI detector, a UV Detector Module 2550 for TDA 305 and a VISCOTEK SEC-MALS 9 light scattering detector. A calibration with polystyrene standards (375 – 177000 Da) was used to determine the molecular weight of the polymers.

3.5.3. Testing of Various Monomers

See procedure described in 3.5.1.

4. Stability of Formulations

4.1. Thermal Stability

To evaluate the thermal stability of the formulations under investigation, DSC experiments were conducted using a Netzsch Jupiter STA 449 F1 thermal analysis tool with an autosampler. The experiments involved a ramp from 25 to 200 °C under N_2 atmosphere (10 K min^{-1}), which was performed twice to gather a baseline. All samples were precisely weighed into aluminum DSC pans (10 ± 2 mg) and subjected to a constant gas flow rate (40 mL min^{-1}).

4.2. Long Time Reactivity *via* Rheology

B-formulations and Cu-formulations were prepared and stored in a fridge for various times until measured: 0week, 2weeks, 3weeks, 4weeks. After the respective time of storage rheology/IR measurements were conducted using these formulations.

Rheology measurements were performed with a real time-near infrared rheometer consisting of an Anton Paar MCR 302 WESP with a P-PTD 200/GL Peltier glass plate and a PP25 measuring system coupled with a Bruker Vertex 80 FTIR spectrometer. An external mirror was used to guide the IR beam from the spectrometer through the glass plate and the sample to the rheology plate, which reflected the beam. The beam was detected with an external MCT detector.

100 mg of each respective 2K-formulation (B-formulation and Cu-formulation) was placed at the center of the glass plate, which was covered with a PE tape and the measurements were conducted at 25 °C with an Anton Paar H-PTD 200 furnace and a gap of 200 µm. The shear strain was set to 1 % and a frequency of 1 Hz.

4.2.1. Stability in 3Mix

See procedure described in 4.2.

4.2.2. Stability in D3MA

See procedure described in 4.2.

4.2.3. Stability in D3MA/BisGMA

See procedure described in 4.2.

5. Reactivity

5.1. Polymerization Temperature Measurements

For the polymerization temperature measurements, 0.9 g of each of the respective 2K formulations (B-formulations and Cu-formulation) were weighed out and mixed in a silicon mold (15 x 15 x 15 mm) under air at room temperature. During the curing of the formulation the temperature was measured with a thermocouple (type K) submerged into the formulation and processed with a Picolog 6.2.6 software.

5.1.1. Investigation of Cu Compounds

See procedure described in 5.1.

5.1.2. Investigation of Diboranes

See procedure described in 5.1.

5.2. Rheology/IR Measurements

Rheology measurements were performed with a real time-near infrared rheometer consisting of an Anton Paar MCR 302 WESP with a P-PTD 200/GL Peltier glass plate and a PP25 measuring system coupled with a Bruker Vertex 80 FTIR spectrometer. An external mirror was used to guide the IR beam from the spectrometer through the glass plate and the sample to the rheology plate, which reflected the beam. The beam was detected with an external MCT detector.

100 mg of each respective 2K-formulation (B-formulation and Cu-formulation) was placed at the center of the glass plate, which was covered with a PE tape and the measurements were conducted at 25 °C with an Anton Paar H-PTD 200 furnace and a gap of 200 μm. The shear strain was set to 1 % and a frequency of 1 Hz.

5.2.1. Investigation of Cu Compounds

See procedure described in 5.2

5.2.2. Investigation of Diboranes

See procedure described in 5.2

5.2.3. Concentration Dependency of B6-1/Cu(acac)$_2$

See procedure described in 5.2

5.3. Reactivity: Diborane/Cu vs. State of the Art

See procedure described in 5.2

6. Polymer Properties

6.1. Tensile Tests

For the tensile tests, polymer specimens were fabricated by pouring a 50wt%:50wt% mixture of the two respective formulations (B-formulation and Cu-formulation) into the respective silicon mold and letting it polymerize under air at room temperature. Subsequently, the specimens were post-cured for 24 h at 37 °C. The dog chew bone-shaped samples met the requirements for ISO 527 test specimen 5b (total length of 35 mm and a parallel region dimension of 2 × 2 × 12 mm). Five specimens were tested per sample. The tests themselves were performed on a Zwick Z050 with a maximum test force of 50 kN. The specimens were fixed between two clamps and strained with a traverse speed of 5 mm min^{-1}. A stress–strain plot was recorded simultaneously.

ATR-IR experiments of the specimens were performed on a PerkinElmer Spectrum 65 FT-IR Spectrometer, using a Specac MKII Golden Gate Single Reflection ATR System and evaluated with PerkinElmer Spectrum 10.03.07.0112. Therefore, the uncured monomer formulation was measured and the ratio between the integral of the double bond band and the carbonyl band was calculated. This ratio was then also measured for cured samples and the conversion of double bonds was calculated.

6.1.1. Post-Curing Efficiency

See procedure described in 6.1, however post-curing was done for 1h, 1d and 7d.

6.1.2. Investigation of Cu Compounds

6.1.2.1. B6-1/Cu Compounds

See procedure described in 6.1.

6.1.2.2. B5-1/Cu Compounds

See procedure described in 6.1.

6.1.3. Investigation of Diboranes

6.1.3.1. Cu(acac)$_2$/Diboranes

See procedure described in 6.1.

6.1.3.2. Concentration Dependency of B6-1/Cu(acac)2

See procedure described in 6.1.

6.1.4. Tensile Tests: Diborane/Cu vs. State of the Art

See procedure described in 6.1.

6.2. Dynamic Mechanical Thermal Analysis (DMTA)

For the DMTA measurements, polymer specimens were fabricated by pouring a 50wt%:50wt% mixture of the two respective formulations (F-red and F-ox) into a silicone mold (sticks, $5 \times 2 \times 40$ mm) and letting it polymerize under air at room temperature. Subsequently, the specimens were post-cured for 24 h at 37 °C. Thereafter, the specimens were sanded until uniform dimensions ($< \pm 0.1$ mm) were reached.

DMTA measurements were performed with an Anton Paar MCR 301 with a CTD 450 oven and an SRF 12 measuring system. Polymer specimens were tested in torsion mode with a frequency of 1 Hz and strain of 0.1%. The temperature was increased from -100 °C to 200 °C with a heating rate of 2 °C min^{-1}. The storage modulus and the loss factor of the polymer samples was recorded with the software Rheoplus/32 V3.40 from Anton Paar.

ATR-IR experiments of the specimens were performed on a PerkinElmer Spectrum 65 FT-IR Spectrometer, using a Specac MKII Golden Gate Single Reflection ATR System and evaluated with PerkinElmer Spectrum 10.03.07.0112. Therefore, the uncured monomer formulation was measured and the ratio between the integral of the double bond band and the carbonyl band was calculated. This ratio was then also measured for cured samples and the conversion of double bonds was calculated.

6.2.1. Investigation of Cu Compounds

6.2.1.1. B6-1/Cu Compounds

See procedure described in 6.2.

6.2.1.2. B5-1/Cu Compounds

See procedure described in 6.2.

6.2.2. Investigation of Diboranes

6.2.2.1. Cu(acac)$_2$/Diboranes

See procedure described in 6.2.

6.2.2.2. Concentration Dependency of B6-1/Cu(acac)$_2$

See procedure described in 6.2.

6.2.3. DMTA: Diborane/Cu vs. State of the Art

See procedure described in 6.2.

Materials and Methods

1. Materials

Name	Supplier
1-(2-hydroxypropylamino)propan-2-ol	Thermo Scientific
1-Ethyl-3-(3-dimethylaminopropyl)carbodiimid hydrochlorid (EDC.HCl)	abcr
2-(4,4,5,5-Tetramethyl-1,3,2-dioxaborolan-2-yl)-2,3-dihydro-1H-naphtho[1,8-de][1,3,2]diazaborinine	chemPUR
2-(Dimethylphenylsilyl)-4,4,5,5-tetramethyl-1,3,2- dioxaborolan (SiB-1)	Merck
2-[(2-hydroxyethyl)-N-methylamino]ethanol	Merck
2-ethylhexylacid (EHA)	Thermo Scientific
3-methylbutane-1,3-diol	Merck
4,4,4',4',6,6,6',6'- Octamethyl-2,2'-bi(1,3,2-dioxaborinane (B6-2)	BLD Pharm
4,4,4',4',5,5,5',5'-Octamethyl-2,2'- bi-1,3,2-dioxaborolan (B5-1)	Merck
4,8-Dimethyl-2-(4,4,5,5-tetramethyl-1,3,2-dioxaborolan-2- yl)-1,3,6,2-dioxazaborocane (BN-2)	abcr
5,5,5',5'-Tetramethyl-2,2'-bi-1,3,2-dioxaborinan (B6-1)	BLD Pharm
acetic acid (AcOH)	Sigma
acetonitrile (ACN)	Sigma
acrylomorpholine (A-Morph)	Sigma
acrylonitrile (AN)	ACROS
Ag(I)ac	Fisher
benzene	Sigma
benzyl bromide	Sigma
benzylacrylate (BzA)	TCI
benzylmethacrylate (BzMA)	Sigma
Bis-(catecholato)-diboran	chemPUR
Bis[(-)-pinanediolato]diboron	BLDPharm
bisphenol-A-glycidyl-dimethacrylate (BisGMA)	Ivoclar AG
Cd(II)acac$_2$	abcr
CDCl$_3$	TCI
Co(II)acac$_2$	Aldrich

Materials and Methods

Name	Supplier
Co(III)acac$_3$	abcr
Cr(III)acac$_3$	TCI
Cu(ac)	abcr
Cu(ac)$_2$	Merck
Cu(acac)$_2$	Merck
Cu(hfacac)$_2$	Merck
Cu(tfacac)$_2$	abcr
cumene hydroperoxide (80% solution in cumene) (CHP)	Sigma
D$_2$O	TCI
decanedioldimethacrylate (D3MA)	Ivoclar AG
dichloromethane (DCM)	Sigma
diethylether (Et$_2$O)	Sigma
dimethylacrylamide (DMAA)	Sigma
dimethylphenyldisilane (DMPDS)	abcr
dimethylsulfoxide (DMSO)	Sigma
4-(Dimethylamino)pyridin (DMAP)	Sigma
DMSO-d6	TCI
ethylacetate	Sigma
Fe(III)acac$_3$	Sigma
ferrocene	Sigma
HCl	Sigma
hexamethydigermane (HMDG)	abcr
hexamethyldisilane (HMDS)	fluka
hexaphenyldisilane (HPDS)	Sigma
hypodiboronic acid	BLDPharm
isobutylvinylether (isoBVE)	TCI
K$_2$CO$_3$	Thermo Scientific
methanol (MeOH)	Sigma
methylmethacrylate (MMA)	VWR
Mn(III)acac$_3$	Sigma
Na$_2$SO$_4$	Sigma
n-hexane	Sigma

Name	Supplier
Ni(II)acac$_2$	abcr
	Thermo
palladium on carbon (Pd/C)	Scientific
palmoyl vitcamin C (PalmVitC)	Sigma
Pd(II)(PPh$_3$Fc)Cl$_2$	BLDPharm
Pd(II)ac$_2$	Aldrich
Pd(II)acac$_2$	Sigma
petrolether	Sigma
Pt(II)acac$_2$	abcr
pyridine	Sigma
Rh(I)(PPh$_3$Cl)	Sigma
Rh(III)acac$_3$	abcr
styrene (ST)	ACROS
TEMPO	Sigma
tert-butyl hydroperoxide (*t*BuHP)	Sigma
tetra-butylammonium hexafluorophosphate	Aldrich
tetrahydrofurane (THF)	Sigma
tetrakis(dimethylamino)diboron	BLD Pharm
thiourea reference compound (TU-Ref)	Ivoclar AG
toluene	Sigma
urethanedimethacrylate (UDMA)	Ivoclar AG
V(III)acac$_3$	Aldrich
V(IV)Oacac$_3$	TCI
vitamin-C (VitC)	Sigma

2. Methods

2.1. Thin layer chromatography

TLC was carried out using TLC-aluminum foils, coated with silica gel 60 F254 from Merck

2.2. Column chromatography

Column chromatography was carried out using a Büchi MPLC system equipped with a C-620 control unit, a C-660 fraction collector and a C-635 UV photometer. The stationary Merck silica gel 60 (0.040-0.063 mm) was used as the stationary phase.

2.3. Melting points

The melting points were determined using an Optimelt MPA100 automatic melting point apparatus.

2.4. NMR

NMR spectra were recorded on a Bruker DPX-200 FT-NMR spectrometer at 200 MHz for ^{1}H and 50 MHz for ^{13}C, as well as on a Bruker Avance DRX-400 FT-NMR spectrometer at 400 MHz for ^{1}H and 100 MHz for ^{13}C. The signals are recorded according to their chemical shifts, which were reported in ppm (s = singlet, d = doublet, t = triplet, q = quartet, qn = quintet, sep = septet, m = multiplet, bs = brad singlet) in comparison to tetramethylsilane (d = 0 ppm). The spectra awere then referenced on the used NMR-solvent [^{1}H: $CDCl_3$ (7.26 ppm), ^{13}C: $CDCl_3$ (77.16 ppm)]. The analysis of the spectra was performed with MestReNova version 14.3.3-33362.

2.5. Ultra-high pressure liquid chromatography – mass spectroscopy (UPLC-MS)

A Nexera X2® UHPLC system (Shimadzu®), consisting of LC-30AD pumps, SIL-30AC autosampler, CTO-20AC column oven and DGU-20A5/3 degassing module, was used in combination with an SPD-M20A photodiode array detector, an RF-20Axs fluorescence detector, an ELS-2041 evaporative light scattering detector (JASCO®) and an LC-MS-2020 mass spectrometer (ESI/APCI). All separations were performed using a Waters® XSelect® CSHTM C18 2.5 μm (3.0 x 50 mm) column XP at 40 °C and a flow rate of 1.7 ml/min with water/acetonitrile + 0.1 % formic acid gradient elution.

2.6. Cyclovoltammetry

An Ag/AgCl reference electrode, a glassy carbon working electrode as well as a Pt counter electrode was used. The potentiostat used was a Metrohm Autolab PGStat302N with the Nova

2.1.4 software. The potential was varied between -1500 mV and 2200 mV with a rate of 50 mV/s.

2.7. SEC

SEC measurements were carried out on a Waters GPC using 3 columns (Styragel HR 0.5, Styragel HR 3 and Styragel HR 4) and a Waters 2410 RI detector, a UV Detector Module 2550 for TDA 305 and a VISCOTEK SEC-MALS 9 light scattering detector. A calibration with polystyrene standards (375 – 177000 Da) was used to determine the molecular weight of the polymers. The investigated polymer was dissolved in THF and filtered before conducting the measurement.

2.8. EPR-ST

Stock solutions of the copper salts and the boron compounds in acetonitrile were prepared. The stock solutions were combined with a spin trap (DMPO; 5,5-dimethyl-1-pyrrolin-Noxide). The final concentrations were: 0.57 mM Cu-salt, 10 mM boron compound and 50 mM spin trap. The mixture was filled into a capillary and EPR spectra were recorded on a Bruker EMX spectrometer. For simulations the WinSIM software was used.

2.9. Polymerization temperature measurements

For the polymerization temperature measurements, 0.9 g of each of the respective 2K formulations were weighed out and mixed in a silicon mold (15 x 15 x 15 mm) under air at room temperature. During the curing of the formulation the temperature was measured with a thermocouple (type K) submerged into the formulation and processed with a Picolog 6.2.6 software.

2.10. DSC

DSC experiments were conducted using a Netzsch Jupiter STA 449 F1 thermal analysis tool with an autosampler. The experiments involved a ramp from 25 to 200 °C under N_2 atmosphere (10 K min^{-1}), which was performed twice to gather a baseline. All samples were precisely weighed into aluminum DSC pans (10 ± 2 mg) and subjected to a constant gas flow rate (40 mL min^{-1}).

2.11. Rheology/IR

Rheology measurements were performed with a real time-near infrared rheometer consisting of an Anton Paar MCR 302 WESP with a P-PTD 200/GL Peltier glass plate and a PP25 measuring

system coupled with a Bruker Vertex 80 FTIR spectrometer. An external mirror was used to guide the IR beam from the spectrometer through the glass plate and the sample to the rheology plate, which reflected the beam. The beam was detected with an external MCT detector.

2.12. Tensile Tests

The tests were performed on a Zwick Z050 with a maximum test force of 50 kN. The specimens were fixed between two clamps and strained with a traverse speed of 5 mm min^{-1}. A stress−strain plot was recorded simultaneously.

2.13. ATR-IR

ATR-IR experiments of the specimens were performed on a PerkinElmer Spectrum 65 FT-IR Spectrometer, using a Specac MKII Golden Gate Single Reflection ATR System and evaluated with PerkinElmer Spectrum 10.03.07.0112.

2.14. DMTA

DMTA measurements were performed with an Anton Paar MCR 301 with a CTD 450 oven and an SRF 12 measuring system. Polymer specimens were tested in torsion mode with a frequency of 1 Hz and strain of 0.1%. The temperature was increased from -100 °C to 200 °C with a heating rate of 2 °C min^{-1}. The storage modulus and the loss factor of the polymer samples was recorded with the software Rheoplus/32 V3.40 from Anton Paar.

2.15. Research Tools

Literature searches were performed using SciFinder-n by CAS, Google Scholar and Reaxys. Writing was done using Microsoft® Word 2019 MSO. Textediting and paraphrasing were done with the help of deepl.com and ChatGPT 3.5. Citations were added using EndNote X9.1 software. Diagrams were plotted using Origin 2019b and Microsoft® Excel 2019 MSO. Chemical drawings were created using ChemDoodle® V 10.3.0 software from iChemLabsTM and figures were refined using Microsoft® PowerPoint® 2019 MSO.

Abbreviations

Abbrev.

2K	two-component
APT	attached proton test
ATR-IR	attenuated total reflection infrared spectroscopy
BPO	dibenzoyl peroxide
CV	cyclovoltammetry
DBC	double bond conversion
DBC_{ATR-IR}	double bond conversion determined via ATR-IR
DBC_{gel}	double bond conversion at gel point
DC	dual-cure
DMTA	dynamical mechanical thermal analysis
DSC	differential scanning calorimetry
E_{ox}	oxidation potential
EPR-ST	electron paramagnetic resonance spectroscopy with spin-trapping
eq.	equivalents
E_{red}	reduction potential
EWG	electron withdrawing group
F_N	normal force
F-ox	formulation containing an oxidizing agent
F-red	formulation containing a reducing agent
FRP	free-radical polymerization
G'	storage modulus
G''	loss modulus
$G'_{25°C}$	storage modulus at 25°C
G'_{end}	storage modulus at the end of the measurement
HOMO	highest occupied molecular orbital
HPLC-MS	high pressure liquid chromatography coupling with mass spectrometry
HSQC	heteronuclear single quantum coherence spectroscopy
IR	infrared
LUMO	lowest unoccupied molecular orbital

MABLI	metal acetylacetonate-bidentate ligand interaction
M_n	number average molecular weight
NIR	near infrared
NMR	nuclear magnetic resonance spectroscopy
Ox	oxidation
Red	reduction
Ref	reference system
R_f	retention factor
RT	room temperature
SC	self-cure
SEC	size exclusion chromatography
SET	single electron transfer
$\tan\delta$	loss factor
T_g	glass transition temperature
t_{gel}	gel point
T_{max}	highest temperature in polymerization temperature measurements
t_{max}	time of highest temperature in polymerization temperature measurements
U_T	tensile toughness
w%	weight percent
$\Delta\sigma/\Delta\varepsilon$	slope of the stress/strain curve in linear section
ε_M	maximum elongation
σ_M	maximum stress

Appendix

1. Further Studies

1.1. Stabilization with TEMPO

The effect of the stabilizer TEMPO on the long-time reactivity in 3Mix was investigated. Therefore, formulations were prepared according to Table 71.

Table 71: Formulations prepared for long time reactivity studies consisting of Cu(acac)$_2$ and BN-2 in 3Mix with various concentrations of TEMPO.

	B-formulation	Cu-formulation
BN-2 (mol%)	3.5	-
Cu(acac)$_2$ (mol%)	-	0.2
TEMPO (mol%)	0 / 0.01 / 0.1 / 0.5	-
3Mix (mol%)	96.5 / 96.49 / 96.4 / 96.0	99.8

The measurements were evaluated and the respective t_{k-max} values t0 are depicted in Figure 174 for all investigated concentrations of TEMPO.

Figure 174 Values for t_{k-max} of the polymerization reaction in Rheo/IR measurements observed for different concentrations of TEMPO with BN-2 and Cu(acac)$_2$ in 3Mix.

It was shown that with higher concentration of TEMPO in the respective formulations the reactivity decreases which is reflected in the increase of t_{k-max}. The stable TEMPO radicals can react with the radical species generated during the initiation and the propagation and therefore slow down the initiation as well as the propagation process. To investigate whether

the addition of TEMPO would increase the long-time reactivity these formulations were measured again after one week of storage in the fridge at 8 °C depicted in Figure 175.

Figure 175: Fully drawn: Values for t_{k-max} of the polymerization reaction in Rheo/IR measurements observed for different concentrations of TEMPO with BN-2 and Cu(acac)$_2$ in 3Mix. Dashed: Values for t_{k-max} of the polymerization reaction in Rheo/IR measurements observed for different concentrations of TEMPO with BN-2 and Cu(acac)$_2$ in 3Mix after one week of storage at 8 °C.

The t_{k-max} is increasing after one week already for every formulation. It is shown that TEMPO does not increase the long-time reactivity. The instability of the diborane formulation is not enhanced by the addition of TEMPO

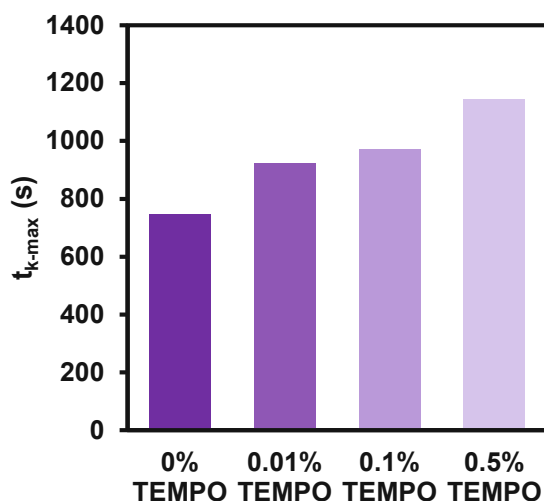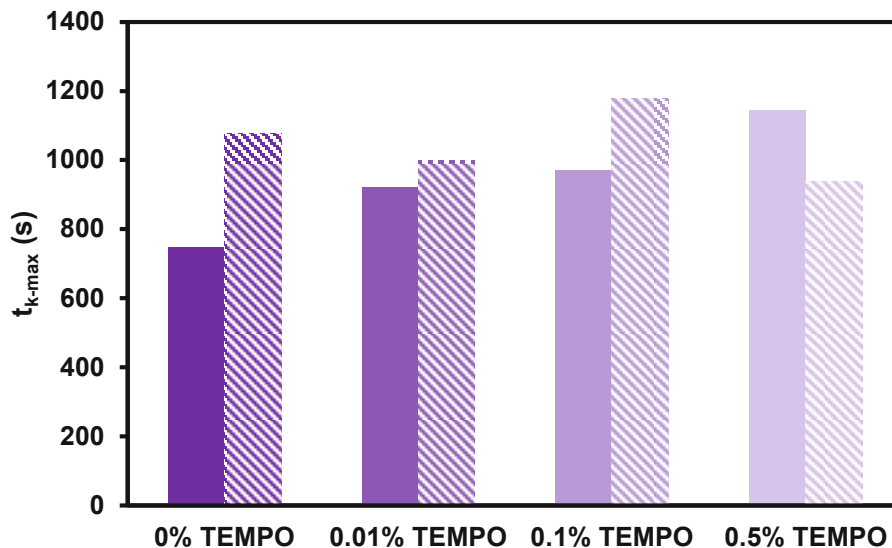Table 72: Values for t_{k-max} of the polymerization reaction in Rheo/IR measurements observed for different concentrations of TEMPO with BN-2 and Cu(acac)$_2$ in 3Mix at t_0 and after one week of storage at 8 °C.

	t_0	1 week
	t_{k-max} (s)	
0% TEMPO	747	1077
0.01% TEMPO	923	999
0.1% TEMPO	971	1179
0.5% TEMPO	1145	939

1.1.1.   Influence of TEMPO on Polymer Properties

Dynamic mechanical thermal analysis (DMTA) was carried out to study the temperature dependency of the mechanical properties of the polymers. Conclusions can be drawn regarding the network properties, the T_g and post-curing effects.

The thermomechanical properties of polymerized 3Mix were compared, applying BN-2/Cu(acac)$_2$ with 0.1mol% TEMPO. The B-formulations and respective Cu-formulation were mixed in w% 50:50 ratio and cured inside a mold for DMTA specimens. Thereafter, the specimens were stored for 24 h at 37 °C and subsequently the measurements were performed. The formulations were prepared according to Table 73.

Table 73: Formulations prepared for DMTA measurements of Cu(acac)$_2$ and BN-2 in 3Mix with various concentrations of TEMPO.

	B-formulation	Cu-formulation
BN-2 (mol%)	3.5	-
Cu(acac)$_2$ (mol%)	-	0.2
TEMPO (mol%)	0 / 0.1	-
3Mix (mol%)	96.5 / 96.4	99.8

The storage modulus (G') of the respective specimens is plotted against the temperature increase from -100 °C to 200 °C. Another important parameter is the loss factor (tanδ) which is the quotient of G' and the loss modulus (G''). In the following Figure 176 G' and tanδ are depicted for samples polymerized with BN-2 and BN-2 + 0.1mol% TEMPO.
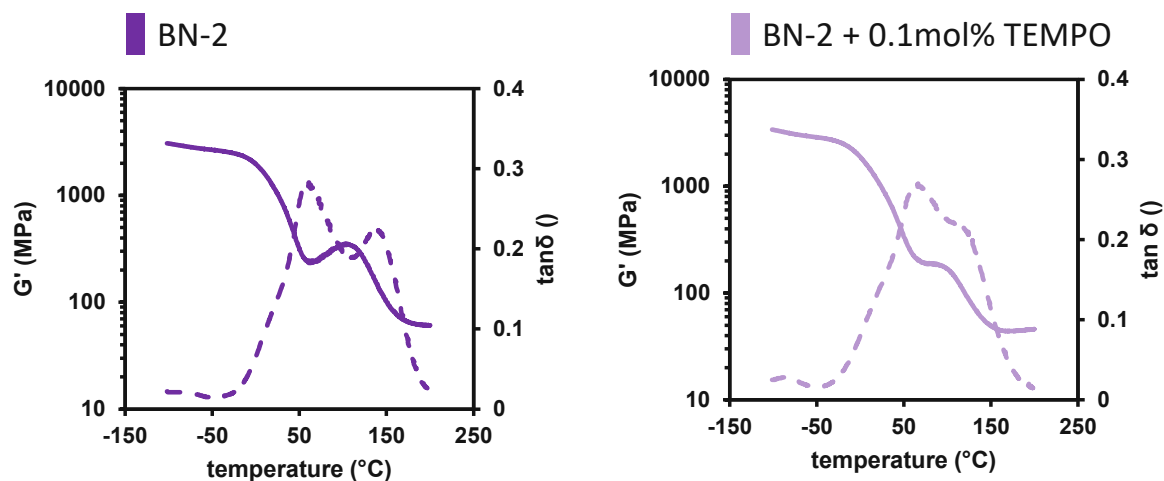
Figure 176: DMTA curves with G' (fully drawn) and tanδ (dashed line) of samples derived from BN-2 and BN-2 + 0.1mol% TEMPO with Cu(acac)$_2$ in 3Mix.

The main difference in thermomechanical properties that comes with the addition of 0.1 mol% TEMPO is that the thermal post-curing is almost vanished, which is why no second T_g is observable. This is due to TEMPO radicals that are still available and can deactivate any thermally generated radicals readily. The mechanical properties as well as the double bond conversion is lower for the sample with addition of TEMPO. The first T_g of the network is very similar to the sample without TEMPO.

Table 74: Values for G'$_{25°C}$, T_g1, T_g2 and DBC$_{ATR-IR}$ of samples derived from BN-2 and BN-2 + 0.1mol% TEMPO with Cu(acac)$_2$ in 3Mix.

	G'$_{25°C}$ (MPa)	T_g1 (°C)	T_g2 (°C)	DBC$_{ATR-IR}$ (%)
BN-2	1037	63.0	136.8	58.4
BN-2 + 0.1% TEMPO	962	62.2	-	33.1

Not only thermomechanical properties as obtained from DMTA measurements are necessary to characterize polymer specimen sufficiently. Tensile Tests give a great insight in the mechanical properties of the polymer, including stress at break (σ), elongation at break (ε) and Δσ/Δε, an approximate value for the Young's modulus.

Formulations were prepared according to Table 75 and mixed in a w% 50:50 ratio and transferred to a silicon mold for tensile test specimens. After polymerization the specimens were stored for 24 h at 37 °C, after which the measurements were performed.

Table 75: Formulations prepared for tensile tests of Cu(acac)$_2$ and BN-2 in 3Mix with various concentrations of TEMPO.

	B-formulation	Cu-formulation
BN-2 (mol%)	3.5	-
Cu(acac)$_2$ (mol%)	-	0.2
TEMPO (mol%)	0 / 0.1	-
3Mix (mol%)	96.5 / 96.4	99.8

Interestingly, the results of the DMTA measurement would suggest similar mechanical properties at 25 °C, however, the tensile tests showed a significant decrease of mechanical properties with the addition of 0.1 mol% TEMPO (Figure 177).
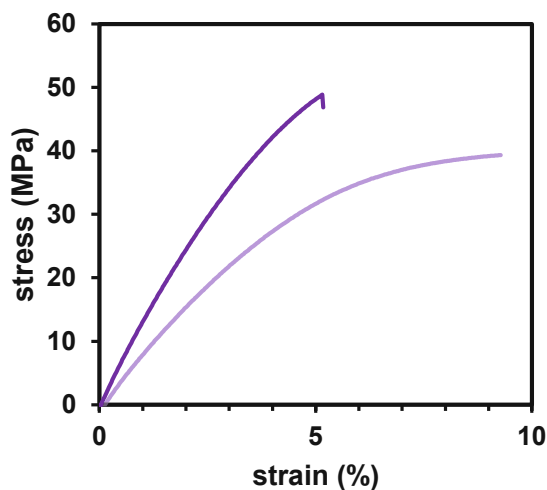
Figure 177: Stress/strain diagram of tensile tests of samples derived from BN-2 and BN-2 + 0.1mol% TEMPO with Cu(acac)$_2$ in 3Mix.

The addition of TEMPO comes with a decrease in the DBC, measured via ATR-IR, which explains the more flexible and less brittle polymer. The stress at break is decreased and the elongation at break is increased.

Table 76: Results of tensile tests of specimen derived from different BN-2 and BN-2 + 0.1 mol% TEMPO with Cu(acac)$_2$ in 3Mix, including stress at break, elongation at break, $\Delta\sigma/\Delta\varepsilon$ and DBC$_{ATR-IR}$.

	stress at break (MPa)	elongation at break (%)	$\Delta\sigma/\Delta\varepsilon$ (MPa)	DBC$_{ATR-IR}$ (%)
BN-2 0% TEMPO	47.9±0.7	4.8±0.3	13.5	58.4
BN-2 0.1% TEMPO	36.4±2.3	9.3±1	8.9	33.1

Although the (thermo)mechanical properties of the final polymer were not overly influenced no real increase in stability was observed via the addition of TEMPO. The diborane/Cu system is better stabilized via the choice of monomer as shown in previous discussions.

1.2. Concentration Dependency of SiB-1/Cu(acac)$_2$ in 3Mix
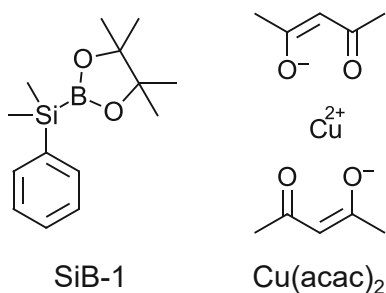
Figure 178: Chemical structure of the SiB-1 and Cu(acac)$_2$

Furthermore, the higher reactive SiB-1 was studied with Cu(acac)$_2$ via rheology-IR measurements to investigate the polymerization process of 3Mix in more detail. Formulations were prepared according to Table 77.

Table 77: Formulations used in the Rheology-IR experiments studying the SiB/Cu system with constant 0.2 mol% Cu

	Cu-formulation	SiB-formulation
3Mix (mol%)	99.8	93/ 96.5 / 98.2
Cu(acac)$_2$ (mol%)	0.2	-
SiB-1 (mol%)	-	7 / 3.5 / 1.8

For the rheology-IR experiments 100 mg of Cu-formulation and 100 mg of SiB-formulation was applied to the glass plate of the measuring device. The measurement was started

immediately, mixing the two monomer formulations for 45 s with the rotating stamp, then the recording of moduli and IR would start. The resulting curves of G' and DBC are depicted in

Figure 179: The left diagram shows the storage modulus G' during the polymerization reaction and the right graph the according DBC. 7 mol% SiB-1 (●), 3.5 mol% SiB-1 (●) and 1.8 mol% SiB-1 (○) in 3Mix with 0.2 mol% Cu in 3Mix.

It is shown that the speed of the polymerization is very fast in the case of the 7 mol% SiB-1 formulation. However, also the lower concentrated formulations are fast considering the amount of initiator. A formulation that contains 1.8 mol% SiB-1 and 0.2 mol% Cu initiator in each respective formulation results in a total concentration of 0.9 mol% SiB-1 and 0.1 mol% $Cu(acac)_2$ in the mixed formulation. When looking at the DBC over time, a very fast increase for the 7 mol% SiB-1 system can be seen, where even a little polymerization during the mixing phase might have occurred. However, interestingly the DBC curve for the 1.8 mol% SiB-1 formulation shows an almost linear increase in DBC for a 1000 s before slowing down. This would suggest a living polymerization and will be investigated in more detail, however, it was only observed in this concentration and no other formulation had shown that behavior.

The t_{50} value reflects the speed of the polymerization very well and it can be seen that with increasing concentration of SiB-1 the speed increases. The 7 mol% SiB-1 formulation was more than two minutes faster than the reference system and also the 3.5 mol% SiB-1 formulation was only one minute slower compared to the reference. The final double bond conversion increases again with increasing concentration of SiB-1 from around 40% to 50% (Table 78).

Table 78: Rheology-IR results of 7 mol% SiB-1, 3.5 mol% SiB-1 and 1.8 mol% SiB-1, showing the t_{k-max} value, representing the speed of the polymerization and the final DBC.

	t_{k-max} (s)	G'_{final} (Pa)	DBC_{end} (%)
1.8 mol% SiB-1	1052	$4.91*10^5$	41
3.5 mol% SiB-1	881	$4.16*10^5$	47
7 mol% SiB-1	357	$5.28*10^5$	52

Since the results so far were very clear and a dependence of the speed of the polymerization as well as the final DBC on the concentration of SiB-1 could be distributed, also the Cu concentration was varied in the following experiment. The SiB-1 concentration was held constant at 3.5mol% and the Cu concentration set to 0.01 mol%, 0.1 mol% or 0.2 mol% respectively (Table 79).

Table 79: Formulations used in the Rheology-IR experiments studying the SiB-1 with Cu(acac)$_2$ system with constant 3.5 mol% SiB-1.

	Cu-formulation	SiB-formulation
3Mix (mol%)	99.8 / 99.9 / 99.99	96.5
Cu(acac)$_2$ (mol%)	0.2 / 0.1 / 0.01	-
SiB-1 (mol%)	-	3.5

For the rheology-IR experiments ~100 mg of Cu-formulation and ~100 mg of SiB-1 formulation was applied to the glass plate of the measuring device. The measurement was started immediately, mixing the two monomer formulations for 45 s with the rotating stamp, then the recording of moduli and IR would start. The resulting curves are depicted in Figure 180.

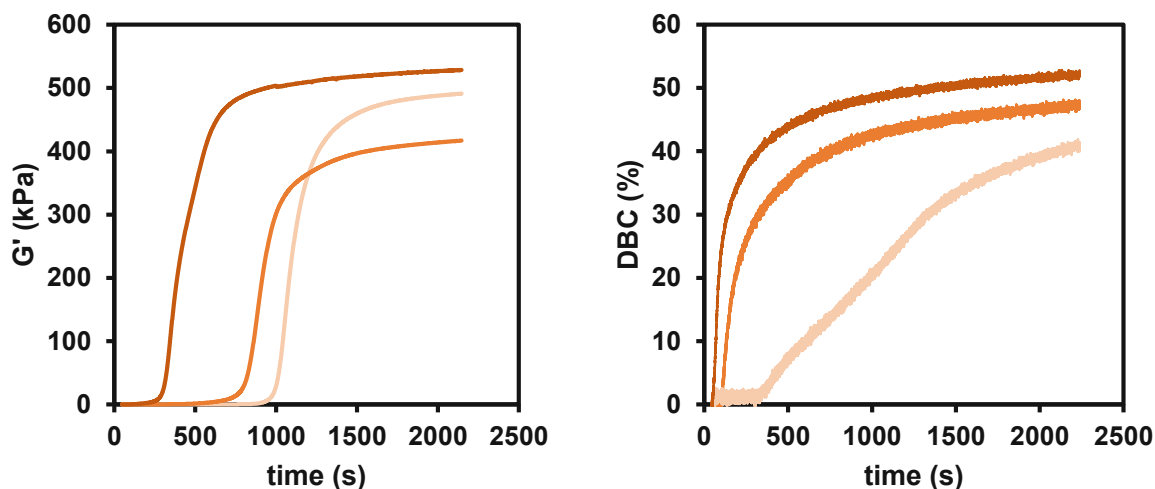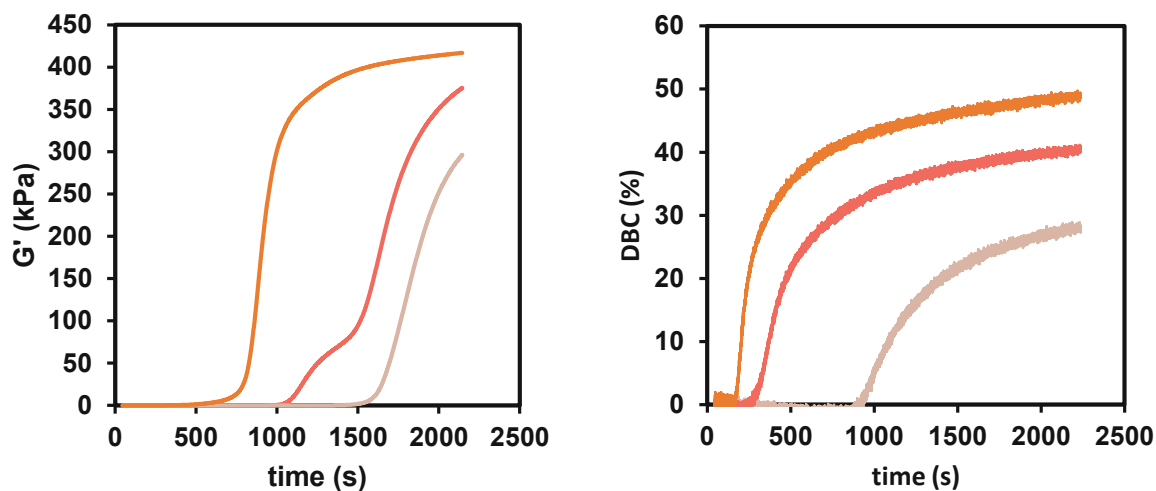Figure 180: The left diagram shows the storage modulus G' during the polymerization reaction and the right graph the according DBC. 0.1w% Cu (●), 0.025w% Cu (●) and 0.005w% Cu (●) in 3Mix with 1w% SiB in 3Mix.

It is shown that with decreasing Cu(acac)$_2$ concentration the time until the polymerization starts is highly delayed. The same trend as for decreasing SiB concentrations was observed in this case. The increase of the polymerization speed with higher Cu(acac)$_2$ concentration, however, excludes a catalytic role of the Cu(acac)$_2$ and assigns it to an actively initiating role. This is a key finding in order to optimize this kind of polymerization system. Not only is the t_{k-max} value much lower, also the final DBC is significantly less with less Cu concentration.

It is to note that the delay time until the polymerization starts shows really no increase in DBC. This indicates that a reaction between SiB-1 and Cu(acac)$_2$ has to occur to a very high degree until finally radical species are formed that can start the polymerization reaction. This reaction seems to be very dependent on the amount of Cu(acac)$_2$ in the formulation and occurs faster with a higher Cu(acac)$_2$ concentration.

In this case, also a decrease in the mechanical properties was observed that very much reflects the trend of the DBC. The polymers with less DBC show a significantly lower final storage modulus.

Table 80 Rheology-IR results of 0.2 mol% Cu, 0.1 mol% Cu and 0.01 mol% Cu with constant 3.5 mol% SiB-1, showing the t_{k-max} value, representing the speed of the polymerization, the final storage modulus G' and the final DBC.

	t_{k-max} (s)	G'_{final} (Pa)	DBC (%)
0.2% Cu	880	$4.17*10^5$	47
0.1% Cu	1622	$3.73*10^5$	40
0.01% Cu	1785	$2.93*10^5$	28

1.3. Concentration Dependency of B5-1/Cu(acac)2 in 3Mix

In the previously discussed diborane/Cu systems very low concentrations of the Cu species of 0.2 mol% is employed. This has solubility reasons, as higher concentrations of up to 2 mol% do not remain fully dissolved in 3Mix over time, as well as coloration reasons, as with a higher Cu(acac)$_2$ concentration the formulations start get blue/grey. Despite that, the reactivity properties were investigated using the formulations shown in Table 81.

Table 81: Formulations prepared for Rheo/IR measurements as well as DMTA measurements regarding concentrations of Cu(acac)$_2$ up to 2 mol%.

	B-formulation	Cu-formulation
B5-1 (mol%)	3.5	-
Cu (mol%)	-	0.2 / 0.5 / 1 / 2
3Mix (mol%)	96.5	99.8 / 99.5 / 99 / 98

It could be shown in Rheo/IR experiments that an increase in Cu(acac)$_2$ concentration enhances the polymerizations reactivity from 0.2 mol% - 1 mol%. (Figure 181)

■ 2 mol%   ■ 1 mol%   ■ 0.5 mol%   ■ 0.2 mol%
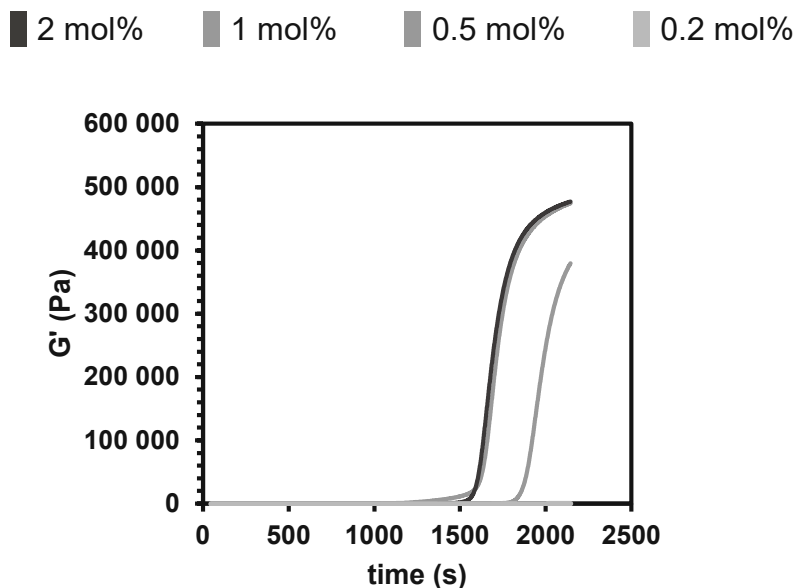
Figure 181: Storage modulus (G') during the polymerization of 3Mix with diborane/Cu employing B5-1 and Cu(acac)$_2$ in different concentrations.

The concentrations increase from 1 mol% to 2 mol% did not have any impact on the reactivity of the formulations. These results do support the catalytic cycle that is employed in the initiation mechanism as with very high concentrations the reactivity does not further increase.

The thermomechanical properties were investigated via DMTA measurements and no significant improvements were observed with the increase of Cu(acac)$_2$ concentration.

1.4.   FurtherTensile Tests SiB/Cu(acac)2 in 3Mix

Specimens for tensile tests were prepared from formulations of 3Mix with 7 mol% SiB-1, 3.5 mol% SiB-1 and 1.8 mol% SiB-1 respectively and 0.2 mol% Cu(acac)$_2$ (Table 82). The Cu-formulation was mixed with the respective SiB-1-formulation in a 1:1 (w%) ratio. The samples containing high concentrations of SiB-1, especially the 7 mol% SiB-1 formulation polymerized very fast in the molds, resulting in unavoidable bubbles.

Table 82: Formulations used in the tensile tests studying the SiB-1/Cu system with constant 0.2 mol% Cu(acac)$_2$

	Cu-formulation	SiB-1-formulation
3Mix (mol%)	99.8	93/ 96.5 / 98.2
Cu(acac)$_2$ (mol%)	0.2	-
SiB-1 (mol%)	-	7 / 3.5 / 1.8

The tensile curve fitting the best to the average obtained values is displayed in Figure 182.
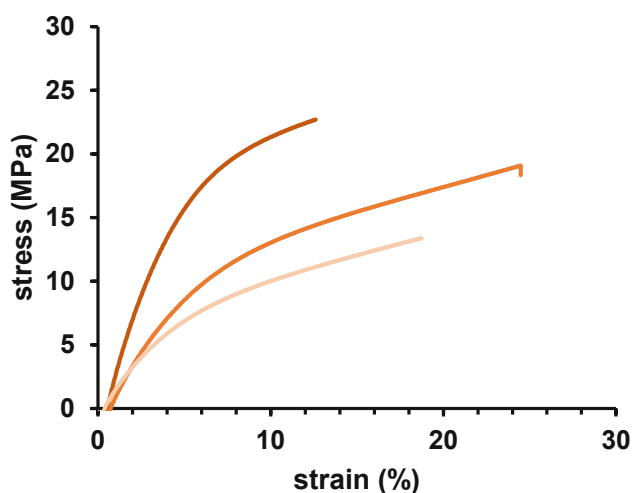
Figure 182: Tensile curves of polymer specimens polymerized with 7 mol% SiB-1 (●), 3.5 mol% SiB-1 (●) and 1.8 mol% SiB-1 (●) in 3Mix with 0.2 mol% Cu(acac)$_2$ in 3Mix.

It is shown that a higher SiB-1 concentration results in a stiffer polymer with a higher stress at break and a lower elongation at break due to a higher crosslinking density. The stress at break as well as the elongation at break is listed in Table 83 below. The shown Δσ/Δε was calculated from the curve's linear region with an R^2>0.99.

Table 83: Results from the tensile tests of polymer specimens polymerized with 7 mol% SiB-1 , 3.5 mol% SiB-1 and 1.8 mol% SiB-1 in 3Mix with 0.2 mol% Cu(acac)$_2$ in 3Mix. Values for stress at break, elongation at break, Δσ/Δε as well as DBC$_{ATR-IR}$ are displayed.

	stress at break (MPa)	elongation at break (%)	Δσ/Δε (MPa)	DBC$_{ATR-IR}$ (%)
7 mol% SiB-1	20.7±2.9	10.7±2.7	5.9	46±5
3.5 mol% SiB-1	16.7±2.4	17.6±6.2	3.5	56±5
1.8 mol% SiB-1	10±4.1	14.5±6.1	2.6	24±5

Interestingly, the concentration of 3.5 mol% SiB-1 results in rather stiff polymers with still a high elongation at break. The measured DBC of the respective specimens via ATR-IR also shows that the 3.5 mol% SiB-1 formulation has a higher conversion than e.g. the 7 mol% SiB-1 formulation. However, usually, it is suggested that with lower SiB-1 concentration also the DBC is lower (as previously discussed in Rheology/IR measurements). Δσ/Δε is decreasing with lower SiB-1 concentration, following the trend of the stress at break.

Specimens for tensile tests were prepared from formulations of 3Mix with 7 mol% SiB-1, 3.5 mol% SiB-1 and 1.8 mol% SiB-1 respectively and 0.01 mol% Cu(acac)$_2$ (Table 84). The Cu-formulation was mixed with the respective SiB-1-formulation in a 1:1 (w%) ratio.

Table 84: Formulations used in the tensile tests studying the SiB-1/Cu system with constant 0.01 mol% Cu(acac)$_2$

	Cu-formulation	SiB-1-formulation
3Mix (mol%)	99.99	93/ 96.5 / 98.2
Cu(acac)$_2$ (mol%)	0.01	-
SiB-1 (mol%)	-	7 / 3.5 / 1.8

The tensile curve fitting the best to the average obtained values is displayed in Figure 183.

Figure 183: Tensile curves of polymer specimens polymerized with 7 mol% SiB-1 (●), 3.5 mol% SiB-1 (●) and 1.8 mol% SiB-1 (●) in 3Mix with 0.01 mol% Cu(acac)$_2$ in 3Mix.

It is shown that with higher SiB-1 concentration the samples are getting stiffer. However, in comparison to the 0.2 mol% Cu(acac)$_2$ samples, the 0.01 mol% Cu(acac)$_2$ samples are still very soft and more elastomer like. Very high elongations at break are achieved with only very little stress at break. This is also well reflected in the $\Delta\sigma/\Delta\varepsilon$ of the samples which is decreasing with lower SiB-1 concentration. The very soft behavior of the samples is easily explained by the low DBC observed in ATR-IR. The low Cu(acac)$_2$ concentration definitely results in a lower DBC and therefore in lighter crosslinked softer materials. The experimental data is shown in Table 85.
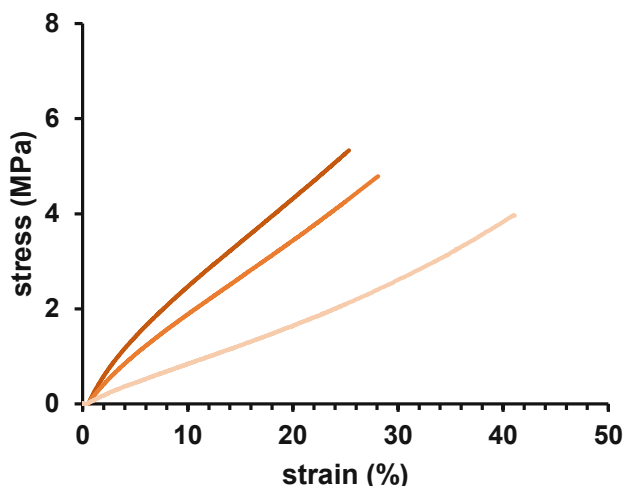
Appendix

Table 85: Results from the tensile tests of polymer specimens polymerized with 7 mol% SiB-1 , 3.5 mol% SiB-1 and 1.8 mol% SiB-1 in 3Mix with 0.2 mol% Cu(acac)$_2$ in 3Mix. Values for stress at break, elongation at break, Δσ/Δε as well as DBC$_{ATR-IR}$ are displayed.

	stress at break (MPa)	elongation at break (%)	Δσ/Δε (MPa)	DBC$_{ATR-IR}$ (%)
7 mol% SiB-1	4.2±1.2	21.1±5.6	0.53	41±5
3.5 mol% SiB-1	3.5±1	22.3±5.3	0.34	14±5
1.8 mol% SiB-1	3.2±1.2	36.2±3.8	0.11	8±5

Tensile test specimens were prepared of formulations of 3Mix containing 3.5 mol% B5-1 or 3.5 mol% SiB-1 respectively, combined with 3Mix containing 0.2 mol% Cu(acac)$_2$ (Table 86). The Cu-formulation was mixed with the respective SiB-1-formulation in a 1:1 (w%) ratio. All samples had a reasonable working time before the polymerization and bubble free specimens were achieved.

Table 86: Formulations used in the tensile tests studying the post-curing of the B5-1/Cu and the SiB-1/Cu system with constant 0.2 mol% Cu(acac)$_2$ in 3Mix.

	Cu-formulation	B5-1-formulation	SiB-1-formulation
3Mix (mol%)	99.8	96.5	96.5
Cu(acac)$_2$ (mol%)	0.2	-	-
B5-1 (mol%)	-	3.5	-
SiB-1 (mol%)	-	-	3.5

After the preparation of the samples, a third of them was immediately measured (1h). In Figure 184 the diagrams show the tensile test curves that fit the best to the average of the measurements. Interestingly, after 1h there is no significant difference between the specimens. The elongation at break is in the same range, as well as the stress at break and Δσ/Δε. However, it is to note that the measured DBC of the SiB-1 sample is double the DBC of the B5-1 sample, which is not reflected in the mechanical properties. After one day of storage at 37 °C another third was measured. The diagram shows clearly the difference that the storage time makes on the mechanical properties. Both, the B5-1 and the SiB-1 samples, show an increase in stress at break as well as Δσ/Δε, and a decrease in elongation at break. The DBC

is increased as well after one day for both samples. The BPB samples have a much higher increase in their mechanical properties compared with the SiB-1 samples. That can be well explained by the increase in the DBC, since for the SiB-1 sample it increases for 4%. The DBC of the B5-1 samples however doubles from 12% to 25% in one day.
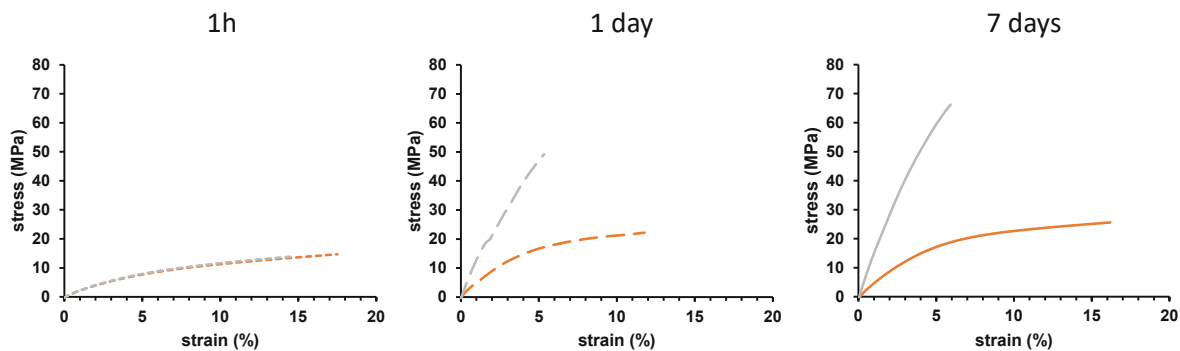

Figure 184: Curves of the tensile tests of the specimen polymerized with 3.5 mol% B5-1 (●) or 3.5 mol% SiB-1 (●) with 0.2 mol% Cu(acac)$_2$. In the left graph the measurements were conducted after 1h, in the middle graph the measurements were conducted after one day of storage at 37 °C and in the right graph the measurements were conducted after 7 days of storage 37 °C.

The very right diagram in Figure 184 shows the tensile tests curves from the measurement after 7 days of storage at 37 °C. In the case of the B5-1 sample, the stress at break increases again together with the $\Delta\sigma/\Delta\varepsilon$, and the elongation at break decreases. The SiB-1 sample shows an increase in stress at break as well as the elongation at break, while employing an almost constant $\Delta\sigma/\Delta\varepsilon$. The rise in DBC from one day of storage to 7 days of storage is immense for both samples. This increase in DBC, however, is not reflected in mechanical properties of the samples. The experimental data is displayed in Table 87.

Table 87: Results from the tensile tests of polymer specimens polymerized with 3.5 mol% B5-1 or 3.5 mol% SiB-1 in 3Mix with 0.2 mol% Cu(acac)$_2$ in 3Mix. Values for stress at break, elongation at break, $\Delta\sigma/\Delta\varepsilon$ as well as DBC$_{ATR-IR}$ are displayed.

	stress at break (MPa)	elongation at break (%)	$\Delta\sigma/\Delta\varepsilon$ (MPa)	DBC$_{ATR-IR}$ (%)
1h B5-1	13.2±0.9	14±1.6	2.5	12.2±1.8
1d B5-1	52.4±7.9	6.6±1.5	13.4	24.6±4.9
7d B5-1	66.2±5.2	5.9±0.8	15.8	84.3±2
1h SiB-1	10.4±2.8	10.9±5	2.4	25.7±2.8
1d SiB-1	17.6±4.9	7.7±3.1	5.1	29.8±2.8
7d SiB-1	23.9±1.5	15.2±0.8	5.2	72.5±3.9

In Figure 185 it is clearly visible that with time, the mechanical properties improve drastically, especially during the first day of post-curing. Also, the DBC is over time is displayed. The SiB-1 sample starts at a higher DBC right after the polymerization, however benefits less from the post-curing time. In contrast, the B5-1 sample starts at a lower DBC right after the polymerization, but its DBC increases almost linear over the course of one week. The DBC increase very much reflects a higher crosslinking density of the polymer network, therefore resulting in the observed better mechanical properties. It is, however interesting that the degree of increase in the mechanical properties is not corresponding to the degree of increase in the DBC.
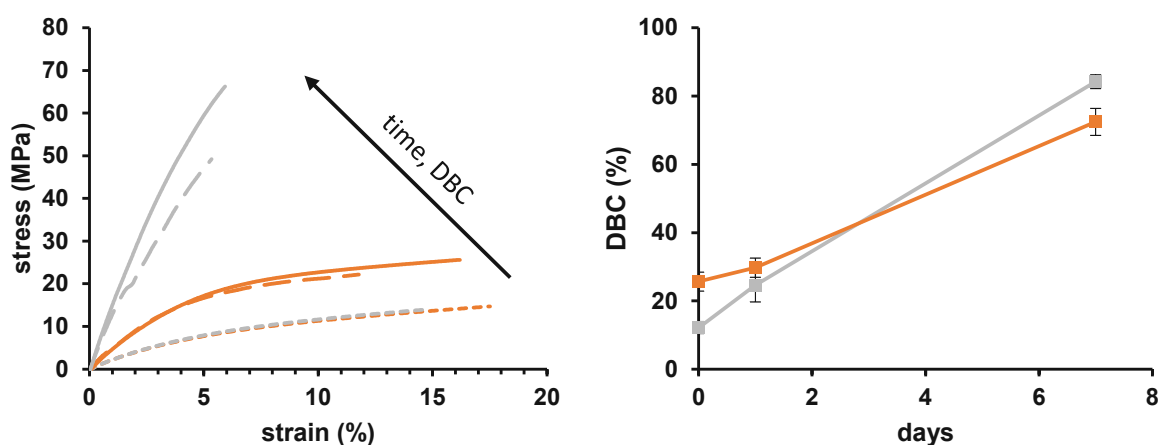
Figure 185: Curves of the tensile tests of the specimen polymerized with 3.5 mol% B5-1 (⬤) or 3.5 mol% SiB-1 (⬤) with 0.2 mol% Cu(acac)$_2$ in the left graph. Dotted lines were measured after 1h, dashed lines after 1 day and full lines after 7 days. In the right graph the according DBC is displayed at the time measured.

1.5. Further DMTA using SiB-1/Cu(acac)2 in 3Mix

Specimens for DMTA measurements were prepared from formulations of 3Mix with 7 mol% SiB-1, 3.5 mol% SiB-1 and 1.8 mol% SiB-1 respectively and 0.2 mol% Cu(acac)$_2$ (Table 88). The Cu-formulation was mixed with the respective SiB-1 formulation in a 1:1 ratio. The samples containing high concentrations of SiB-1, especially the 7 mol% SiB-1 formulation polymerized very fast in the molds.

Table 88: Formulations used in the DMTA measurements studying SiB-1 with Cu(acac)$_2$ in 3Mix with constant 0.2 mol% Cu(acac)$_2$.

	Cu-formulation	SiB-1-formulation
3Mix (mol%)	99.8	93/ 96.5 / 98.2
Cu(acac)$_2$ (mol%)	0.2	-
SiB-1 (mol%)	-	7 / 3.5 / 1.8

A very intense double peak or a peak with a shoulder is observed for the tanδ values. This peak is also strongly reflected in the storage modulus that has its highest degree of decrease at the tanδ maximum and then shows an almost constant value (7 mol% SiB-1) or even an increase at higher temperatures (3.5 mol% SiB-1 and 1.8 mol% SiB-1) before ending up on a fixed value. This is explained by a highly inhomogeneous network formation. The highest reactive monomers in the 3Mix seem to polymerize selectively and form a network (T_g1=~79 °C). The other monomers are loosely polymerized into that network, however when the SiB-1 concentration is increased more of these monomers are included in the network pushing the T_g1 to a higher temperature. At a certain temperature a post-curing effect occurs where all the non-reacted monomers are at least partly polymerized into the network resulting in an increase of the storage modulus at higher temperatures for the 3.5 mol% SiB-1 and 1.8 mol% SiB-1 specimens. It is also noted that the broadness of the tanδ peak increases with higher SiB-1 concentration and the height decreases simultaneously, which both indicates a higher crosslinked network. The G' at 100 °C reflects that very well, as it decreases with lower SiB-1 concentration. (Figure 186, left diagram).
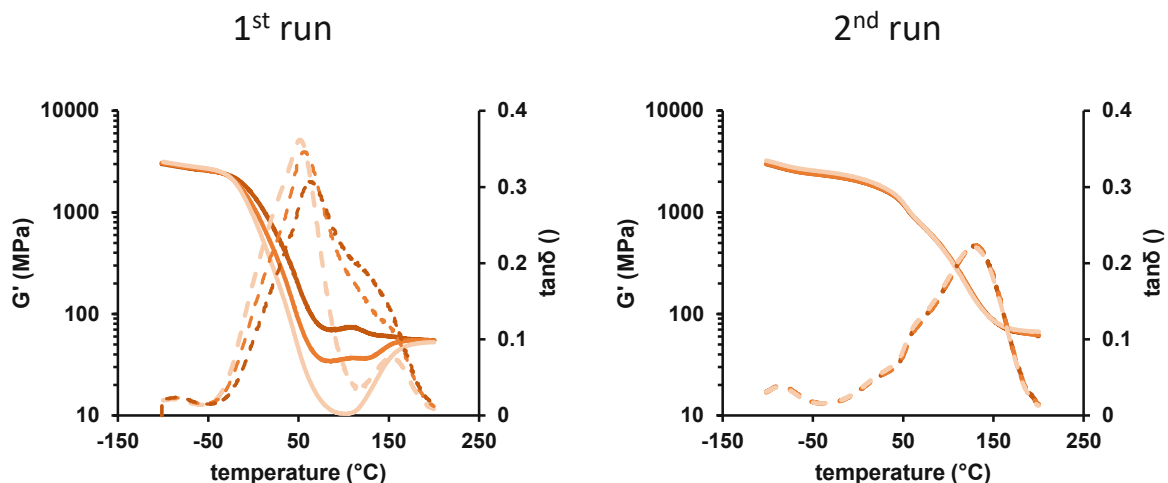
1st run   2nd run

Figure 186: Consecutive Lines: Storage modulus (G') of polymer specimens polymerized with 7 mol% SiB-1 (●), 3.5 mol% SiB-1 (●) and 1.8 mol% SiB-1 (○) in 3Mix with 0.2 mol% Cu in 3Mix. Dashed Lines: tanδ of polymer specimens polymerized with 7 mol% SiB-1 (●), 3.5 mol% SiB-1 (●) and 1.8 mol% SiB-1 (○) in 3Mix with 0.2 mol% Cu in 3Mix.

The postulated post-curing effect is clearly visible when looking at the right diagram in Figure 186. The storage modulus shows a much slower decrease and the tanδ is shifted to much higher temperatures. It is noted that all three specimens showed the almost exact same behavior, from which one can conclude that already 1.8 mol% SiB-1 are enough to provide the full post-curing effect. The absolute height of the tanδ curve is also much less than in the first run, meaning a higher crosslinked network. However, a shoulder is now visible at around 60 °C, which might be the not fully post-cured leftovers of the first network. All the experimental data is listed in Table 89.

Table 89: Results from the DMTA measurements of polymer specimens polymerized with 7 mol% SiB-1, 3.5 mol% SiB-1 and 1.8 mol% SiB-1 in 3Mix with 0.2mol% Cu in 3Mix. Values for T_g1, T_g2, G' at 100°C and T_g-2nd run are displayed.

	T_g1 (°C)	T_g2 (°C)	$G'_{100°C}$ (MPa)	T_g-2nd run (°C)
7 mol% SiB-1	81	-	72	128
3.5 mol% SiB-1	78	-	36	128
1.8 mol% SiB-1	76	153	10	128

2. Silane/Iodonium Salt Redox System

The redox system depicted Figure 187 was investigated as a 2K system with difunctional methacrylates as monomers. Previous experiments showed, that the system polymerizes well, however, when adding filler materials, the polymerization is inhibited.
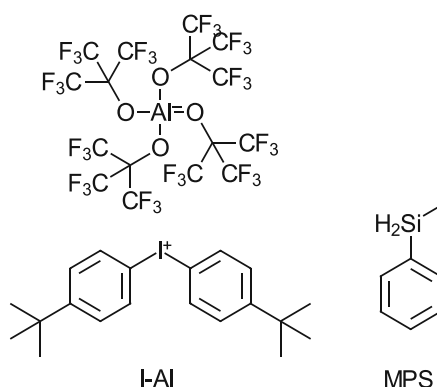
Figure 187: I-Al and MPS redox initiation system

The formulations which were used for the experiments with this system are shown below in Table 90. The F1-formulations always refer to the iodonium salt containing formulations and the F2-formulations always refer to the MPS containing formulations.

Table 90: Composition of the target formulations F1 and F2

F1	target (w%)	F2	target (w%)
BisGMA	30.90%	BisGMA	30.92%
UDMA	43.33%	UDMA	44.33%
E3-BisGMA	21.73%	E3-BisGMA	22.75%
I-Al	4.00%	MPS	2.00%
TEMPO	0.04%		

For the experiments four different filler materials were used, Sphaerosil, Ox50, Glasfüller and YbF filler.

2.1. Filler Screening

Formulations of F1 and F2 were prepared with each containing 50w% of the respective filler. In addition, the formulations F1 and F2 were prepared without filler as well.

2.1.1. Polymerization Temperature Measurements

When using the pyrometer setup, 0.5 g of the respective F1 formulation and 0.5 g of the respective F2 formulation were weighed out and subsequently mixed. The pyrometer measurement was started immediately afterwards and the temperature of the formulation as a function of time was detected. Below, an exemplary diagram of such a measurement is shown of the formulations F1 and F2 without filler.
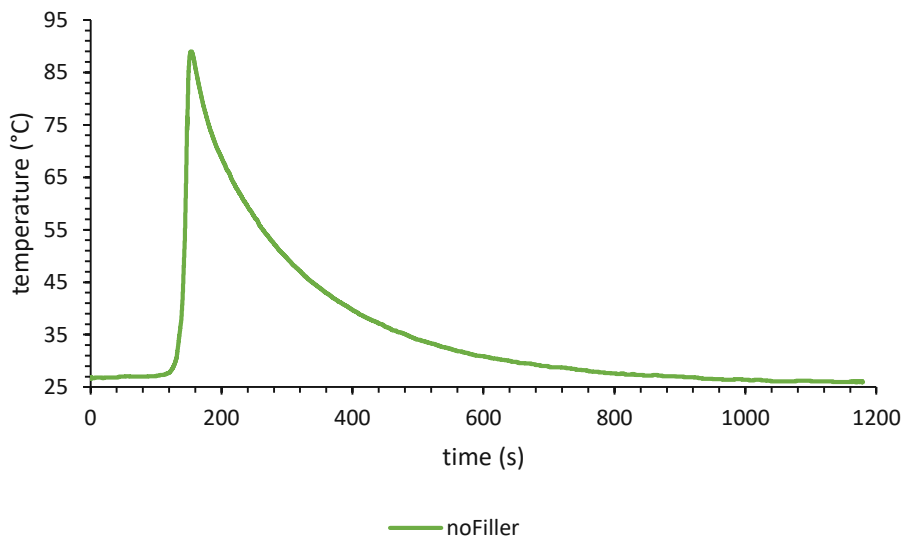

Figure 188: Temp/time-diagram of F1 and F2 without filler

Below, the Table 91 shows an overview over the polymerizations of the formulations with either of the four fillers.

Table 91: Formulations F1 and F2 with either or both containing filler; time of maximum temperature and maximum temperature of the polymerization

Filler	Name	Time (s)	Temperature (°C)
Sphaerosil	F1 + F2Sph	296	35.4
	F1Sph + F2	268	40.8
	F1Sph + F2Sph	-	-
Ox50	F1 + F2Ox50	703	42.3
	F1Ox50 + F2	557	31.5
	F1Ox50 + F2Ox50	-	-
Glasfüller	F1 + F2Glas	409	43.4
	F1Glas + F2	678	37.6
	F1Glas +F2Glas	-	-
YbF	F1 + F2YbF	302	53.9
	F1YbF + F2	58	88.7
	F1YbF + F2YbF	237	42
	no Filler	157	87.7

Indeed, the reactions of F1 with F2 where both formulations contained filler materials were unsuccessful and did not polymerize, except for the YbF filler. However, this is explainable, since the density of the YbF filler is higher than the other ones, so there is less material in the formulation to get to 50w% filler content. In total it clearly shows, that the reactions of the formulations where only one formulation contained filler material showed a polymerization. This gives evidence, that the filler does not necessarily interact with the iodonium or silane part of the initiating system, since the formulations where only one contained a filler always showed a polymerization.

The reactivity of the polymerization reaction seems to depend on the concentration of the filler material.

2.2. Filler Concentration

In an exemplary experiment, Glasfüller was used as the filler material and formulations of F1 and F2 were prepared containing 20w%, 30w% and 40w% of the filler.

2.2.1. Polymerization Temperature Measurements

Again, pyrometric measurements were performed of the reactions of F1 and F2 with the different filler contents. The results are shown in the Table 92 below.

Table 92: Polymerization of F1 and F2 with different concentrations of Glasfüller

Filler content (w%)	Time (s)	Temperature (°C)
20	296	30.4
30	1037	31.5
40	-	-
50	-	-

It clearly shows that the polymerization reaction rapidly slows down with increasing filler content. The formulations with a filler content over 30w% do not show any polymerization anymore. This emphasizes the theory, that the total amount of filler in the final mixed formulation determines the reactivity of the polymerization.

2.2.2. Rheology Measurements

In addition to pyrometric measurements, rheology measurements were performed to obtain the gel point and the modulus of the final composite material. Below are shown the rheology diagrams of the formulations with 20w%, 30w% and 40w% Glasfüller (Figure 189 - Figure 191).
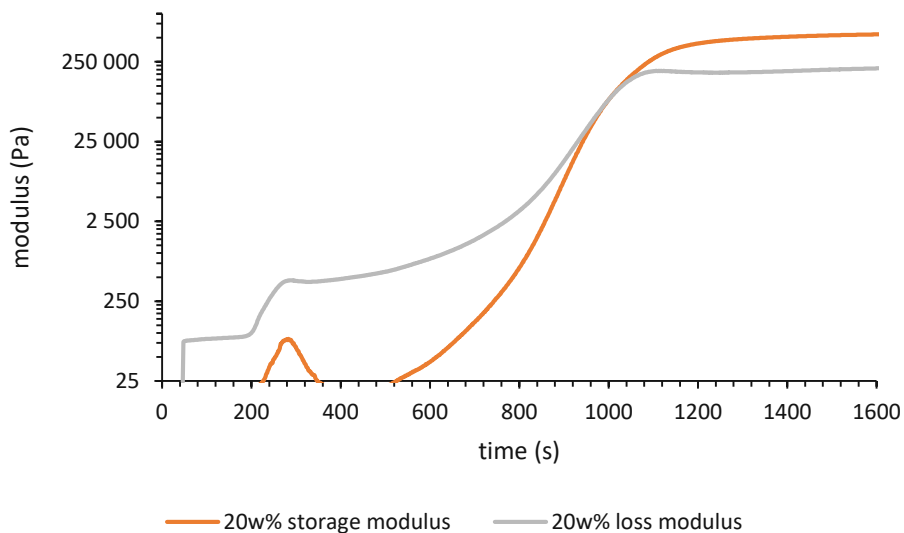

Figure 189: Storage modulus and loss modulus of the polymerization of F1 + F2 with 20w% Glasfüller each
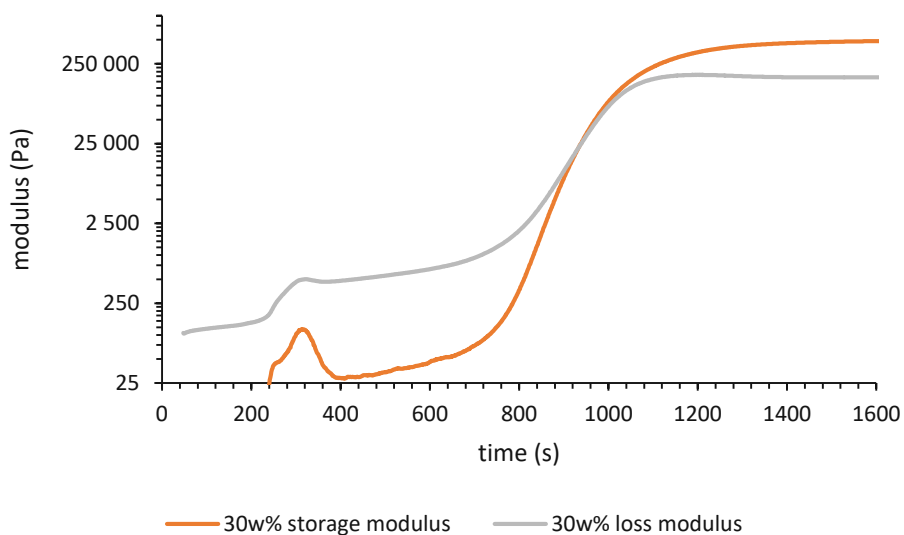
Figure 190: Storage modulus and loss modulus of the polymerization of F1 + F2 with 30w% Glasfüller each
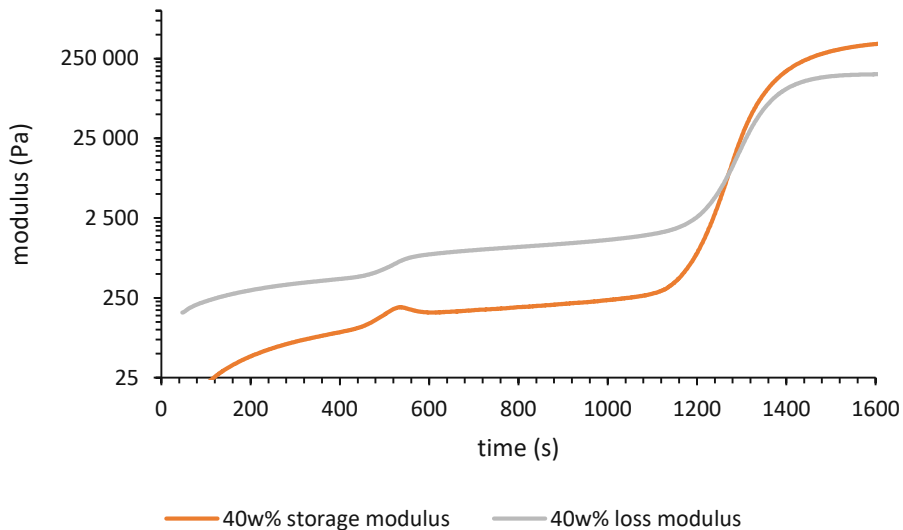
Figure 191: Storage modulus and loss modulus of the polymerization of F1 + F2 with 40w% Glasfüller each

The results are summarized in Table 93.

Table 93: Gelpoints and storage moduli of the different formulations

	t_{gel} (s)	storage modulus end (Pa)
20w%	963	$5.59 * 10^5$
30w%	1053	$4.76 * 10^5$
40w%	1414	$4.44 * 10^5$

It is clearly visible that the gel point is increasing with higher filler content, while the storage modulus is decreasing. This is as well emphasizing the theory, that the reactivity is decreasing dramatically with increasing filler content. This might be due to lower double bond conversions (DBC) of the methacrylic network. For that reason, the DBC of these formulations will be investigated.

2.3. Long Time Reactivity *via* Rheology

In previous experiments, the effect of the filler in the two different formulations F1 and F2 was investigated, since it was assumed that the filler materials might interact with one of the initiating components I-Al or MPS. The polymerization was monitored via pyrometric measurements of the temperature after mixing the two formulations. It was concluded that the filler has no impact on one of the initiating components, since the reactivity of the formulations did not change when filling only F1 or F2. However, the overall concentration of filler has a significant impact on the reactivity of the formulations, which was supported by subsequent rheology measurements of the formulations with various filler contents.

All formulations were prepared according to Table 90 and then used to prepare the composite formulations. The respective filler content as well as F1 and F2 were weighed out and the formulations were homogenized in a Speedmixer at 3000 rpm for 2 min.

2.3.1. Filler Concentration

To investigate the polymerization of the filled systems at different times, rheology/IR measurements were performed right after mixing the formulations and after one week stored at RT. In the following diagrams, rheology measurements of the formulations with 0 -40w% Sphärosil filler are depicted. They were recorded on the same day the formulations were prepared, and one week later respectively.

t0

1 week
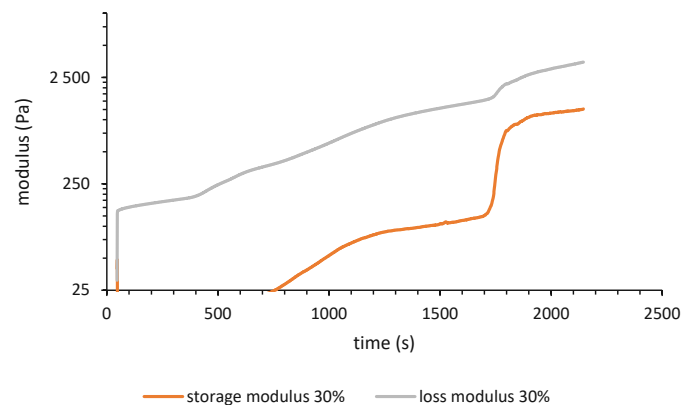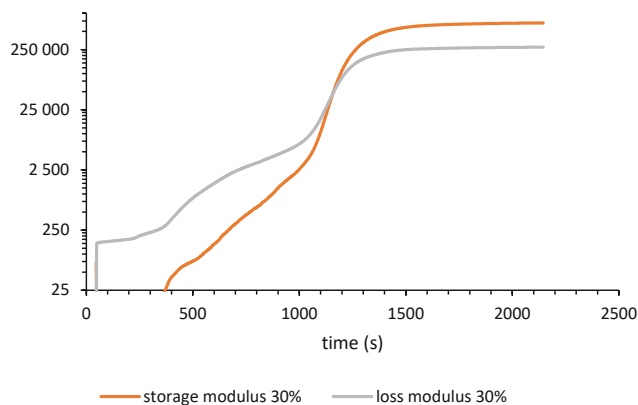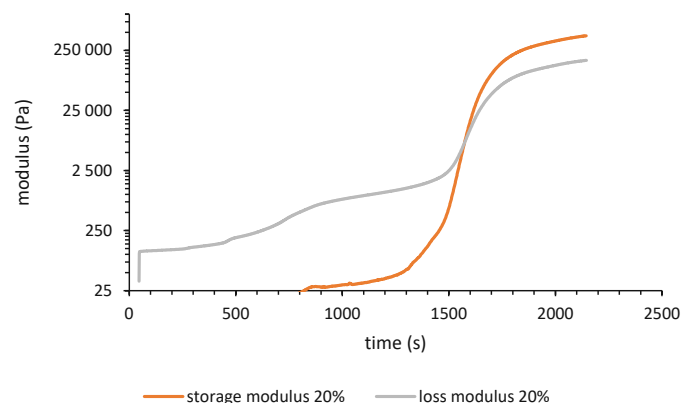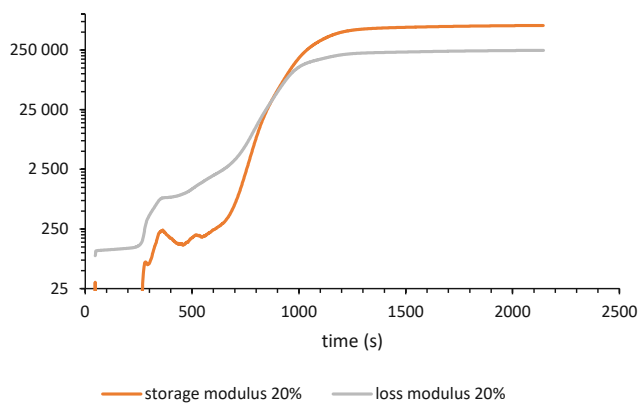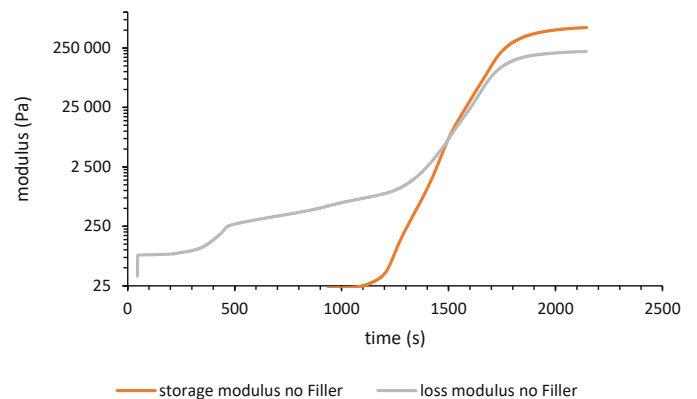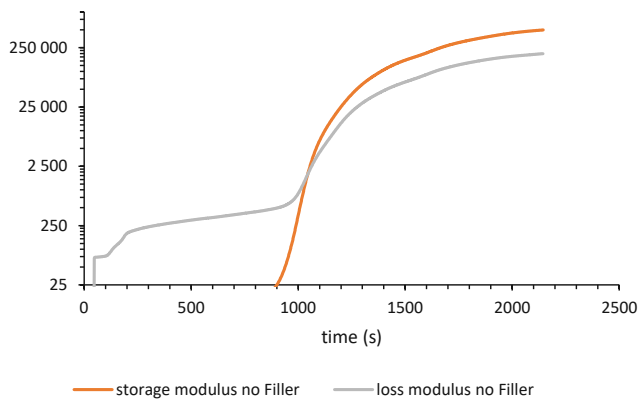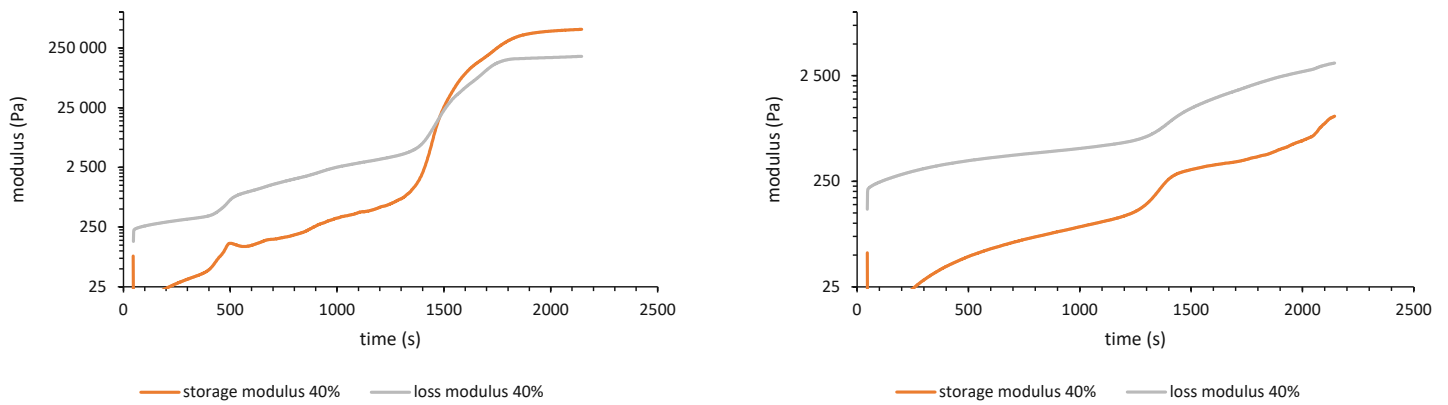
Figure 192: Rheology measurements of the Silane / I-Al system with different Sphärosil filler content directly after mixing (left) in comparison with 1 week later (right)

The diagrams in Figure 192 show the trend already observed, namely that with higher filler content the t_{gel} is also shifted to the right to longer times. Interestingly, the formulation without a filler polymerizes slower, than the respective formulation with 20w% filler content in the case of the t0 diagrams. Another noticeable feature depicted is a short increase of the storage and loss moduli before the gelpoint and the subsequent relaxation, which is the case for every formulation. The comparison of the measurements directly after mixing to the measurements after 1 week clearly show a slowdown of the polymerization speed, since the t_{gel} is drastically shifted to the right to longer times. In the case of the 1 week 30w% and 40w% measurements, no t_{gel} is visible anymore, as it is shifted to longer times than 2100 s (35 min). The observed storage moduli and t_{gel} as well as the simultaneously recorded double bond conversion (DBC) are summarized in the table below.

Table 94: Storage modulus (Pa), t_{gel} (s) and DBC$_{end}$ (%) of the silane / I-Al Formulation with different Sphärosil filler content directly after mixing in comparison with 1 week later

	storage modulus end (Pa)		t_{gel} (s)		DBC$_{end}$ (%)	
	t0	1 week	t0	1 week	t0	1 week
no filler	$6.27*10^5$	$5.53*10^5$	1001	1497	47.3	40.9
20%	$6.45*10^5$	$4.39*10^5$	876	1574	50.3	37.8
30%	$6.94*10^5$	-	1160	-	45.3	25.7
40%	$5.13*10^5$	-	1482	-	35.9	19.5

Table 94 clearly shows a decrease in the storage modulus within one week with respect to the directly measured samples (t0). Also, the DBC is decreasing for every filler content when comparing the measurement times. When looking at the different filler concentrations, the DBC is decreasing with increasing filler content. This is in accordance with the observed loss in reactivity when increasing the filler content.

The intensities of the peak at 6150 cm^{-1} were also compared at the start of each measurement (t0 and 1week). This was done to check if a polymerization (and therefore a relative decrease of the peaks intensity) can be observed during the week stored at RT. However, no discrepancy was found, since all the peak intensities match at the start of each measurement, for the same filler concentration respectively. However, a slower conversion is observed, when looking at the decrease of the peak's intensity (Figure 193). For the other filler concentrations, the same trend was observed, which does fit the detected slower t_{gel}.
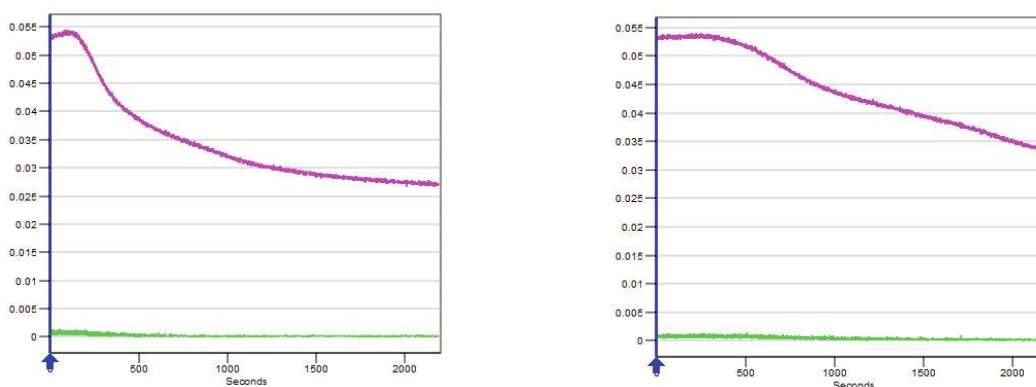
Figure 193: Decrease of the double bond peak at 6150 cm^{-1} over time for the 20% t0 formulation (left) and the 20% 1 week formulation (right)

2.3.2. Storage Conditions

Polymerization experiments were performed of the stored formulations with freshly prepared formulations and were monitored via rheology/IR. The measured matrix is shown in Figure 194. It is noteworthy, that the measurements between the stored samples at RT and 50 °C were spared out, because no relevant information would be obtained. For these measurements the formulations depicted in Table 90 were used and were stored at RT/50 °C for one week.
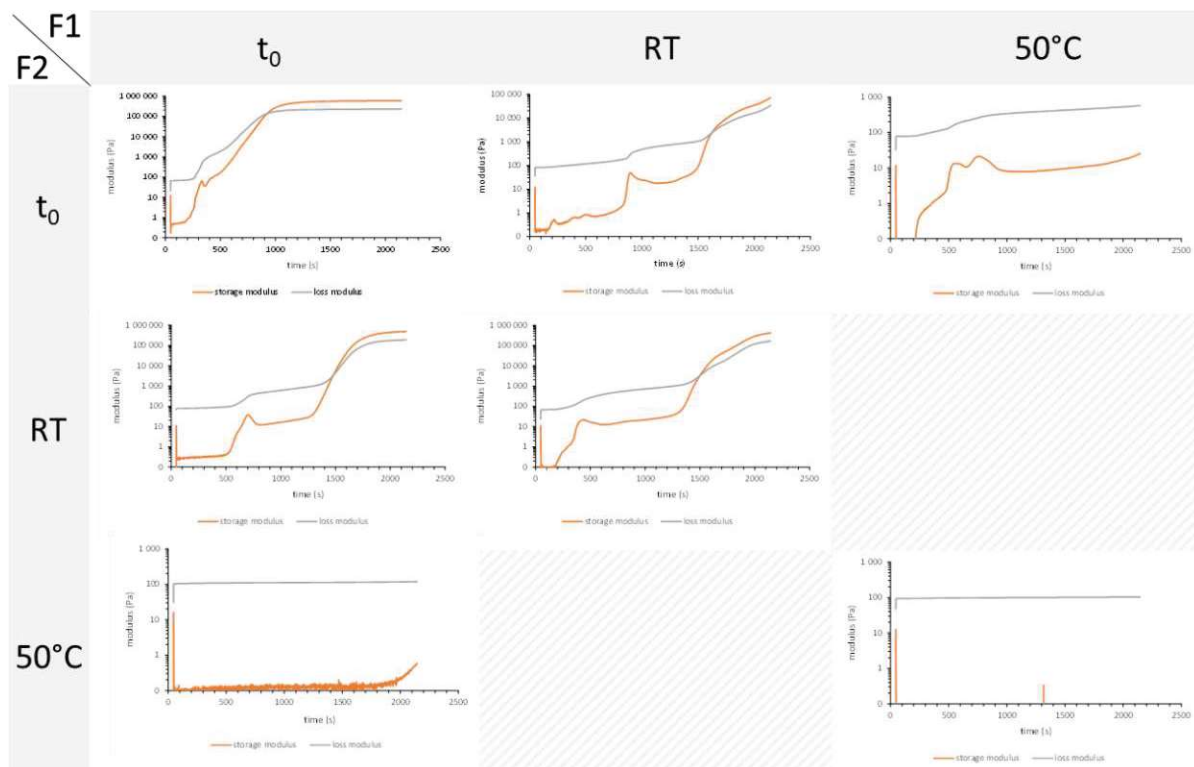
Figure 194: Matrix of the measured formulations in which the stored samples (RT and 50°C) were always combined with a freshly prepared one (t0) and amongst themselves

The formulations, that were stored at 50°C did not polymerize in combination with the fresh formulations. This is true for neither formulation F1 nor F2. Interestingly, both combinations of the formulations stored at room temperature did polymerize, however slowly. No significant difference between the measurements of the RT samples was observed. The geltimes (t_{gel}) as well as the DBC are shown in Table 95 and Table 96.

Table 95: Geltimes (s) of the measured formulations with different storage conditions

		F1		
		t_0	RT	50°C
	t_0	920	1630	-
F2	RT	1500	1540	x
	50°C	-	x	-

x.. not measured

-.. no polymerization

Table 96: DBC$_{end}$ (%) of the measured formulations with different storage conditions

		F1		
		t_0	RT	50°C
	t_0	58.3	12.8	4.1
F2	RT	18.3	19.0	x
	50°C	0	x	0

x.. not measured

The already observed trend, that storage effects the geltime is continued here, as even the measurements where only one formulation was stored at RT for one week show a dramatic increase in the geltime. In addition, the difference between the measurement where only one formulation was stored, and the measurement where both formulations were stored, is insignificant. This states that no conclusion, which formulation is responsible for the increase in geltime can be drawn from these measurements. However, the samples stored at 50°C show no polymerization activity anymore, which is also reflected in the observed DBC. Also, the very low DBC of 4.1% of the fresh F2 with 50°C F1 can be easily seen in the respective rheology measurement, as some polymerization is occurring. Over all, it can be concluded, that both formulations affect the lower reactivity to the same extent.

2.4. Viscosity

A reason for the decreasing reactivity within one week could be an instability of the formulations. Therefore, viscosity measurements were performed over time for the different fillers with a filler content of 50w% to see if the viscosity increases because of an occuring autopolymerization of the respective formulations F1 and F2.

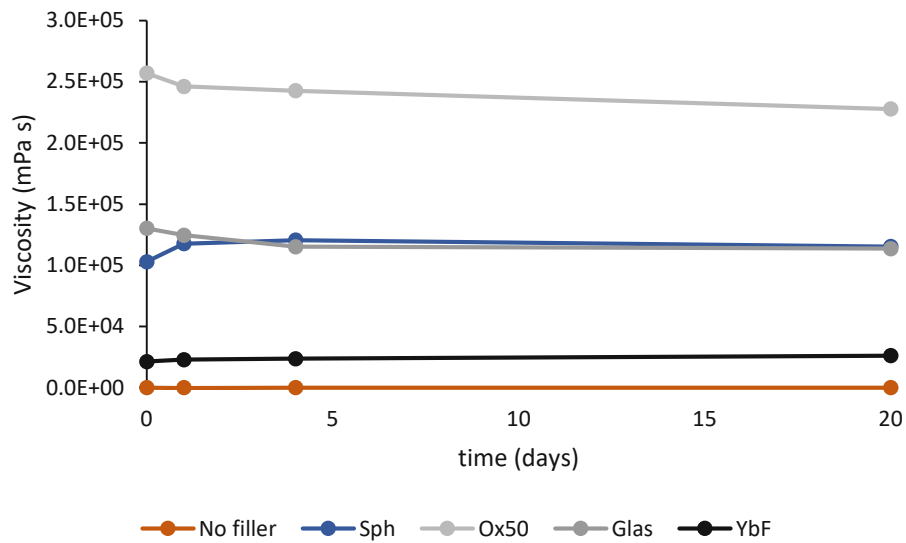The viscosity of F1 (Figure 195) and F2 (Figure 196) over time is depicted in the figures below.

Figure 195: Viscosity (mPa s) of the formulation F1 over 20 days
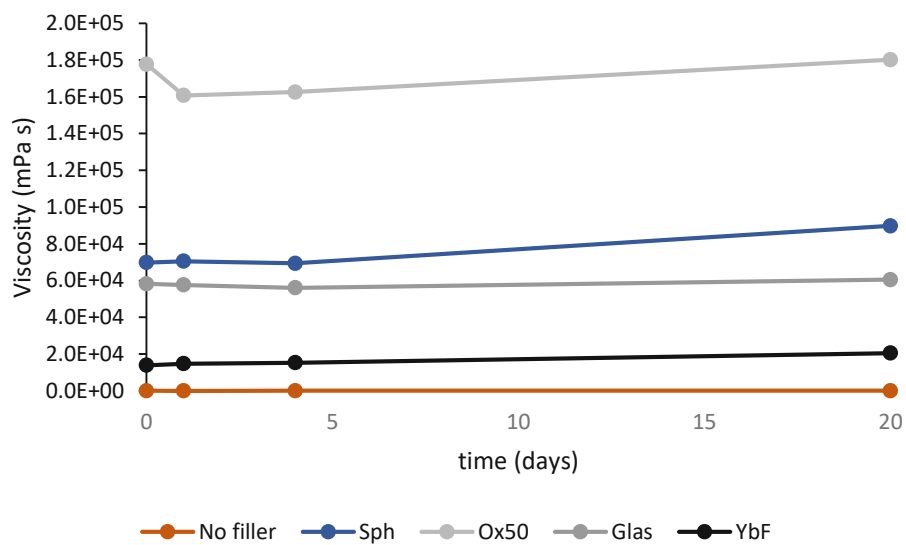
Figure 196: Viscosity (mPa s) of the formulation F2 over 20 days

The viscosity of both formulations, F1 and F2, is relatively constant over 20 days. Formulation F2 shows a slight increase in viscosity, however that is mostly attributable to inhomogeneity of the formulation or inaccuracy of the device. It can be concluded, that no autopolymerization reaction occurs in any of the filled formulations, regardless of type of filler, which is also supported by the previously stated peak intensity check.

2.5. Rheology with PEG Filler

Regarding that the filler is not interacting with the formulations in any other way than increasing the viscosity, a neutral polymer was used as a filling material to see just the effect of viscosity. Therefore, formulations of F1 and F2 were prepared, each containing 20w% PEG (4kDa). Efforts were made to also mix formulations with higher PEG content, however 20w% was the maximum soluble amount possible.
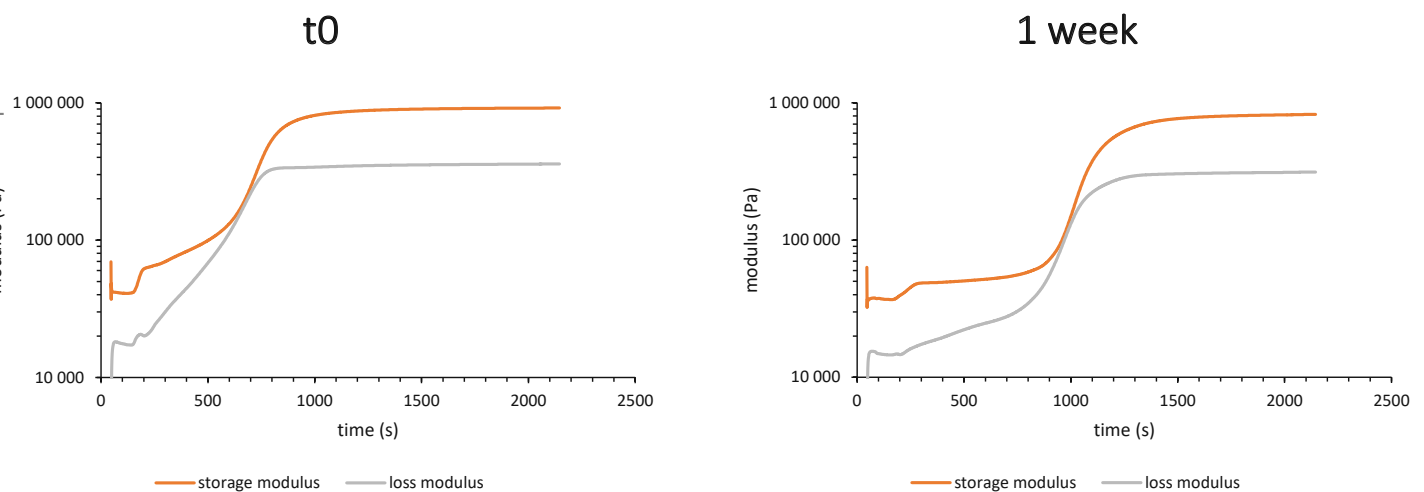
Figure 197: Rheology measurements of the polymerization of the 20w% PEG formulations directly after mixing (left) and 1 week later (right)

As can be seen in Figure 197, the polymerization is slowed down with the 20w% PEG formulations as well after one week. An exact gelpoint is not legible since the storage and loss modulus do not overlap, however the point of the steepest increase of storage modulus was referred to as t_{gel}. Also, the DBC was calculated and is depicted in Table 97 together with the rheological data.

Table 97: Storage modulus (Pa), gelpoint and DBC of the rheology measurements of 20w% PEG formulations

	storage modulus end (Pa)	t_{gel} (s)	DBC_{end} (%)
t0	$9.16 \cdot 10^5$	715	57.5
1 week	$8.22 \cdot 10^5$	1027	57.3

Interestingly, the DBC is not affected over time in this case, whereas the Sphärosil filled system showed a decrease of the DBC for every filler concentration. However, these measurements show that the DBC is not decreased while the t_{gel} is significantly shifted to the right for more than 300 s. This means, that a slowdown of the polymerization reaction is observed, while the DBC in the end is the same.

References

(1) (WHO), W. H. O. Oral Health https://www.who.int/news-room/fact-sheets/detail/oral-health. **2021**.

(2) Albert, P.; Dermann, K.; Rentsch, H. Amalgam und die Alternativen. *Chemie in unserer Zeit* **2000**, *34* (5), 300-305. DOI: https://doi.org/10.1002/1521-3781(200010)34:5<300::AID-CIUZ300>3.0.CO;2-0.

(3) Kingston, G. The rise and fall of mercury amalgam. *Prim Dent J* **2013**, *2* (3), 74-75. DOI: 10.1308/205016813807439913 PubMed.

(4) WebMD. Picture of the Teeth, https://www.webmd.com/oral-health/picture-of-the-teeth. **2021**.

(5) Arola, D. D.; Gao, S.; Zhang, H.; Masri, R. The Tooth: Its Structure and Properties. *Dental Clinics of North America* **2017**, *61* (4), 651-668. DOI: https://doi.org/10.1016/j.cden.2017.05.001.

(6) Ferracane, J. L. Resin composite--state of the art. *Dental materials : official publication of the Academy of Dental Materials* **2011**, *27* (1), 29-38. DOI: 10.1016/j.dental.2010.10.020 From NLM.

(7) Aminoroaya, A.; Neisiany, R. E.; Khorasani, S. N.; Panahi, P.; Das, O.; Madry, H.; Cucchiarini, M.; Ramakrishna, S. A review of dental composites: Challenges, chemistry aspects, filler influences, and future insights. *Composites Part B: Engineering* **2021**, *216*, 108852. DOI: https://doi.org/10.1016/j.compositesb.2021.108852.

(8) Moszner, N.; Salz, U. Recent Developments of New Components for Dental Adhesives and Composites. *Macromolecular Materials and Engineering* **2007**, *292* (3), 245-271. DOI: https://doi.org/10.1002/mame.200600414.

(9) Moszner, N., Salz, U., . New developments of polymeric dental composites. *Progress in Polymer Science* **2001**, *26*, 535-576.

(10) Moszner, N.; Gianasmidis, A.; Klapdohr, S.; Fischer, U. K.; Rheinberger, V. Sol-gel materials 2. Light-curing dental composites based on ormocers of cross-linking alkoxysilane methacrylates and further nano-components. *Dental materials : official publication of the Academy of Dental Materials* **2008**, *24* (6), 851-856. DOI: 10.1016/j.dental.2007.10.004 From NLM.

(11) Yagci, Y.; Jockusch, S.; Turro, N. J. Photoinitiated Polymerization: Advances, Challenges, and Opportunities. *Macromolecules* **2010**, *43* (15), 6245-6260. DOI: 10.1021/ma1007545.

(12) Purbrick, M. D. Photoinitiation, photopolymerization and photocuring. J.-P. Fouassier. Hanser Publishers, Munich, 1995. pp. xii + 375, price DM198.00, sFr175.00, öS1466.00, US$138.00, £84.00. ISBN 3-446-17069-3. *Polymer International* **1996**, *40* (4), 315-315. DOI: https://doi.org/10.1002/(SICI)1097-0126(199608)40:4<315::AID-PI566>3.0.CO;2-T.

(13) Fukuda, T. Fundamental kinetic aspects of living radical polymerization and the use of gel permeation chromatography to shed light on them. *Journal of Polymer Science Part A: Polymer Chemistry* **2004**, *42* (19), 4743-4755. DOI: https://doi.org/10.1002/pola.20325.

(14) Pierrel, J.; Ibrahim, A.; Croutxé-Barghorn, C.; Allonas, X. Effect of the oxygen affected layer in multilayered photopolymers. *Polymer Chemistry* **2017**, *8* (31), 4596-4602, 10.1039/C7PY00974G. DOI: 10.1039/C7PY00974G.

(15) Palin, W. M.; Ferracane, J. L. Resin-based cements used in dentistry. In *Handbook of Oral Biomaterials*, 2014; pp 213-254.

(16) Garra, P.; Dietlin, C.; Morlet-Savary, F.; Dumur, F.; Gigmes, D.; Fouassier, J.-P.; Lalevée, J. Redox two-component initiated free radical and cationic polymerizations: Concepts, reactions and applications. *Progress in Polymer Science* **2019**, *94*, 33-56. DOI: https://doi.org/10.1016/j.progpolymsci.2019.04.003.

(17) Duymus, Z. Y.; Yanikoğlu, N. D.; Alkurt, M. Evaluation of the flexural strength of dual-cure composite resin cements. *Journal of Biomedical Materials Research Part B: Applied Biomaterials* **2013**, *101B* (5), 878-881. DOI: https://doi.org/10.1002/jbm.b.32892.

(18) FERRACANE, J. L.; STANSBURY, J. W.; BURKE, F. J. T. Self-adhesive resin cements – chemistry, properties and clinical considerations. *Journal of Oral Rehabilitation* **2011**, *38* (4), 295-314. DOI: https://doi.org/10.1111/j.1365-2842.2010.02148.x.

(19) Wang, R.; Liu, H.; Wang, Y. Different depth-related polymerization kinetics of dual-cure, bulk-fill composites. *Dental Materials* **2019**, *35* (8), 1095-1103. DOI: https://doi.org/10.1016/j.dental.2019.05.001.

(20) Catel, Y.; Angermann, J.; Grob, B.; Fässler, P.; Lamparth, I.; Schnur, T. Acylthiourea oligomers as promising reducing agents for dimethacrylate-based two-component dental materials. *Dental Materials* **2023**, *39* (10), 886-893. DOI: https://doi.org/10.1016/j.dental.2023.07.007.

(21) Székely, A.; Klussmann, M. Molecular Radical Chain Initiators for Ambient- to Low-Temperature Applications. *Chemistry – An Asian Journal* **2019**, *14* (1), 105-115. DOI: https://doi.org/10.1002/asia.201801636.

(22) Achilias, D. S.; Sideridou, I. D. Kinetics of the benzoyl peroxide/amine initiated free-radical polymerization of dental dimethacrylate monomers: Experimental studies and mathematical modeling for TEGDMA and Bis-EMA. *Macromolecules* **2004**, *37* (11), 4254-4265, Article. DOI: 10.1021/ma049803n Scopus.

(23) Sideridou, I. D.; Achilias, D. S.; Karava, O. Reactivity of Benzoyl Peroxide/Amine System as an Initiator for the Free Radical Polymerization of Dental and Orthopaedic Dimethacrylate Monomers: Effect of the Amine and Monomer Chemical Structure. *Macromolecules* **2006**, *39* (6), 2072-2080. DOI: 10.1021/ma0521351.

(24) Zoller, A.; Gigmes, D.; Guillaneuf, Y. Simulation of radical polymerization of methyl methacrylate at room temperature using a tertiary amine/BPO initiating system11Electronic supplementary information (ESI) available: Further information on the experimental section and a detailed model development. See DOI: 10.1039/c5py00229j. *Polymer Chemistry* **2015**, *6* (31), 5719-5727. DOI: https://doi.org/10.1039/c5py00229j.

(25) Nayak, P. L.; Lenka, S. Redox Polymerization Initiated by Metal Ions. *Journal of Macromolecular Science, Part C* **1980**, *19* (1), 83-134. DOI: 10.1080/00222358008081047.

(26) Fenton, H. J. H. LXXIII.—Oxidation of tartaric acid in presence of iron. *Journal of the Chemical Society, Transactions* **1894**, *65* (0), 899-910, 10.1039/CT8946500899. DOI: 10.1039/CT8946500899.

(27) Murinov, Y. I.; Grabovskiy, S. A.; Kuramshina, A. R.; Antipin, A. V.; Kabal'Nova, N. N. The role of oxygen in the reaction of ferrocene with benzoyl peroxide. *Russian Journal of General Chemistry* **2015**, *85* (1), 123-125, Article. DOI: 10.1134/S1070363215010211 Scopus.

(28) Murinov, Y. I.; Grabovskiy, S. A.; Islamova, R. M.; Kuramshina, A. b. R.; Kabal'nova, N. N. Mechanism of Methyl Methacrylate Polymerization Initiated by Benzoyl Peroxide and Ferrocene in the Presence of Oxygen. *Mendeleev Communications* **2013**, *23* (1), 53-55. DOI: https://doi.org/10.1016/j.mencom.2013.01.020.

(29) Voloshanovskii, I. S.; Shevchenko, O. V.; Burenkova, E. V. Benzoyl peroxide-cobalt(II) vinyl-β-diketonate systems as initiators of styrene and methyl methacrylate polymerization. *Russian Journal of Applied Chemistry* **2008**, *81* (6), 1033-1036, Article. DOI: 10.1134/S1070427208060219 Scopus.

(30) Kameda, N.; Ishii, E. Polymerization of methyl methacrylate initiated by a Rh(I) complex and benzoyl peroxide. *Die Makromolekulare Chemie* **1983**, *184* (9), 1901-1906. DOI: https://doi.org/10.1002/macp.1983.021840916.

(31) Berry, K. L.; Peterson, J. H. Tracer Studies of Oxidation—Reduction Polymerization and Molecular Weight of "Teflon" Tetrafluoroethylene Resin. *Journal of the American Chemical Society* **1951**, *73* (11), 5195-5197. DOI: 10.1021/ja01155a057.

(32) Worzakowska, M. Studyof polymerization kinetics of the unsaturated polyester resin usingacetylacetone peroxide and Co(II)octoate. *Journal of Thermal Analysis and Calorimetry* **2007**, *88* (2), 441-448. DOI: 10.1007/s10973-006-8055-7.

(33) Garra, P.; Kermagoret, A.; Al Mousawi, A.; Dumur, F.; Gigmes, D.; Morlet-Savary, F.; Dietlin, C.; Fouassier, J. P.; Lalevée, J. New copper(i) complex based initiating systems in redox polymerization and comparison with the amine/benzoyl peroxide reference. *Polymer Chemistry* **2017**, *8* (28), 4088-4097, 10.1039/C7PY00726D. DOI: 10.1039/C7PY00726D.

(34) Garra, P.; Dumur, F.; Gigmes, D.; Al Mousawi, A.; Morlet-Savary, F.; Dietlin, C.; Fouassier, J. P.; Lalevée, J. Copper (Photo)redox Catalyst for Radical Photopolymerization in Shadowed Areas and

Access to Thick and Filled Samples. *Macromolecules* **2017**, *50* (10), 3761-3771. DOI: 10.1021/acs.macromol.7b00622.

(35) Kim, K.; Singstock, N. R.; Childress, K. K.; Sinha, J.; Salazar, A. M.; Whitfield, S. N.; Holder, A. M.; Stansbury, J. W.; Musgrave, C. B. Rational Design of Efficient Amine Reductant Initiators for Amine–Peroxide Redox Polymerization. *Journal of the American Chemical Society* **2019**, *141* (15), 6279-6291. DOI: 10.1021/jacs.8b13679.

(36) Buback, M.; Frauendorf, H.; Günzler, F.; Vana, P. Electrospray ionization mass spectrometric end-group analysis of PMMA produced by radical polymerization using diacyl peroxide initiators. *Polymer* **2007**, *48* (19), 5590-5598. DOI: https://doi.org/10.1016/j.polymer.2007.07.041.

(37) Merz, J. H.; Waters, W. A. A. - Electron-transfer reactions. The mechanism of oxidation of alcohols with Fenton's reagent. *Discussions of the Faraday Society* **1947**, *2*, 179-188, Review. DOI: 10.1039/DF9470200179 Scopus.

(38) Wissbrun, K. F. The Photolysis of Polymethylvinyl Ketone and Polymethyl Isopropenyl Ketone1. *Journal of the American Chemical Society* **1959**, *81* (1), 58-62. DOI: 10.1021/ja01510a013.

(39) Kolthoff, I. M.; Medalia, A. I.; Raaen, H. P. The Reaction between Ferrous Iron and Peroxides. IV. Reaction with Potassium Persulfate1a. *Journal of the American Chemical Society* **1951**, *73* (4), 1733-1739. DOI: 10.1021/ja01148a089.

(40) Orr, R. J.; Williams, H. L. The Efficiency of Initiation by Cumyloxy and Sulfoxy Radicals in Free Radical Polymerization1. *Journal of the American Chemical Society* **1955**, *77* (14), 3715-3720. DOI: 10.1021/ja01619a012.

(41) Garra, P.; Morlet-Savary, F.; Graff, B.; Dumur, F.; Monnier, V.; Dietlin, C.; Gigmes, D.; Fouassier, J. P.; Lalevée, J. Metal Acetylacetonate–Bidentate Ligand Interaction (MABLI) as highly efficient free radical generating systems for polymer synthesis. *Polymer Chemistry* **2018**, *9* (12), 1371-1378, 10.1039/C8PY00238J. DOI: 10.1039/C8PY00238J.

(42) Garra, P.; Dumur, F.; Gigmes, D.; Nechab, M.; Morlet-Savary, F.; Dietlin, C.; Gree, S.; Fouassier, J. P.; Lalevée, J. Metal Acetylacetonate–Bidentate Ligand Interaction (MABLI) (Photo)activated Polymerization: Toward High Performance Amine-Free, Peroxide-Free Redox Radical (Photo)initiating Systems. *Macromolecules* **2018**, *51* (7), 2706-2715. DOI: 10.1021/acs.macromol.8b00163.

(43) Le Dot, M.; Giacoletto, N.; Morlet-Savary, F.; Graff, B.; Monnier, V.; Gigmes, D.; Nechab, M.; Dumur, F.; Gerard, P.; Lalevée, J. Synergistic approach of type I hybrid complexes for highly efficient metal-based initiating strategies: Toward low energy-consuming polymerization for thermoplastic composite implementation. *European Polymer Journal* **2023**, *186*, 111871. DOI: https://doi.org/10.1016/j.eurpolymj.2023.111871.

(44) Crivello, J. V. Cationic polymerization — Iodonium and sulfonium salt photoinitiators. In *Initiators — Poly-Reactions — Optical Activity*, Berlin, Heidelberg, 1984//, 1984; Springer Berlin Heidelberg: pp 1-48.

(45) Crivello, J. V. Redox Initiated Cationic Polymerization: Reduction of Triarylsulfonium Salts by Silanes. *Silicon* **2009**, *1* (2), 111-124. DOI: 10.1007/s12633-009-9007-1.

(46) Arar, A.; Mokbel, H.; Dumur, F.; Lalevée, J. High Performance Redox Initiating Systems Based on the Interaction of Silane with Metal Complexes: A Unique Platform for the Preparation of Composites. *Molecules* **2020**, *25* (7), 1602.

(47) Arar, A.; Mousawi, A. A.; Boyadjian, C.; Garra, P.; Fouassier, J. P.; Lalevee, J. Diphenylsilane-Manganese Acetylacetonate Redox Initiating Systems: Toward Amine-Free and Peroxide-Free Systems. *Macromol. Chem. Phys.* **2020**, *221* (11), 2000058. DOI: 10.1002/macp.202000058.

(48) Wang, D.; Garra, P.; Fouassier, J. P.; Lalevée, J. Silane/iodonium salt as redox/thermal/photoinitiating systems in radical and cationic polymerizations for laser write and composites. *Polymer Chemistry* **2020**, *11* (4), 857-866, 10.1039/C9PY01819K. DOI: 10.1039/C9PY01819K.

(49) Wang, D.; Garra, P.; Szillat, F.; Fouassier, J. P.; Lalevée, J. Silane Based Redox Initiating Systems: Toward a Safer Amine-Free, Peroxide-Free, and Metal-Free Approach. *Macromolecules* **2019**, *52* (9), 3351-3358. DOI: 10.1021/acs.macromol.9b00233.

(50) Moszner, N.; Hirt, T. New polymer-chemical developments in clinical dental polymer materials: Enamel–dentin adhesives and restorative composites. *Journal of Polymer Science Part A: Polymer Chemistry* **2012**, *50* (21), 4369-4402. DOI: https://doi.org/10.1002/pola.26260.

(51) Yuji I, Y. K., Kawashima T. Polymerization initiator composition controlling polymerization at interface and curable composition containing same. . *EP0480785B1*.

(52) Guggenberger RA, H. R., Ludsteck M, Raia G, Stippschild-Boxler Twocomponent self-adhesive dental composition, process of production and use thereof. *US10932994B2*.

(53) Hecht R, L. M. Initiator system for acid dental formulations. *US6953535B2*.

(54) Falsafi A, K. R., Oxman JD. Dental compositions and methods with arylsulfinate salts. . *US7465758B2.*

(55) Kawashima M, O. I. Polymerizable Composition. *EP0408357B1*.

(56) Tehfe, M.-A.; Dumur, F.; Graff, B.; Morlet-Savary, F.; Gigmes, D.; Fouassier, J.-P.; Lalevée, J. Push–pull (thio)barbituric acid derivatives in dye photosensitized radical and cationic polymerization reactions under 457/473 nm laser beams or blue LEDs. *Polymer Chemistry* **2013**, *4* (13), 3866-3875, 10.1039/C3PY00372H. DOI: 10.1039/C3PY00372H.

(57) Ikemura, K.; Endo, T. Effect on adhesion of new polymerization initiator systems comprising 5-monosubstituted barbituric acids, aromatic sulfinate amides, and tert-butyl peroxymaleic acid in dental adhesive resin. *Journal of Applied Polymer Science* **1999**, *72* (13), 1655-1668. DOI: https://doi.org/10.1002/(SICI)1097-4628(19990624)72:13<1655::AID-APP2>3.0.CO;2-0.

(58) Ikemura, K.; Endo, T. A review of our development of dental adhesives — Effects of radical polymerization initiators and adhesive monomers on adhesion. *Dental Materials Journal* **2010**, *29* (2), 109-121. DOI: 10.4012/dmj.2009-057.

(59) Arar, A.; Mousawi, A. A.; Morlet-Savary, F.; Lalevée, J. Peroxide-free redox initiating systems for polymerization in mild conditions. *Polymer Chemistry* **2021**, *12* (12), 1816-1822, 10.1039/D1PY00172H. DOI: 10.1039/D1PY00172H.

(60) Yu, F.-E.; Hsu, J.-M.; Pan, J.-P.; Wang, T.-H.; Chern, C.-S. Kinetics of Michael addition polymerizations of n,n'-bismaleimide-4,4'-diphenylmethane with barbituric acid. *Polymer Engineering & Science* **2013**, *53* (1), 204-211. DOI: https://doi.org/10.1002/pen.23248.

(61) Mukherjee, A. R.; Pal , R.; Amarendra; Biswas, M.; Maiti, S. Redox-initiated vinyl polymerization with thiourea as the reductant. *Journal of Polymer Science Part A-1: Polymer Chemistry* **1967**, *5* (1), 135-149. DOI: https://doi.org/10.1002/pol.1967.150050112.

(62) Singh, B. C.; Mohanty, T. R.; Nayak, P. L. Polymerization of acrylonitrile initiated by thiourea-vanadium(V) redox system. *European Polymer Journal* **1976**, *12* (6), 371-376. DOI: https://doi.org/10.1016/0014-3057(76)90105-1.

(63) Moszner, N.; Catel, Y.; Lamparth, I.; Angermann, J. Dental materials on the basis of polymerizable thiourea derivatives. EP4039220, 2022.

(64) Moszner, N.; Burtscher, P.; Gianasmidis, A. Photopolymerizable and dual curing dental materials based on thiourea derivatives. EP2921154, 2015.

(65) Morandi, P.; Catel, Y.; Angermann, J.; Fässler, P.; Robin, J.-J.; Monge, S. Synthesis of original polymeric hydroperoxides as innovative oxidizing agents for self-cure dental materials. *Polymer Chemistry* **2023**, *14* (34), 3950-3961, 10.1039/D3PY00639E. DOI: 10.1039/D3PY00639E.

(66) Noirbent, G.; Dumur, F. Recent Advances on Copper Complexes as Visible Light Photoinitiators and (Photo) Redox Initiators of Polymerization. *Catalysts* **2020**, *10* (9), 953.

(67) Lv, Y.; Liu, Z.; Zhu, A.; An, Z. Glucose oxidase deoxygenation–redox initiation for RAFT polymerization in air. *Journal of Polymer Science Part A: Polymer Chemistry* **2017**, *55* (1), 164-174. DOI: https://doi.org/10.1002/pola.28380.

(68) Njus, D.; Kelley, P. M.; Tu, Y.-J.; Schlegel, H. B. Ascorbic acid: The chemistry underlying its antioxidant properties. *Free Radical Biology and Medicine* **2020**, *159*, 37-43. DOI: https://doi.org/10.1016/j.freeradbiomed.2020.07.013.

(69) Garra, P.; Dumur, F.; Al Mousawi, A.; Graff, B.; Gigmes, D.; Morlet-Savary, F.; Dietlin, C.; Fouassier, J. P.; Lalevée, J. Mechanosynthesized copper(i) complex based initiating systems for redox

References

polymerization: towards upgraded oxidizing and reducing agents. *Polymer Chemistry* **2017**, *8* (38), 5884-5896, 10.1039/C7PY01244F. DOI: 10.1039/C7PY01244F.

(70) Zhao, Y.; Qu, B.; Wu, X.; Li, X.; Liu, Q.; Jin, X.; Guo, L.; Hai, L.; Wu, Y. Design, synthesis and biological evaluation of brain targeting l-ascorbic acid prodrugs of ibuprofen with "lock-in" function. *Eur J Med Chem* **2014**, *82*, 314-323. DOI: 10.1016/j.ejmech.2014.05.072 PubMed.

(71) Tanini, D.; Gori, M.; Bicocchi, F.; Ambrosi, M.; Nostro, P. L.; Capperucci, A. Synthesis and spectroscopic characterization of double chained and sulfurated derivatives of L-ascorbic acid. *ARKIVOC* **2016**, *2017* (2), 407-420. DOI: 10.24820/ark.5550190.p009.781.

(72) Koepp, H.-M.; Wendt, H.; Stkehlow, H. Der Vergleich der Spannungsreihen in verschiedenen Solventien. II. *Zeitschrift für Elektrochemie, Berichte der Bunsengesellschaft für physikalische Chemie* **1960**, *64* (4), 483-491. DOI: https://doi.org/10.1002/bbpc.19600640406.

(73) Pisoschi, A. M.; Danet, A. F.; Kalinowski, S. Ascorbic Acid Determination in Commercial Fruit Juice Samples by Cyclic Voltammetry. *Journal of Automated Methods and Management in Chemistry* **2008**, *2008*, 937651. DOI: 10.1155/2008/937651.

(74) Elgrishi, N.; Rountree, K. J.; McCarthy, B. D.; Rountree, E. S.; Eisenhart, T. T.; Dempsey, J. L. A Practical Beginner's Guide to Cyclic Voltammetry. *Journal of Chemical Education* **2018**, *95* (2), 197-206. DOI: 10.1021/acs.jchemed.7b00361.

(75) Korolev, B. A.; Lachinov, M. B.; Dreval, V. Y.; Zubov, V. P.; Vinogradov, G. V.; Kabanov, V. A. Rheological study of the mechanism of gel-effect in radical polymerization of butyl methacrylate in bulk. *Polymer Science U.S.S.R.* **1983**, *25* (11), 2826-2831. DOI: https://doi.org/10.1016/0032-3950(83)90363-5.

(76) Suzuki, Y.; Mishima, R.; Kato, E.; Matsumoto, A. Analysis of the glass effect and Trommsdorff effect during bulk polymerization of methyl methacrylate, ethyl methacrylate, and butyl methacrylate. *Polymer Journal* **2023**, *55* (3), 229-238. DOI: 10.1038/s41428-022-00746-5.

(77) Barron, E. S. G.; DeMeio, R. H.; Klemperer, F. STUDIES ON BIOLOGICAL OXIDATIONS: V. COPPER AND HEMOCHROMOGENS AS CATALYSTS FOR THE OXIDATION OF ASCORBIC ACID. THE MECHANISM OF THE OXIDATION. *Journal of Biological Chemistry* **1936**, *112* (2), 625-640. DOI: https://doi.org/10.1016/S0021-9258(18)74946-6.

(78) Ligon, S. C.; Husár, B.; Wutzel, H.; Holman, R.; Liska, R. Strategies to reduce oxygen inhibition in photoinduced polymerization. *Chemical reviews* **2014**, *114* (1), 557-589. DOI: 10.1021/cr3005197 From NLM.

(79) Gorsche, C.; Harikrishna, R.; Baudis, S.; Knaack, P.; Husar, B.; Laeuger, J.; Hoffmann, H.; Liska, R. Real Time-NIR/MIR-Photorheology: A Versatile Tool for the in Situ Characterization of Photopolymerization Reactions. *Analytical Chemistry* **2017**, *89* (9), 4958-4968. DOI: 10.1021/acs.analchem.7b00272.

(80) Thetiot, E.; Ohl, C.; Vidal, L.; Catel, Y.; Lamparth, I.; Fässler, P.; Lalevée, J. Reactivity of dihydropyridines as reducing agents in redox initiating systems. *European Polymer Journal* **2024**, *209*, 112905. DOI: https://doi.org/10.1016/j.eurpolymj.2024.112905.

(81) https://polymerinnovationblog.com/thermoset-characterization-part-17-applications-dynamic-mechanical-analysis-dma-part-2/ (15.12.2023).

(82) Grellmann, W. S., S. Kunststoffprüfung. *Carl Hanser Verlag GmbH & Co. KG* **2011**, p 739.

(83) Kabalka, G. W.; Das, B. C.; Das, S. Rhodium-catalyzed 1,4-addition reactions of diboron reagents to electron deficient olefins. *Tetrahedron Letters* **2002**, *43* (13), 2323-2325. DOI: https://doi.org/10.1016/S0040-4039(02)00261-7.

(84) Baker, R. T.; Nguyen, P.; Marder, T. B.; Westcott, S. A. Transition Metal Catalyzed Diboration of Vinylarenes. *Angewandte Chemie International Edition in English* **1995**, *34* (12), 1336-1338. DOI: https://doi.org/10.1002/anie.199513361.

(85) Lennox, A. J. J.; Lloyd-Jones, G. C. Selection of boron reagents for Suzuki–Miyaura coupling. *Chemical Society Reviews* **2014**, *43* (1), 412-443, 10.1039/C3CS60197H. DOI: 10.1039/C3CS60197H.

(86) Mo, F.; Jiang, Y.; Qiu, D.; Zhang, Y.; Wang, J. Direct Conversion of Arylamines to Pinacol Boronates: A Metal-Free Borylation Process. *Angewandte Chemie International Edition* **2010**, *49* (10), 1846-1849. DOI: https://doi.org/10.1002/anie.200905824.

(87) Pubill-Ulldemolins, C.; Bonet, A.; Gulyás, H.; Bo, C.; Fernández, E. Essential role of phosphines in organocatalytic β-boration reaction. *Organic & Biomolecular Chemistry* **2012**, *10* (48), 9677-9682, 10.1039/C2OB26899J. DOI: 10.1039/C2OB26899J.

(88) Kou, T.; Tatsuo, I.; Norio, M. Addition and Coupling Reactions of Bis(pinacolato)diboron Mediated by CuCl in the Presence of Potassium Acetate. *Chemistry Letters* **2000**, *29* (9), 982-983. DOI: 10.1246/cl.2000.982.

(89) Mun, S.; Lee, J.-E.; Yun, J. Copper-catalyzed beta-Boration of alpha,beta-unsaturated carbonyl compounds: rate acceleration by alcohol additives. *Organic letters* **2006**, *8* (21), 4887-4889. DOI: 10.1021/ol061955a PubMed.

(90) Lalevée, J.; Tehfe, M. A.; Allonas, X.; Fouassier, J. P. Boryl Radicals as a New Photoinitiating Species: A Way to Reduce the Oxygen Inhibition. *Macromolecules* **2008**, *41* (23), 9057-9062. DOI: 10.1021/ma8018848.

(91) Lalevée, J.; Blanchard, N.; Tehfe, M.-A.; Chany, A.-C.; Fouassier, J.-P. New Boryl Radicals Derived from N-Heteroaryl Boranes: Generation and Reactivity. *Chemistry – A European Journal* **2010**, *16* (43), 12920-12927. DOI: https://doi.org/10.1002/chem.201001440.

(92) Tehfe, M.-A.; Makhlouf Brahmi, M.; Fouassier, J.-P.; Curran, D. P.; Malacria, M.; Fensterbank, L.; Lacôte, E.; Lalevée, J. N-Heterocyclic Carbenes–Borane Complexes: A New Class of Initiators for Radical Photopolymerization. *Macromolecules* **2010**, *43* (5), 2261-2267. DOI: 10.1021/ma902492q.

(93) Himmel, H.-J. Nucleophilic Neutral Diborane(4) Compounds with sp3–sp3-Hybridized Boron Atoms. *European Journal of Inorganic Chemistry* **2018**, *2018* (20-21), 2139-2154. DOI: https://doi.org/10.1002/ejic.201800031.

(94) Wu, C.; Hou, X.; Zheng, Y.; Li, P.; Lu, D. Electrophilicity and Nucleophilicity of Boryl Radicals. *The Journal of Organic Chemistry* **2017**, *82* (6), 2898-2905. DOI: 10.1021/acs.joc.6b02849.

(95) Flinker, M.; Yin, H.; Juhl, R. W.; Eikeland, E. Z.; Overgaard, J.; Nielsen, D. U.; Skrydstrup, T. Efficient Water Reduction with sp3-sp3 Diboron(4) Compounds: Application to Hydrogenations, H–D Exchange Reactions, and Carbonyl Reductions. *Angewandte Chemie International Edition* **2017**, *56* (50), 15910-15915. DOI: https://doi.org/10.1002/anie.201709685.

(96) Yoshida, H.; Seki, M.; Kageyuki, I.; Osaka, I.; Hatano, S.; Abe, M. B(MIDA)-Containing Diborons. *ACS Omega* **2017**, *2* (9), 5911-5916. DOI: 10.1021/acsomega.7b01042.

(97) Marcuccio, S. M. Boronic Compounds. 2002.

(98) Gao, M.; Thorpe, S. B.; Kleeberg, C.; Slebodnick, C.; Marder, T. B.; Santos, W. L. Structure and Reactivity of a Preactivated sp2–sp3 Diboron Reagent: Catalytic Regioselective Boration of α,β-Unsaturated Conjugated Compounds. *The Journal of Organic Chemistry* **2011**, *76* (10), 3997-4007. DOI: 10.1021/jo2003488.

(99) Pieringer, F.; Knaipp, K.; Liska, R.; Moszner, N.; Catel, Y.; Gescheidt, G.; Knaack, P. Boron–boron bonds: boldly breaking boundaries towards amine- and peroxide-free 2K radical polymerization. *Polymer Chemistry* **2024**, 10.1039/D4PY00445K. DOI: 10.1039/D4PY00445K.

(100) Lawlor, F. J.; Norman, N. C.; Pickett, N. L.; Robins, E. G.; Nguyen, P.; Lesley, G.; Marder, T. B.; Ashmore, J. A.; Green, J. C. Bis-Catecholate, Bis-Dithiocatecholate, and Tetraalkoxy Diborane(4) Compounds: Aspects of Synthesis and Electronic Structure. *Inorganic Chemistry* **1998**, *37* (20), 5282-5288. DOI: 10.1021/ic980425a.

(101) Suginome, M.; Ito, Y. Transition-Metal-Catalyzed Additions of Silicon–Silicon and Silicon–Heteroatom Bonds to Unsaturated Organic Molecules. *Chemical reviews* **2000**, *100* (8), 3221-3256. DOI: 10.1021/cr9902805.

(102) Marder, T. B.; Norman, N. C. Transition metal catalysed diboration. *Topics in Catalysis* **1998**, *5* (1), 63-73. DOI: 10.1023/A:1019145818515.

(103) Kleeberg, C.; Borner, C. On the Reactivity of Silylboranes toward Lewis Bases: Heterolytic B–Si Cleavage vs. Adduct Formation. *European Journal of Inorganic Chemistry* **2013**, *2013* (15), 2799-2806. DOI: https://doi.org/10.1002/ejic.201300119.

(104) Misra, G. S.; Bajpai, U. D. N. Redox polymerization. *Progress in Polymer Science* **1982**, *8* (1), 61-131. DOI: https://doi.org/10.1016/0079-6700(82)90008-9.

(105) Garra, P.; Dumur, F.; Nechab, M.; Morlet-Savary, F.; Dietlin, C.; Graff, B.; Gigmes, D.; Fouassier, J.-P.; Lalevée, J. Stable copper acetylacetonate-based oxidizing agents in redox (NIR photoactivated) polymerization: an opportunity for the one pot grafting from approach and an example on a 3D printed object. *Polymer Chemistry* **2018**, *9* (16), 2173-2182, 10.1039/C8PY00341F. DOI: 10.1039/C8PY00341F.
(106) Adamczyk-Woźniak, A.; Jakubczyk, M.; Sporzyński, A.; Żukowska, G. Quantitative determination of the Lewis acidity of phenylboronic catechol esters — Promising anion receptors for polymer electrolytes. *Inorganic Chemistry Communications* **2011**, *14* (11), 1753-1755. DOI: https://doi.org/10.1016/j.inoche.2011.08.002.
(107) Clegg, W.; R. F. Johann, T.; B. Marder, T.; C. Norman, N.; Guy Orpen, A.; M. Peakman, T.; J. Quayle, M.; R. Rice, C.; J. Scott, A. Platinum-catalysed 1,4-diboration of 1,3-dienes. *Journal of the Chemical Society, Dalton Transactions* **1998**, (9), 1431-1438, 10.1039/A800108A. DOI: 10.1039/A800108A.